

Electronic Thesis and Dissertation Repository

2-24-2021 2:00 PM

Metabolic Reprogramming By DNA Tumour Viruses

Martin Prusinkiewicz, *The University of Western Ontario*

Supervisor: Mymryk, Joe S., *The University of Western Ontario*

A thesis submitted in partial fulfillment of the requirements for the Doctor of Philosophy degree in Microbiology and Immunology

© Martin Prusinkiewicz 2021

Follow this and additional works at: <https://ir.lib.uwo.ca/etd>



Part of the [Cancer Biology Commons](#)

Recommended Citation

Prusinkiewicz, Martin, "Metabolic Reprogramming By DNA Tumour Viruses" (2021). *Electronic Thesis and Dissertation Repository*. 7667.

<https://ir.lib.uwo.ca/etd/7667>

This Dissertation/Thesis is brought to you for free and open access by Scholarship@Western. It has been accepted for inclusion in Electronic Thesis and Dissertation Repository by an authorized administrator of Scholarship@Western. For more information, please contact wlsadmin@uwo.ca.

Abstract

Viruses are the etiological agents of approximately 12% of human cancers. However, only a subset of viral infections eventually progress to cancer. As obligate intracellular parasites, viruses create a host-cell environment that is amenable to virus replication. These changes to host-cell processes during infection are enacted by virally-encoded proteins that act as molecular hubs. When these processes intersect with pathways that encourage the development of cancer, such as the p53 tumour suppressor pathway, these virally-encoded molecular hub proteins function as viral oncoproteins. One major requirement of both virus infected cells and rapidly growing cancer cells is an altered metabolism that provides the rapid production of energy and macromolecules required for either viral or cellular replication. Typically, this metabolic phenotype involves an increased rate of glycolysis and a decreased rate of cellular respiration despite the presence of ample oxygen that would otherwise encourage respiration. The purpose of this thesis is to investigate how viruses belonging to a subset viruses known as DNA tumour viruses can reprogram cellular metabolism. We hypothesize that DNA tumour viruses cause a cancer-like metabolic phenotype in the infected cell or cancerous tissue, which is similar to, but still distinct from, the metabolic phenotype in corresponding non-virally induced cancers. First, we determined that the 13S isoform of the E1A oncoprotein found in human adenovirus is responsible for causing an increase in glycolysis both as an endogenously expressed protein and in HAdV infected cells. Next, we utilized The Cancer Genome Atlas, a repository of patient tumour data, to determine that human papillomavirus-positive (HPV+) head and neck squamous cell carcinoma (HNSCC) have a distinct metabolism-related transcriptome when compared to HPV- HNSCC, and that some of these metabolic genes are associated with patient survival. Finally, we confirm that DNA tumour virus-induced cancers do have a distinct metabolism-related transcriptome in the context of another cancer, Epstein-Barr virus associated gastric cancer. These findings highlight that the metabolic phenotypes of virally infected cells and cancer cells, while superficially similar, are distinct enough to represent potential novel druggable targets or biomarkers.

Summary for Lay Audience

In rare cases, cancer can develop from infections caused by certain viruses. Even before a virus causes cancer in an infected cell, the metabolism of the infected cell begins to resemble that of a cancer cell. Specifically, how that cell produces energy and what molecules it produces as building blocks for the production of new virus are very similar to the ways in which a cancer cell performs the same tasks to grow. The purpose of this thesis is to compare the metabolism of virus-infected cells and cancers to the metabolism of those that are not caused by a virus. The three viruses I discuss in this thesis are human adenovirus, human papillomavirus and Epstein-Barr virus. Human adenovirus does not cause cancers in humans, but it can cause cancers in rodent cells. Human adenovirus is frequently used to study how virus-induced cancer proceeds in cells. In the first part of my thesis, I explore how one of the tools used by human adenovirus, a viral protein called E1A, changes the metabolism of an infected cell to resemble that of cancer. Adenovirus can produce different versions of E1A. We identified that one version, 13S, is responsible for increasing cellular sugar consumption, a process known as glycolysis, both by itself and as part of a whole virus. Next we wanted to determine whether human cancers caused by viruses used different metabolic processes than similar non-viral cancers. The first cancer we examined was head and neck cancer caused by human papillomavirus (HPV). We used a database of patient tumours called The Cancer Genome Atlas, which contains information about the genetic messages (mRNA) produced by a cancer that codes for the cellular machines (enzymes) responsible for metabolism in the cancer. We found that head and neck cancer caused by HPV had a different set of messages than the same cancer that was not caused by the virus. We also found that the levels of these messages within HPV-induced head and neck cancers appeared to correlate with, but not necessarily cause, differences in patient survival. We performed a similar analysis for stomach cancers that were caused by Epstein-Barr virus. Once again, it appeared that the Epstein-Barr virus containing cancers had a different set of messages for metabolism-related enzymes than other stomach cancers. In conclusion, my thesis shows that cancers caused by viruses might produce energy and molecular building blocks in a way that differs from non-viral cancers. This could have implications for the treatment of cancers caused by viruses.

Keywords

Human adenovirus, HAdV, Early region 1A, E1A, Human Papillomavirus, HPV, Epstein-Barr Virus, EBV, Metabolism, Glycolysis, Cellular Respiration, Oxidative Phosphorylation, Glutaminolysis, Warburg effect, Cancer, Head and neck squamous cell carcinoma, Gastric cancer, Oncoprotein

Co-Authorship Statement

Sections of Chapter 1 of this thesis were published as review article in *Viruses*, 2019; 11:141. I was the primary author of this manuscript.

Chapter 2 of this thesis was published in *Viruses*, 2020; 12:610. I was the primary author of this manuscript. I performed all extracellular flux experiments, the E1A western blot included in the manuscript, and a number of the RT-qPCR experiments, which were otherwise performed under my supervision by Jessie Tu whom I trained to perform the technique. Katelyn M. MacNeil performed another western blot under my supervision, which ultimately was not included in the manuscript, but was invaluable for framing some of the ideas included within. Sandi Radko-Juettner and Peter Pelka from the University of Manitoba created the E1A-expressing A549 cell lines used for this manuscript and generated the RNAseq data for virally infected IMR-90 cells. Gregory J. Fonseca from McGill University contributed to analysis of the RNAseq data. All other authors provided invaluable feedback regarding the writing of the manuscript.

Chapter 3 of this thesis was published in *Cancers*, 2020; 12:253. I was the primary author of this manuscript. I was responsible for the primary analysis and interpretation of the data. Steven F. Gameiro and Farhad Ghasemi were invaluable to the generation of data from the TCGA database. Peter Y.F. Zeng performed additional analyses that were ultimately not included in the manuscript, but were invaluable for framing some of the ideas therein. Hanna Maekebay was responsible for early data analysis under my supervision. John W. Barrett, Anthony C. Nichols and Joe S. Mymryk were responsible for supervision of all authors involved in the project. All authors provided invaluable feedback regarding the writing of the manuscript.

Chapter 4 of this thesis contains an unpublished manuscript of which I was the primary author. I was responsible for the primary analysis and interpretation of the data. Farhad Ghasemi was invaluable to the generation of data from the TCGA database. Mackenzie J. Dodge was responsible for early data analysis under my supervision. All other authors provided invaluable feedback regarding the writing of the manuscript.

Acknowledgments

I would like to express my immense gratitude and thanks to my supervisor, Dr. Joe Mymryk, who gave me the freedom to explore an area of research that was new to the lab. His abundant patience and mentorship saw my early fumbling thoughts and experiments through to published manuscripts. He was also an endless source of interesting information on every topic under the sun during my time in the lab.

Much thanks to my committee members throughout the years of my PhD, the input and feedback I have received from Dr. Trevor Shepherd, Dr. Rod DeKoter and Dr. Hon Leong. Your feedback and guidance helped focus my thesis into a finished product.

Thank you to the multitude of people that have been members of the Mymryk lab throughout the years. I learned a lot from each of you. Special thanks to Dr. Steven Gameiro, Tanner Tessier, Katelyn MacNeil, Wyatt Anderson and Mackenzie Dodge (“You’ve got this!”) for your collegiality and friendship during the later years of my thesis. It was great to be a part of the team that was the Mymryk lab. Also, thank you to the past members of the Mymryk lab, including Dr. Greg Fonseca, Dr. Cason King, Dr. Mike Cohen, Ali Zhang, Kristianne Galpin, Jessica Hill and Gloria Thomson. Thanks to the undergraduate students in the lab throughout the years, especially Jessie Tu and Sarah Denford, it was a wonderful experience mentoring both of you and you both became impressively self-sufficient by the end of your projects. An acknowledgement goes out to the PEL high school students who had the opportunity to experience a university research environment during their program in the lab, especially Hanna Maekebay who was the first student I was involved in supervising directly.

Thank you to Dr. Anthony Nichols and all the members of the Nichols lab, especially Dr. Farhad Ghasemi, Dr. John Barrett, Peter Zeng, Dr. Nicole Pinto and Dr. Kara Ruicci. I would also like to thank Dr. Tim Regnault and the members of his lab, especially Dr. Christie Vanderboor and Zach Easton for allowing me unlimited access to their lab space and use of the Seahorse XF analyzer. It was a huge help and is very much appreciated.

I appreciate the funding that I have received throughout my PhD and I would like to acknowledge support from the Schulich School of Medicine & Dentistry, the Department of Microbiology & Immunology at Western, the National Sciences and Engineering Research Council, and the generous financial support from Dr. Mymryk.

Finally, a huge thanks goes out to my wife, Martina Mudri, and my family and for their continuous love and support throughout this process. They gave me the energy to keep going and helped me keep everything in perspective.

Table of Contents

Abstract.....	ii
Summary for Lay Audience.....	iii
Co-Authorship Statement.....	v
Acknowledgments.....	vi
Table of Contents.....	viii
List of Tables.....	xiii
List of Figures.....	xv
List of Abbreviations.....	xviii
Chapter 1.....	1
1 Introduction.....	1
1.1 Virus Structure and Classification.....	1
1.2 The Essentials of DNA Tumour Viruses.....	3
1.3 Discovery of Human Adenovirus, Human Papillomavirus and Epstein-Barr Virus	4
1.4 Overview of Human Adenovirus Proteins.....	6
1.5 Human Adenovirus Reprogramming of Host-cell Metabolism.....	8
1.5.1. The Earliest Observations of Metabolic Changes due to HAdV Infection	8
1.5.2. Metabolomic and Proteomic Analyses of Adenovirus Infection.....	11
1.5.3. E4ORF1 Positively Regulates Glycolysis and Glutamine Catabolism..	19
1.5.4. E1A as a Regulator of Cellular Metabolism During Infection.....	23
1.6 Human Adenovirus and Cancer.....	29
1.7 Overview of Human Papillomavirus Proteins.....	31
1.8 Human Papillomavirus Reprogramming of Host-cell Metabolism.....	34
1.9 Human Papillomavirus and Cancer.....	34
1.10 Overview of Epstein-Barr Virus Proteins.....	36
1.11 Epstein-Barr Virus Reprogramming of Host-cell Metabolism.....	38
1.12 Epstein-Barr Virus and Cancer.....	38
1.13 Glycolysis and the Warburg Effect.....	40
1.14 Parallels Between the Metabolism of Cancer Cells and Virally Infected Cells.	42

1.15	Why Study Metabolism	44
1.16	Thesis Overview	47
1.16.1.	Hypothesis, Rationale, and Approach.....	47
1.16.2.	Chapter 2: Differential Effects of Human Adenovirus E1A Protein Isoforms on Aerobic Glycolysis in A549 Human Lung Epithelial Cell	48
1.16.3.	Chapter 3: Survival-Associated Metabolic Genes in Human Papillomavirus-Positive Head and Neck Cancers.....	49
1.16.4.	Chapter 4: Expression and Patient Survival Associations for Metabolic Enzyme Genes in Epstein-Barr Virus Associated Gastric Cancer.....	50
Chapter 2	52
2	Differential Effects of Human Adenovirus E1A Protein Isoforms on Aerobic glycolysis in A549 Human Lung Epithelial Cells	52
2.1	Introduction.....	52
2.2	Materials and Methods.....	54
2.2.1	Cell Culture	54
2.2.2	Protein Extraction and Western Blot	54
2.2.3	Seahorse Glycolytic Stress Test.....	55
2.2.4	Seahorse Mitochondrial Stress Test.....	55
2.2.5	RNA Extraction and qPCR	55
2.2.6	RNA Sequencing Analysis	57
2.2.7	Statistics	57
2.3	Results.....	58
2.3.1	A549-13S Cells Increased Baseline Glycolysis and Decreased Maximum Respiration	58
2.3.2	Glycolytic Genes Are Upregulated in A59-13S Cells	62
2.3.3	Pentose Phosphate Pathway Genes Are Differentially Regulated in A549-13S Cells.....	65
2.3.4	Tricarboxylic Acid Cycle Genes Are Upregulated in A549-13S Cells .	65
2.3.5	Oxidative Phosphorylation Genes Are Downregulated in A549-13S Cells	69

2.3.6	13S E1A Influences Metabolism to a Greater Extent than 12S E1A in HAdV-5 Infected Primary IMR-90 Cells	69
2.4	Discussion	74
2.5	Conclusions.....	78
Chapter 3	80
3	Survival-Associated Metabolic Genes in Human Papillomavirus-Positive Head and Neck Cancers	80
3.1	Introduction.....	80
3.2	Materials and Methods.....	82
3.2.1	Data collection	82
3.2.2	RNA expression comparisons.....	82
3.2.3	Survival analysis	84
3.2.4	Gene Enrichment Analysis	84
3.2.5	Analysis of differential cell line sensitivity to tyrosine kinase inhibitors based on HPV status	84
3.3	Results.....	85
3.3.1	Expression of Pathway-specific Metabolic Genes were Altered Between HPV+, HPV-, and Normal Control Samples from The TCGA HNSC Cohort.....	85
3.3.2	Low Expression of Genes Encoding Multiple Components of the Mitochondrial Electron Transport Chain are Associated with Improved Patient Survival in HPV+ HNSCC	87
3.3.3	Low Expression of ELOVL6, Involved in Fatty Acid Synthesis, is Associated with Better Overall Survival in Patients with HPV+ HNSCC	92
3.3.4	Low Expression of GOT2, Involved in Amino Acid Metabolism, is Associated with Better HPV+ HNSCC Patient Survival.....	92
3.3.5	Low Expression of SLC16A2, a Thyroid Hormone Transporter, in HPV+ HNSCC is Associated with Better Overall Survival.	95
3.3.6	COX16, COX17, and SLC16A2 are Independently Correlated with Favourable Survival Outcomes in HPV+ HNSCC	95
3.4	Discussion	97

3.5	Conclusions.....	104
Chapter 4.....		106
4	Expression and patient survival associations for metabolic enzyme genes in Epstein-Barr virus associated gastric cancer	106
4.1.	Introduction.....	106
4.2.	Materials and Methods.....	108
4.2.1.	RNA Expression Analysis	108
4.2.2.	Venn Diagram Visualization.....	108
4.2.3.	Survival analysis	109
4.3.	Results.....	109
4.3.1.	Glycolysis	109
4.3.2.	Tricarboxylic Acid Cycle.....	115
4.3.3.	Cellular Respiration	118
4.3.4.	Fatty Acid Metabolism	124
4.3.5.	Glutaminolysis	127
4.3.6.	Pentose Phosphate Pathway	129
4.3.7.	Monocarboxylate Transporters	132
4.4.	Discussion.....	135
4.5.	Conclusions.....	140
Chapter 5.....		142
5	Discussion.....	142
5.1	Thesis Summary.....	142
5.2	Viral Oncogenes and Metabolism.....	144
5.2.1	Viral Oncoprotein Regulation of MYC	146
5.2.2	Viral Oncoprotein Regulation of p53	149
5.2.3	Viral Oncoprotein Regulation of pRb/E2F	153
5.3	The Importance of Biomarkers in Metabolism.....	153
5.4	Limitations of this Work.....	156
5.5	Future Work	157
References.....		161
Appendix.....		205

Curriculum Vitae209

List of Tables

Table 1.1. Characteristics of DNA tumour viruses discussed in this thesis.	5
Table 1.2. Different HAdV species and associated types, tissue tropisms and clinically associated infections.	7
Table 1.3. Cell lines used in studies of metabolism in HAdV infected cells.....	12
Table 1.4 Different HPV species and associated types, tissue tropisms and clinically associated infections.	32
Table 3.1. Univariate and multivariate analysis of the association of clinical variables and expression of metabolic genes with overall survival in HPV+ HNSCC.	96
Table 4.1 Glycolysis genes that were differentially regulated in EBVaGC.	111
Table 4.2. TCA cycle genes that were differentially regulated in EBVaGC.....	117
Table 4.3. Respiratory complex I genes that were differentially regulated in EBVaGC.	119
Table 4.4. Respiratory complex II genes that were differentially regulated in EBVaGC.	119
Table 4.5. Respiratory complex III genes that were differentially regulated in EBVaGC.	119
Table 4.6. Respiratory complex IV genes that were differentially regulated in EBVaGC.	120
Table 4.7. Fatty acid synthesis genes that were differentially regulated in EBVaGC.....	125
Table 4.8. Beta-oxidation genes that were differentially regulated in EBVaGC.....	126
Table 4.9. Glutaminolysis genes that were differentially regulated in EBV+ STAD.....	128

Table 4.10. Pentose phosphate pathway genes that were differentially regulated in
EBVaGC. 130

Table 4.11. Monocarboxylic acid transport genes that were differentially regulated in
EBVaGC. 133

List of Figures

Figure 1.1. Key advances in metabolism research, adenovirus research and technology.	10
Figure 1.2. Factors influencing host-cell metabolism with HAdV infection.....	15
Figure 1.3. Schematic of how E4ORF1 contributes to MYC-regulated transcription of genes involved in glycolysis.	21
Figure 1.4. Putative mechanisms by which HAdV E1A regulates transcription of host-cell metabolic genes based on models derived from the literature.	28
Figure 1.5. Viruses and cancers co-opt many cellular metabolic pathways to satisfy their metabolic requirements.	41
Figure 1.6 The Warburg Effect in cancer cells and virus infected cells.	43
Figure 1.7. Carbon metabolism under different oxygen availabilities.....	46
Figure 2.1. Western blot of E1A expression levels in A549-EV, A549-12S and A549-13S cell lines.	59
Figure 2.2. A549-13S cells have a unique functional glycolytic and oxidative phosphorylation metabolism when compared to A549-12S and A549-EV cells.	61
Figure 2.3. Relative expression levels of mRNA for glycolytic genes in 13S and 12S expressing A549 cells.	64
Figure 2.4. Relative expression of mRNA for pentose phosphate pathway genes in 13S and 12S expressing A549 cells.	66
Figure 2.5. Relative expression of mRNA for tricarboxylic acid cycle genes in 13S and 12S expressing A549 cells.	68
Figure 2.6. Relative expression of mRNA for cellular respiration genes in 13S and 12S expressing A549 cells.	70
Figure 2.7. RNAseq analysis of metabolic genes from IMR-90 lung fibroblasts infected with either dl520, pm975 or an E1A-deleted HAdV-5 control virus.	73
Figure 3.1. Genes differentially expressed between HPV-positive (HPV+) head and neck squamous cell carcinomas (HNSCC), HPV-negative (HPV-) HNSCC, and normal control tissues by metabolic pathway.....	86
Figure 3.2. Low expression of SDHC is associated with favorable survival outcomes in HPV+ HNSCC.	88
Figure 3.3. Low expression of three mitochondrial respiration complex IV genes in HPV+ HNSCC is associated with improved survival.....	91

Figure 3.4. Low expression of ELOVL6, GOT2 and SLC16A2 is associated with improved patient survival in HPV+ HNSCC.....	94
Figure 3.5. HPV+ HNSCC patient survival stratified by double low or double high expression of survival-associated metabolic genes.....	98
Figure 3.6. Correlation plots of independently significant genes identified by multivariate analysis.....	99
Figure 3.7. Tyrosine kinase inhibitor activity in 27 HNSCC cell lines based on HPV status.	103
Figure 4.1. Venn diagram of differentially regulated glycolysis-related genes in GC. ...	112
Figure 4.2 Expression of two transcripts that encode glycolytic enzymes were associated with EBVaGC patient survival outcomes.	114
Figure 4.3. Venn diagram of differentially regulated TCA cycle-related genes in GC. For each GC subtype, gene expression was compared to non-cancerous tissue.	116
Figure 4.4. Venn diagrams of differentially regulated cellular respiration complex genes in GC.....	122
Figure 4.5. Five-year survival outcomes dichotomized by median expression of the cellular respiration complex I component encoding transcript NDUFA4L2.....	123
Figure 4.6. Venn diagrams of differentially regulated fatty acid synthesis-related genes, and beta-oxidation-related genes in GC.....	125
Figure 4.7. Two transcripts that encode fatty acid synthesis enzymes were associated with EBVaGC patient survival outcomes.	126
Figure 4.8. Venn diagram of differentially regulated glutaminolysis-related genes in GC.	128
Figure 4.9. Venn diagram of differentially regulated pentose phosphate pathway-related genes in GC.....	130
Figure 4.10. Five-year survival outcomes dichotomized by median expression of the pentose phosphate pathway enzyme-encoding transcript RPE.....	131
Figure 4.11. Five-year survival outcomes dichotomized by median expression of the monocarboxylate transporter encoding transcript SLC16A13.	133
Figure 4.12. Venn diagram of differentially regulated monocarboxylic acid transport-related genes in GC.....	134
Figure 5.1. Regulation of MYC by DNA tumour virus oncoproteins.	150

Figure 5.2. Regulation of p53 by DNA tumour virus oncoproteins.152
Figure 5.3. Regulation of pRb/E2F by DNA tumour virus oncoproteins.154

List of Abbreviations

α -TOS	α -tocopheryl succinate
ACAA	Acetyl-CoA acyltransferases
ACACB	Acetyl-CoA carboxylase beta
ACAD	Acyl-CoA dehydrogenase family
ACADL	Acyl-CoA dehydrogenase long chain
ACADM	Acyl-CoA dehydrogenase medium chain
ACADSB	Acyl-CoA dehydrogenase short/branched chain
ACADVL	Acyl-CoA dehydrogenase very long chain
ACAT	Acetyl-CoA acetyltransferase
ACLY	ATP citrate lyase
ACO	Aconitase
ACSS	Acyl-CoA synthetase short chain family member
ACTB	Actin beta
ADP	Adenosine diphosphate
AKR1C3	Aldo-keto reductase family 1 member C3
AKT	RAC-alpha serine/threonine-protein kinase
ALDOB	Aldolase, fructose-bisphosphate B
ALDOC	Aldolase, fructose-bisphosphate C
ALG6	Alpha-1,3-glucosyltransferase
ANOVA	Analysis of variance
ATF	Activating transcription factor
ATP	Adenosine triphosphate
A549	Lung epithelial carcinoma cell line
BART	BamHI-A region rightward transcript (in Epstein-Barr virus)
BCKDHA	Branched chain keto acid dehydrogenase E1 subunit alpha
BFRF1	Nuclear egress protein 2 (in Epstein-Barr virus)
BFRF2	Tegument protein (in Epstein-Barr virus)
BHRF1	BamHI fragment H rightward open reading frame 1 (in Epstein-Barr virus)
BLAST	Basic local alignment search tool

BRLF1	Replication and transcription activator (in Epstein-Barr virus)
BZLF1	Trans-activator protein BZLF1 (in Epstein-Barr virus)
Caco-2	Primary hepatocyte cells
CAD	Carbamoyl phosphate synthetase-aspartate transcarbamylase-dihydroorotase
cDNA	Complimentary DNA
ChIP-qPCR	Chromatin immunoprecipitation quantitative polymerase chain reaction
CIN	Chromosomal instability
CMV	Cytomegalovirus
COA	Coenzyme A
COX6A1	Cytochrome C oxidase subunit 6A1
COX6A2	Cytochrome C oxidase subunit 6A2
COX7A1	Cytochrome C oxidase subunit 7A1
COX15	Cytochrome C oxidase assembly homolog COX15
COX16	Cytochrome C oxidase assembly factor COX16
COX17	Cytochrome C oxidase copper chaperone COX17
COX18	Cytochrome C oxidase assembly factor COX18
COX20	Cytochrome C oxidase assembly factor COX20
CREB	cAMP response element binding protein
CR3	Conserved region 3
CS	Citrate synthase
CT	Critical threshold
CYP11A1	Cytochrome P450 family 11 subfamily A member 1
D-PBS	Dulbecco's phosphate-buffered saline
DMEM	Dulbecco's modified eagle media
DNA	Deoxyribonucleic acid
DP-1	Transcription factor Dp-1
dsDNA	Double-stranded deoxyribonucleic acid
dsRNA	Double-stranded ribonucleic acid
EBER	EBV-encoded noncoding RNAs

EBNA1	Epstein-Barr nuclear antigen 1
EBNA2	Epstein-Barr nuclear antigen 2
EBNA3	Epstein-Barr nuclear antigen 3
EBNALP	Epstein-Barr nuclear antigen leader protein
EBV	Epstein-Barr virus
EBV+	Epstein-Barr virus-positive
EBV-	Epstein-Barr virus-negative
EBVaGC	Epstein-Barr virus-associated gastric cancer
ECAR	Extracellular acidification rate
ECI	Enoyl-CoA delta isomerase
EGF	Epidermal growth factor
ELO	Fatty acid elongase
ELOVL	Elongation of very long chain fatty acids
EnAd	Enadenotucirev
ENO	Enolase
ERK	Extracellular signal-regulated kinases
EV	Empty vector
E1	Early region 1 (in human papillomavirus)
E1A	Early region 1A (in human adenovirus)
E1B	Early region 1B (in human adenovirus)
E2	Early region 2 (in human papillomavirus)
E2A	Early region 2A (in human adenovirus)
E2B	Early region 2B (in human adenovirus)
E2F	Retinoblastoma-associated protein
E3	Early region 3 (in human adenovirus)
E4	Early region 4 (in human adenovirus)
E4	Early region 4 (in human papillomavirus, commonly a E1 ^{E4} fusion protein)
E4ORF1	Early region 4, open reading frame 1 (in human adenovirus)
E4ORF3	Early region 4, open reading frame 3 (in human adenovirus)
E4ORF4	Early region 4, open reading frame 4 (in human adenovirus)

E4ORF6	Early region 4, open reading frame 6 (in human adenovirus)
E5	Early region 5 (in human papillomavirus)
E6	Early region 6 (in human papillomavirus)
E7	Early region 7 (in human papillomavirus)
E8	Early region 8 (in human papillomavirus; commonly an E8 ^{E2} fusion protein)
FA	Fatty acid
FASN	Fatty acid synthase
FCCP	carbonyl cyanide-4-(trifluoromethoxy)phenylhydrazine
FDR	False discovery rate
FH	Fumarate hydratase
GAPDH	Glyceraldehyde 3-phosphate dehydrogenase
GC	Gastric cancer
GCK	Glucokinase
GDP	Guanosine diphosphate
GK	Glycerol kinase
GlcNAc	N-acetylglucosamine
GLOBOCAN	Global cancer observatory
GLS	Glutaminase
GLUT	Glucose transporter
GO	Gene ontology
GOT	Glutamic-oxaloacetic transaminase
GPI	Glucose-6-phosphate isomerase
GPT	Glutamic--Pyruvic Transaminase
GS	Genomically stable
G6PD	Glucose-6-phosphate dehydrogenase
HADH	Hydroxyacyl-CoA dehydrogenase
HADHA	Hydroxyacyl-CoA dehydrogenase trifunctional multienzyme complex subunit alpha
HADHB	Hydroxyacyl-CoA dehydrogenase trifunctional multienzyme complex subunit beta

HAdV	Human adenovirus
HEK	Human embryonic kidney cells
HeLa	Henrietta Lacks cells
HK	Hexokinase
HLA-DPA1	Major histocompatibility complex, class II, DP alpha 1
HLA-DPB1	Major histocompatibility complex, class II, DP beta 1
HNSC	Head and neck squamous cell carcinoma
HNSCC	Head and neck squamous cell carcinoma
hpi	Hours post infection
HPV	Human papillomavirus
HPV+	Human papillomavirus-positive
HPV-	Human papillomavirus-negative
HS68	Primary human foreskin fibroblast cells
H2AFY	H2A histone family, member Y
H3K9	Lysine residue 9 of histone H3
IDH	Isocitrate dehydrogenase
IDH3A	Isocitrate dehydrogenase (NAD(+)) 3 non-catalytic subunit alpha
IDH3B	Isocitrate dehydrogenase (NAD(+)) 3 non-catalytic subunit beta
IDH3G	Isocitrate dehydrogenase (NAD(+)) 3 non-catalytic subunit gamma
IMR-90	Normal lung fibroblast cell line
IVa2	Adenovirus protein IVa2
JNK	Mitogen-activated protein kinase 8
kb	kilobases
LC-MS	Liquid chromatography-mass spectrometry
LC-MS/MS	Liquid chromatography-tandem mass spectrometry
LDHA	Lactate dehydrogenase A
LDHB	Lactate dehydrogenase B
LMP1	Latent membrane protein 1 (in Epstein-Barr virus)
LMP2A	Latent membrane protein 2A (in Epstein-Barr virus)
LY6K	Lymphocyte antigen 6 family member K
L1	Late region 1 (in human adenovirus)

L1	Late region 1 (in human papillomavirus)
L2	Late region 2 (in human papillomavirus)
L5	Late region 5 (in human adenovirus)
MAPK	Mitogen-activated protein kinase
MCF10A	Mammary epithelial cell line
MCT	Monocarboxylic acid transporter
MDH	Malate dehydrogenase
ME	Malic enzyme
MHC-II	Major histocompatibility complex class II
miRNA	microRNA
MIZ	Myc-interacting zinc finger protein
mRNA	Messenger RNA
MSI	Microsatellite instable
MYC	MYC proto-oncogene, BHLH transcription factor
N stage	Nearby lymph nodes
NAD	Nicotinamide adenine dinucleotide
NADPH	Nicotinamide adenine dinucleotide phosphate
NDUFA4L2	NDUFA4 mitochondrial complex associated like 2
NDUFB9	NADH:Ubiquinone oxidoreductase subunit B9
NDUFS2	NADH:Ubiquinone oxidoreductase core subunit S2
NDUFV2	NADH:Ubiquinone oxidoreductase core subunit V2
Nf- κ B	Nuclear factor kappa B subunit 1
NHBE	Normal human bronchial epithelial cells
NK	Natural killer
NRF2	Nuclear factor, erythroid 2 like 2
NuA4	A multicomponent histone acetyltransferase complex
OCR	Oxygen consumption rate
OGDH	Oxoglutarate dehydrogenase
ORF	Open reading frame
PAK	p21-activated protein kinase
PANTHER	Protein analysis through evolutionary relationships

PDH	Pyruvate dehydrogenase
PDHB	Pyruvate dehydrogenase E1 subunit beta
PDHX	Pyruvate dehydrogenase complex component x
PDK4	Pyruvate dehydrogenase kinase 4
PDP	Pyruvate dehydrogenase phosphatase
PDZ	Post synaptic density protein, drosophila disc large tumor suppressor, zonula occludens-1 protein structural domain
PFKFB2	6-phosphofructo-2-kinase/Fructose-2,6-biphosphatase 2
PFKFB3	6-Phosphofructo-2-kinase/Fructose-2,6-biphosphatase 3
PFKFB4	6-Phosphofructo-2-kinase/Fructose-2,6-biphosphatase 4
PFKL	Phosphofructokinase, liver
PFKM	Phosphofructokinase, muscle
PFKP	Phosphofructokinase, platelet
PGAM	Phosphoglycerate mutase
PGD	Phosphogluconate dehydrogenase
PGK	Phosphoglycerate kinase
PGM	Phosphoglucomutase
pIX	Adenovirus protein IX
PI3K	Phosphatidylinositol 3-kinase
PKM	Pyruvate kinase M1/2
PLPP3	Phospholipid phosphatase 3
PPP	Pentose phosphate pathway
pRb	RB Transcriptional corepressor 1
PRPS2	Phosphoribosyl pyrophosphate synthetase 2
p300	E1A binding protein P300
p38	Mitogen-activated protein kinase 14
p53	Tumor protein P53
qPCR	Quantitative polymerase chain reaction
RAS	Rat sarcoma viral oncogene homolog
RdRP	RNA-dependent RNA polymerase
Resp	Respiratory

RNA	Ribonucleic acid
RNAseq	RNA sequencing
ROS	Reactive oxidative species
RPE	Ribulose-5-phosphate-3-epimerase
RPEL1	Ribulose-5-phosphate-3-epimerase like 1
RPIA	Ribose 5-phosphate isomerase A
RSEM	RNA-sequencing by expectation maximization
RQ	Relative quantity
RT	Reverse transcriptase
SARS-CoV-2	Severe acute respiratory syndrome coronavirus 2
SCD	Stearoyl-CoA desaturase
SCO2	Synthesis of cytochrome C oxidase 2
SDH	Succinate dehydrogenase
SDHC	Succinate dehydrogenase complex subunit C
SEM	Standard error of the mean
shRNA	Short hairpin RNA
SKOV3	Ovarian carcinoma cell line
SLC1A5	Solute carrier family 1 member 5
SLC2A3	Solute carrier family 2 member 3
SLC7A5	Solute carrier family 7 member 5
SLC16A2	Solute carrier family 16 member 2
SLC16A7	Solute carrier family 16 member 7
SLC16A8	Solute carrier family 16 member 8
SLC16A9	Solute carrier family 16 member 9
SLC16A11	Solute carrier family 16 member 11
SLC16A13	Solute carrier family 16 member 13
SLC16A14	Solute carrier family 16 member 14
ssDNA	Single-stranded deoxyribonucleic acid
ssRNA(+)	Single-stranded ribonucleic acid, positive sense
ssRNA(-)	Single-stranded ribonucleic acid, negative sense
STAD	Stomach adenocarcinoma

SUCLA2	Succinate-CoA ligase ADP-forming subunit beta
SUCLG1	Succinate-CoA ligase GDP/ADP-forming subunit alpha
SUCLG2	Succinate-CoA ligase GDP-forming subunit beta
T stage	Size and extent of tumour
TALDO	Transaldolase
TCA	Tricarboxylic acid
TCGA	The cancer genome atlas
TIGAR	TP53 induced glycolysis regulatory phosphatase
TKI	Tyrosine kinase inhibitor
TKT	Transketolase
TPI	Triosephosphate isomerase
TRIB1	Tribbles pseudokinase 1
tRNA	Transfer RNA
TRRAP	Transformation/transcription domain associated protein
T3	Triiodothyronine
T4	Thyroxine
UDP	Uridine diphosphate
UQCRB	Ubiquinol-cytochrome C reductase binding protein
UQCRC2	Ubiquinol-cytochrome C reductase core protein 2
UQCRH	Ubiquinol-cytochrome C reductase hinge protein
UQCRQ	Ubiquinol-cytochrome C reductase complex III subunit VII
UQCR10	Ubiquinol-cytochrome C reductase, complex III subunit X
UQCR11	Ubiquinol-cytochrome C reductase, complex III subunit XI
XF	Extracellular flux
1G3	Human amniocyte-derived cell line
2-DG	2-deoxyglucose
6PGL	6-phosphogluconolactonase

Chapter 1

1 Introduction

1.1 Virus Structure and Classification

Viruses are obligate intracellular parasites that employ a variety of strategies and genotypic structures in order to replicate successfully in the infected host cell. In general, viruses have a genome that is comprised of either deoxyribonucleic acid (DNA) or ribonucleic acid (RNA). These molecules differ in their sugar backbone, with RNA containing ribose and DNA containing deoxyribose, which has one less oxygen molecule in its structure. The four main DNA nucleotides are adenine and guanine, which are purines; thymine and cytosine, which are both pyrimidines. RNA utilizes the nucleotide uracil rather than thymine. These four nucleotides encode the genetic instructions for the proteins that a living cell utilizes to carry out its key functions for life. Each set of three nucleotides, called a codon, corresponds to the code for one amino acid. This leads to the central dogma of molecular biology (Crick, 1970), in which the flow of information is through DNA to protein. That is, the DNA within the nucleus of the cell contains the information required to build all of the proteins or other functional elements, such as microRNAs, within a cell. However, in order for these proteins to be produced, the DNA code must be first transcribed to messenger-RNA (mRNA), strands of which can then exit the nucleus and be translated to proteins within the cytosol. Translation involves the shuttling of amino acids by transfer-RNA (tRNA) that can read the mRNA sequence loaded onto a ribosome. Ribosomes are complexes in which proteins are constructed within a cell, and ensure that the amino acids are placed in the correct order to build a functional protein. Within a cell, it is typically considered impossible for the flow of biological information to occur in the reverse order, which is from protein to RNA and back to DNA. However, viruses can be interesting exceptions to these rules (Baltimore, 1970; Temin and Mizutami, 1970).

In order to understand how viruses can circumvent the central dogma, one must appreciate the different classes of viruses that exist. The standard viral classification system is called the Baltimore Classification (Baltimore, 1971), after the scientist who devised the system in 1971, David Baltimore. There are seven classes or groups of viruses. Group I are the

double stranded DNA viruses (dsDNA), that replicate in a manner that is more or less consistent with the central dogma. The viral genome of dsDNA viruses replicates and is transcribed within the nucleus of the host cell, typically utilizing its replication machinery, such as polymerases. The transcribed viral mRNA is then translated in the cytosol of the host cell. However, there are exceptions to this, such as poxvirus, which can replicate entirely in the cytoplasm as it encodes its own polymerase in its large linear genome, which can range from 130 to 230 kb (Moss, 2013). Group II are the single-stranded DNA (ssDNA) viruses. Although these viruses are packaged within the viral virion as single strands (Hayashi et al., 1963), they quickly form double stranded intermediates for genome replication and transcription within the host cell nucleus. ssDNA viruses can have a negative or positive genome polarity and therefore can be further classified as ssDNA(-) or ssDNA(+) viruses. In some cases the replicated ssDNA virus can have its genome oriented in either polarity in which case these viruses can be subclassified as ssDNA(+/-). Group III are double-stranded RNA viruses (dsRNA) and are capable of replicating entirely within the cytoplasm of the infected host cell. Group IV are positive-sense single-stranded RNA (ssRNA(+)) viruses. These viruses can be immediately translated in the cytoplasm, rendering them very efficient. Group V viruses are negative-sense single-stranded RNA (ssRNA(-)) viruses. The negative-sense RNA genome of these viruses must first be replicated into positive-sense RNA, which requires a virally encoded protein, RNA-dependent RNA polymerase (RdRP). Group VI viruses are ssRNA(+) RNA viruses that encode a reverse transcriptase protein capable of generating a double stranded DNA molecule (ssRNA(+)-RT), a direct contradiction of the central dogma of molecule biology. This viral dsDNA genome can become integrated into the host-genome rendering these viruses especially difficult to remove from the infected cell. The final Baltimore classification is Group VII viruses. These viruses are dsDNA viruses that encode a viral reverse transcriptase and have an RNA step in their cycle of viral replication.

Viral genomes are packaged within protective protein structures known as capsids. These structures are repetitive, giving virions a highly organized geometric pattern (Roos et al., 2007). Some, but not all viruses, are further packaged within a lipid bilayer known as the viral envelope which provides further protection to the virus (Perlmutter and Hagan, 2015). Nearly all of these components that comprise the virus structure, from nucleic acids to

proteins and lipids must be derived from the metabolites in the infected host cell (Goodwin et al., 2015). To force the host cell to produce these metabolites, many viruses encode proteins that function as molecular hubs, which means they are capable of altering the function of many proteins within the host cell (Brito and Pinney, 2017; Pelka et al., 2008; Rozenblatt-Rosen et al., 2012; Zheng et al., 2014). Some of these target proteins are integral in the functioning of metabolic processes. Therefore, by altering the function of these metabolism-related proteins, viruses can direct the cell to produce metabolites in certain quantities and at certain stages during infection to benefit the viral replication process. Interestingly, this virally induced increase in the activity of host cell metabolic processes is typically accompanied by other changes in the host cell that may resemble cell replication. Virally induced changes to host cell metabolism and growth processes typically serve to aid the processes of viral replication, typically leading to the release of replicated virus by cell lysis or via a continuous productive infection that releases viral progeny without cell lysis. However, in rare occasions these viral replication processes malfunction in the host cell leading to uncontrolled cell growth and replication (Gaglia and Munger, 2018). It is these abnormal infections that can lead to a variety of cancers (Chang et al., 2017).

1.2 The Essentials of DNA Tumour Viruses

While viruses from a variety of Baltimore classifications may be associated with cancer, a large number of Group I viruses, the dsDNA viruses, are capable of causing cancer in a small percentage of infections. The three dsDNA tumour viruses that will be discussed in this thesis are human adenovirus (HAdV), human papillomavirus (HPV), and Epstein-Barr virus (EBV). These three viruses vary drastically in the size of their genomes, with HPV genomes being the smallest at approximately 8 kilobases, followed by HAdV genomes at 36 kilobases, and EBV genomes at approximately 170 kilobases. In addition, the genome structure of these three viruses vary. HPV has a circular genome (Crawford, 1965; Klug and Finch, 1965), while both HAdV (Green et al., 1967) and EBV (Schulte-Holthausen and Hausen, 1970) have linear genomes. However, in the context of oncogenesis, which will be discussed in specific detail for each virus below, these viruses can potentially induce cellular oncogenesis in a similar manner. Usually, a sequence of the DNA tumour virus

becomes stably expressed in the host cell either through an integration event into the host-cell genome during viral genome replication, or as a distinct episome that lingers in the host-cell (Choo et al., 1987; Delecluse et al., 1993; Matsukura et al., 1989). This is associated with immune evasion that allows the foreign DNA to remain within the cell (Mahr and Gooding, 1999; Rensing et al., 2015; Tindle, 2002). Abnormal expression of one or more virally encoded hub proteins leads to uncontrollable activation of host cell metabolic, growth and replication processes leading to the development of cancer. The physical attributes of each virus are found in Table 1.1.

1.3 Discovery of Human Adenovirus, Human Papillomavirus and Epstein-Barr Virus

HAdV was discovered in 1953 by Wallace Rowe and his collaborators from human adenoid tissue, hence the name adenovirus (Rowe et al., 1953). However, the tissue tropism of HAdV is quite varied, and has been found in tissues ranging from gastrointestinal tissue, respiratory tissue, ocular tissue, kidney tissue, and urethral tissue (Lion, 2014). The diseases caused by HAdV vary, depending on the infected tissue type and HAdV type, of which there are, by some counts, over 90 (Zhang and Huang, 2019). Although HAdV has not yet been conclusively shown to be associated with human cancers, HAdV is capable of robustly transforming rodent cells, and for this reason was the first recognized DNA tumour virus (Trentin et al., 1962).

HPV was first discovered to be an etiological agent of human cervical cancer by Dr. Harald zur Hausen and colleagues in 1983 (Durst et al., 1983). Dr. zur Hausen would go on to win the Nobel Prize in Physiology or Medicine for this discovery in 2008. In 2003, HPV was recognized to be the etiological agent for certain head and neck cancers by the International Agency for Research on Cancer (Herrero et al., 2003).

EBV is an ubiquitous virus, and over 90% of the world's population is infected by this virus, which predominantly infects B cells (Faulkner et al., 2000). EBV was discovered in 1964 by the team of Michael Anthony Epstein and Yvonne Barr, the individuals from

Table 1.1. Characteristics of DNA tumour viruses discussed in this thesis.

Virus	Genome Size (Approx.)	Genome Organization	Enveloped (Yes/No)	Capsid Geometry and Complexity	Oncogenic to Humans (Yes/No)	Integrated or Episomal in Associated Cancers
HAdV	36 kb	Linear	No	Icosahedral (pseudo T=25)	No	N/A
HPV	8 kb	Circular	No	Icosahedral (T=7)	Yes	Integrated
EBV	170 kb	Linear	Yes	Icosahedral (T=16)	Yes	Episome

which the virus obtained its name, when they observed EBV particles in cells derived from a B cell cancer, Burkitt lymphoma (Epstein et al., 1964). EBV was also the first virus discovered to cause human cancers (Ko, 2015).

1.4 Overview of Human Adenovirus Proteins

HAdVs are non-enveloped, linear double-stranded DNA tumour viruses with a genome of approximately 36 kilobase pairs. There are approximately 90 specific types distributed across 7 species, termed A through G, based on genetic and biological characteristics (Table 1.2). HAdVs exhibit a variety of tissue tropisms, often dependent on HAdV type, including preference for respiratory, gastrointestinal, ocular, or renal tissues (Lenaerts et al., 2008; Lion, 2014). HAdVs generally cause acute, lytic infections with a replicative cycle of typically several days between exposure and production of new viruses in quiescent epithelial cells. In one round of infection, a single infectious virion leads to the production of thousands of infectious progeny. Viral replication requires the substrates and energy provided by the host cell, and an optimized environment within the virus infected cell ensures maximal HAdV progeny production. HAdV proteins interact with host-cell proteins to modify cellular functions, creating amenable conditions for virus replication and virion production regardless of any pre-existing cell state.

The adenovirus genome is organized into early and late regions, corresponding to the temporal kinetics of transcription of these regions (Nash and Parks, 2017). The early region consists of multiple transcription units, termed E1A, E1B, E2A, E2B, E3 and E4 (Lenaerts et al., 2008). The products of the E1A transcription unit function to control transcription of viral genes, as well as modify host-cell gene expression to benefit viral reproduction (Pelka et al., 2008). The E1B products modulate host-cell proliferation, apoptosis and assist with viral replication (Nash and Parks, 2017). The products from the E2 transcription units are primarily involved in viral DNA replication (Nash and Parks, 2017). The E3 transcription unit encodes viral proteins that subvert host immune responses (Nash and Parks, 2017). The E4 transcription unit is comprised of 7 open reading frames (ORFs), the products of which act to modulate cellular function and assist with viral DNA replication and RNA

Table 1.2. Different HAdV species and associated types, tissue tropisms and clinically associated infections. The last column indicates whether the species contains the metabolism-associated E4ORF1 viral gene.

Species	Types	Tissue Tropism (Types)	Associated Infections	Contains E4ORF1 (Y/N)
A	12, 18, 31, 61	Gastrointestinal	Gastroenteritis	Yes
B	3, 7, 11, 14, 16, 21, 34, 35, 50, 55, 66, 68, 72, 79	Respiratory (3, 7, 16, 21, 50) Urinary/Renal (11, 14, 34, 35) Ocular (3, 7, 11, 14)	Acute respiratory disease, conjunctivitis, nephritis	Yes
C	1, 2, 5, 6, 57	Respiratory, Ocular (5)	Acute respiratory disease, conjunctivitis	Yes
D	8-10, 13, 15, 17, 19, 20, 22-30, 32, 33, 36-39, 42-49, 51, 53, 54, 56, 58-60, 62-65, 67, 69, 70, 71, 73-75, 81, 83-85, 90	Ocular, Gastrointestinal (36, 37)	Follicular conjunctivitis, pharyngeal conjunctival fever, epidemic keratoconjunctivitis, gastroenteritis	Yes
E	4	Respiratory, Ocular	Acute respiratory disease, conjunctivitis	Yes
F	40, 41	Gastrointestinal	Gastroenteritis	No
G	52	Gastrointestinal	Gastroenteritis	Yes
Unclassified/No record	76-78, 80, 82, 86-89	-	-	-

processing (Weitzman, 2005). There is a single late transcription unit that is alternatively spliced to yield five groups of mRNAs termed L1 through L5. Late mRNAs encode products that are viral structural proteins or contribute to virion production (Nash and Parks, 2017). Other transcription units expressed during intermediate timepoints of infection, such as pIX and IVa2, perform structural functions or play a role in viral packaging (Nash and Parks, 2017). In addition, some of the viral proteins are oncoproteins capable of inducing cancer-like phenotypes. For example, the HAdV E1A oncoprotein is capable of transforming many cell types (Whyte et al., 1988a) in conjunction with a second oncoprotein, such as RAS, or the HAdV E1B oncoproteins. E4ORF1, another HAdV protein (Javier, 1994), can influence host-cell metabolism.

1.5 Human Adenovirus Reprogramming of Host-cell Metabolism

1.5.1. The Earliest Observations of Metabolic Changes due to HAdV Infection

Shortly after adenoviruses were discovered in 1953 by Wallace Rowe and colleagues (Rowe et al., 1953), the effects of HAdV infection on metabolism were explored in cell culture (Figure 1.1). During these early investigations, similarities in metabolic reprogramming between HAdV types were recognized (Fisher and Ginsberg, 1957; Levy et al., 1957; Rozee et al., 1957). For example, HAdV species B type 7 (HAdVB-7) (Table 1.2) infection of HeLa cells (Table 1.3) was noted to exhibit increased lactic acid production, likely due to an increase in glucose utilization, when compared to uninfected HeLa cells (Rozee et al., 1957). This increased lactic acid production corresponded to a 2-fold increase in lactate dehydrogenase activity in infected cells (Rozee et al., 1957). In addition, the tricarboxylic acid (TCA) cycle was necessary for HAdVB-7 replication, as inhibition of this pathway with sodium fluoroacetate decreased viral titre by 300× (Rozee et al., 1957), serving as a precursor to the subsequent recognition of the importance of glutamine and glutaminolysis for viral replication (Thai et al., 2014, 2015).

The upregulation of nucleotide biosynthesis by HAdV infection was also discovered in the early years of HAdV research. In 1964, HAdV species C type 5 (HAdVC-5) (Table 1.2)

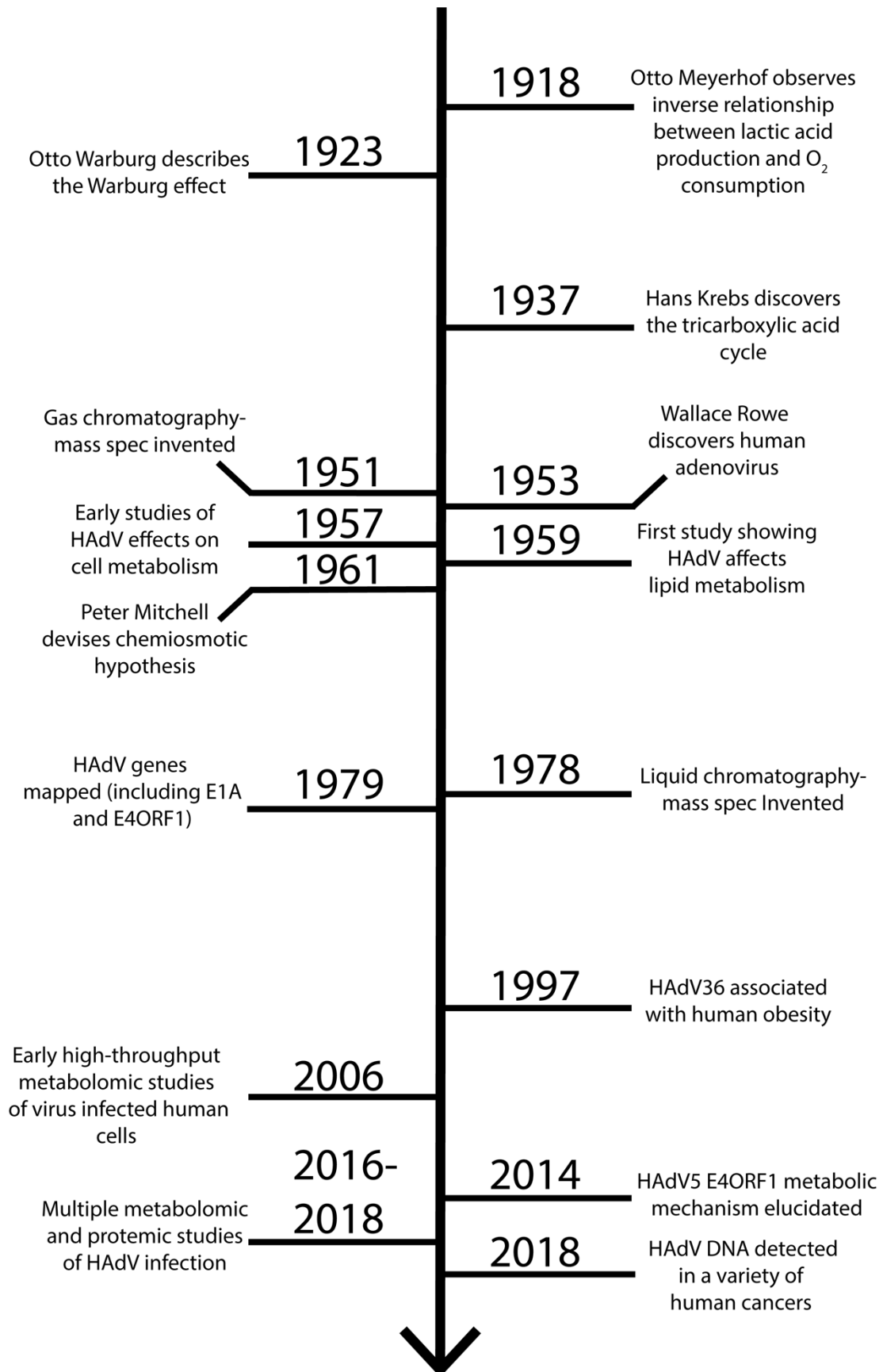


Figure 1.1. Key advances in metabolism research, adenovirus research and technology. These allowed for contemporary high-throughput studies on the effect of HAdV infection on cellular metabolism. The early 20th century featured many insights into the basics of cellular metabolism. The discovery of HAdV and early studies on the effect of HAdV on host-cell metabolism were performed in the 1950s. Little further research on the influence of HAdV on cellular metabolism was performed until the 21st century, when advances in metabolomic, proteomic and genomic technology allowed for thorough study of host-cell metabolic changes.

was found to cause a 2- to 3-fold increase in aspartate transcarbamylase activity at 18 hours post infection (hpi) in HeLa cells (Consigli and Ginsberg, 1964). Aspartate transcarbamylase activity is a function of the first enzyme in the pyrimidine biosynthesis pathway, carbamoyl phosphate synthetase-aspartate transcarbamylase-dihydroorotase (CAD) (Huang and Graves, 2003). In another paper from 1971, increased cellular lipid metabolism, primarily triglyceride production, was associated with HAdVC-5 infection of human embryonic kidney (HEK) cells (Table 1.3) (McIntosh et al., 1971). As expected, these lipids were not incorporated into the HAdVC-5 structure, since HAdV is a non-enveloped virus (McIntosh et al., 1971). As this increase in lipid metabolism could similarly be induced by a UV-inactivated virus, a structural feature of the virus was possibly responsible for the upregulation (McIntosh et al., 1971). Indeed, exposure of the cell to purified HAdV structural proteins indicated that the penton and penton-base proteins, but not the fiber or hexon proteins, were at least partially responsible for this increase in lipid metabolism (McIntosh et al., 1971).

Many years passed between these initial observations and advances in high-throughput metabolomics technology that allowed for the first metabolomics study of virus-infected human cells in 2006 (Munger et al., 2006). Indeed, thorough metabolomic studies of HAdV infected cells began in 2016 (Silva et al., 2016). These metabolomic studies of HAdV infected cells will be discussed in the next section. Important relevant discoveries in metabolism, HAdV virology and high-throughput metabolomics technologies are summarized in the timeline depicted in Figure 1.1.

1.5.2. Metabolomic and Proteomic Analyses of Adenovirus Infection

Since 2016, many high-throughput metabolic studies on HAdV infected cells have been performed. Key studies will be summarized in this section. Recent genomic and proteomic studies of HAdV infected cells in the context of host-cell metabolic changes will also be summarized.

An investigation using $^1\text{H-NMR}$ spectroscopy looked for changes in 35 metabolite concentrations in HEK293 (Table 1.3) and human amniocyte derived 1G3 cells (Table 1.3) during infection with E1-region deleted HAdVC-5 (Silva et al., 2016). Although cells were

Table 1.3. Cell lines used in studies of metabolism in HAdV infected cells. Unless noted otherwise, all cell lines are human.

Cell Line	Donor Characteristics	Date Established	Cell Morphology	Tissue of Origin	Transformation Status
HeLa	Female—31 years old	1951 (Gey et al., 1952)	Epithelial	Cervical adenocarcinoma	HPV transformed
HEK ¹	Fetus	1970 (Mayyasi et al., 1970)	Epithelial	Embryonic kidney	Primary
HEK293	Female—Fetus	1977 (Graham et al., 1977)	Epithelial	Embryonic kidney	HAdV5 E1A transformed
1G3 ²	Fetus	2015 (Silva et al., 2015)	Amniocyte	Amniotic fluid	HAdV5 E1A transformed
IMR-90	Female—Fetus (16 weeks)	1977 (Nichols et al., 1977)	Fibroblast	Lung	Primary
A549	Male—58 years old	1973 (Giard et al., 1973)	Epithelial	Lung adenocarcinoma	Transformed
SKOV3	Female—64 years old	1973 (Fogh and Trempe, 1975)	Epithelial	Ovarian adenocarcinoma ascites	Transformed
MCF10A	Female—36 years old	1990 (Line et al., 1990)	Epithelial	Fibrocystic breast mammary gland	Spontaneously immortalized
NHBE	Human ³	N.A. ³	Epithelial	Bronchial	Primary
3T3-L1	Mouse—Fetus	1973 (Green and Kehinde, 1974)	Fibroblast	Embryonic – pre-adipose	Spontaneously immortalized
BRK	Rat—Neonate	N.A. ³	Epithelial	Kidney	Primary
HS68	Newborn	1969 (Yateman, 1995)	Fibroblast	Foreskin	Primary

¹ Noted to be HeLa contaminated and is not the parent line of HEK293 cells; ² Not to be confused with the mouse-derived hybridoma of the same name; ³ Batch-specific.

infected with an E1-region deleted HAdVC-5, this study essentially measured the effects of wild type HAdVC-5 infection as both HEK293 and 1G3 cells effectively complement the viral defect by expressing the E1A and E1B regions of HAdVC-5. The main finding of this study was that glucose consumption doubles and lactate secretion increases 4-fold compared to respective uninfected cells (Silva et al., 2016).

This study also examined the effects of cell density on metabolic changes induced by HAdVC-5 infections. Lower cell density at infection was associated with better HAdVC-5 production and more extreme metabolic responses (Silva et al., 2016). Interestingly, glutamine exhaustion was limiting for HAdV replication, especially at higher cell densities (Silva et al., 2016). In addition, this study explored whether glutamine replenishment and pH control with cells grown in a bioreactor yielded a similar metabolic phenotype upon HAdVC-5 infection. The results of these experiments suggest that 1G3 cells are less reliant on glutamine during infection (Silva et al., 2016). In short, cellular density at infection had significant effects on metabolism (Silva et al., 2016) (Figure 1.2). While glucose consumption trends were similar in both 1G3 and HEK293 cells, consumption and production of other metabolites (Supplementary Table 1.1) could vary with cell type (Figure 1.2B) and growth phase (Silva et al., 2016) (Figure 1.2C), especially when the slower replication rate of HAdV in primary cells is considered (Crisostomo et al., 2019; Granberg et al., 2006; Miller et al., 2007).

Another study measured the metabolic flux of [1,2-¹³C] glucose and [U-¹³C] glutamine in 1G3 cells infected with E1-deleted HAdVC-5, conditions which again essentially recapitulated a wild type HAdVC-5 infection [46] (Supplementary Table 1.1). In 1G3 cells infected with HAdVC-5 during exponential growth, glycolysis was upregulated by 17%, as evidenced by higher ¹³C incorporation in glycolytic intermediates than TCA cycle intermediates, with a corresponding 4-fold increase in the pentose phosphate pathway (PPP) [46]. Lactate production also increased with glucose production, as observed in other studies (Silva et al., 2016; Thai et al., 2014). Increases in other metabolites, such as amino acids, under these conditions are shown in Supplementary Table 1.1

That study also reported an interesting 2-fold increase in acetyl-CoA production from

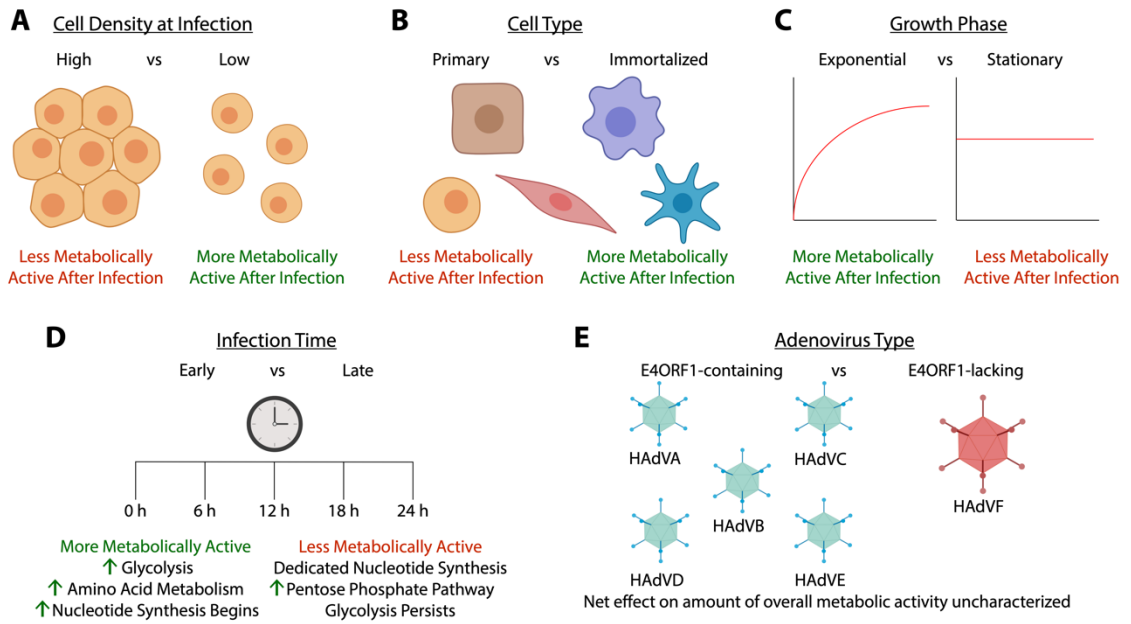


Figure 1.2. Factors influencing host-cell metabolism with HAdV infection. (A) HAdV induced changes in cellular metabolism are less drastic in cells infected at a high cellular density in comparison to cells infected at a low cellular density (Silva et al., 2016). (B) Cell type can influence the metabolic reprogramming enacted by HAdV. Primary cells are usually slower growing than immortalized cells, which is reflected in a lower metabolic rate. Although metabolism is changed across various cell types upon HAdV infection (Silva et al., 2016), the rate of that change is likely faster in immortalized cells and contributes to rapid viral replication in immortalized cells (Crisostomo et al., 2019; Granberg et al., 2006; Miller et al., 2007). However, even among immortalized cells, those with a phenotype more closely resembling the Warburg effect appear primed for HAdV replication and experience more drastic metabolic changes than immortalized cells with a metabolic phenotype reliant on oxidative phosphorylation (Dyer et al., 2018). (C) Growing and dividing cells infected with HAdV show more drastic metabolic changes than infected quiescent cells (Carinhas et al., 2017). (D) The metabolic profile of HAdV infected cells changes throughout the course of infection (Valdés et al., 2018). Initially, HAdV infected cells typically exhibit upregulated glycolysis, amino acid metabolism and nucleotide biosynthesis pathways (Valdés et al., 2018). Towards the later stages of infection, HAdV infected cells still perform glycolysis, but the majority of metabolic activity is directed towards nucleotide biosynthesis and an upregulation of the PPP occurs (Valdés et al., 2018). (E) Different HAdV types regulate metabolism through mechanisms related to the functions of HAdV E4ORF1 proteins. Some HAdV types (e.g., HAdVF-40) do not have E4ORF1 and clearly rely on other HAdV proteins to regulate metabolism (Guissoni et al., 2018). E1A, which also varies among HAdV types, is another potential regulator of cell metabolism during infection (Ferrari et al., 2014; Pelka et al., 2011; Zhao et al., 2017). Created with BioRender.

citrate (Carinhas et al., 2017), a process associated with fatty acid biosynthesis. Increased lipid biosynthesis is a logical requirement for enveloped viruses, and both enveloped and non-enveloped viruses can increase lipid biosynthesis for the expansion of membrane bound viral replication compartments (reviewed in (Chukkapalli et al., 2012; Heaton and Randall, 2011)). However, HAdV replication compartments are located in the nucleus and are not surrounded by a membrane (Hidalgo et al., 2016). This leaves the reasons for the potential increase of lipid biosynthesis during HAdV infection unclear.

While overall metabolic activity was increased in 1G3 cells infected with HAdVC-5 during stationary phase, which was induced by a combination of cell confluency and serum deprivation for 36 hours, these metabolic changes were different compared to 1G3 cells infected during exponential growth (Carinhas et al., 2017). Metabolic changes that occurred in infected stationary 1G3 cells included a 1.5-fold increase in glutamine catabolism (Carinhas et al., 2017), which serves to replenish TCA cycle intermediates when they might be limited due to the conversion of pyruvate to lactate by the Warburg effect (DeBerardinis et al., 2007). A corresponding 1.5-fold increase in the TCA cycle itself also occurred in infected stationary 1G3 cells (Carinhas et al., 2017). Glucose consumption in HAdVC-5-infected stationary 1G3 cells increased, with a corresponding increase in lactate production (Carinhas et al., 2017). Production of specific amino acids also increased (Supplementary Table 1.1) (Carinhas et al., 2017). An increase in acetyl-CoA production from citrate was observed with HAdVC-5 infection of growth arrested 1G3 cells (Carinhas et al., 2017). However, the PPP was not stimulated and overall HAdVC-5 production decreased 4-fold when compared to exponentially growing HAdVC-5-infected 1G3 cells (Carinhas et al., 2017).

The metabolic state of HAdV infected cells also changes longitudinally (Figure 1.4D). A study analyzing changes in cellular protein expression of HAdV species C type 2 (HAdVC-2) (Table 1.2) infected growth-arrested IMR-90 cells (Table 1.3) at 6, 12, 24 and 36 hpi identified a variety of metabolism related proteins with differential expression throughout infection. Early during infection, starting at 6 hours and persisting through to 12 hpi, proteins encoding enzymes involved in glycolysis and *de novo* purine and pyrimidine synthesis were upregulated (Valdés et al., 2018). The upregulation of glycolytic and

nucleotide biosynthesis proteins persisted through to the later 24 and 36 hpi time points (Valdés et al., 2018). Unique to the 6 and 12 hour time points was an upregulation of proteins involved in glutathione metabolism (Valdés et al., 2018) (Supplementary Table 1.2), which is responsible for detoxifying reactive oxidative species, perhaps generated as a result of virus infection (Li et al., 2017). An analysis of upregulated pathways indicated that at the earliest time point (6 hpi) serine glycine biosynthesis (Supplementary Table 1.2), and mannose metabolism (Supplementary Table 1.2) were upregulated (Valdés et al., 2018). The serine glycine biosynthesis pathway converts 3-phosphoglycerate into serine, and eventually glycine (Yang and Vousden, 2016), which could account for some of the increased intracellular amino acid concentrations noted in the two studies mentioned above (Carinhas et al., 2017; Thai et al., 2015). Mannose metabolism is responsible for contributing to protein glycosylation (Ichikawa et al., 2014; Sharma et al., 2014). Later, at 12 hpi, proteins involved in fructose galactose metabolism (Supplementary Table 1.2) were upregulated and likely contribute to the upregulated glycolysis occurring at all time points (Valdés et al., 2018). There were also two enzymes from the PPP that were upregulated at 12 hpi (Supplementary Table 1.2). At 24 hpi, most proteins involved in the PPP were upregulated, although the authors did not find any changes in mRNA expression for PPP genes (Valdés et al., 2018). This may be due to changes in expression based on cell type and/or differences in infection timing between these two studies. At 24 hpi, a few proteins involved in serine glycine biosynthesis continued to be upregulated (Supplementary Table 1.2), which could contribute to the production of glycine used for purine biosynthesis (Yang and Vousden, 2016).

In the same study, an analysis of putative transcription factors regulating the expression of metabolic genes during HAdV infection indicated that MYC was significantly upregulated at all time points (Valdés et al., 2018). Another transcription factor potentially responsible for the upregulation of metabolic genes in HAdV infection was E2F1 (Valdés et al., 2018). The ATF/CREB family of transcription factors were also upregulated (Valdés et al., 2018). ATF/CREB transcription factors are responsible for upregulating metabolism (Desvergne et al., 2006) and are also known targets of E1A (Flint and Shenk, 1989; Lee et al., 1996; Liu and Green, 1990). Finally, the transcription factor NRF2, which has metabolism associated regulatory functions (Hayes and Dinkova-Kostova, 2014), was potentially

responsible for the expression of a wide variety of metabolic genes at all time points during HAdV infection (Valdés et al., 2018). The metabolic functions of NRF2 include inhibiting lipogenesis, activating fatty acid oxidation, influencing the PPP, as well as enhancing purine biosynthesis and NADPH production (Hayes and Dinkova-Kostova, 2014).

Another study compared the effects of infection with HAdVC-5, wild-type HAdV species B type 11p (HAdVB-11p) (Table 1.2), and an oncolytic HAdV, enadenotucirev (EnAd, formerly ColoAd1), on metabolism of A549 cells (Table 1.3) and SKOV3 ovarian carcinoma cells (Table 1.3) (Dyer et al., 2018). HAdV infection increased glycolysis and glutaminolysis (Dyer et al., 2018), as expected (Carinhas et al., 2017; Thai et al., 2014, 2015; Valdés et al., 2018). However, counterintuitively, the authors found that inhibiting glycolysis with 2-deoxyglucose (2DG) or limiting glucose availability increased viral genome replication and packaging efficiency in both A549 cells and SKOV3 cells (Dyer et al., 2018). Inhibition of glycolysis in SKOV3 cells, which, unlike A549 cells, exhibit a metabolic phenotype that does not resemble the Warburg effect (Hatzivassiliou et al., 2005), also increased the speed of EnAd and HAdVB-11p viral replication and progeny production (Dyer et al., 2018). Glucose limitation is hypothesized to be beneficial to the expression of late proteins during HAdV infection, which could explain why HAdV progeny production was increased with 2DG (Dyer et al., 2018). These results were maintained when viral replication was measured in SKOV3 cells lacking functional endogenous glycolysis, in primary human ascites cells and an in vivo xenograft mouse model treated with 2DG (Dyer et al., 2018). Furthermore, A549 cells grown in glutamine limiting conditions had a 1×10^5 -fold reduction in the production of infectious EnAd or HAdVB-11p virions (Dyer et al., 2018). These results indicate that glycolysis is expendable, and perhaps even detrimental to viral replication at higher levels. However, HAdV infected cells generally require glutamine, but the extent to which glutamine is required may vary with HAdV type, as HAdVC-5 did not appear to have a similar dependence (Dyer et al., 2018).

When a variety of other TCA cycle intermediates were supplemented to glutamine limited A549 or SKOV3 cells infected with EnAd, only α -ketoglutarate, not oxaloacetate or pyruvate, was able to completely rescue HAdV virion production (Dyer et al., 2018). This

suggests that rather than wholly being used to fuel the TCA cycle, glutamine may also be broken down to α -ketoglutarate, which is used for production of other macromolecules required for viral replication, including amino acids and/or lipids.

An LC-MS proteomic study of A549 cells infected at confluency with HAdV species F type 40 (HAdVF-40) (Table 1.2) and examined at 30 hpi indicated that 206 host-cell proteins were upregulated and 130 host-cell proteins were downregulated by infection (Guissoni et al., 2018). Many of these were involved in metabolism and energy production pathways. Specifically, these included glycolysis, the TCA cycle, cellular respiration, beta-oxidation, the PPP, and amino acid metabolism (Guissoni et al., 2018). Interestingly, the authors observed higher mitochondrial activity in HAdVF-40 infected cells (Guissoni et al., 2018). In addition, two glycolytic proteins upregulated by HAdVC-5 infection, HK2 and PFKM, were not induced in HAdVF-40 infected cells (Guissoni et al., 2018). HAdVF-40 does not encode an E4ORF1 equivalent, which may explain why these two specific glycolytic enzymes are not upregulated by HAdVF-40 infection (Guissoni et al., 2018). This also suggests that, despite E4ORF1 being the only HAdV protein currently implicated in transcriptionally regulating metabolism upon infection, HAdV proteins other than E4ORF1 contribute to transcriptional regulation of host-cell metabolism gene expression (Figure 1.2E).

1.5.3.E4ORF1 Positively Regulates Glycolysis and Glutamine Catabolism

The only concrete mechanism by which adenovirus is currently known to regulate host-cell metabolism is through its E4ORF1 protein (Thai et al., 2014, 2015). E4ORF1 is a viral oncoprotein that can transform rat embryonic fibroblasts through its C-terminal PDZ-binding domain (Chung et al., 2007; Javier, 1994). This PDZ-binding domain binds host-cell PDZ domain proteins and mediates the activation of PI3K and AKT, leading to oncogenic transformation (Chung et al., 2007). However, the ability of E4ORF1 to regulate glycolysis is independent of this C-terminal domain (Thai et al., 2014).

Thai et al observed that MCF10A breast epithelial cells (Table 1.3) infected with wild type HAdVC-5 had increased glucose consumption and increased lactate production compared

to uninfected cells (Thai et al., 2014) (Supplementary Table 1.1). These metabolic changes were accompanied with decreased oxygen consumption and presumably less oxidative phosphorylation compared to uninfected cells (Thai et al., 2014). Thai et al found that cells infected with a non-replicating $\Delta E4$ HAdVC-5 mutant did not have increased glycolysis or decreased oxidative phosphorylation (Thai et al., 2014). When MCF10A cells were engineered to express the adenovirus E4 region alone, glycolysis was increased, as indicated by increased glucose consumption and lactate production (Thai et al., 2014). However, oxidative phosphorylation was not affected, as there was no change in oxygen consumption in these cells (Thai et al., 2014). E4ORF1 was identified to be the viral protein responsible for these metabolic changes, but these changes were enhanced in the presence of E4ORF6, which is known to have a stabilizing effect on E4ORF1 (Thai et al., 2014). Microarray with gene set enrichment analysis (GSEA) in MCF10A cells constitutively expressing E4ORF6 and transfected with either E4ORF1 or an empty vector identified genes regulated by MYC as being particularly upregulated by E4ORF1 (Thai et al., 2014). This MYC upregulation agrees with another high throughput study looking at transcription factors regulated by HAdV infection (Valdés et al., 2018). Chromatin immunoprecipitation quantitative polymerase chain reaction (ChIP-qPCR) analysis indicated that MYC binding to glycolytic genes was increased in E4ORF1 transfected cells and E4ORF1 was also found bound to some glycolytic genes (Thai et al., 2014) (Figure 1.3). E4ORF1 formed a physical interaction with MYC, supported by E4ORF6, and this increased MYC localization to the nucleus (Thai et al., 2014). These changes corresponded to increased *HK2* and *PFKMI* mRNA levels in E4ORF1-expressing cells (Thai et al., 2014). In agreement with this, A549 cells infected with HAdVF-40, which does not contain E4ORF1, do not exhibit elevated levels of HK2 or PFKM protein (Guissoni et al., 2018).

Thai et al identified that E4ORF1 was responsible for regulating metabolic changes, as a point mutation in this viral protein, D68A, abrogated all of the metabolic changes associated with E4ORF1 in both vector transfection and mutant virus infection (Thai et al., 2014). shRNA knockdown of MYC also abrogated the glycolytic metabolic changes

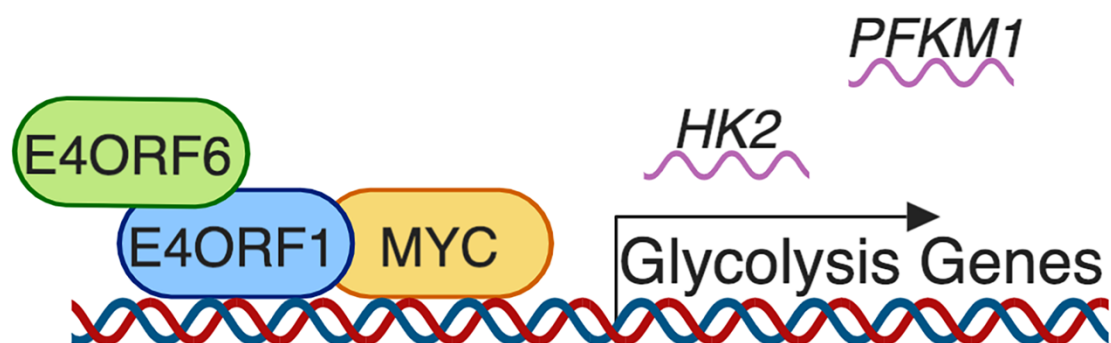


Figure 1.3. Schematic of how E4ORF1 contributes to MYC-regulated transcription of genes involved in glycolysis. E4ORF1 binds to MYC, enhancing the transcriptional activity of MYC, leading to increased transcription of metabolic genes such as HK2 and PFKM1 (Thai et al., 2014). E4ORF1 can also bind glycolytic genes, which may be how E4ORF1 brings MYC into proximity of these target genes. E4ORF6 appears to play a scaffolding role and enhances E4ORF1 binding to MYC, although E4ORF6 does not appear to bind MYC or glycolytic genes itself (Thai et al., 2014). Created with BioRender.

associated with E4ORF1 during HAdV infection (Thai et al., 2014). In addition, MYC knockdown decreased viral titre, providing evidence that metabolic changes do indeed enhance virus yield during infection (Thai et al., 2014). Interestingly, viral titre from cells infected with E4ORF1-D68A mutant HAdVC-5 was only lower in infected HeLa cells, but not in infected MCF10A cells. Thai et al attribute this to the higher glycolytic activity of MCF10A cells (Thai et al., 2014).

Finally, increased nucleotide metabolism is one of the consequences of upregulated glycolysis. Thai et al traced carbon from ^{13}C -labelled glucose to nucleotides during wild type HAdVC-5 infection in normal human bronchial epithelial cells (NHBE) (Table 1.3). Increased ^{13}C incorporation into nucleotides did not occur during infection with HAdVC-5 E4ORF1-D68A (Thai et al., 2014). Correspondingly, transcripts of *RPIA* and *RPE*, two genes involved in the non-oxidative branch of the PPP, were only upregulated in cells infected with wild type HAdVC-5, but not HAdVC-5 E4ORF1-D68A (Thai et al., 2014). This upregulation of the PPP with an increase in glycolysis matches the observations in another high throughput metabolomics study (Carinhas et al., 2017). However, a second high throughput metabolomics study found no changes in mRNA levels for any PPP genes (Valdés et al., 2018).

In a follow-up study, HAdVC-5 infection of NHBE was associated with increased glutamine consumption during early infection (Supplementary Table 1.1), which occurred at approximately 8 to 12 hpi (Thai et al., 2015). This increased consumption was abrogated by shRNA knockdown of MYC, or infection with the non-MYC binding E4ORF1-D68A mutant adenovirus (Thai et al., 2015). miRNAs miR-23a and miR-23b, which are associated with decreased glutaminase expression, were also downregulated starting at 90 minutes post wild type HAdVC-5 infection (Thai et al., 2015). LC-MS/MS U- $^{13}\text{C}_5$ -glutamine labelling indicated that HAdVC-5 infected cells had a pattern of carbon labelling that corresponded to reductive carboxylation (Thai et al., 2015). Reductive carboxylation is the carboxylation of α -ketoglutarate, produced from glutamine, to citrate. This citrate can be used to produce lipids from interconversion to acetyl-CoA or fuel the TCA cycle (Mullen et al., 2012). mRNA transcripts associated with reductive carboxylation were also

upregulated with HAdVC-5 infection (Thai et al., 2015), but not in HAdVC-5 E4ORF1 D68A mutant infections (Thai et al., 2015).

Further emphasizing the importance of glutamine during HAdVC-5 infection, transcripts for glutamine transporter genes *SLC1A5* and *SLC7A5* were higher in HAdVC-5 infected cells (Thai et al., 2015). These transporters exchange glutamine for other amino acids. There were higher intracellular concentrations of both essential and non-essential amino acids in HAdVC-5 infected NHBE cells as compared to uninfected or HAdVC-5 E4ORF1-D68A mutant infected cells (Thai et al., 2015). Increases in intracellular amino acid concentrations (Supplementary Table 1.1) matched what was observed in another high throughput metabolomics study (Carinhas et al., 2017). Concentrations of amino acids likely increase to provide substrates required for virus replication. Another pathway associated with HAdVC-5 infection-induced glutamine metabolism is hexosamine biosynthesis (Thai et al., 2015), which produces UDP-GlcNAc. UDP-GlcNAc can be used for O-GlcNAc protein modification to alter the activity of metabolic enzymes, such as those involved in glycolysis (Hanover et al., 2018). The importance of glutamine for adenovirus replication is also emphasized by the ability of CD-839, an inhibitor of glutaminase, to reduce HAdVC-5 replication at least 80-fold (Thai et al., 2015). However, whether any of these changes in glutamine metabolism are linked to HAdVC-5-infection induced decreases in oxidative phosphorylation remains to be explored.

1.5.4.E1A as a Regulator of Cellular Metabolism During Infection

Although E4ORF1 is the only HAdV protein with conclusive transcriptional effects on cellular metabolism, these studies suggest that at least one other HAdV encoded metabolic regulator exists (Thai et al., 2014). The HAdV oncoprotein E1A has been shown to interact with a wide variety of host-cell proteins that are capable of influencing metabolism independently of an interaction with E1A (King et al., 2018; Nicolay and Dyson, 2013; Pelka et al., 2008; Stine et al., 2015; Zhao et al., 2017). In addition, because E1A is the first HAdV protein expressed during infection, it seems to be ideally positioned to establish early changes in cellular metabolism during HAdV infection.

Perhaps one of the first studies which suggested that E1A could influence cellular energy metabolism was performed in 1990 (Kaddurah-Daouk et al., 1990). Expression of creatine kinase B, an enzyme responsible for maintaining cellular ATP levels (Schlattner et al., 2016), was shown to be induced by E1A (Kaddurah-Daouk et al., 1990). This report represents the first suggestion that E1A may be responsible for inducing a cancer-like metabolic phenotype in human cells during infection. Another paper, published at roughly the same time, indicated that E1A was capable of inducing expression of thymidylate synthase, linking E1A to metabolic changes related to increased DNA synthesis (Zerler et al., 1987).

A thorough metabolomic and transcriptomic study of IMR-90 cells transformed with E1A in conjunction with RAS revealed that glucose consumption and lactate secretion increased, as did glutamine consumption and glutamate secretion with transformation (Supplementary Table 1.1) (Madhu et al., 2015). The authors of this study elected to use E1A and RAS to study transformation as E1A alone only immortalizes, but does not transform, IMR-90 cells (Madhu et al., 2015). This is a caveat for the interpretation of this study towards the role of E1A in HAdV infection, as some of metabolic effects observed may be mediated by RAS rather than E1A. Consumption and secretion of certain carboxylic acids and amino acids increased with transformation, as assayed from the extracellular media (Supplementary Table 1.1) (Madhu et al., 2015). A comparison of intracellular metabolites between E1A/RAS transformed IMR-90 cells versus wild type IMR-90 cells indicated that E1A/RAS transformed IMR-90 cells were much more metabolically active (Madhu et al., 2015). Intracellular glucose and pyruvate levels were lower in E1A/RAS transformed IMR-90 cells, as were concentrations of amino acids (Supplementary Table 1.1) (Madhu et al., 2015). While lower intracellular concentrations of amino acids stand in contrast to what was observed in the context of wild type HAdVC-5 infection by Thai et al (Thai et al., 2015), the increase in extracellular glutamine consumption is consistent with a number of papers examining metabolic changes due to HAdV infection (Silva et al., 2016; Thai et al., 2015). Despite lower intracellular concentrations of amino acids, E1A/RAS transformed IMR-90 cells had increased amino acid consumption (Supplementary Table 1.1) (Madhu et al., 2015). Another indicator that

E1A/RAS transformed IMR-90 cells were more metabolically active than wild type IMR-90 cells was the increase in the phosphocreatine to creatine ratio observed in transformed cells (Madhu et al., 2015). This ratio is a proxy for the cellular ATP/ADP ratio and energy state (Madhu et al., 2015). The higher metabolic activity of E1A/RAS transformed IMR-90 cells was further emphasized by the number of significant internal metabolite correlations within transformed cells (Madhu et al., 2015). There were 72 positive internal correlations and 92 negative internal correlations between the measured intracellular metabolites of E1A/RAS transformed IMR-90 cells, versus 23 positive internal correlations and 26 negative internal correlations in wild type IMR-90 cells (Madhu et al., 2015). The number of internal correlations is indicative of the number of perturbed metabolic pathways (Urbanczyk-Wochniak et al., 2007).

One of the unique correlations among metabolites upregulated in E1A/RAS transformed cells was a positive correlation between the levels of choline, involved in cell membrane structure (Ridgway, 2013), and the levels of the amino acids isoleucine, leucine, phenylalanine, tyrosine and lysine (Madhu et al., 2015). In addition, changes in phosphocholine, another component of cell membrane formation (Ridgway, 2013), was positively correlated with changes in isoleucine, leucine, phenylalanine, tyrosine and lysine (Madhu et al., 2015). It is unclear whether this increase in membrane metabolism components is specific to E1A/RAS transformed cells or is more widely applicable to HAdV infection, even though HAdV is a non-enveloped virus. However, choline consumption was increased in both HAdV infected HEK293 and 1G3 cells as discussed above (Supplementary Table 1.1) (Silva et al., 2016), which may point to an upregulation of cell membrane-component metabolism due to E1A in the context of HAdV infection.

Expression of genes involved in amino acid catabolism in the mitochondria, consistent with amino acid use as a significant energy source, were also upregulated in E1A/RAS transformed IMR-90 cells (Supplementary Table 1.2) (Madhu et al., 2015). Other genes encoding components of amino acid metabolism were similarly upregulated (Supplementary Table 1.2) (Madhu et al., 2015). In addition, genes involved in glucose metabolism were significantly increased in E1A/RAS transformed IMR-90 cells

(Supplementary Table 1.2) (Madhu et al., 2015). Gene correlation analysis within E1A/RAS transformed IMR-90 cells indicated that expression of these amino acid catabolism genes, for example *BCKDHA*, were positively correlated with certain genes involved in the TCA cycle, such as *SUCLG1*, *IDH3B* and certain glycolytic genes, such as *ALDOC* (Madhu et al., 2015). In a number of ways, the phenotype observed with IMR-90 transformation by E1A/RAS follows the traditional definition of the Warburg effect, which is an upregulation of glycolysis and a downregulation of oxidative phosphorylation despite the presence of ample oxygen (Racker, 1972; Warburg, 1925; Warburg et al., 1927). However, the increased consumption and potential utilization of amino acids as an energy source in E1A/RAS transformed IMR-90 cells indicate that oxidative phosphorylation through amino acid catabolism is another important metabolic pathway with nuanced regulation (Madhu et al., 2015). The increase in glycolysis and glutaminolysis occurring from E1A/RAS transformation is very similar to the increase in glycolysis and glutaminolysis attributed to the E4ORF1 protein of HAdV (Thai et al., 2014, 2015). It is an interesting possibility that E1A contributes to cellular metabolic changes during HAdV infection in a manner similar to, but independent of, E4ORF1. If this question were to be examined, one confounding consideration would be that E1A is responsible for inducing transcription of E4ORF1, in addition to its role in modulating expression of many host-cell proteins during infection (King et al., 2018; Nevins, 1981).

The interaction of E1A with host-cell proteins that can influence metabolism is also important when considering the role of E1A in host-cell metabolic reprogramming (Figure 1.4). Like E4ORF1, E1A is capable of influencing MYC activity (Zhao et al., 2017). However, this occurs indirectly via the interaction of E1A with the TRRAP protein of the NuA4 histone acetyltransferase complex, leading to increased transcription of MYC regulated genes (Figure 1.4A) (Zhao et al., 2017). An RNA-seq analysis of HS68 primary human foreskin fibroblast cells (Table 1.3) transduced with the TRRAP interacting region of E1A, indicated that 140 metabolic genes were upregulated, according to the supplementary data from that study (Zhao et al., 2017). An additional 92 metabolic genes were upregulated in conjunction with an interaction of E1A with p300 (Figure 2.6B), again extrapolated from the supplementary data of that paper (Zhao et al., 2017).

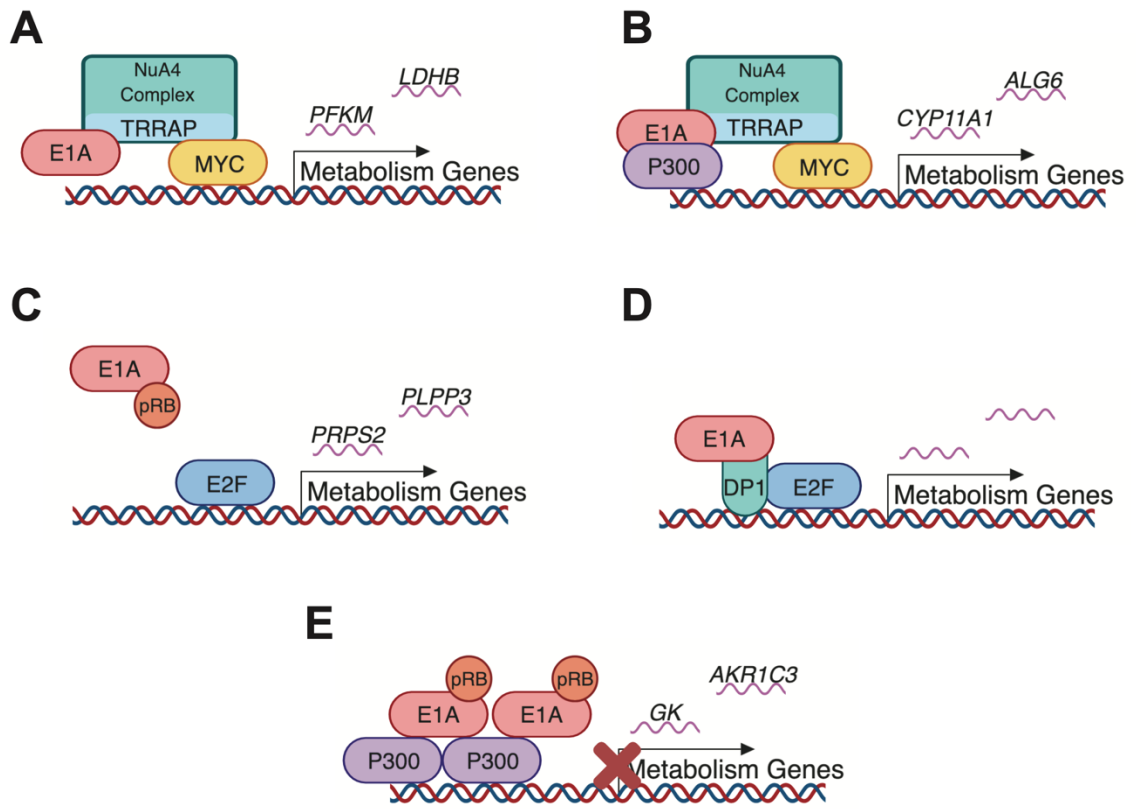


Figure 1.4. Putative mechanisms by which HAdV E1A regulates transcription of host-cell metabolic genes based on models derived from the literature. (A) E1A can regulate metabolic gene expression through an interaction with the transcription factor MYC. E1A binds TRRAP, part of the NuA4 complex, which in turn is bound to MYC leading to increased transcription of metabolic genes (Zhao et al., 2017). PFKM and LDHB are two examples of transcripts that may be regulated due to this interaction based on supplementary data from Zhao et al. (Zhao et al., 2017). (B) The same paper indicated that E1A may be bound to p300 in addition to TRRAP and MYC leading to the expression of other E1A-regulated genes (Zhao et al., 2017). Again, CYP11A1 and ALG6 are two examples of metabolic genes potentially regulated by this interaction based on supplementary data from Zhao et al. (Zhao et al., 2017). (C) E1A can bind to pRB and release the inhibition of E2F-mediated gene transcription by pRB (Ferrari et al., 2014). *PRPS2* and *PLPP3* are examples of two metabolic genes with decreased expression in a HAdVC-5 infection with a non-pRB binding E1A mutant compared to wild type infected cells and therefore could rely on the pRB-binding of E1A for expression during infection (Ferrari et al., 2014). (D) E1A may also mediate the expression of E2F regulated genes through an interaction with DP1, which itself can bind to E2F and activate transcription (Pelka et al., 2011). No specific transcripts are shown, as this study by Pelka et al. did not include an RNA-seq component (Pelka et al., 2011). (E) Finally, an interaction between E1A, p300 and pRB may inhibit transcription of metabolism related genes through histone deacetylation (Ferrari et al., 2014). *GK* and *AKRIC3* are two genes that may be regulated by E1A binding to p300 (Ferrari et al., 2014). Image created with BioRender.

In addition to the targets listed above, E1A can influence the E2F family of transcription factors via its interaction with their negative regulator pRb and pRb family members (Figure 1.4C) (Whyte et al., 1988b), or via a direct interaction with the DP-1 binding partner of the E2Fs (Figure 1.4D) (Pelka et al., 2011). It is well established that E1A sequesters pRb from E2F, leading to E2F activation. A study of transcriptional regulation by E1A indicated that the resulting E2F activation upregulates genes involved with RNA metabolism and biopolymer (macromolecule) metabolism in the host cell (Ferrari et al., 2008). Additionally, E2F1 has been reported to influence oxidative phosphorylation and glycolysis (Nicolay and Dyson, 2013). Another comprehensive RNA-seq study of IMR-90 cells infected with a HAdVC-5 E1A mutant virus deficient for pRB binding, showed an upregulation of one metabolic gene, *TRIB1* (fold-change > 2) and a downregulation of approximately 89 metabolic genes (fold-change < 2) compared to wild type HAdVC-5 infected cells, as extrapolated from the supplementary RNA-seq gene list of that paper (Ferrari et al., 2014). This suggests that pRB binding by E1A likely contributes to the regulation of these genes. This agrees with a high throughput study examining transcription factors potentially altered by HAdV infection, which found that E2F1 activity was increased (Valdés et al., 2018).

Additionally, extrapolation of data from an RNA-seq analysis of IMR-90 cells infected with a HAdVC-5 E1A mutant virus deficient for p300 binding, indicated that 13 metabolic genes were upregulated (fold-change > 2) and 5 metabolic genes were downregulated (fold-change < 2) when compared to wild type HAdVC-5 infected cells (Ferrari et al., 2014). Again, this suggests that the interaction of E1A with p300 (Figure 1.4E) modulates host-cell metabolism during infection. Due to the paucity of studies looking at metabolic effects of HAdV E1A, it seems that additional investigations of this area are clearly warranted. However, the interactions of E1A with MYC, pRB/E2F and p300 are an interesting starting point for understanding how E1A influences host-cell metabolism.

1.6 Human Adenovirus and Cancer

Although HAdV has not been conclusively identified as an etiological agent of human cancers, the presence of HAdV DNA has been identified in some human cancers (Kosulin

et al., 2007, 2013, 2014; Kuwano et al., 1997). However, whether this is at all significant to human oncogenesis is unknown. Despite this, as HAdV robustly transforms rodent cells (Trentin et al., 1962), it was important for elucidating many of the general mechanisms by which DNA tumour viruses transform cells. The main oncoproteins of HAdV are the E1 proteins, E1A and E1B, and some of the E4 proteins (Ip and Dobner, 2019). Interestingly, either E1A or E1B alone are insufficient to transform rodent cells. Both E1A and the E1B-19K and/or E1B-55K proteins are required for a transformation event in rodent cells (Elsen et al., 1983; Gallimore et al., 1986), although E1A alone can immortalize rodent cells (Braithwaite et al., 1983; Houweling et al., 1980). Note that immortalization refers to the ability of a cell to divide indefinitely, but is not necessarily associated with alterations to cell growth and differentiation pathways that are typical of cancerous cells. Transformation refers to a cell that is not only immortalized, but has altered cellular processes that are characteristic of the hallmarks of cancer (Hanahan and Weinberg, 2000). E1A can enact its complex regulation of cellular processes related to growth and division through interactions with host cell molecular hub proteins that can modulate a broad range of host cell functions (King et al., 2018). For this reason E1A itself is termed a viral molecular hub protein (Pelka et al., 2008). E1B is indispensable for transformation in conjunction with E1A because it counteracts the apoptotic pathways activated by E1A, such as the p53 tumour suppressor pathway (Debbas and White, 1993), allowing the transformed cell to proliferate unchecked.

As for the E4 proteins, E4orf1 from species D HAdV has been noted to have oncogenic potential in rodent cells, but this effect of E4orf1 is absent from species A, B or C HAdV (Thomas et al., 1999). PI3K signalling is an important component of how E4orf1 mediates its oncogenicity as E4orf1 contains a PDZ domain that interacts with proteins that in turn influence PI3K (Frese et al., 2003). E4orf3 and E4orf6 can also assist HAdV oncogenic transformation as they can inhibit a variety of tumour suppressor proteins (Nevels et al., 1999a, 2000). As modulation of metabolism is a process that is indispensable to cancer cell growth and proliferation, these HAdV oncoproteins can also influence cellular metabolism. E1A may contribute to the control of cellular metabolism during infection both on a functional level and through altering the expression of mRNA transcripts related to central metabolic pathways. Chapter 2 is an investigation into how E1A may influence cellular

metabolism in a manner that closely resembles the metabolic program typical of cancer cells.

1.7 Overview of Human Papillomavirus Proteins

Human papillomavirus is a non-enveloped virus, with a circular genome of approximately 8 kb. There are over 200 HPV types across at least 50 families. These families are α 1-15, with no HPV types assigned to the α 12 family, β 1-5, γ 1-27, μ 1-3, and ν 1 (Table 1.4). HPV families and types are assigned based on the identity of the L1 major capsid protein sequence. A range of 60% to 70% identity defines a species, and greater than 70% identity defines a type (De Villiers et al., 2004). HPV infects either cutaneous or mucosal tissue, depending on the HPV family and type. While HPV infections generally result in minor skin warts or genital warts, which are cleared in months to years within an immunocompetent individual; however, a small percentage of HPV infections in individuals infected with a high-risk HPV type in mucosal tissue in the oropharynx or anogenital region can progress into head and neck cancer or anogenital cancers, with cervical cancer in women being the most common (de Martel et al., 2017). Indeed, HPV is the cause of nearly all cases of cervical cancer in women (Walboomers et al., 1999). In addition, HPV is responsible for a portion of anal cancers, vaginal cancers, vulval cancers and penile cancers (de Martel et al., 2017). HPV16 and HPV18 are the high risk HPV types responsible for the majority of these cancers (Michaud et al., 2014).

HPV viral proteins can be classified as early proteins or late proteins depending on whether their transcription is under the control of the HPV early or late promoter. Proteins encoded by genes under control of the HPV early promoter include E1, which is an ATPase-dependent helicase (Bergvall et al., 2013); E2, which is capable of regulating the transcription of other HPV-encoded genes (McBride, 2013); E4, which commonly occurs as an E1^{E4} fusion protein, and has functions related to virus release and transmission (Doorbar, 2013); E5, which is a transmembrane protein that can be found localized in various intracellular membranes, including the Golgi apparatus, the endoplasmic reticulum and nuclear membranes (DiMaio and Mattoon, 2001). E5 is responsible for activating

Table 1.4 Different HPV species and associated types, tissue tropisms and clinically associated infections. The last column indicates whether the species includes HPV types that are the causative agent of a high number of head and neck or genitourinary cancers.

Species	HPV Types	Tissue Tropism	Associated Infections	Cancer Risk
Alpha-1	32, 42	Mucosal	Focal Epithelial Hyperplasia (Heck's Disease)	Low
Alpha-2	3, 10, 28, 29, 77, 78, 94, 117, 125, 160	Cutaneous	Flat Warts, Common Warts, Epidermodysplasia Verruciformis	Low
Alpha-3	61, 62, 72, 81, 83, 84, 86, 87, 89, 102, 114	Mucosal/ Cutaneous	Cervical Intraepithelial Neoplasia, Cutaneous Lesions	Low
Alpha-4	2, 27, 57	Mucosal/ Cutaneous	Common Warts, Plantar Warts, Flat Warts, Cervical Intraepithelial Neoplasia	Low
Alpha-5	26, 51, 69, 82	Mucosal/ Cutaneous	Common Warts, Flat Warts, Genital Warts, Cervical Intraepithelial Neoplasia	Low/ High
Alpha-6	30, 53, 56, 66,	Mucosal	Cervical Intraepithelial Neoplasia, Invasive Carcinoma, Cervical Carcinoma	High
Alpha-7	18, 39, 45, 59, 68, 70, 85, 97, 177	Mucosal	Cervical Intraepithelial Neoplasia, Invasive Carcinoma, Genital Warts, Head and Neck Squamous Cell Carcinoma	High
Alpha-8	7, 40, 43, 91	Mucosal/ Cutaneous	Common Warts, Cervical Intraepithelial Neoplasia, Genital Warts	Low
Alpha-9	16, 31, 33, 35, 52, 58, 67	Mucosal/ Cutaneous	Cervical Intraepithelial Neoplasia, Invasive Carcinoma, Cutaneous Lesions, Conjunctival Papillomas/Carcinomas, Head and Neck Squamous Cell Carcinoma	High
Alpha-10	6, 11, 13, 44, 74	Mucosal/ Cutaneous	Genital Warts, Focal Epithelial Hyperplasia (Heck's Disease), Cutaneous Lesions, Recurrent Respiratory Papillomatosis, Conjunctival Papillomas/ Carcinomas, Cervical Intraepithelial Neoplasia	Low
Alpha-11	34, 73	Mucosal/ Cutaneous	Cervical Intraepithelial Neoplasia, Cutaneous Lesions	High
Alpha-13	54	Mucosal	Genital Warts	Low
Alpha-14	71, 90, 106	Mucosal	Genital Warts	Low
Beta-1	5, 8, 12, 14, 19, 20, 21, 24, 25, 36, 47, 93, 98, 99, 105, 118, 124, 143, 152, 195, 196	Mucosal/ Cutaneous	Epidermodysplasia Verruciformis, Cutaneous Lesions, Flat Warts, Head and Neck Squamous Cell Carcinoma	Low
Beta-2	9, 15, 17, 22, 23, 37, 38, 80, 100, 104, 107, 110, 111, 113, 120, 122, 145, 151, 159, 174, 182, 198, 217	Mucosal / Cutaneous	Epidermodysplasia Verruciformis, Cutaneous Lesions, Flat Warts, Head and Neck Squamous Cell Carcinomas	Low
Beta-3	49, 75, 76, 115	Cutaneous	Flat Warts, Cutaneous Lesions	Low
Beta-4	92	Cutaneous	Cutaneous Lesions	Low
Beta-5	96, 150, 185	Cutaneous	Cutaneous Lesions	Low
Beta-unclassified	206, 209	-	-	Low

Gamma-1	4, 65, 95, 173	Cutaneous	Cutaneous Lesions, Plantar Warts, Common Warts	Low
Gamma-2	48, 200	Cutaneous	Cutaneous Lesions	Low
Gamma-4	60	Cutaneous	Cutaneous Lesions	Low
Gamma-5	88	Cutaneous	Cutaneous Lesions	Low
Gamma-6	101, 103, 108	Mucosal	Cervical Intraepithelial Neoplasia	Low
Gamma-7	109, 123, 134, 138, 139, 149, 155, 170, 186, 189, 193, 218	Cutaneous/ Mucosal	Squamous Carcinoma of Skin, Keratotic Lesions	Low
Gamma-8	112, 119, 147, 164, 168, 176	Mucosal	Genital Warts	Low
Gamma-9	116, 129	Mucosal/ Cutaneous	Keratotic Lesions	Low
Gamma-10	121, 130, 133, 142, 180, 191	Mucosal/ Cutaneous	Head and Neck Squamous Cell Carcinoma, Keratotic Lesions	Low
Gamma-11	126, 136, 140, 141, 154, 169, 171, 181, 202	Mucosal/ Cutaneous	Head and Neck Squamous Cell Carcinoma, Flat Warts, Genital Warts	Low
Gamma-12	127, 132, 148, 165, 199	Mucosal/ Cutaneous	Head and Neck Squamous Cell Carcinoma, Keratotic Lesions, Associated with Non-Melanoma Skin Cancer	Low
Gamma-13	128, 153	Mucosal/ Cutaneous	Keratotic Lesions, Genital Warts	Low
Gamma-14	131	Cutaneous	Keratotic Lesions	Low
Gamma-15	135, 146, 179, 192	Mucosal/ Cutaneous	Common Warts	Low
Gamma-16	137	Mucosal	-	Low
Gamma-17	144	Mucosal	-	Low
Gamma-18	156	-	-	Low
Gamma-19	161, 162, 166	Cutaneous	-	Low
Gamma-20	163, 183, 194	Cutaneous	-	Low
Gamma-21	167	Cutaneous	-	Low
Gamma-22	172	Mucosal	-	Low
Gamma-23	175	Mucosal	Genital Warts	Low
Gamma-24	178, 190, 197	Cutaneous	-	Low
Gamma-25	184	Cutaneous	Common Warts	Low
Gamma-26	187	-	-	Low
Gamma-27	201	Mucosal	Genital Warts	Low
Gamma-unclassified	157, 158, 203, 205, 207, 208, 210, 211, 212, 213, 214, 215, 216, 219, 220, 221, 222, 223, 224	Cutaneous	-	Low
Mu-1	1	Cutaneous	Plantar Warts, Common Warts	Low
Mu-2	63	Cutaneous	Plantar Warts	Low
Mu-3	204	-	-	Low
Nu-1	41	Cutaneous	Common Warts, Flat Warts, Cutaneous Lesions	Low

epidermal growth factor (EGF) signaling that promotes cell division (DiMaio and Petti, 2013). Other proteins under the control of the HPV early promoter are E6, which can inhibit and degrade the p53 tumour suppressor, and promote progression of the cell cycle (Vande Pol and Klingelutz, 2013); E7 which can degrade pRb, which leads to the release of the E2F transcription factor, and promotes cell cycle progression (Roman and Munger, 2013); and E8, which can repress HPV gene transcription and HPV replication to ensure appropriate timing of these events during infection (Dreer et al., 2017). E8 is expressed in the form of an E8^{E2} fusion protein (Dreer et al., 2017). The HPV late proteins L1 and L2 are both encoded by genes under control of the HPV late promoter. L1 is the major capsid protein (Buck et al., 2013), while L2 is the minor capsid protein and also plays a role in viral trafficking and entry (Wang and Roden, 2013).

1.8 Human Papillomavirus Reprogramming of Host-cell Metabolism

HPV, or its oncoproteins, typically reprogram cellular metabolism in a manner reminiscent of other viral infections, with an upregulation of glycolysis (Lai et al., 2013; Leiprecht et al., 2011; Mazurek et al., 2001a). Also noted in the literature are increases in nucleotide metabolism (Mazurek et al., 2001a) and glutaminolysis (Mazurek et al., 2001b) as a result of either HPV infection or expression of the E6 and E7 HPV oncoproteins. However, there is one report of a contradictory function of E6, in which it was shown to upregulate cellular respiration (Cruz-Gregorio et al., 2019).

1.9 Human Papillomavirus and Cancer

HPV is a sexually transmitted virus, and infects basal epithelial cell layers in which the epithelium has been disrupted by mechanical abrasions (Zur Hausen, 2002). These infected cells continue to divide and proliferate increasing the number of HPV infected cells. In a subset of infections, portions of the HPV viral genome become integrated with the host-cell genome (McBride and Warburton, 2017) or persist in viral episomes within the infected cell (Oyervides-Muñoz et al., 2018). This can lead to constitutive expression of the HPV oncoproteins E6 and E7. Like the HAdV oncoproteins, the HPV oncoproteins E6

and E7, are capable of inhibiting the p53 and pRB tumour suppressors, allowing for uncontrolled cell growth and proliferation (Fehrmann and Laimins, 2003). Not all HPV types are equally capable of causing cancer and for this reason HPV can be classified as a low-risk or high-risk type, with the highest-risk types being HPV16, which is predominant in both HPV+ cervical and head and neck cancer (Kreimer et al., 2005), and HPV18, which is predominant in HPV+ cervical cancer (Crow, 2012). Interestingly, HPV+ head and neck cancer is associated with better survival outcomes than head and neck cancers with a non-viral origin (Fakhry et al., 2008). As the majority of cervical cancers are HPV+, HPV status is not used as a prognostic indicator for survival outcomes in cervical cancer, in contrast to head and neck cancer (Crow, 2012). The worldwide incidence of HPV+ head and neck cancers and cervical cancers should be decreasing as effective vaccines for HPV have been developed (Koutsky and Harper, 2006; Petrosky et al., 2015) and are beginning to be widely administered as part of a routine immunization schedule (Markowitz et al., 2013).

Only about 25% of head and neck cancers are caused by HPV, and most of these are present in the oropharynx. Other head and neck cancers of a non-viral origin primarily arise from mutations due to excessive smoking and drinking (Tumban, 2019). In addition to distinct etiologies, HPV+ and HPV- HNSCCs have distinct mechanisms of cancer progression (Leemans et al., 2011). This means that disease treatment strategies for HPV+ head and neck cancer may not necessarily be appropriate for HPV- head and neck cancers. For example, the immune landscape between HPV+ and HPV- head and neck cancers differs. HPV+ head and neck cancers have a phenotype that suggests T-cell inflammation while HPV- head and neck cancers do not (Gameiro et al., 2018). HPV+ head and neck cancers may be more susceptible to treatment with immune checkpoint inhibitors than HPV- head and neck cancers (Gameiro et al., 2018). Likewise, other cellular processes, such as metabolism, may differ between HPV+ and HPV- head and neck cancers (Fleming et al., 2019). Chapter 3 of this thesis is an analysis of data available from The Cancer Genome Atlas (TCGA) to determine whether there are differences in survival associated with differing expression of central metabolic genes between HPV+ and HPV- head and neck cancers. This chapter then goes on to speculate which potential pharmacological compounds may be uniquely effective in HPV+ head and neck cancer due to its unique transcriptional profile for metabolism-related genes.

1.10 Overview of Epstein-Barr Virus Proteins

Unlike HAdV and HPV, EBV is a large DNA tumour virus with a genome size of approximately 172 kb. Also in contrast to both HAdV and HPV, EBV has a lipid envelope surrounding its protein capsid. (Möhl et al., 2016) and contains at least 17 tegument proteins (Johannsen et al., 2004). Tegument proteins are unique to herpesviruses (Guo et al., 2010). They are preformed effector proteins that are delivered with the incoming virion and contribute to aspects of viral replication, such as nucleocapsid translocation or expression of EBV immediate-early genes and host-cell genes (Guo et al., 2010). For example, the EBV tegument protein BFRF1 is involved in appropriate translocation of the immature virion from the nucleus (Farina et al., 2005), while BFRF2 is a tegument protein involved in DNA packaging and the primary envelopment step of the EBV replication cycle (Granato et al., 2008).

EBV encodes 85 genes, but of these 85, the latent genes play the most significant role in virally induced cancers (Smatti et al., 2018). While EBV is also known as human gammaherpesvirus 4, there are only two types of EBV identified primarily based on the sequence of their EBV latent proteins, typically EBNA2 or EBNA3 (Choi et al., 2018). Type 1 is the most predominant EBV worldwide, while Type 2 only occurs with equal prevalence to Type 1 in Africa (Choi et al., 2018). Neither type appears to be associated with worse disease outcomes (Puchhammer-Stöckl and Görzer, 2006). EBVs typically infect cells in the oropharynx around the tonsils, including oral epithelia and B cells (Dunmire et al., 2018). Some of these B cells end up in the circulatory system, and other epithelial cells in the nasopharynx and gastric cells can be affected by EBV infection (zur Hausen et al., 1970; Yanai et al., 1997). Over 90% of adults are actively and asymptotically infected with EBV worldwide (Faulkner et al., 2000).

In circumstances where EBV causes disease, it is primarily responsible for infectious mononucleosis, which occurs through infection of tonsillar epithelial cells and B cells (Dunmire et al., 2015; Wang et al., 1998). Typically, infection of epithelial cells by EBV leads to an acute lytic infection (Iizasa et al., 2012) while infection of B cells leads to a persistent, long term latent infection (Küppers, 2003). In a subset of B cell infections, EBV-

positive germinal centre B cells and EBV-positive memory B cells that have re-entered the germinal centre may undergo a transformation event in the cell proliferation-encouraging environment of the germinal centre (Küppers, 2003). The presence of EBV oncoproteins in conjunction with the transformation event in these B cells can lead to cancer when apoptotic mechanisms to remove these aberrant cells are bypassed (Kanzler et al., 1996; Kurth et al., 2003; Niller et al., 2003). For example, expression of EBV proteins in Burkitt lymphoma can overcome potential apoptotic signals that result from a frequent MYC translocation in this cancer (Pajic et al., 2001). In Hodgkin lymphoma, the EBV protein LMP2A may encourage pro-survival pathways in affected B cells (Caldwell et al., 1998; Küppers, 2003). EBV-infected B cells are responsible for infection of other epithelial tissues, including nasopharyngeal and gastric tissue (Iizasa et al., 2012). Cell-to-cell contact of EBV-infected B cells with uninfected epithelial cells triggers a lytic infection in the B cells that is reliant on endocytic machinery in the recipient epithelial cell (Nanbo et al., 2012, 2016). However, non-cell mediated infection of epithelial cells by EBV is another possible, albeit less significant, mechanism of infection (Imai et al., 1998). In a small proportion of epithelial cells infected with EBV, alterations in host-cell genome methylation and gene expression caused by EBV-encoded genes, primarily EBV-encoded noncoding RNAs (EBERs) and microRNAs, can lead to oncogenic transformation and cause epithelial cancers, including nasopharyngeal carcinomas or gastric cancer (Thompson and Kurzrock, 2004).

The EBV latent proteins include EBNA1, which is responsible for p53 degradation, virus persistence, and transactivation of both viral and infected host-cell genes (Frappier, 2015). The second EBV latent protein, EBNA2, can also activate both viral and host-cell gene expression, primarily with the assistance of another EBV latent protein, EBNA1LP (Kempkes and Ling, 2015). EBNA3A modulates the expression of EBNA2 (Allday et al., 2015). EBNA3A can also induce G1 arrest (Allday et al., 2015). EBNA3B can act as a tumour suppressor and can coactivate EBNA2 (Allday et al., 2015). EBNA3C has a wide variety of functions, including inducing pRB degradation, overcoming the DNA damage response, promoting cell proliferation, and inducing G1 arrest (Allday et al., 2015). LMP1 can activate cell survival related cell signalling pathways including the Nf- κ B, JNK and p38 MAPK pathways (Kieser and Sterz, 2015). The LMP2A protein can mimic B-cell

receptor signalling, especially activation of the ERK/MAPK pathways, as well as encourage epithelial cell motility and spreading (Cen and Longnecker, 2015). EBV also has a variety of EBERs that function to confer resistance to apoptosis (Skalsky and Cullen, 2015). microRNAs transcribed by the *Bam*HI-A region rightward transcript (BART) and *Bam*HI fragment H rightward open reading frame 1 (BHRF1) regions of the EBV genome also function to inhibit apoptosis of the infected host-cell (Skalsky and Cullen, 2015) and modulate the immune response (Wang et al., 2018).

1.11 Epstein-Barr Virus Reprogramming of Host-cell Metabolism

Like the other two DNA tumour viruses that will be discussed in this thesis, EBV has also been noted to drive an increase in glucose metabolism in the infected cell (McFadden et al., 2016; Zhang et al., 2017a). Additionally, EBV has been reported to induce one-carbon metabolism, the end products of which are utilized in nucleotide biosynthesis (Wang et al., 2019a). Perhaps contradicting the reliance on glycolysis implied by the metabolic programming associated with the Warburg effect, EBV also increases the activity of the TCA cycle and oxidative phosphorylation (Wang et al., 2019a).

1.12 Epstein-Barr Virus and Cancer

EBV is the etiological agent of a variety of cancers of immune cells, including B cells, T cells and natural killer (NK) cells (Thompson and Kurzrock, 2004). In addition, EBV can cause cancers in epithelial tissues, included, but not limited to, gastric epithelial cells (Tsao et al., 2015). As is common to the other DNA tumour viruses discussed above, evasion of the host immune system contributes to the development of cancer in the EBV infected cell (Ressing et al., 2015). EBV has two distinct lifecycles, the lytic and latent lifecycles, and both the latent and lytic lifecycle have been noted to contribute to oncogenesis (Murata and Tsurumi, 2014). The latent cycle, in which the EBV genome exists in an episome, is the predominant contributor to viral oncogenesis by EBV (Murata et al., 2014). This is because genes controlling growth and proliferation are activated by the immediate-early and early EBV oncoproteins expressed by latent EBV infections (Hoebe et al., 2013; Mauser et al., 2002). However, during the lytic stages of infections, EBV oncogenes become expressed

at higher levels, and some of those induce cytokines and growth factors that can lead to abnormal proliferation of the surrounding latently infected cells (Mosialos, 2001). It is possible that the switching of EBV replication cycles between the lytic and latent cycles could make the host-cell genome especially prone to genomic instability (Fang et al., 2009). Several EBV oncogenes also contribute to EBV-induced oncogenesis. The most predominant oncogenes are the latent membrane proteins LMP1 and LMP2A (Dawson et al., 2012; Scholle et al., 2000; Shair et al., 2012). Both of these proteins can trigger growth-related pathways in the host-cell and can also enact tumour promoting host immune evasion. Despite this, increased inflammation has been associated with EBV-induced gastric cancers (Derks et al., 2016). The EBV nuclear antigen proteins, EBNA1, EBNA2, EBNA3A, and EBNA3C generally promote oncogenesis or transformation with varying degrees of essentiality (Kang and Kieff, 2015). EBNA3B can act as tumour suppressor (Kang and Kieff, 2015). Unlike the other two DNA-tumour viruses discussed above, virally-encoded microRNA and noncoding RNA have a significant role in EBV-induced oncogenesis (Wang et al., 2019c). In terms of gastric cancers induced by EBV, which will be the focus of chapter 4 in this thesis, approximately 9% are caused by EBV (Murphy et al., 2009). EBV was first noted to be a significant factor for classification of stomach adenocarcinomas in 2014 based on a whole tumour TCGA analysis (Bass et al., 2014). Compared to EBV-negative (EBV-) stomach adenocarcinomas, the EBV-positive (EBV+) stomach adenocarcinomas had higher expression of genes related to immune regulation, such as genes related to MHC-II, namely *HLA-DPA1* and *HLA-DPB1*, and genes related to lymphocyte function, such as *LY6K* (Zhang et al., 2020). Also distinct from EBV- stomach adenocarcinomas, the EBV+ stomach adenocarcinomas had increased cell division associated with tumour infiltrating B cells (Zhang et al., 2020), which corresponds to the ability of EBV to infect B cells. However, it remains unclear whether EBV+ stomach adenocarcinomas have an altered metabolic phenotypic corresponding to the unique etiology of this stomach adenocarcinoma and the increased cycling of immune cells. Chapter 4 of this thesis will explore the question of metabolic gene expression in EBV+ stomach adenocarcinomas.

1.13 Glycolysis and the Warburg Effect

Cellular energy production typically begins with the conversion of glucose to pyruvate through glycolysis. Pyruvate is funnelled to the TCA cycle to load electrons onto various coenzymes that can be utilized in the electron transport chain to convert ADP to ATP (Figure 1.5). However, many metabolites within glycolysis and the TCA cycle can be utilized in other pathways to generate precursors for macromolecules required for viral replication. For example, intermediates of glycolysis can be funnelled into the PPP to generate ribose, the sugar backbone of nucleotides (Figure 1.5).

Typically, cells prefer the slower, but more energetically productive electron transport chain as the main source of cellular energy over glycolysis. Glycolysis proceeds rapidly, but produces much less energy. However, under certain conditions, cells appear to utilize glycolysis over cellular respiration, despite the presence of ample oxygen. This is known as the Warburg effect (Figure 1.6), and was first observed in cancer cells (Racker, 1972; Warburg, 1925; Warburg et al., 1927). It is becoming increasingly appreciated that many viruses reprogram cellular metabolism in a similar manner (Figure 1.6). For example, DNA tumour and tumour-associated viruses, such as HPV, Kaposi's sarcoma associated herpesvirus, EBV, human cytomegalovirus, and HAdV, are all noted to increase host cell glycolytic activity (reviewed in (Goodwin et al., 2015; Sanchez and Lagunoff, 2015)).

Some single-stranded RNA viruses, such as poliovirus, dengue virus, hepatitis C virus and influenza A virus have also been noted to increase glycolysis (Goodwin et al., 2015; Sanchez and Lagunoff, 2015). In addition, the Warburg effect is more complex than initially appreciated, as it is commonly accompanied by glutaminolysis (Vander Heiden et al., 2009) (Figure 2.2), which includes the utilization of glutamine as a substrate in the TCA cycle. This means that cells exhibiting the Warburg effect still utilize cellular respiration, albeit to a lesser extent than cells with a normal metabolic phenotype.

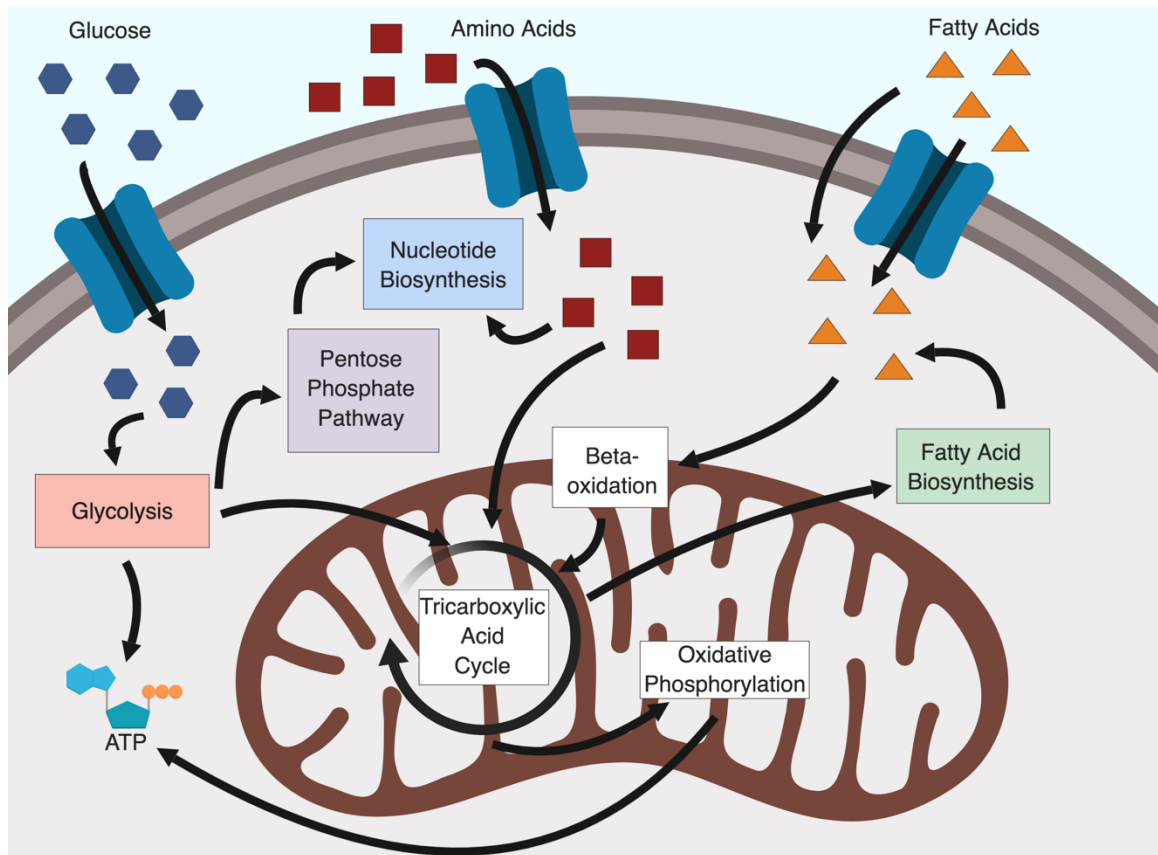


Figure 1.5. Viruses and cancers co-opt many cellular metabolic pathways to satisfy their metabolic requirements. These pathways include those used for energy production, primarily glycolysis and oxidative phosphorylation, and macromolecule production, such as for the synthesis of nucleotides or fatty acids. Created with BioRender.

1.14 Parallels Between the Metabolism of Cancer Cells and Virally Infected Cells

Both cancer and the viral infections described above are disease states that promote rapid cellular growth and proliferation. To sustain this growth, virally infected cells and cancer cells must increase the production of metabolites to provide the raw materials required for the production of the biomolecules necessary for cellular and/or viral replication (Currie et al., 2013; Goodwin et al., 2015; Lunt and Vander Heiden, 2011; Mikawa et al., 2015; Noch and Khalili, 2012). This includes, but is not limited to, nucleotides, proteins, carbohydrates, and lipids. Interestingly, both disease processes can rely on similar pathways to enact these metabolic changes. MYC is one common metabolism-related transcription factor that is employed by a variety of viruses and cancer types to stimulate metabolism and create an environment permissive to replication (Stine et al., 2015; Thai et al., 2015). A well-established result of MYC activation is a metabolic phenotype historically referred to as the Warburg effect (Warburg, 1925). This involves an upregulation of glycolysis, which is the metabolic pathway in which glucose is converted into pyruvate or lactic acid depending on the availability of oxygen and a few molecules of ATP, normally 2 molecules, with a concurrent decrease in cellular respiration, in which oxygen is utilized in conjunction with a variety of electron carriers to produce high quantities of ATP, approximately 34 ATP molecules. The Warburg effect is now more typically referred to as aerobic glycolysis, in contrast to anaerobic glycolysis.

To understand this distinction, one must appreciate the difference between how glycolysis proceeds under typical normoxic conditions (Figure 1.7A), hypoxic conditions (Figure 1.7B) and under the unique conditions surrounding virus infection or cancer (Figure 1.7C). Under normoxic conditions, glycolysis serves to generate two molecules of pyruvate, which are further broken down in the TCA cycle into a variety of intermediates with the end result of the electrons from these molecules being shuffled to electron carriers that can be used to fuel the electron transport chain (Dashty, 2013). However, under hypoxic conditions, pyruvate continues to be converted into another product of glycolysis, lactic acid (van den Beucken et al., 2006). The conversion of pyruvate to lactic acid generates an additional two molecules of ATP that would otherwise be unavailable due to the hypoxic

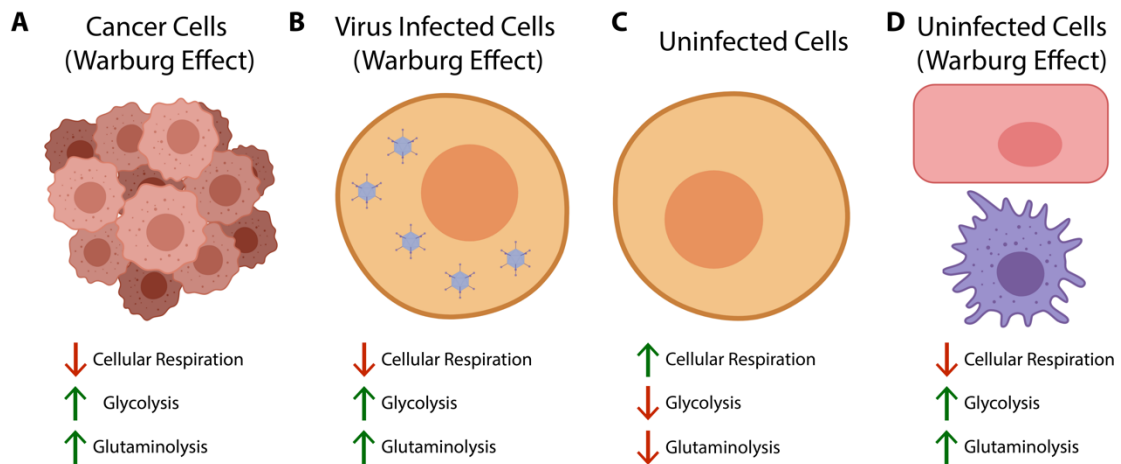


Figure 1.6 The Warburg Effect in cancer cells and virus infected cells. Both cancer cells (A) and virus infected cells (B) often exhibit a characteristic metabolic phenotype known as the Warburg effect. This phenotype is associated with an increase in cellular glycolysis and a concurrent decrease, albeit not a complete reduction, of cellular respiration despite the availability of ample oxygen. In contrast, healthy, uninfected cells (C) preferentially utilize cellular respiration over glycolysis as the main ATP generating pathway. Glutaminolysis is also less active in uninfected non-transformed cells. However, there are uninfected cells (D) that preferentially utilize the Warburg effect. For example, endothelial cells consistently have a Warburg effect-like metabolic phenotype (Eelen et al., 2015). Activated immune cells, such as effector T cells, activated macrophages, and activated dendritic cells, also shift to a Warburg effect-like metabolic phenotype (Domblides et al., 2018). Created with BioRender.

environment limiting the progression of the TCA cycle and the electron transport chain. However, in aerobic glycolysis, which occurs during a variety of viral infections and cancers, a large fraction of pyruvate is converted to lactic acid, despite conditions that would otherwise be favourable for the progression of pyruvate into the TCA cycle (Lunt and Vander Heiden, 2011).

While the reason why viral infections and cancer cells utilize this type of metabolic program is not completely understood, theories include the possibility that since aerobic glycolysis proceeds more rapidly than the electron transport chain, it can provide energy in the form of ATP more readily to the replicating virus or cancer cell (Lunt and Vander Heiden, 2011). The second theory is that an increase in aerobic glycolysis generates an abundance of the metabolite precursors required by the rapidly replicating virus or cell (Lunt and Vander Heiden, 2011). For example, glycolytic intermediates can be funnelled into the PPP which generates ribose, which is the sugar backbone of nucleotides (Patra and Hay, 2014). As further evidence that this might be the case, many viral infections and cancer cells upregulate the TCA cycle without upregulating the electron transport chain (Jin et al., 2016; Sanchez and Lagunoff, 2015). Many intermediates of the TCA cycle can also be used as precursors for the synthesis of other macromolecules required for viral or cellular replication. Additionally, this altered regulation of the TCA cycle can occur at various points due to the activity of other metabolic pathways whose products can continue into the TCA cycle. For example, glutaminolysis is the breakdown of glutamine into intermediates that can enter the TCA cycle, which can then be used for the synthesis of other molecules (Akins et al., 2018). The overarching purpose of this thesis is to explore how certain aspects of viral infection program the infected cell into becoming more metabolically cancer-like, and to expand this idea to how the metabolic program initiated by viral infections persists into cancers induced by viral oncogenesis.

1.15 Why Study Metabolism

The question remains, what is the benefit of understanding the myriad of metabolism-associated changes in virally infected cells or virally induced cancers? In terms of virally infected cells, a thorough appreciation of the metabolic changes induced by a certain virus

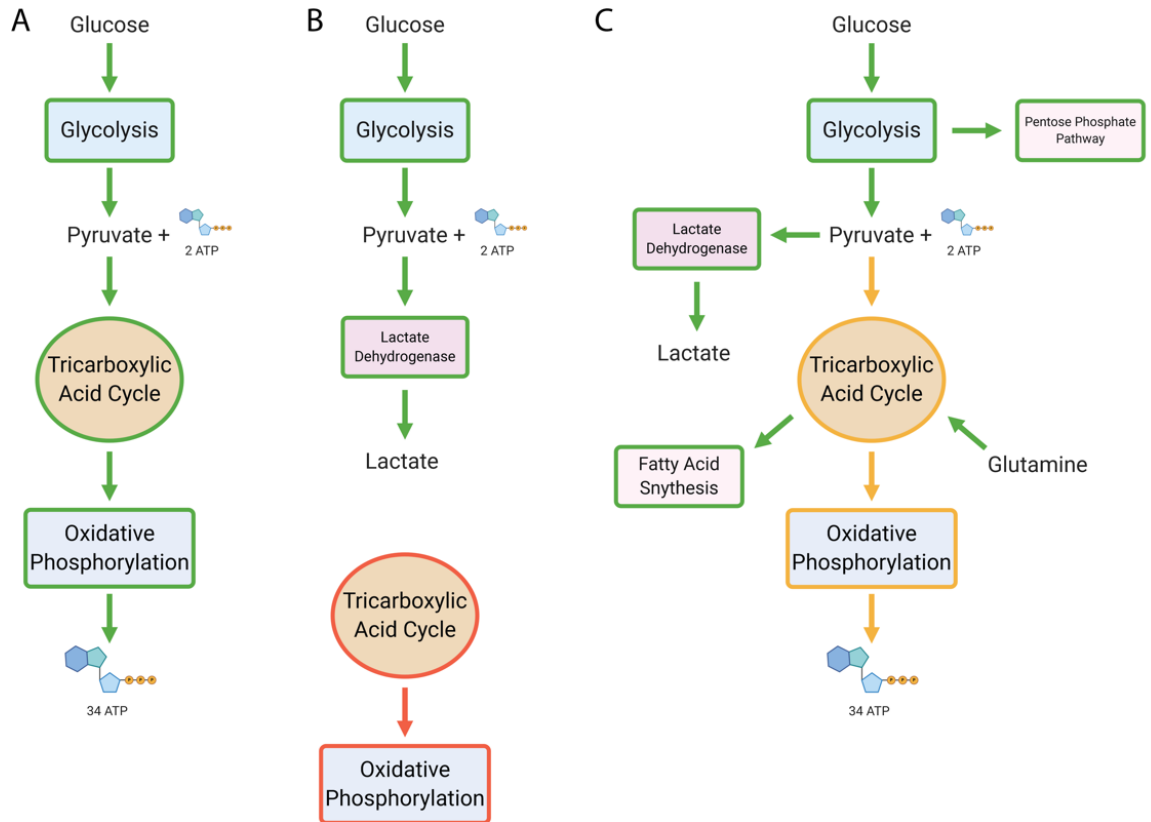


Figure 1.7. Carbon metabolism under different oxygen availabilities. (A) Under normoxic conditions, glycolysis converts glucose into two molecules of pyruvate and two molecules of ATP. Each pyruvate molecule enters the TCA cycle in which the pyruvate is broken down into intermediates whose electrons are donated to the electron carriers NADH and FADH₂. These electron carriers are used to create a hydrogen gradient through the electron transport chain. This hydrogen gradient powers the conversion of ADP to ATP. Oxygen is required for the electron transport chain as it is the final electron acceptor. (B) Under anaerobic conditions, glycolysis proceeds with the formation of pyruvate from glucose, but pyruvate does not proceed into the TCA cycle. Pyruvate is converted to lactate by lactate dehydrogenase, which is then transported out of the cell. (C) In cancer and most virus infections, cells perform aerobic glycolysis, whereby some pyruvate proceeds through the TCA cycle. Most of the pyruvate produced is converted to lactate by lactate dehydrogenase. As these cells are rapidly growing, some glycolytic intermediates are funnelled into the PPP to produce ribose, the sugar backbone of nucleotides. In addition, these cells can utilize glutamine as an alternative carbon source for the TCA cycle in a process called glutaminolysis. It is not uncommon for TCA intermediates to be utilized in other anabolic pathways, such as fatty acid synthesis.

can lead to an identification of parallels or differences between other virus infections (Goodwin et al., 2015; Sanchez and Lagunoff, 2015; Thaker et al., 2019). Metabolic processes that are altered in a similar manner across a number of viruses could represent a useful druggable target, especially when that metabolic difference varies greatly from the normal parameters of the uninfected host-cell. Additionally, while many virally induced cancers appear similar to non-virally induced cancers in the same tissue type, these similarities may exist only on a superficial level. Understanding the unique phenotype of virus-induced cancers can lead to an increased ability to differentiate and potentially treat virus-induced cancers in comparison to their non-virally induced counterparts. For example, differences in mRNA expression for certain metabolic genes can act as prognostic indicators for survival in HPV+ head and neck cancers, but not HPV- head and neck cancers. Additionally, if it appears that a whole pathway might be differentially regulated in a certain virally induced cancer when compared to a non-virally induced cancer in the same tissue, these pathways may represent unique druggable targets that can selectively target the virus induced cancer.

1.16 Thesis Overview

1.16.1. Hypothesis, Rationale, and Approach

The main scientific problem addressed by this thesis is how the metabolic phenotypes induced by DNA tumour viruses, or their viral oncoproteins, differ from those of corresponding cancers with a non-viral origin. We hypothesize that DNA tumour viruses cause a cancer-like metabolic phenotype in the infected cell or cancerous tissue, which is similar to, but still distinct from, the metabolic phenotype in non-virally induced cancers. The rationale for this hypothesis is partially based on the observation that disease severity and survival outcomes for a number of virally-induced cancers are significantly better for individuals with a virus-positive subtype of a certain cancer when compared to individuals with a virus-negative subtype of the same cancer (Bratman et al., 2016; Constanza Camargo et al., 2014; Fakhry et al., 2008; Goodman et al., 2015; Hino et al., 2008; O'Rorke et al., 2012; Song et al., 2010). Additionally, DNA tumour viruses can induce a metabolic phenotype that closely resembles the Warburg effect observed in cancer cells with an upregulation of glycolysis and a corresponding decrease in cellular respiration, despite

conditions that would otherwise preferentially favour cellular respiration (Goodwin et al., 2015). However, the mechanisms by which these metabolic changes are enacted in DNA tumour virus-positive cancers, which are frequently driven by viral oncoproteins (Thaker et al., 2019), likely differs from that of non-virally induced cancers. This could result in a metabolic phenotype that has characteristics unique to the virally-induced cancer when compared to its non-viral counterpart. These metabolic differences could have implications for patient survival when the viral and non-viral subtypes of a cancer are compared to one another.

The work in this thesis approaches the question of how DNA tumour viruses influence metabolism from two different angles. The first angle is from the model DNA tumour virus, HAdV, and how specific oncoproteins from this virus may influence cellular metabolism in a manner that enhances aerobic glycolysis and the TCA cycle, without necessarily enhancing the electron transport chain. While the HAdV metabolism literature has identified E4orf1 as one of the HAdV proteins responsible for metabolic reprogramming during HAdV infection, a portion of this introduction discussed the evidence that another HAdV oncoprotein, E1A, may also affect cellular metabolism. This idea is expanded upon in chapter 2, which shows that E1A may be capable of modulating metabolism in isolation within a cell and in the context of HAdV infection. However, understanding how viral oncoproteins may influence metabolism in a context that does not lead to oncogenesis is only a partial picture of the unique ways DNA tumour viruses program cancer-like metabolic phenotypes. In chapters 3 and 4 of this thesis, data from the TCGA is analyzed in the context of two different virally induced cancers. Chapter 3 shows that in HPV+ head and neck cancers, but not HPV- head and neck cancers, transcripts which encode enzymes involved in the TCA cycle are upregulated, and could serve as an important prognostic indicator. In chapter 4, a similar approach is utilized to understand the expression of transcript-encoding metabolic genes in EBV+ gastric cancers.

1.16.2. Chapter 2: Differential Effects of Human Adenovirus E1A Protein Isoforms on Aerobic Glycolysis in A549 Human Lung Epithelial Cells.

The purpose of this study was to determine whether HAdV E1A was capable of influencing cellular metabolism either as an endogenously expressed protein or within the context of

an HAdV infection. We hypothesized that since E1A is the first HAdV protein expressed and is capable of influencing a wide range of host-cell regulatory proteins (King et al., 2018; Pelka et al., 2008), some of which are reportedly capable of influencing metabolism independently of an interaction with E1A (Nicolay and Dyson, 2013; Stine et al., 2015; Vousden and Ryan, 2009), it is very likely that E1A plays a role in the regulation of host-cell metabolism. Our aims for this study were to determine: 1) whether A549 cells expressing either the 13S or 12S isoforms of E1A were able to influence cellular glycolytic and cellular respiration rates; 2) whether either E1A isoform was associated with changes in the transcription of genes involved in cellular metabolism; and 3) whether HAdV mutants limited to expressing only one of the two E1A isoforms had a different metabolic transcriptome in comparison to the other.

To examine these questions, functional metabolism was measured in A549 cells expressing endogenous 13S E1A or 12S E1A using extracellular flux analyses, mRNA levels in these cells were measured with RT-qPCR, and transcriptomic data from HAdV infected IMR-90 cells was analyzed. A549 cells that expressed the 13S isoform of E1A had higher baseline rates of glycolysis and lower maximum respiration rates when compared to 12S expressing A549 cells. In addition, these 13S containing A549 cells expressed more glycolysis-related transcripts and fewer cellular respiration transcripts than 12S containing A549 cells. Transcripts encoding TCA cycle enzymes were also upregulated in 13S containing A549 cells. Transcripts encoding glycolytic enzymes and TCA cycle enzymes were upregulated in greater number in IMR-90 cells infected with HAdV expressing only the 13S isoform of E1A, when compared to IMR-90 cells infected with HAdV expressing only the 12S isoform of E1A. We concluded that the 13S and 12S E1A isoforms have different influences on glycolysis and cellular respiration, and the 13S isoform appears to influence cellular metabolism more drastically towards a cancer-like metabolic phenotype.

1.16.3. Chapter 3: Survival-Associated Metabolic Genes in Human Papillomavirus-Positive Head and Neck Cancers.

The purpose of this study was to determine whether a virally induced cancer, HPV+ HNSCC, a cancer driven by the E6 and E7 oncogenes, had a different metabolism-related transcriptome when compared to HNSCC of a non-viral origin and to determine whether

any of these genes were associated with survival outcomes in HPV+ HNSCC patients. In light of the evidence from chapter 2, namely that E1A, a viral oncoprotein from the model DNA-tumour virus HAdV, can alter metabolism in cell culture, and evidence from the literature that in cell culture E6 can induce increased mitochondrial respiration (Cruz-Gregorio et al., 2019), we hypothesized that HPV+ HNSCC would therefore have a greater number of upregulated mRNA transcripts related to the TCA cycle and cellular respiration when compared to HPV- HNSCC.

Our aims for this study were to determine: 1) whether HPV+ HNSCC had a different metabolism-related transcriptomic profile when compared to HPV- HNSCC; 2) which genes would make good preliminary candidates for druggable targets in HPV+ HNSCC; and 3) identify whether any of these metabolism-related genes were associated with survival outcomes in HPV+ HNSCC, and whether double high or low expression of these genes had additive effects on survival. To examine this question we analyzed the expression of 229 metabolism genes in both HPV+ and HPV- HNSCC from TCGA RNAseq data. Next we examined whether stratifying the expression of these genes by the median level of expression in HPV+ HNSCC indicated any significant differences in patient survival, based on associated patient data available from the TCGA. We found that HPV+ HNSCCs had lower expression of glycolytic genes and higher expression of TCA cycle genes, cellular respiration genes, and beta-oxidation genes than HPV- HNSCC. In addition low expression of *SDHC*, *COX7A1*, *COX16*, *COX17*, *ELOVL6*, *GOT2*, and *SLC16A2* correlated with improved patient survival in HPV+ HNSCC.

1.16.4. Chapter 4: Expression and Patient Survival Associations for Metabolic Enzyme Genes in Epstein-Barr Virus Associated Gastric Cancer.

The purpose of this study was to determine whether tumours from another virally derived cancer, in this case EBV-associated gastric cancer (EBVaGC), were distinct from corresponding gastric cancer tumours of non-viral etiologies. As HPV+ HNSCC was distinct from HPV- HNSCC, shown in chapter 3, we hypothesized that EBVaGC would likewise have distinct regulation of metabolism-related transcripts when compared to other gastric cancers. The aims of this study were to: 1) identify the metabolic genes that were differentially regulated in all gastric cancer types, including EBVaGC, when compared to

non-cancerous tissue; 2) determine whether any differentially regulated genes were uniquely up- or downregulated in EBVaGC; and 3) determine whether any of these genes were associated with survival outcomes in EBVaGC. To address this question, we analyzed RNAseq expression data and survival data from four different gastric cancer subtypes, these being EBVaGC, microsatellite instable gastric cancer, genomically stable gastric cancer, and gastric cancers with chromosomal instability.

We identified that expression of glycolysis-related and PPP-related genes were upregulated in EBVaGC, while genes involved in the TCA cycle, cellular respiration and beta-oxidation were downregulated in EBVaGC when compared to non-cancerous tissue. In addition, EBVaGC had genes that were uniquely regulated in glycolysis, cellular respiration complexes I and IV, fatty acid synthesis and beta-oxidation when compared to gastric cancers of other subtypes. Finally high levels of expression of *PFKM*, *ACLY*, *SCD*, *RPE*, and *SLC16A13* and low expression of *ALDOB* and *NDUFA4L2* were associated with survival in EBVaGC, although these genes did not continue to be significant after false discovery correction with the Benjamini-Hochberg procedure.

Chapter 2

2 Differential Effects of Human Adenovirus E1A Protein Isoforms on Aerobic glycolysis in A549 Human Lung Epithelial Cells

2.1 Introduction

Viruses are obligate intracellular parasites as they are only capable of replicating within the infected host cell. Viruses co-opt a wide variety of host cell pathways to meet the requirements for replication. This includes reprogramming cellular metabolism to provide the substrates and energy required for successful replication (Goodwin et al., 2015). Typically, this metabolic reprogramming involves an upregulation of glycolysis and a downregulation of cellular respiration despite the presence of ample oxygen (Goodwin et al., 2015). This is known as aerobic glycolysis. Interestingly, this metabolic phenotype was first observed in cancer cells by Otto Heinrich Warburg in the 1920s (Warburg, 1925), and is also referred to as the Warburg effect. For this reason, it is possible there are similarities between the reprogramming of metabolism by viruses and cancer cells. Aside from aerobic glycolysis, viruses can modify a wide range of metabolic pathways including nucleotide biosynthesis, glutamine metabolism, and lipid metabolism (Sanchez and Lagunoff, 2015). The mechanisms by which different viruses enact these metabolic changes can be specific to the virus (Thaker et al., 2019). For example, viruses with larger genomes, such as herpes simplex virus 1, may encode some of their own metabolic enzymes (Thaker et al., 2019). However, the extent to which metabolism can be directly altered by natively encoded viral metabolic proteins is still limited, and virtually non-existent for small viruses, including human adenovirus (HAdV) (Prusinkiewicz and Mymryk, 2019). Consequently, viruses must enact metabolic changes indirectly by altering the regulation and function of host-cell enzymes and pathways. Typically, this is achieved by a viral protein that acts as a molecular hub. These proteins are capable of regulating the function of other host-cell regulatory proteins, which in turn affect a multitude of cellular processes, including metabolism.

HAdV can dysregulate metabolism (Prusinkiewicz and Mymryk, 2019), potentially through the HAdV early proteins which can enact broad regulatory changes in the host cell

(Ou et al., 2011). Currently, only the HAdV protein E4orf1 has been implicated in cellular metabolic reprogramming during HAdV infection by causing an increase in glycolysis and glutaminolysis through regulation of the cellular transcription factor MYC (Thai et al., 2014, 2015). While the effects of E4orf1 on cellular metabolism appear to be its most well characterized functions, E4orf1 can also act as an oncoprotein (Frese et al., 2003), interact with other host-cell proteins through a PDZ domain (Lee et al., 1997), and potentially contribute to the lytic lifecycle of adenovirus (Dix and Leppard, 1993). However, E4orf1 cannot explain the entirety of the metabolic phenomena associated with HAdV infection, including the downregulation of cellular respiration that is noted to occur during infection (Thai et al., 2014). Little is known about how the other HAdV oncoproteins regulate metabolism. HAdV E1A is an attractive candidate for contributing to HAdV metabolic reprogramming because it is a viral molecular hub protein (Pelka et al., 2008). This means that E1A is capable of influencing a wide range of host-cell proteins that regulate various cellular functions, which potentially includes cellular metabolism (King et al., 2018). Interestingly, this regulation may occur at the transcriptional level due to the ability of E1A to interact with a wide variety of transcription factors that can in turn influence the expression of transcripts encoding enzymes in metabolic pathways (reviewed in (Prusinkiewicz and Mymryk, 2019)). In addition, E1A is the first temporally expressed HAdV protein, which means it could be responsible for influencing early-infection metabolic changes (Crisostomo et al., 2019; Zhao et al., 2007). In HAdV-5, the primary E1A transcript is differentially spliced into five isoforms. The two isoforms of E1A encoded by the 13S and 12S mRNAs are predominantly expressed during early infection and are responsible for the majority of the functions of E1A (Nevins, 1987; Radko et al., 2015). They differ only in the presence or absence of one conserved region, known as conserved region 3 (CR3) (Lillie et al., 1987). However, there are functional differences between these two isoforms, which could contribute to differences in how each influence cellular metabolism. For example, the 13S isoform appears to function more readily as an activator of transcription (Pelka et al., 2009; Stevens et al., 2002), while the 12S isoform regulates cellular activity through transcriptional repression (Pelka et al., 2009) or by influencing localization of host-cell proteins (Madison et al., 2002). However, both isoforms are important for productive adenovirus infection and contribute to activating

cellular processes related to immortalization and transformation (Moran and Mathews, 1987). The purpose of this study was to determine whether the HAdV E1A protein is capable of enacting cellular metabolic changes on its own. To test this, we measured the functional glycolytic and oxidative phosphorylation rates with extracellular flux assays and determined whether they corresponded to changes in the expression of transcripts encoding metabolic genes in A549 cells that stably and endogenously expressed either the 13S or 12S encoded isoforms of E1A. We corroborated these data with RNAseq data from IMR-90 lung fibroblasts infected with mutant variants of HAdV-5 that expressed either the 13S or 12S encoded isoform of E1A. As these isoforms differ only in whether they contain the CR3 region, any differences in metabolism or transcript expression between these two cell lines or viral infections could be ascribed to this region.

2.2 Materials and Methods

2.2.1 Cell Culture

Low passage (<20) A549 cells with endogenous expression of the 13S encoded E1A isoform of HAdV-5 (A549-13S), the 12S encoded isoform of HAdV-5 E1A (A549-12S) or empty vector transduced control cells (A549-EV) were cultured in Dulbecco's modified Eagle's medium (DMEM) with 4.5 g/L glucose, L-glutamine, sodium pyruvate, and phenol red (Wisent Inc, Saint-Jean-Baptiste, QC, Canada) supplemented with 10% fetal bovine serum (Wisent Inc), and 1% penicillin-streptomycin (Wisent Inc). The A549-13S cells were previously described in Soriano et al., 2019 as A549-E1A289R cells. The A549-12S and A549-EV cells were generated concurrently with the A549-13S cells and in a similar manner. This involved the use of a LNSX retrovirus vector (described in (Miller and Rosman, 1989)) with either 12S or 13S E1A cDNA inserted, while the A549-EV cells have the LNSX empty vector inserted. A pool of transduced cells was used to avoid clonal variation. Cells were passaged every 2 to 3 days and split at 70%–80% confluency. Unless otherwise indicated, cells were plated in the above media for all experiments.

2.2.2 Protein Extraction and Western Blot

Protein extraction from A549-13S, A549-12S, and A549-EV cells and subsequent Western blots were performed as described previously (Zhang et al., 2018). The primary antibody

used was a mixture of two E1A-specific mouse monoclonal antibodies, M37 and M58 (Harlow et al., 1985). The blot was imaged using a ChemiDoc XRS+ (Bio-Rad, Hercules, CA, USA).

2.2.3 Seahorse Glycolytic Stress Test

A549-13S, A549-12S and A549-EV cells were seeded on XFe24 microplates (Agilent, Santa Clara, CA, USA) at a density of 1×10^5 cells/ml for 24 hours. Following this, cells were washed in D-PBS (Wisent Inc) and incubated in Seahorse XF base medium (DMEM-based with no bicarbonate, glucose, or pyruvate; Agilent) supplemented with 2 mM L-glutamine at 37 °C in a CO₂-free incubator for 60 minutes. The microplate was transferred to a Seahorse XFe24 Analyzer (Agilent) to measure the extracellular acidification rate (ECAR). Basal ECAR was recorded for 3 measurement cycles before injection of glycolytic stress test compounds. Measurements were taken during sequential cycles of exposure to 10 mM glucose (3 measurement cycles), 1.5 µg/mL oligomycin (3 measurement cycles), and 50 mM 2-deoxyglucose (2-DG) (3 measurement cycles). The ECAR was normalized to the third measurement prior to injection of the first compound.

2.2.4 Seahorse Mitochondrial Stress Test

Cells were seeded on XFe24 microplates as above, however the Seahorse XF base medium was supplemented with 2 mM L-glutamine, 10 mM glucose, and 2 mM sodium pyruvate. The microplate was transferred to a Seahorse XFe24 Analyzer to measure the oxygen consumption rate (OCR). Basal OCR was recorded for 3 measurement cycles before injection of mitochondrial stress test compounds. Measurements were taken during sequential cycles of exposure to 1.5 µg/ml oligomycin (3 measurement cycles), 1 µM carbonyl cyanide-4-(trifluoromethoxy)phenylhydrazone (FCCP) (3 measurement cycles), and 0.5 µM rotenone/antimycin A (3 measurement cycles). The OCR was normalized to the third measurement prior to injection of the first compound.

2.2.5 RNA Extraction and qPCR

A549-13S, A549-12S, and A549-EV cells were grown on 100 mm cell culture dishes until 70%–80% confluency. Cells were trypsinized and collected in a cell pellet. Total RNA was

extracted with a PureLink RNA mini kit (Invitrogen, Waltham, MA, USA) according to the manufacturer's guidelines. A total of 1 μg of total RNA was used in a reverse transcription reaction with a SuperScript VILO cDNA synthesis kit (Invitrogen) according to the manufacturer's guidelines. Primer sequences were generated *de novo* using Primer-BLAST (Ye et al., 2012) with requirements that the primer pair span an exon-exon junction and be separated by at least one intron when possible. All primer efficiencies were verified using a five-point standard curve with 400 ng, 200 ng, 100 ng, 50 ng and 25 ng of cDNA. A list of primer sequences used in this study can be found in Supplementary Table 2.1. A total of 50 ng of cDNA per reaction was used for subsequent qPCR characterization of mRNA expression. All qPCR reactions were performed on a QuantStudio 5 Real-Time PCR system (Applied Biosystems, Foster City, CA, USA). *H2AFY* and *ACTB* were used as reference genes.

Data were analyzed using the $2^{-\Delta\Delta\text{Ct}}$ method (Livak and Schmittgen, 2001). First, the Ct values from the three technical replicates for each sample were averaged to provide a single value for one biological replicate. There were three biological replicates for each of A549-13S, A549-12S and A549-EV. A reference Ct value for every biological replicate was calculated from the geometric mean of *H2AFY* and *ACTB* Ct values for that replicate. A ΔCt value was calculated for each biological replicate by subtracting the Ct value for a target gene of interest, such as *HK2*, from the geometric mean. The three biological replicate ΔCt values were then averaged together to provide the $\Delta\text{Ct}_{\text{avg}}$. The standard deviation of these three biological replicate ΔCt values was also calculated as $\Delta\text{Ct}_{\text{SD}}$. Next, the $\Delta\Delta\text{Ct}$ value was calculated by subtracting the ΔCt of the condition, in this case A549-13S or A549-12S cells, from the ΔCt of the control sample, A549-EV. Technically, the $\Delta\Delta\text{Ct}$ value is also calculated for the control, A549-EV, but this value is always zero as the ΔCt for A549-EV is subtracted from itself. Next the standard deviation, $\Delta\text{Ct}_{\text{SD}}$, of the corresponding $\Delta\Delta\text{Ct}$ values were added or subtracted from the $\Delta\Delta\text{Ct}$ for each cell type and gene of interest. These values, $\Delta\Delta\text{Ct}$, $\Delta\Delta\text{Ct} + \Delta\text{Ct}_{\text{SD}}$ and $\Delta\Delta\text{Ct} - \Delta\text{Ct}_{\text{SD}}$, were used to calculate the relative quantity (RQ) where $\text{RQ} = 2^{-\Delta\Delta\text{Ct}}$, the maximum possible RQ error value (RQ_{Max}) where $\text{RQ}_{\text{Max}} = 2^{-(\Delta\Delta\text{Ct} - \Delta\text{Ct}_{\text{SD}})}$, and the minimum possible RQ error value (RQ_{Min}) where $\text{RQ}_{\text{Min}} = 2^{-(\Delta\Delta\text{Ct} + \Delta\text{Ct}_{\text{SD}})}$. This method of calculation yields an error range for all RQ values, including for the control group (Livak and Schmittgen, 2001). T-test

analysis was performed on the ΔC_t values prior to $2^{-\Delta\Delta C_t}$ transformation to generate applicable p -values (Yuan et al., 2006). See appendix 1 for a sample calculation.

2.2.6 RNA Sequencing Analysis

IMR-90 primary lung fibroblasts (American Type Culture Collection, Manassas, VA, USA) were contact arrested for 72-hours and infected for 16 hours with either a *dl520* HAdV-5 mutant (Haley et al., 1984) (from Dr. S.T. Bayley (McMaster University, Hamilton, ON, Canada)), which expressed the 12S encoded E1A isoform; a *pm975* HAdV-5 mutant (Montell et al., 1982) (from Dr. S.T. Bayley), which expressed the 13S encoded E1A isoform; or an E1A-deleted HAdV-5 mutant control at a multiplicity of infection of 10. The control virus had the E1 region replaced with CMV-driven beta-galactosidase. Total RNA from infected IMR-90 cells were collected with TRIzol reagent (Sigma, St. Louis, MO, USA) according to the manufacturer's protocol, with each infection repeated for a total of two biological replicates. Collected RNA was sent to Genome Quebec for processing and sequencing using Illumina's HiSeq platform. Bam sequencing files were aligned to the hg38 (human) genome using STAR (Dobin et al., 2013). Tag directories were produced using the homer (Heinz et al., 2010) function `makeTagDirectories` and RNA reads were quantified using `analyzeRepeats`. Differential expression was calculated using DESeq2 (Love et al., 2014) at a cut-off p -value of 0.05.

2.2.7 Statistics

Normalized Seahorse XFe24 Analyzer data were analyzed in GraphPad Prism 8 (San Diego, CA, USA) using a two-way ANOVA in which the ECAR or OCR was defined as the continuous dependent variable, cell line was one categorical independent variable, and injection was the second categorical independent variable. The two-way ANOVA was followed by a Tukey's multiple comparison test in which each cell mean was compared to every other cell mean on that row. A separate analysis was performed for the glycolytic stress test data and mitochondrial stress test data. qPCR data were analyzed using Microsoft Excel 365 (Redmond, WA, USA) and comparisons between groups were performed using a Student's t -test.

2.3 Results

2.3.1 A549-13S Cells Increased Baseline Glycolysis and Decreased Maximum Respiration

To examine the role of adenovirus E1A in changing cellular metabolism, we examined extracellular metabolic flux, with a Seahorse XFe24 analyzer, in A549 cells expressing either the 13S encoded HAdV-5 E1A isoform (A549-13S), the 12S encoded isoform (A549-12S), or an empty vector control (A549-EV). The expression of E1A in these cell lines was confirmed by Western blot (Figure 2.1). The extracellular acidification rate of these three cell lines, a readout of glycolytic function, is shown in Figure 2.2A. The A549-EV and A549-12S cell lines had very similar glycolytic profiles. The minimal basal rate of glycolysis, induced by glucose after two hours of serum starvation, was similar between the two cell lines. To determine their maximal glycolytic potential, cells were stimulated with oligomycin. Oligomycin inhibits ATP synthase, forcing cells to increase glycolysis to a maximal rate. Maximal glycolysis was significantly higher in A549-EV cells than in A549-12S cells. In contrast, A549-13S cells reached their maximal glycolytic rate immediately after the addition of glucose, which implied that the baseline rate of glycolysis in A549-13S cells was higher than in A549-12S cells or A549-EV cells. Importantly, glycolysis in A549-13S cells could not be increased to a higher maximal rate with the addition of oligomycin. In fact, the rate of glycolysis after oligomycin addition was the lowest in A549-13S cells in comparison to both the A549-12S and A549-EV cells. All cell lines responded similarly to 2-DG, which was used to shut down glycolysis and terminate the experiment.

We next assessed oxygen consumption rates, a readout of cellular respiration. The only observed differences in oxygen consumption were in the maximal respiration rates (Figure 2.2B). Maximal respiration was induced by FCCP, which uncouples oxidation from phosphorylation in mitochondria rendering them inefficient. This causes the cell to increase its rate of cellular respiration to compensate for the mitochondrial inefficiency. The A549-13S containing cells had a lower rate of cellular respiration compared to the A549-12S containing cells or the A549-EV containing cells, which were otherwise equivalent. No

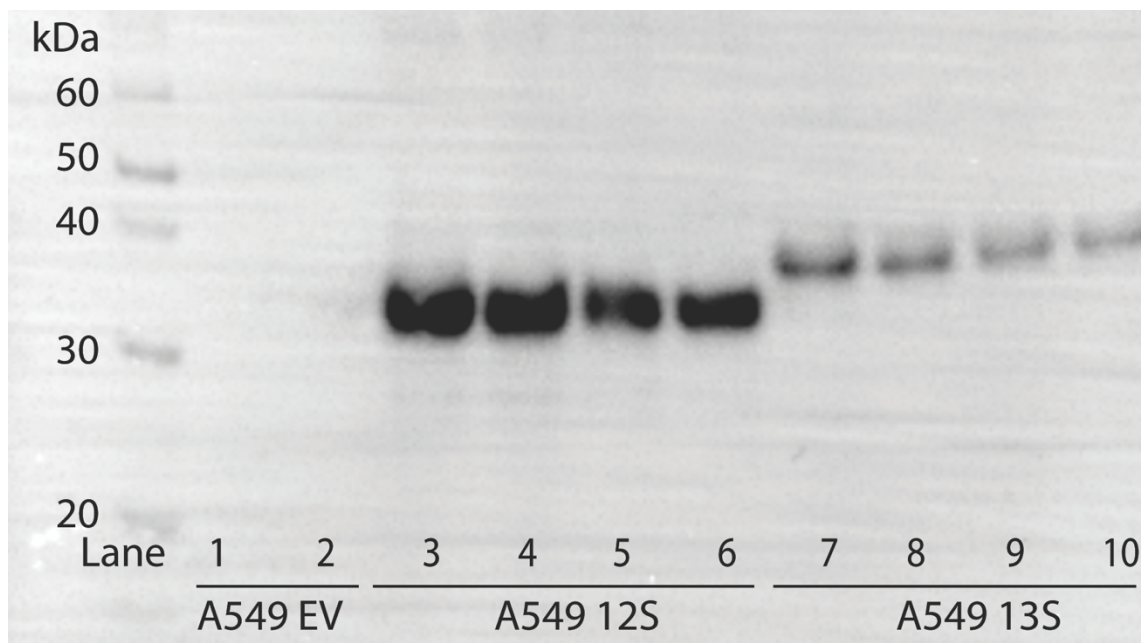


Figure 2.1. Western blot of E1A expression levels in A549-EV, A549-12S and A549-13S cell lines. Replicate cell lysates were resolved by electrophoresis, transferred to a membrane and blotted with a mixture of M37 and M58 E1A-specific mouse antibodies. No E1A was detected in lanes 1 and 2, corresponding to the A549-EV cells that do not express E1A. As expected, A549-12S cells (lanes 3-6) transduced with a vector expressing the smaller major isoform of E1A showed a band with a lower molecular weight than A549-13S cells (lanes 7-10) transduced with a vector expressing the larger major isoform of E1A. Note that each consecutive pair of lanes corresponds to protein from a single sample

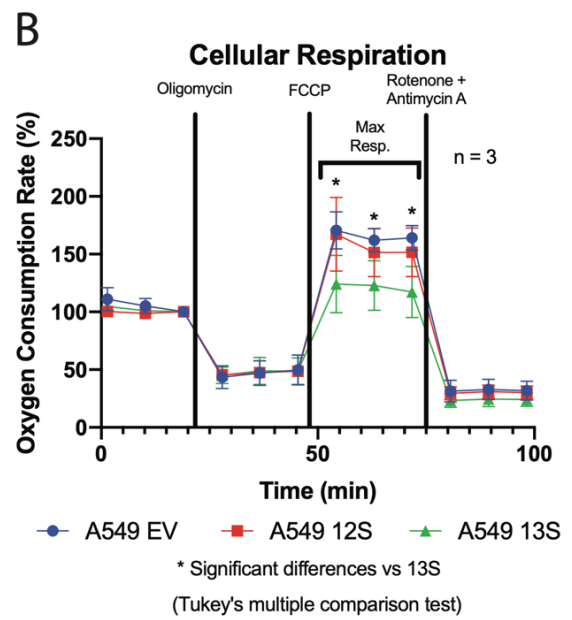
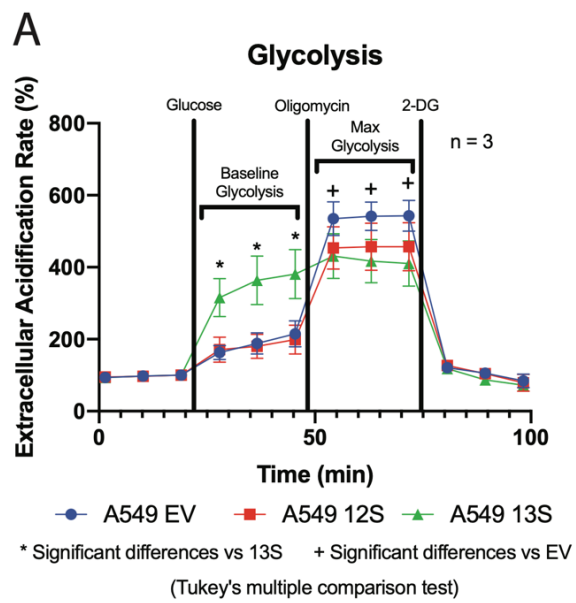


Figure 2.2. A549-13S cells have a unique functional glycolytic and oxidative phosphorylation metabolism when compared to A549-12S and A549-EV cells.

(A) Seahorse XFe24 assay of extracellular acidification rates, a readout of glycolysis. Extracellular acidification rates were highest in A549-13S cells after addition of glucose, which is a reflection of the baseline glycolytic rate after stimulation. However, A549-EV cells had the highest maximum extracellular acidification rates after addition of oligomycin, which forces maximal glycolysis by inhibition of ATP synthase. There were no differences in response after the addition of 2-deoxyglucose (2-DG) to shut down glycolysis and end the experiment. * = $p < 0.05$ in a comparison between A549-13S and either A549-12S or A549-EV cell lines. += $p < 0.05$ in a comparison between A549-EV and either A549-12S or A549-13S cell lines. (B) Seahorse XFe24 assay of oxygen consumption rates, a readout of oxidative phosphorylation. The amount of cellular respiration dedicated to ATP production was no different between the cell lines as indicated by oligomycin treatment. Maximal oxygen consumption rates, induced by carbonyl cyanide-4-(trifluoromethoxy)phenylhydrazone (FCCP) which decouples the mitochondria, were lowest in A549-13S cells. There were also no differences between the cell lines after the addition of rotenone and antimycin A used to terminate the experiment. * = $p < 0.05$ in a comparison between A549-13S and either A549-12S or A549-EV cell lines. 2-DG, 2-deoxyglucose; FCCP, carbonyl cyanide-4-(trifluoromethoxy)phenylhydrazone.

differences in response between the cell lines were observed when they were treated with oligomycin, which is used to determine the amount of cellular respiration dedicated to ATP production. Cells were treated with rotenone and antimycin A to completely shut down cellular respiration and terminate the experiment. There were also no differences in response to rotenone and antimycin A between the cell lines.

2.3.2 Glycolytic Genes Are Upregulated in A59-13S Cells

To determine how these functional differences in metabolism are reflected by the transcription of metabolic genes, we first examined genes involved in glycolysis with qPCR (Figure 2.3). mRNA for the glucose transporter SLC2A3 was 26-fold higher in the A549-13S cells than either the A549-12S cells or the A549-EV cells (Figure 2.3A). Interestingly, hexokinase 1 (*HK1*) mRNA, which encodes the enzyme used in the first step of glycolysis, was significantly lower in A549-13S cells than A549-12S or A549-EV cells (Figure 2.3B).

There were no differences in mRNA expression of glucose-6-phosphate isomerase (*GPI*) mRNA, which encodes the second enzyme involved in glycolysis, across the three cell lines (Figure 2.3C). Expression of mRNA encoding phosphofructokinase (PFK) isoforms, involved in the third step of glycolysis, varied across its five isoforms. *PFKP* and *PFKFB3* mRNAs were significantly lower in A549-13S cells than either A549-EV or A549-12S cells (Figure 2.3D,G). *PFKM*, *PFKFB2* and *PFKFB4* mRNAs were significantly higher in A549-13S cells when compared to A549-EV cells (Figure 2.3E,F,H).

Aldolase (*ALDOA*) mRNA, encoding the enzyme involved in the fourth step of glycolysis, was only significantly higher in A549-12S cells compared to the other two cell lines (Figure 2.3I). Triose-phosphate isomerase (*TPI*) mRNA, which encodes the fifth glycolytic enzyme, was higher in both the A549-13S and A549-12S cells than the A549-EV cells (Figure 2.3J). Glyceraldehyde 3-phosphate dehydrogenase (*GAPDH*) mRNA, encoding the sixth glycolytic enzyme, was only significantly higher in A549-12S cells (Figure 2.3K). mRNA for phosphoglycerate kinase 1 (*PGK1*), which is the seventh glycolytic enzyme, was significantly higher in A549-13S cells than either A549-EV or A549-12S cells (Figure 2.3L). Transcript levels for phosphoglycerate mutase (*PGAM1*), which encodes the eighth

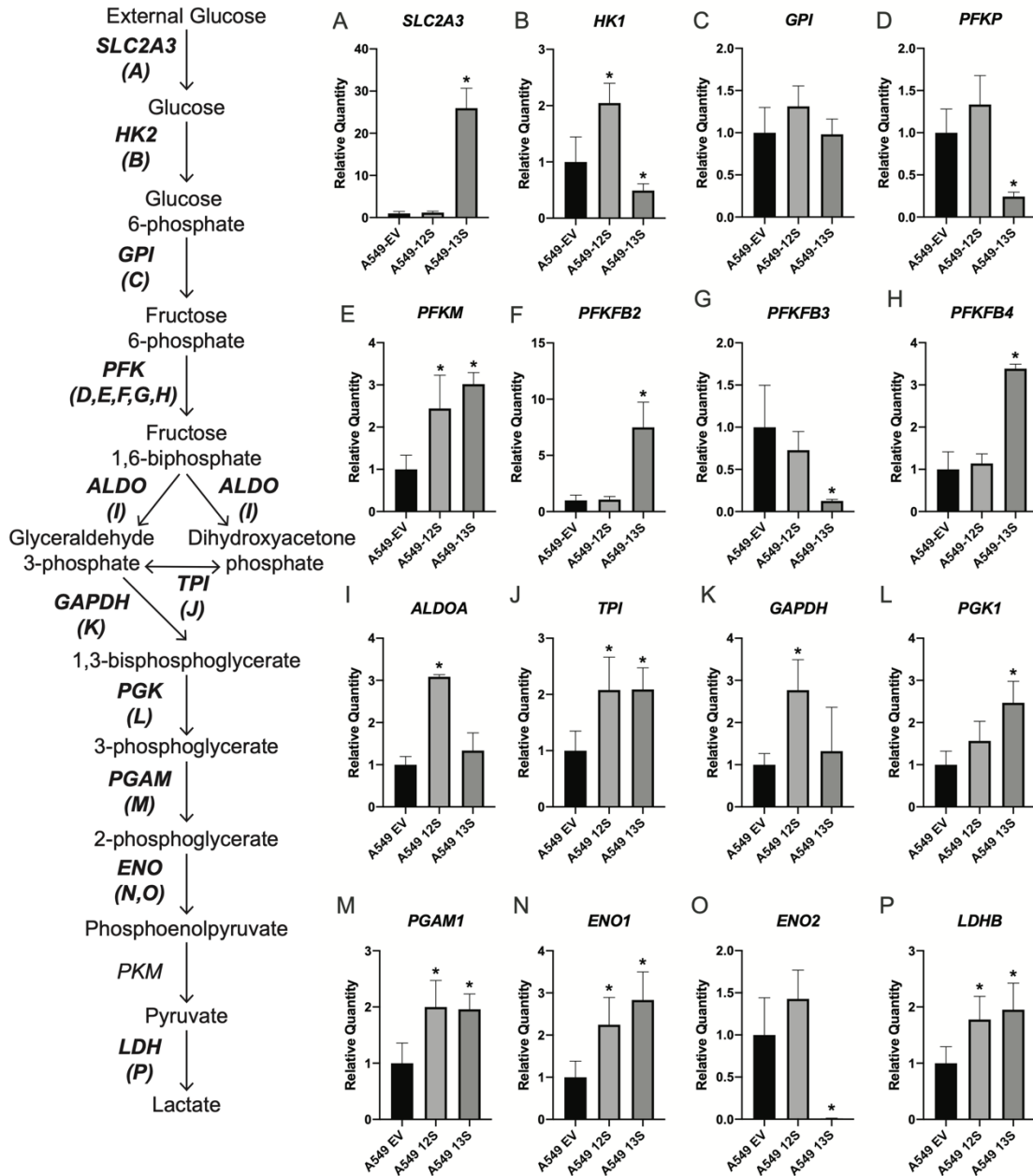


Figure 2.3. Relative expression levels of mRNA for glycolytic genes in 13S and 12S expressing A549 cells. The mRNA expression for 16 genes encoding components of glycolysis were measured with qPCR (A–P). A549-13S cells had higher expression of nine genes (A,E,F,H,J,L,M,N,P) and lower expression of four genes (B,D,G,O) when compared to A549 cells expressing an empty vector. A549-12S cells had higher expression of eight genes (B,E,I,J,K,M,N,P) when compared to A549-EV cells. The combination of differential mRNA expression in the A549-13S cells may contribute to their unusual glycolytic phenotype. H2AFY was used as a reference gene. Asterisks (*) indicate $p < 0.05$. $n = 3$ per group for all panels. SLC2A3, Solute carrier family 2 member 3; HK, hexokinase; GPI, Glucose-6-phosphate isomerase; PFKP, Phosphofructokinase, platelet; PFKM, Phosphofructokinase, muscle; PFKFB, 6-phosphofructo-2-kinase/fructose-2,6-biphosphatase; ALDO, Aldolase, fructose biphosphate; TPI, triosephosphate isomerase; GAPDH, Glyceraldehyde 3-phosphate dehydrogenase; PGK, Phosphoglycerate kinase; PGAM1, Phosphoglycerate mutase; ENO, enolase; PKM, Pyruvate kinase M1/2; LDH, Lactate dehydrogenase.

enzyme in glycolysis, were equally high in both A549-13S and A549-12S cells when compared to A549-EV cells (Figure 2.3M). mRNA expression of enolase 1 (ENO1), the ninth glycolytic enzyme, was higher in both A549-12S and A549-13S cells when compared to A549-EV (Figure 2.3N). However, mRNA for another enolase isoform, enolase 2 (ENO2) was virtually non-existent in the A549-13S containing cells, while the amount of ENO2 mRNA was not significantly different between A549-EV and A549-12S containing cells (Figure 2.3O). mRNA expression of lactate dehydrogenase B (*LDHB*) which encodes the enzyme responsible for the conversion of pyruvate to lactate in aerobic glycolysis was identified to be significantly higher in A549-13S and A549-12S cells when compared to A549-EV cells (Figure 2.3P).

2.3.3 Pentose Phosphate Pathway Genes Are Differentially Regulated in A549-13S Cells

The mRNA expression levels of five genes involved in the pentose phosphate pathway (PPP) were also characterized in these three A549 derived cell lines. mRNA of glucose-6-phosphate dehydrogenase (*G6PD*), which encodes the first enzyme of the PPP oxidative branch, was significantly lower in the A549-13S cells than either the A549-EV or A549-12S cells (Figure 2.4A). However, mRNA for 6-phosphogluconolactonase (*6PGL*), which encodes the second enzyme of the PPP oxidative branch, was significantly higher in A549-13S cells (Figure 2.4B).

The mRNA expression levels of ribulose-5-phosphate-3-epimerase (*RPE*), which encodes the enzymatic link between the oxidative and non-oxidative branches of the PPP, was not significantly different across the three cell lines (Figure 2.4C). mRNA transcripts for transketolase (*TKT*) and transaldolase 1 (*TALDO1*), which encode the two enzymes involved in the non-oxidative branch of the PPP, were significantly lower in A549-13S cells, but not in A549-12S cells or A549-EV cells (Figure 2.4D,E).

2.3.4 Tricarboxylic Acid Cycle Genes Are Upregulated in A549-13S Cells

The upregulation of many glycolytic genes by E1A, including LDHB, suggested that A549-13S cells were preferentially utilizing aerobic glycolysis. However, this does not

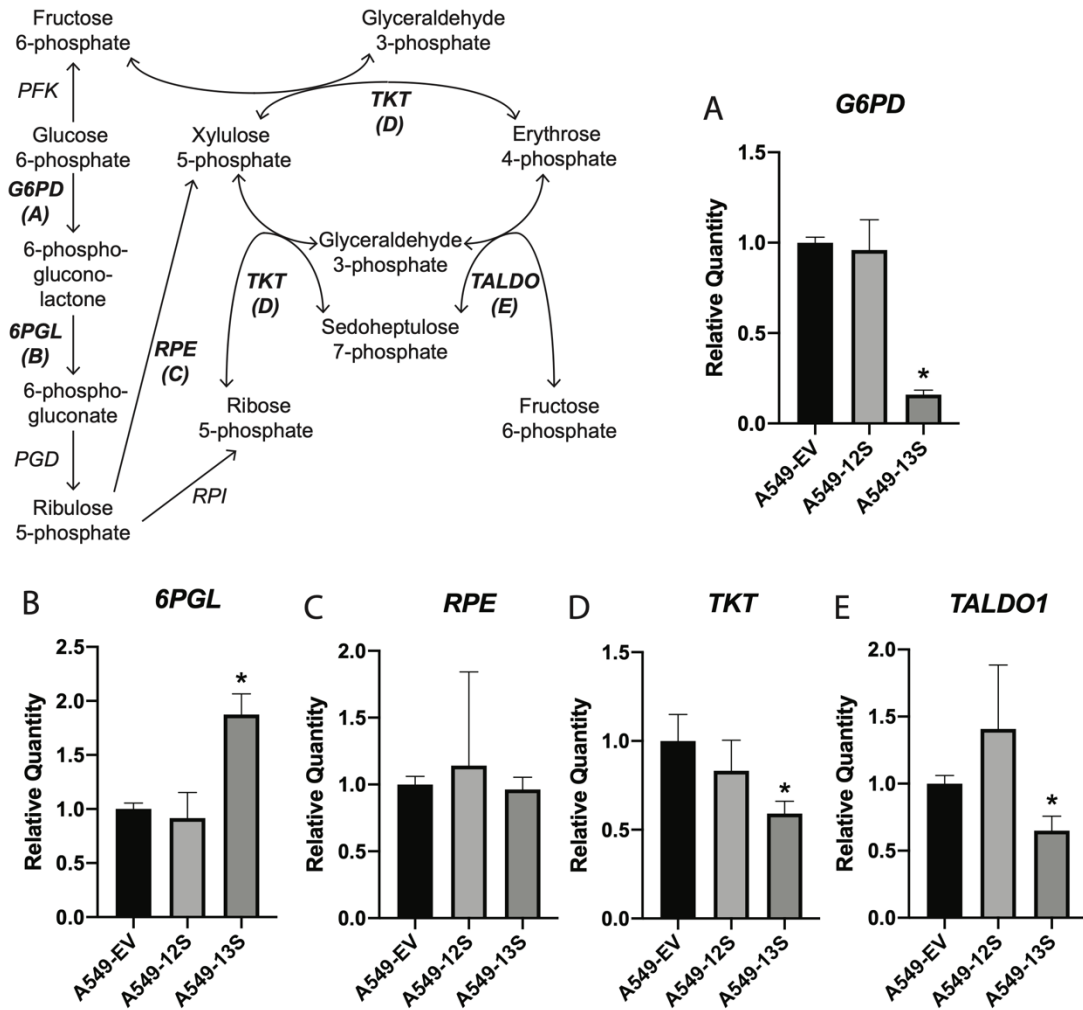


Figure 2.4. Relative expression of mRNA for pentose phosphate pathway genes in 13S and 12S expressing A549 cells. The mRNA expression for five genes encoding components of the pentose phosphate pathway were measured with qPCR (A–E). The pentose phosphate pathway relies on the products of glycolysis. Only A549-13S cells displayed differential regulation of transcripts in this pathway. Of the five pentose phosphate pathway genes measured, three were downregulated (A,D,E) and one was upregulated in the A549-13S cells (B). *H2AFY* was used as a reference gene. Asterisks (*) indicate $p < 0.05$. $n =$ three per group for all panels. G6PD, Glucose-6-phosphate dehydrogenase; 6PGL, 6-phosphogluconolactonase; PGD, Phosphogluconate dehydrogenase; RPE, Ribulose-5-phosphate-3-epimerase; RPI, Ribose 5-phosphate isomerase; TKT, Transketolase; TALDO, Transaldolase;

preclude an upregulation of the tricarboxylic acid (TCA) cycle. For example, many cancer cells and virally infected cells upregulate select enzymes involved in the TCA cycle to promote glutaminolysis and other anaplerotic reactions (Carinhas et al., 2017; Pavlova and Thompson, 2016; Vastag et al., 2011). Indeed, when we measured the expression of 15 genes involved in the TCA cycle with qPCR, six were upregulated only in A549-13S cells (Figure 2.5).

The first was pyruvate dehydrogenase complex component x (*PDHX*) mRNA, which encodes a component of the pyruvate dehydrogenase complex that is responsible for converting pyruvate to acetyl-CoA (Figure 2.5B). The next upregulated transcript was aconitase 2 (*ACO2*) mRNA, which encodes an enzyme responsible for the second step of the TCA cycle. In this step the metabolite citrate is converted into isocitrate through the intermediate cis-aconitate. Expression of *ACO2* was expressed over 2-fold more in A549-13S cells than A549-EV cells (Figure 2.5G). The third upregulated transcript is isocitrate dehydrogenase (NAD(+)) 3 non-catalytic subunit gamma (*IDH3G*) mRNA, which encodes a subunit of the isocitrate dehydrogenase complex. This complex is responsible for the third step of the TCA cycle, the conversion of isocitrate into α -ketoglutarate. *IDH3G* was upregulated 1.5-fold compared to the A549-EV (Figure 2.5J). The following upregulated TCA cycle transcript was oxoglutarate dehydrogenase (*OGDH*) mRNA. This gene encodes a component of the 2-oxoglutarate dehydrogenase complex, which is responsible for the conversion of α -ketoglutarate into succinyl-CoA. *OGDH* expression was three-fold higher in A549-13S cells than A549-EV cells (Figure 2.5K). The final two upregulated TCA cycle transcripts in A549-13S cells encode components of succinyl-CoA synthetase, which is responsible for the conversion of succinyl-CoA to succinate. These transcripts were succinate-CoA ligase GDP-forming subunit beta (*SUCLG2*) mRNA and succinate-CoA ligase ADP-forming subunit beta (*SUCLA2*) mRNA. *SUCLG2* expression was two-fold higher (Figure 2.5M) and *SUCLA2* expression was 1.5-fold higher (Figure 2.5N) in A549-13S cells than A549-EV cells. Interestingly, there were no significant differences in TCA cycle gene expression between the A549-12S cells and the A549-EV cells.

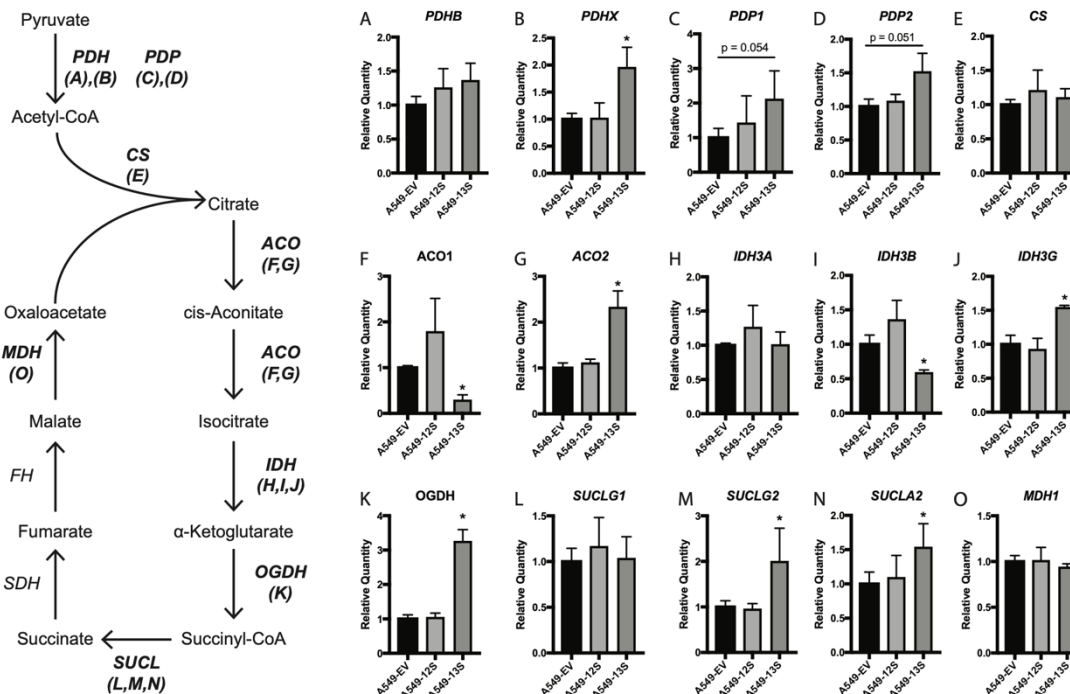


Figure 2.5. Relative expression of mRNA for tricarboxylic acid cycle genes in 13S and 12S expressing A549 cells. (A–O) The mRNA expression for 15 genes encoding components of the tricarboxylic acid (TCA) cycle were measured with qPCR. A549-13S cells displayed upregulated mRNA levels of enzymes involved in the TCA cycle. A549-13S cells had statistically significant upregulation of transcripts encoding six enzymes involved in the TCA cycle (B,G,J,K,M,N) and downregulation of two TCA cycle enzyme encoding transcripts (F,I). In contrast, A549-12S cells did not exhibit any statistically significant differences in TCA cycle transcript expression compared to the A549-EV cells. The geometric mean of two reference genes, *H2AFY* and *ACTB* was used. Asterisks (*) indicate $p < 0.05$. $n =$ three per group for all panels. PDH, pyruvate dehydrogenase; PDP, Pyruvate dehydrogenase phosphatase; CS, Citrate synthase; ACO, Aconitase; IDH, Isocitrate dehydrogenase; OGDH, Oxoglutarate dehydrogenase; SUCLG1, Succinate-CoA ligase GDP/ADP-forming subunit alpha; SUCLG2, Succinate-CoA ligase GDP-forming subunit beta; SDH, Succinate dehydrogenase; FH, Fumarate hydratase; MDH, Malate dehydrogenase.

2.3.5 Oxidative Phosphorylation Genes Are Downregulated in A549-13S Cells

An upregulation of genes involved in the TCA cycle may allow for increased glutaminolysis or anaplerotic pathways rather than impacting cellular respiration. This would likely be reflected in a decrease in the expression of cellular respiration genes, despite the upregulation of TCA cycle genes. We determined the expression levels of two transcripts that encoded components of cellular respiration complex IV, cytochrome C oxidase assembly factor COX16 (*COX16*) mRNA (Figure 2.6A) and cytochrome C oxidase copper chaperone COX17 (*COX17*) mRNA (Figure 2.6B). The expression of both *COX16* and *COX17* was significantly lower in A549-13S cells. This paralleled the decreased oxygen consumption rate observed in A549-13S cells (Figure 2.2B). There were no differences in the expression of these two genes in A549-12S cells when compared to A549-EV cells.

2.3.6 13S E1A Influences Metabolism to a Greater Extent than 12S E1A in HAdV-5 Infected Primary IMR-90 Cells

To determine the physiological relevance of the 13S encoded E1A isoform on cellular metabolic reprogramming in the context of infection, in contrast to the 12S encoded isoform, IMR-90 primary lung fibroblast cells were grown to confluence for 72 hours and infected with mutant HAdV-5 expressing either the 13S or 12S E1A isoforms. Cells were infected with either the *pm975* mutant of HAdV-5, which predominantly expressed the 13S, but not the 12S encoded E1A isoform; the *dl520* HAdV-5 mutant, which predominantly expressed the 12S, but not the 13S isoform; or an E1A-deleted HAdV-5 mutant as a control. RNA from these cells was collected at 16 hours post infection, which corresponds to a relatively early timepoint during infection, at which E1A should be influencing cellular gene expression (Radko et al., 2015). The expression of RNA from these cells was determined using RNAseq.

Expression of the metabolic genes analyzed in the above RT-qPCR experiments was extracted from the RNAseq data allowing for the comparison of *dl520* infected cells versus control virus infected cells, *pm975* infected cells versus control virus infected cells, and *pm975* infected cells versus *dl520* infected cells (Figure 2.7). In terms of glycolytic mRNA

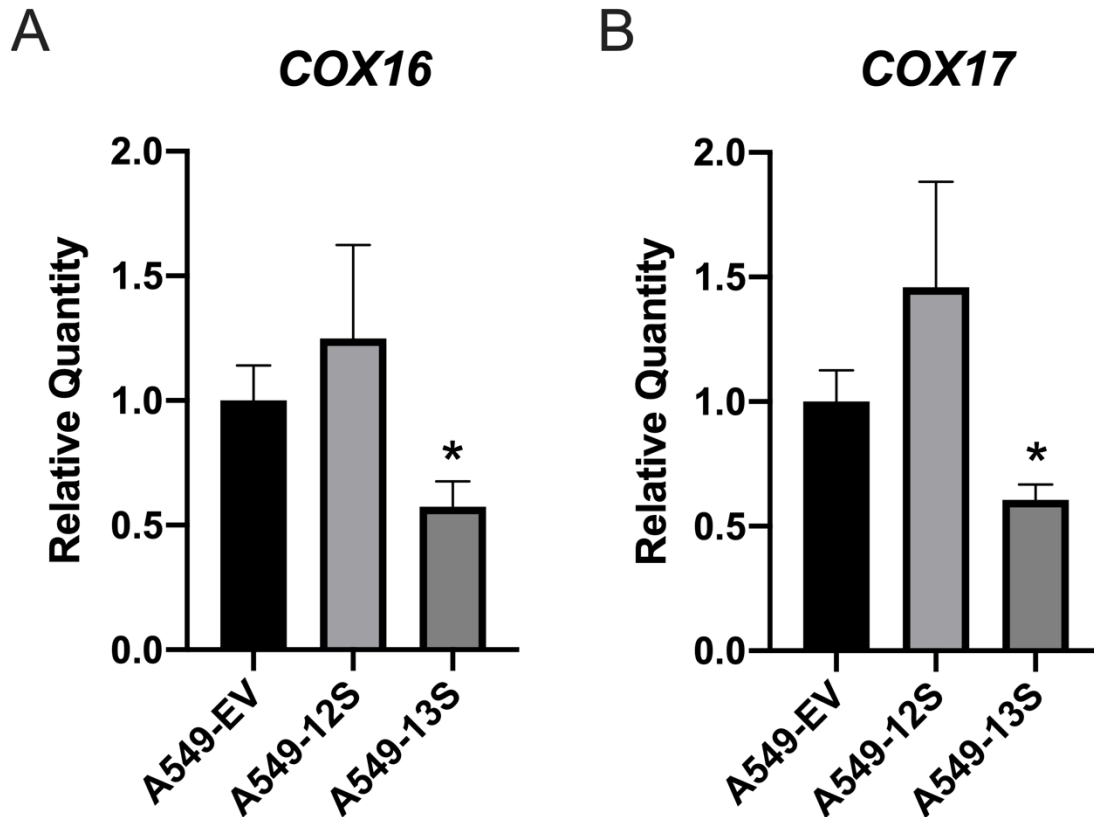


Figure 2.6. Relative expression of mRNA for cellular respiration genes in 13S and 12S expressing A549 cells. The mRNA expression for two genes encoding components of the TCA cycle were measured with qPCR. A549-13S cells exhibit downregulated expression of genes encoding components of cellular respiration complex IV. Both (A) *COX16* and (B) *COX17* mRNA expression was significantly lower in A549-13S cells compared to A549-EV cells. A549-12S cells did not show statistically significant expression differences when compared to A549-12S cells. The geometric mean of two reference genes, *H2AFY* and *ACTB* was used. Asterisks (*) indicate $p < 0.05$. $n =$ three per group for all panels. COX16; Cytochrome C oxidase assembly factor COX16; COX17, Cytochrome C oxidase copper chaperone

expression (Figure 2.7A), 10 of the transcripts were more highly upregulated in *pm975* infected cells than in *dl520* infected cells. In agreement with the A549 cell line results presented above (Figure 2.3), suggesting that the 13S encoded isoform of E1A had a more pronounced role in promoting glycolytic metabolic reprogramming than the 12S encoded isoform during infection. However, both HAdV-5 mutants appeared to upregulate glycolytic transcript expression to a greater extent than E1A-deleted HAdV-5. The expression of transcripts for enzymes in the TCA cycle appeared to be less regulated by E1A at 16 hours post infection than was observed with the A549 cell lines (compare Figure 2.5 and Figure 2.7B). However, there were still some differences in TCA cycle transcript expression between the *pm975* and the *dl520* mutant infections. *PDHB*, *PDP2*, and *SUCLG2* were all more highly downregulated in *pm975* infected cells than in *dl520* infected cells, while *CS*, and *IDH3B* were more highly upregulated. *ACO2*, *IDH3A*, *IDH3G*, *OGDH*, *SUCLA2*, and *MDHI* had higher levels of transcript expression in both *pm975* and *dl520* infected cells when compared to E1A-deleted control HAdV-5 infected cells, but the expression of these transcripts was not significantly different between *pm975* and *dl520* infected cells.

Transcripts encoding enzymes involved in the PPP (Figure 2.7C) appeared to be upregulated in *pm975* infected cells when compared to either *dl520* infected cells or the E1A-deleted control. While the expression of *G6PD* was lower in both *pm975* and *dl520* infected cells when compared to the E1A-deleted control HAdV-5 infected cells, *G6PD* was less drastically downregulated in the *pm975* infected cells. In addition, transcripts for PPP enzymes in the non-oxidative branch, *RPE*, *TKT*, and *TALDO1*, were significantly higher in *pm975* infected cells than either *dl520* or E1A-deleted control HAdV-5 infected cells. The expression of these three genes was significantly lower in the *dl520* infected cells when compared to the E1A-deleted HAdV-5 infections.

Finally, for the two cellular respiration related transcripts, expression of *COX16* showed an upregulation in both *dl520* and *pm975* infected cells when compared to E1A-deleted HAdV-5 control infections, but not to each other. Transcript expression of *COX17* was also up in both *dl520* and *pm975* infections, but this upregulation was less drastic in the *pm975* infected cells when compared to *dl520* infected cells.

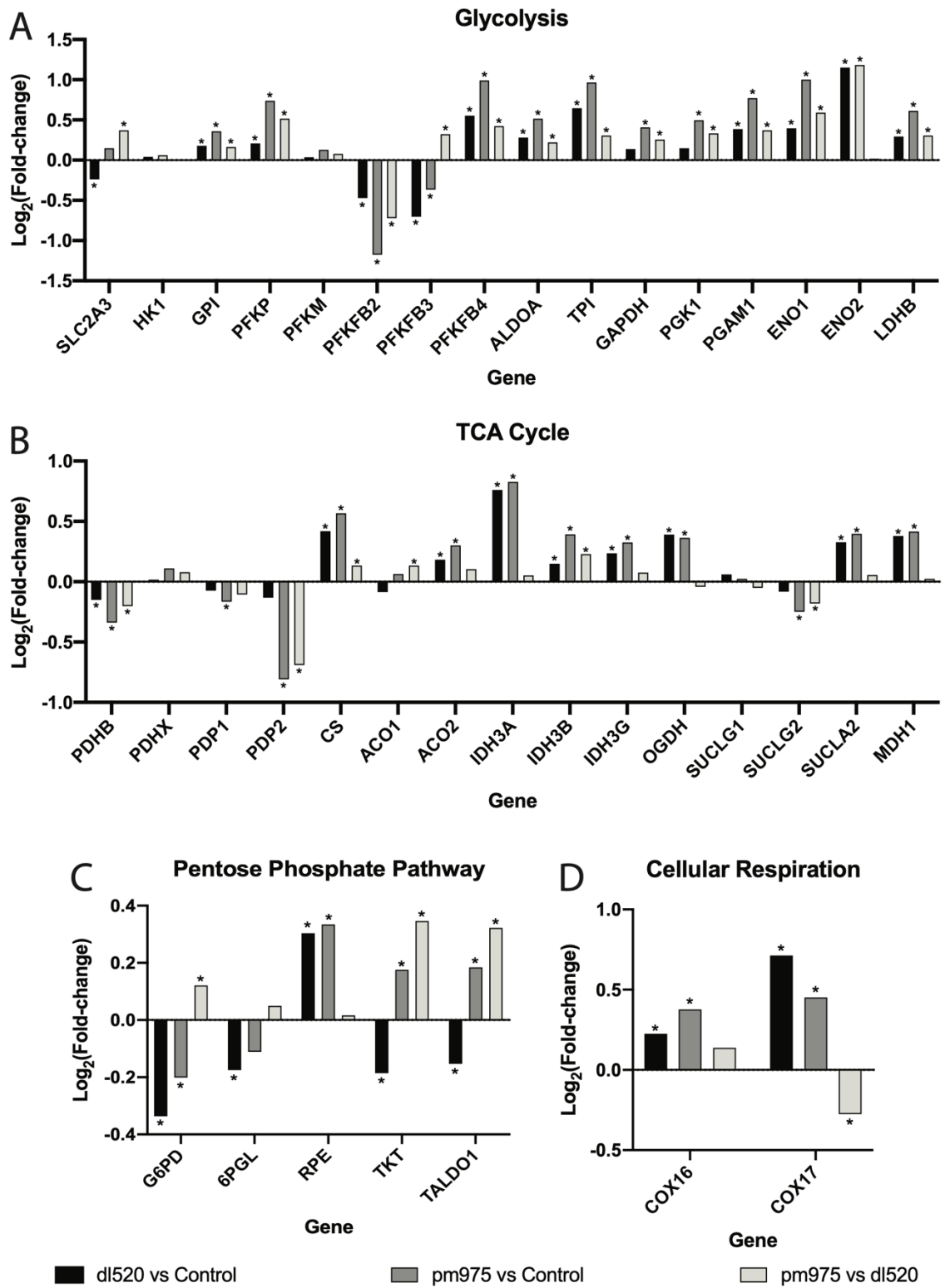


Figure 2.7. RNAseq analysis of metabolic genes from IMR-90 lung fibroblasts infected with either *dl520*, *pm975* or an E1A-deleted HAdV-5 control virus. (A) RNA expression of glycolytic enzyme-encoding transcripts was often greater in *pm975* infected cells than *dl520* infected cells. However, *dl520* infected cells also expressed glycolytic genes at consistently higher levels than in an E1A-deleted control HAdV-5 infection. (B) RNA expression of transcripts encoding TCA cycle enzymes, were more highly up- or downregulated in *pm975* infected cells when compared to *dl520* infected cells. (C) Transcripts encoding PPP intermediates in the non-oxidative PPP branch were more highly upregulated in *pm975* infected cells than in *dl520* infected cells. (D) Both *COX16* and *COX17* transcripts, which encode components of the TCA cycle, are upregulated in both *pm975* and *dl520* infected cells, although to a lesser extent in the *pm975* infection. Asterisks (*) indicate an adjusted p-value < 0.05. n = two per group for all panels. Gene names are defined in Figures 2.3–2.6.

2.4 Discussion

To determine the role that E1A plays in altering cellular metabolism, we investigated the impact of constitutive expression of either of the two major E1A isoforms on the metabolism of A549 lung epithelial cells. Interestingly, A549-13S cells reached a high maximal level of glycolysis after the addition of glucose, unlike the A549-12S cells or the A549-EV controls. The A549-12S and A549-EV cells required the ATP synthase inhibitor oligomycin to reach a maximum ECAR. Oligomycin has been suggested to promote glycolysis by inducing the translocation of GLUT1 glucose transporters to the plasma membrane (Hamrahian et al., 1999). As hypothesized, E1A appeared to be at least partially responsible for controlling these changes at a transcriptional level. In our analysis of the mRNA expression for genes involved in glycolysis, *SLC2A3*, which encodes the glucose transporter GLUT3, was 26-fold higher in the A549-13S cells than the A549-12S or A549-EV cells. This suggests that E1A 13S was also capable of inducing glycolysis through upregulation of glucose transporters, which could explain why the addition of oligomycin to further induce glycolysis was ineffective in these cells. The upregulation of *SLC2A3* transcript expression in only the A549-13S cells may explain why these cells exhibited constitutively high levels of glycolysis while the A549-12S cells did not, despite both cells upregulating some glycolysis genes in comparison to the A549-EV cells. An additional indication that A549-13S cells could functionally upregulate glycolysis while the A549-12S cells could not, was that a greater number of glycolytic genes appeared to be upregulated in the A549-13S cells than the A549-12S cells. However, there were glycolytic transcripts uniquely upregulated in the A549-12S cells and not the A549-13S cells, these being *HK1*, *ALDOA*, and *GAPDH*. Conversely, the glycolytic transcripts *HK1*, *PFKP*, *PFKFB3*, and *ENO2* were uniquely downregulated in A549-13S cells. Both of these results suggested that the regulation of glycolysis by E1A may not be solely dependent on direct transcriptional regulation. The products of these transcripts with apparently paradoxical up- or downregulation in relation to the functional glycolytic extracellular flux data could be regulated post-transcriptionally in an appropriate manner. This could include regulation of metabolic enzymes with post-translational modifications, competition between metabolite intermediates, and feedback loops (reviewed in (Watson et al., 2015; Wegner et al., 2015; Wellen and Thompson, 2012)). Future work exploring how E1A influences

metabolism through these mechanisms could reveal the extent that E1A regulates metabolism in ways unrelated to transcription.

Many metabolic pathways use glycolytic intermediates as precursors. For example, the PPP relies on glucose-6-phosphate as a precursor to produce the ribose sugar backbone of nucleotides (Figure 2.4). However, while *6PGL*, from the oxidative branch of the PPP, was upregulated in the A549-13S cells, expression of *G6PD* from the oxidative branch was downregulated. In addition, the expression of two genes encoding enzymes from the nonoxidative branch of the PPP, *TKT* and *TALDO1*, were both lower. This suggests that E1A 13S inhibited the PPP. Peak nucleotide production occurs at time points that follow peak E1A expression (Valdés et al., 2018). Perhaps E1A 13S plays a role in modulating the timing of nucleotide production by downregulation of the PPP. It is also interesting to note that none of the A549-12S cells had any statistically significant differences in mRNA expression in the PPP when compared to the A549-EV cells, which may further support the idea that the E1A 12S isoform was not involved in the regulation of metabolism during infection.

The TCA cycle is another metabolic pathway that utilizes glycolytic products to provide biosynthetic intermediates that can be utilized in other pathways. The TCA cycle also pulls electrons from intermediates to later produce energy through the electron transport chain. Interestingly, the TCA cycle gene that had the highest level of expression in the A549-13S cells was *OGDH*, which was three-fold higher than in A549-EV cells. OGDH is a subunit of the α -ketoglutarate dehydrogenase complex, which is responsible for converting α -ketoglutarate into succinyl-CoA. Cells that utilize aspartate for anaplerotic metabolism are particularly reliant on OGDH (Allen et al., 2016), which suggests that the TCA cycle in A549-13S cells may be utilized for biomolecule synthesis. In addition, the α -ketoglutarate dehydrogenase complex represents a key step of glutaminolysis (Mullen et al., 2012), which again points towards A549-13S cells utilizing the TCA cycle for biosynthetic metabolic reactions rather than the electron transport chain. Two genes, *SUCLG2* and *SUCLA2*, which encode components of succinyl-CoA synthetase, the complex which immediately follows α -ketoglutarate dehydrogenase in the TCA cycle, were also uniquely upregulated in the A549-13S cells. Succinyl-CoA synthetase activity has also been

implicated in anaplerotic metabolism (Stark et al., 2009). Finally, there is an opposing upregulation of *IDH3G* and downregulation of *IDH3B* in A549-13S cells, both of which encode components of isocitrate dehydrogenase, the complex immediately preceding the α -ketoglutarate dehydrogenase complex in the TCA cycle. However, *IDH3B* has been suggested to be a hub gene that drives tumour associated cellular pathways (Chou et al., 2014), and it could be functioning in a similar manner when its expression is potentially driven by E1A 13S. A decreased rate of functional cellular respiration in the A549-13S cells, combined with lower expression of *COX16* and *COX17* in these cells is another indication that the TCA cycle is being reprogrammed for biosynthetic or anaplerotic reactions.

It should also be noted that the A549 parent cell line, used to generate the cell lines expressing either the 13S or 12S encoded isoforms of E1A, is derived from a human epithelial lung carcinoma. This means at baseline it is expected that this cell line would exhibit some aspects of the Warburg effect in relation to a primary cell line from the same tissue. However, as the A549-13S cells exhibited a drastic increase in glycolysis and drastic decrease to cellular respiration when compared to either the A549-12S or A549-EV cell lines, this reveals the existence of overriding effects of the 13S encoded E1A isoform on host-cell metabolic reprogramming. It is possible that if a similar experiment were conducted using transduced lung primary cell lines, an even more drastic upregulation of glycolysis and downregulation of cellular respiration might be observed. While this study shows that the 13S encoded isoform of E1A will likely influence metabolism in primary cells, it does not definitively exclude the possibility that 12S encoded E1A isoform could have lesser effects on reprogramming primary cell metabolism to more closely resemble the Warburg effect.

The question remains as to how these two different E1A isoforms may specifically influence metabolism in the context of adenovirus infection. Considering that HAdV infected cells tend to exhibit an upregulation of glycolysis and a downregulation of oxidative phosphorylation (Carinhas et al., 2017; Thai et al., 2014) similar to the A549-13S cells in this study, it is likely that this isoform contributes to metabolic reprogramming during HAdV infection. The effect of the 13S isoform on metabolism may be especially

predominant as expression of the 12S isoform is typically three times higher than the 13S isoform when both are at their peak at approximately 24 hours post infection (Radko et al., 2015).

To explore this question, RNAseq data from IMR-90 cells infected for 16 hours were analyzed for expression of the genes used for our qPCR analysis. In terms of glycolysis, the 13S encoded isoform of E1A altered expression of these genes to a greater extent than the 12S encoded isoform. However, a lesser upregulation of glycolysis-related transcript expression was also observed in cells infected with the HAdV-5 mutant that expressed the 12S E1A isoform compared to the control virus infected cells. This suggests that while the 13S isoform likely plays a more significant role in the upregulation of glycolysis during infection, the 12S isoform may still influence glycolysis. While changes in the expression of TCA cycle transcripts did not appear to be greatly different between the *pm975* and *dl520* infected cells, TCA cycle transcripts were still much higher than control virus infected cells. It is possible that the TCA cycle is partially upregulated at 16 hours post infection to provide some of the substrates and energy required for viral replication, and this is driven in part by E1A. In addition, some of the upregulated transcripts were unique to *pm975* HAdV-5 infected cells, which matches our qPCR data in which A549 cells expressing the 13S isoform uniquely upregulated a greater number of different TCA cycle genes compared to cells expressing the 12S isoform.

Interestingly, transcripts encoding enzymes in the nonoxidative branch of the PPP were uniquely upregulated in cells infected with *pm975*, again suggesting that the 13S encoded isoform of E1A promotes host-cell metabolic activity during infection. Although this was opposite to the observed downregulation of nonoxidative branch PPP transcripts observed in A549-13S cells, in both cases the 13S encoded isoform of E1A appears to be regulating the PPP. It appears that during *dl520* infection, the 12S isoform is downregulating the nonoxidative branch of the PPP. Finally, and unexpectedly, the two examined transcripts encoding components of cellular respiration, *COX16* and *COX17* were upregulated in both *dl520* and *pm975* infected cells. This could imply that at this early infection timepoint, the infected cell is being driven into a highly metabolically active state to promote viral replication, and cellular respiration may contribute to this process, at least marginally. It

would be useful to determine whether the 13S encoded E1A isoform coordinates a downregulation of cellular respiration transcripts at later stages of infection.

In addition, although the smaller isoforms of E1A, such as the 9S, 10S and 11S encoded E1A isoforms become more predominant during later stages of infection (Radko et al., 2015), it is unclear whether they would contribute to regulation of host-cell metabolism during HAdV infection. Perhaps they could modulate metabolic pathways regulated during later stages of infection, such as nucleotide production, but this remains to be explored.

Understanding how viruses alter host-cell metabolic processes during infection could yield insight into potential antiviral interventions. For example, understanding the parallels between HAdV-5 metabolic reprogramming of infected host cells with that of other viruses, such as influenza (Smallwood et al., 2017), could have implications for the universal treatment of viruses with compounds that target similar viral processes during infection. In addition, this study provides more evidence for the outsized role the 13S encoded isoform of E1A could have in deregulating host-cell processes during HAdV infection. As the 13S encoded isoform differs from the 12S encoded isoform of E1A by CR3, this region could represent a unique and targetable weak point of HAdV. For example, the 13S encoded E1A isoform is especially important for productive lytic infection of HAdV in A549 cells, while the 12S encoded isoform is less efficient at promoting HAdV induced lysis (Moran et al., 1986). It would be interesting to determine whether simply modulating metabolic pathways upregulated by the 13S encoded isoform would be enough to hinder productive HAdV infection.

2.5 Conclusions

The purpose of this study was to determine whether either of the two major isoforms of HAdV-5 E1A, the 13S or the 12S encoded isoforms, were able to modulate cellular metabolism in cell lines that endogenously expressed these proteins. The difference between the 13S and 12S encoded isoforms is the presence or absence of the CR3 region in the larger major E1A protein (Hošek et al., 2016), which targets and modulates the activity of a distinct set of host-cell regulatory proteins that are primarily involved in transcriptional regulation (Ablack et al., 2010; Gallimore and Turnell, 2001). Given the

similarity between these E1A isoforms, differences in metabolic function or the transcription of metabolic genes between these two isoforms is likely related to the presence of this region. Interestingly, we observed that A549-13S cells had robust glycolytic capacity and reduced cellular respiration when compared to A549-12S or A549-EV cells. This corresponded to a unique upregulation of transcripts encoding enzymes involved in glycolysis and a downregulation of transcripts encoding enzymes involved in cellular respiration in the A549-13S cells compared to the other lines. This was also accompanied by a downregulation of PPP transcripts in A549-13S cells, and an upregulation of TCA cycle transcripts consistent with anaplerotic metabolism. This enhanced upregulation of glycolysis was also apparent in primary IMR-90 lung fibroblasts infected with a HAdV-5 mutant virus that expressed the 13S isoform of E1A. E1A is a viral oncoprotein (Boulanger and Blair, 1991), and it is also interesting that the larger E1A isoform can reprogram metabolism in a manner that resembles the Warburg effect, including an upregulation of baseline glycolysis and downregulation of cellular respiration. This work strongly suggests that E1A is an additional HAdV protein capable of influencing cellular metabolism.

Chapter 3

3 Survival-Associated Metabolic Genes in Human Papillomavirus-Positive Head and Neck Cancers

3.1 Introduction

As of 2018, head and neck squamous cell carcinomas (HNSCC), namely cancers of the oral cavity, oropharynx, nasopharynx, larynx, and hypopharynx, had the 8th highest combined incidence rate and the 5th highest 5-year prevalence as interpreted from GLOBOCAN data (Bray et al., 2018; Ferlay et al., 2018). This translates to 834,860 new head and neck cancers per year and 2,164,271 active head and neck cancers within the past five years worldwide (Bray et al., 2018; Ferlay et al., 2018). Recent incidence rates of some oropharyngeal cancers, such as those of the tonsils and base of the tongue, have been rapidly increasing due to high-risk human papillomavirus (HPV) infection (de Martel et al., 2017). Infection by specific high-risk HPVs, such as HPV16, was only recognized as a contributing factor for oropharyngeal cancer by the International Agency for Research on Cancer in 2003 (Herrero et al., 2003). However, the number of oropharyngeal cancers caused by HPV has risen at epidemic rates over the last decades in many parts of the world (Michmerhuizen et al., 2016), while the number of HNSCCs caused by exposure to mutagens from excessive smoking and drinking has been decreasing (Chaturvedi et al., 2011).

HPV-positive (HPV+) HNSCCs are distinct from their HPV-negative (HPV-) counterparts from a molecular perspective, with characteristic genetic, epigenetic, and protein expression profiles (Gameiro et al., 2018; Seiwert et al., 2015; Worsham et al., 2013). In addition, patient outcomes are generally far more favorable for HPV+ than HPV- HNSCC (Fakhry et al., 2008). The underlying molecular reasons for this difference are not entirely clear. However, approximately 10% of all HPV+ HNSCC patients still succumb to their disease (Weller et al., 2017). Identification of prognostic markers predicting favorable survival outcomes in patients could allow for treatment deintensification, thereby avoiding potential lifelong complications from unnecessarily aggressive treatments. Alternatively, identification of cellular pathways contributing to poor prognosis could lead to the

development of new effective therapies for those not responding to the current standard of care.

Altered metabolism is a cancer hallmark that was recognized decades ago with the discovery of the Warburg effect, also known as aerobic glycolysis (Lunt and Vander Heiden, 2011). Aerobic glycolysis involves an upregulation of glycolysis despite the presence of ample oxygen for efficient cellular respiration. Many tumours exhibit this metabolic phenotype, as it provides rapid energy and an ample supply of precursors for macromolecule biosynthesis. Tumours can also rely on cellular respiration, often via glutaminolysis, which is the breakdown of glutamine into intermediates of the tricarboxylic acid (TCA) cycle (Vander Heiden and DeBerardinis, 2017). TCA intermediates can be funneled off for macromolecule biosynthesis. Many viruses are known to extensively modulate cellular metabolic processes to facilitate infection (Goodwin et al., 2015). These changes can include similar tumour-associated metabolic changes as described above. Infection with HPV has been shown to phenocopy cancer-like metabolic changes that are maintained in HPV+ HNSCC (Fleming et al., 2019). Examination of how the metabolic phenotype differs between HPV+ and HPV- HNSCC could lead to the identification of targetable metabolic changes and potential new treatment options that are specific for either HPV+ HNSCCs or HPV- HNSCCs. Admittedly, cancer metabolism is complex as it impinges on a variety of other cellular processes and can vary across an individual tumour (Montrose and Galluzzi, 2019). In addition, tumours can be highly adaptive to metabolic perturbations (Montrose and Galluzzi, 2019). Identifying multiple metabolic targets that are specific to a cancer type from a large dataset that contains information from an extensive number of tumours, such as The Cancer Genome Atlas (TCGA), is an ideal step towards selecting or generating useful anti-metabolic cancer therapeutics.

In this study, we used RNA-seq data from over 500 HNSCC primary tumour samples from the TCGA to comprehensively compare the expression of genes across key cellular metabolic pathways between HPV+, HPV-, and normal-adjacent control tissues. Expression of a number of metabolic genes were significantly altered in HPV+ versus HPV- HNSCC. Specifically, genes involved in glycolysis were expressed at lower levels in HPV+ compared to HPV- HNSCC. In contrast, genes involved in the TCA cycle,

oxidative phosphorylation, and β -oxidation exhibited higher expression in HPV+ samples compared to their HPV- counterparts. Importantly, we identified that low expression of multiple metabolic genes—*SDHC*, *COX7A1*, *COX16*, *COX17*, *ELOVL6*, *GOT2*, and *SLC16A2*—correlated with markedly improved patient survival in HPV+, but not HPV- HNSCC. The products of these genes could potentially be exploited as targets for therapeutic intervention. Furthermore, the low expression of these seven genes appears useful in predicting improved overall survival in HPV+ HNSCC and could serve as biomarkers of patient outcome.

3.2 Materials and Methods

3.2.1 Data collection

Level 3 RNA-seq by Expectation Maximization normalized Illumina HiSeq RNA expression data (build 2016012800) for the TCGA HNSC cohort, was downloaded from the Broad Genome Data Analysis Centers Firehose server (<https://gdac.broadinstitute.org/>). Patient survival data for the TCGA HNSC cohort, as reported by the Pan-Cancer Atlas (The Cancer Genome Atlas Research Network et al., 2013) was downloaded from: <https://www.cell.com/cms/10.1016/j.cell.2018.02.052/attachment/f4eb6b31-8957-4817-a41f-e46fd2a1d9c3/mmc1.xlsx>.

3.2.2 RNA expression comparisons

RNA-seq by Expectation Maximization normalized expression data for the TCGA HNSC cohort was extracted and analyzed as described previously (Gameiro et al., 2017). Briefly, primary patient samples with known HPV status were manually grouped as HPV+, HPV-, or normal-adjacent control tissue based on other previously published datasets (Bratman et al., 2016; The Cancer Genome Atlas Network, 2015). In these datasets, HPV status was assigned by aligning RNA-seq reads for the HPV oncogenes expressed in the tumours to the different high risk HPV types. This resulted in 73 HPV+, 442 HPV-, and 43 normal-adjacent control samples with data available for gene expression comparisons. Note that all HPV+ samples had high risk HPV as follows: HPV16 (61 samples), HPV33 (8 samples), HPV35 (3 samples), and HPV56 (1 sample). The five-number summary, mean, and pairwise statistical tests were calculated using R (version 3.4.0) for all 229 metabolic

genes analyzed (see supplementary table 3.1). These 229 genes were manually selected (supplementary table 3.1) as they are involved in eight central cellular metabolic pathways or processes, of which cellular respiration was then separated into its respective complexes. The number of genes examined from each pathway was as follows: glycolysis, 36 genes (adapted from GO:0061621 and (Bolaños et al., 2010)); TCA cycle, 20 genes (adapted from GO:0006099 and (Chen and Russo, 2012)); mitochondrial respiratory complex I, 43 genes (adapted from GO:0045333, GO:0046043 and (Sharma et al., 2009)); mitochondrial respiratory complex II, 4 genes (adapted from GO:0045333, GO:0046043 and (Kluckova et al., 2013)); mitochondrial respiratory complex III, 9 genes (adapted from GO:0045333, GO:0046043 and (Guo et al., 2016; Owens et al., 2011)); mitochondrial respiratory complex IV, 31 genes (adapted from GO:0045333, GO:0046043 and (Mansilla et al., 2018)); mitochondrial ATPase, 16 genes (adapted from GO:0046043 and (Jonckheere et al., 2012)); fatty acid synthesis, 21 genes (adapted from GO:0019368, GO:0046949, GO:0006629 and (Currie et al., 2013; Guillou et al., 2010; Koundouros and Poulgiannis, 2019; Kuo and Ann, 2018)); β -oxidation, 18 genes (adapted from GO:0003995, GO:0003985, GO:0004300 and (Houten and Wanders, 2010)); glutaminolysis, 7 genes (adapted from GO:0004069, GO:0004352, GO:0004359, GO:0004021 and (Jin et al., 2016)); pentose phosphate pathway, 11 genes (GO:0006098 and (Patra and Hay, 2014)); monocarboxylic acid transport (MCT) family, 13 genes (adapted from GO:0008028 and (Fleming et al., 2019)). Boxplot comparisons of gene expression were made with GraphPad Prism v7.0 (Graphpad Software, Inc., San Diego, California, USA). For the boxplots, center lines show the medians, box limits indicate the 25th and 75th percentiles, and whiskers extend 1.5 times the interquartile range from the 25th and 75th percentiles. P-values were assigned using a two-tailed non-parametric Mann-Whitney U test using Graphpad Prism. Bivariate analysis for selected genes was performed through R (version 3.4.0) using the Spearman rank correlation coefficient. The proportion of genes in each pathway that were up or downregulated among each comparison was represented in a bar graph and was calculated as follows: number of genes upregulated (or downregulated) in a comparison (e.g., HPV+ HNSCC vs HPV- HNSCC) divided by the total number of genes in that pathway. The proportion of downregulated genes were represented as a negative value.

3.2.3 Survival analysis

Five-year overall survival outcomes were compared in both HPV+ and HPV- subsets of HNSCC patients dichotomized by median expression for all metabolic genes listed in supplementary table 3.1. Log-rank statistical p-values were calculated for each Cox survival model. The derived log-rank p-values for all tested genes (listed in supplementary table 3.2) were assessed for significance after correcting for false discovery rate (FDR) using the Benjamini–Hochberg method, and an FDR threshold of 0.1 was set for significance. Univariate analysis was performed through R (version 3.4.0) based on a Cox Proportional Hazard Model using the survival package (version 2.41-3). Stepwise bidirectional multivariate analysis was then carried out with clinical variables (sex, age, subsite, T stage, N stage, Overall stage, and HPV type), and *SDHC*, *COX7A1*, *COX16*, *COX17*, *ELOVL6*, *GOT2*, and *SLC16A2* expression—low expression of these 7 genes were found to be statistically correlated with improved survival after univariate analysis. The p-values derived from the Wald test on survival coefficients were reported for investigated variables. Furthermore, a second set of survival outcomes were determined to compare HPV+ tumours expressing low levels of each combination of genes that were significantly correlated with improved survival after multivariate analysis—*COX16*, *COX17*, and *SLC16A2*.

3.2.4 Gene Enrichment Analysis

We performed a gene enrichment analysis on our seven survival-associated genes using the Go Enrichment Analysis feature on <http://geneontology.org> (Ashburner et al., 2000; The Gene Ontology Consortium, 2018). This analysis is powered by PANTHER14.1 (PANTHER Overrepresentation Test) using the “GO cellular component complete” annotation data set with a Fisher’s exact test followed by a calculation of false discovery rate (cut-off = FDR $P < 0.05$) to determine statistical significance (Mi et al., 2019).

3.2.5 Analysis of differential cell line sensitivity to tyrosine kinase inhibitors based on HPV status

B-scores (mean \pm SEM) reflecting drug activity were extracted from a previously conducted high throughput drug screen using 27 HNSCC cell lines (Ghasemi et al.,

2018). The average B-scores for the indicated tyrosine kinase inhibitors (TKIs) was calculated for the 6 HPV+ and 21 HPV- HNSCC lines and plotted.

3.3 Results

3.3.1 Expression of Pathway-specific Metabolic Genes were Altered Between HPV+, HPV-, and Normal Control Samples from The TCGA HNSC Cohort

In order to identify differences in metabolic gene expression between HPV+ and HPV- HNSCC, we analyzed the TCGA Illumina HiSeq RNA expression dataset from the HNSC cohort for expression of 229 metabolic genes in central metabolic pathways (supplementary table 3.1). This clinical cohort is comprised of 73 HPV+, 442 HPV-, and 43 normal control samples with available RNA-seq data. Significant differences were seen in a subset of genes in each pathway between HPV+ and HPV- HNSCC. In addition, significant changes were observed between either HPV+ HNSCC or HPV- HNSCC and normal control tissue. To simplify interpretation of these differences, we plotted the fraction of genes in each pathway that were significantly different for each pairwise comparison (Figure 3.1).

This analysis illustrates that glycolytic genes in HPV- HNSCC tissue are more upregulated in comparison to normal tissue than in HPV+ HNSCC when compared to normal tissue. This is particularly evident between HPV+ HNSCC and HPV- HNSCC tissues, since most glycolytic genes are downregulated in HPV+ HNSCC when compared to HPV- HNSCC. However, genes involved in the TCA cycle, oxidative phosphorylation, and β -oxidation were downregulated in both HPV+ and HPV- HNSCC in comparison to normal control tissue. This means that, despite differences in metabolic gene expression between HPV+ and HPV- HNSCC, the metabolism of both types of tumours could resemble the Warburg effect, with lower cellular respiration rates compared to normal control tissue. When compared to one another, HPV+ HNSCC had generally higher expression of these genes than HPV- HNSCC. Other metabolic pathways appeared to have a more similar split between upregulated and downregulated genes in all comparisons, suggesting that the presence of HPV may have minimal impact on transcriptionally mediated changes in these pathways. Overall, it appears that HPV+ HNSCC may be more reliant on cellular

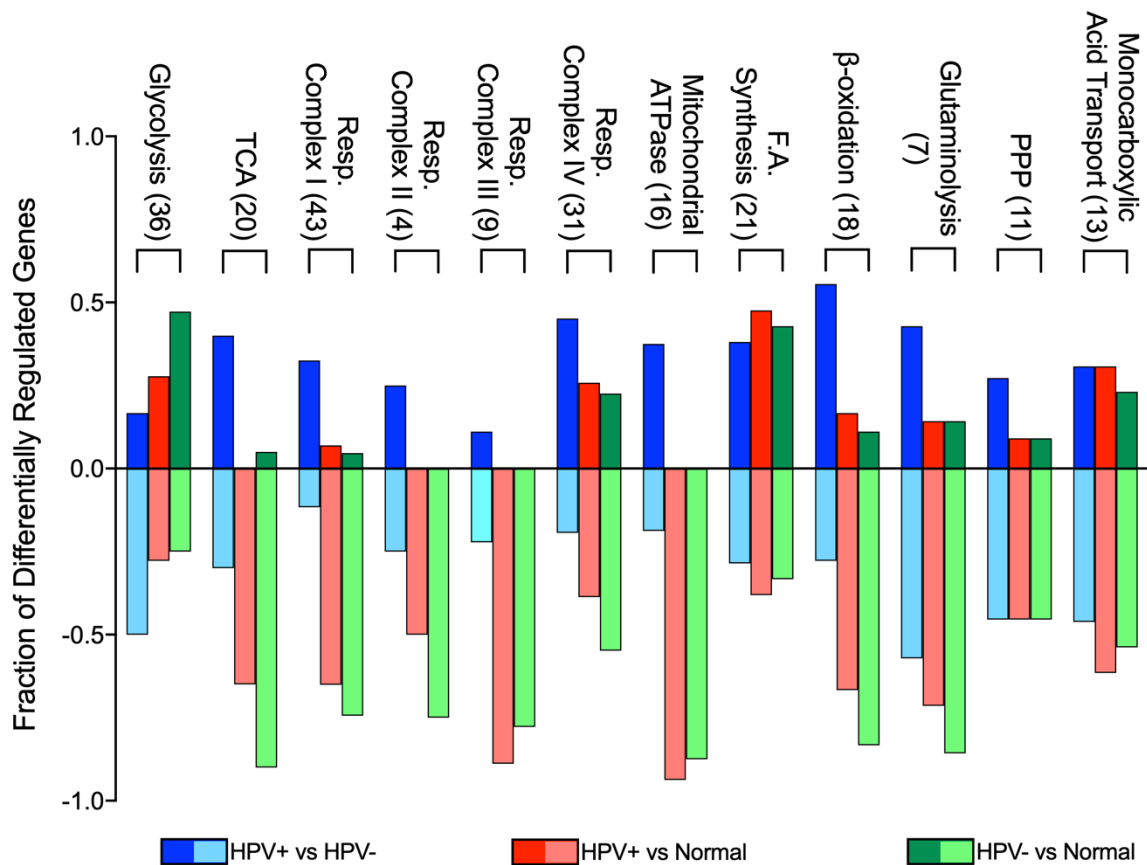


Figure 3.1. Genes differentially expressed between HPV-positive (HPV+) head and neck squamous cell carcinomas (HNSCC), HPV-negative (HPV-) HNSCC, and normal control tissues by metabolic pathway. The y-axis reflects the proportion of genes that are up or downregulated in a given pathway comparison. For example, the positive fraction of genes reflects the proportion of genes upregulated in the first group (e.g., HPV+) when compared to the second group (e.g., HPV-). The negative fraction of genes reflects the proportion of genes downregulated in the same comparison. Blue = HPV+ tissue vs HPV- tissue comparison; Red = HPV+ tissue vs normal control tissue comparison; Green = HPV- tissue vs normal control tissue comparison. Numbers in brackets denote total number of genes analyzed from each pathway. Abbreviations: TCA, tricarboxylic acid cycle; Resp., respiratory; F.A., fatty acid; PPP, pentose phosphate pathway.

respiration than HPV- HNSCC.

3.3.2 Low Expression of Genes Encoding Multiple Components of the Mitochondrial Electron Transport Chain are Associated with Improved Patient Survival in HPV+ HNSCC

Tumour-associated metabolic alterations have functional consequences that impact disease progression, response to therapy, and patient survival. We dichotomized the expression data for each of the 229 metabolic genes by median expression and calculated the impact of high versus low expression on overall patient survival for HPV+ HNSCC patients, as well as HPV- HNSCC patients (supplementary table 3.2). We identified seven genes that were significantly associated with patient survival in HPV+, but not HPV- HNSCC patients. These genes were *SDHC*, part of the mitochondrial respiratory complex II; *COX7A1*, *COX16*, and *COX17*, all part of the mitochondrial respiratory complex IV; *ELOVL6*, involved in fatty acid elongation; *GOT2*, involved in amino acid metabolism; and *SLC16A2* (also known as *MCT8*), which encodes a thyroid hormone transporter. We performed a pathway enrichment analysis of our seven significant genes utilizing a PANTHER overrepresentation test which indicated that 5 of these 7 genes were significantly associated with the mitochondria ($p = 5.10 \times 10^{-5}$; FDR = 1.46×10^{-2}). These genes were *SDHC*, *COX7A1*, *COX16*, *COX17*, and *GOT2*. Detailed studies of the relative expression of each of these genes in HPV+, HPV- and normal control tissue, as well as their association with overall patient survival are presented below.

Previous studies indicate that HPV+ HNSCC is more reliant on oxidative phosphorylation as an energy source than HPV- HNSCC (Fleming et al., 2019). Oxidative phosphorylation requires electron transport via mitochondrial cellular respiratory complexes I-IV (Enríquez, 2016). Reduced expression of *SDHC*, which encodes a component of the mitochondrial cellular respiration complex II, correlated with increased HPV+ HNSCC patient survival (Figure 3.2).

Overall expression of *SDHC* was not significantly different between HPV+ and HPV- HNSCC, and both types of HNSCC expressed lower levels of *SDHC* than normal control

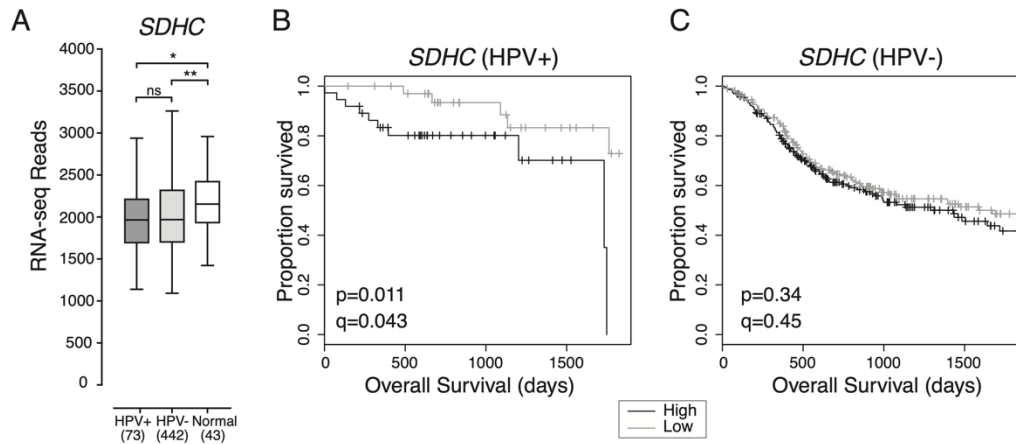


Figure 3.2. Low expression of SDHC is associated with favorable survival outcomes in HPV+ HNSCC.

(A) Transcript levels of SDHC across all HNSCC tissues samples and normal control tissues. Bracketed numbers refer to the sample size of each group.

Overall five-year survival outcomes in (B) HPV+ HNSCC and (C) HPV- HNSCC patients dichotomized by SDHC expression. p = Two-sided log-rank test, q = Benjamini-Hochberg FDR method. Gray = low transcript expression, Black = high transcript expression. * $p \leq 0.05$, ** $p \leq 0.01$, ns (not significant).

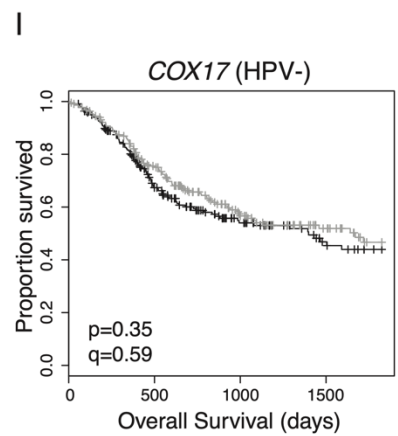
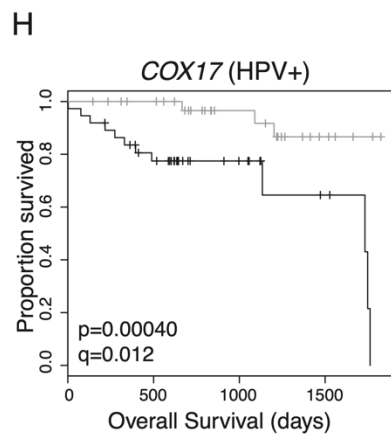
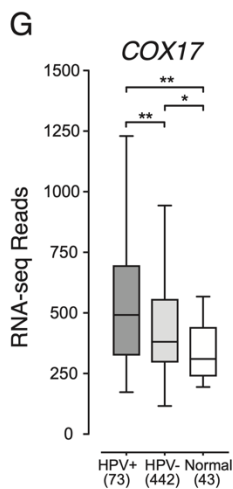
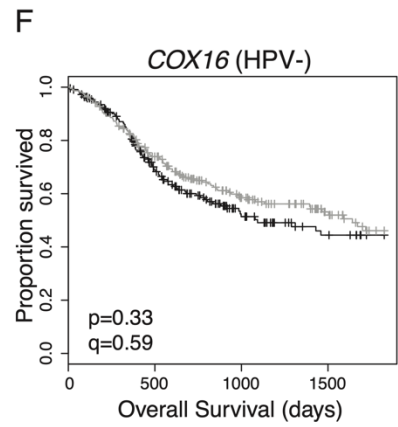
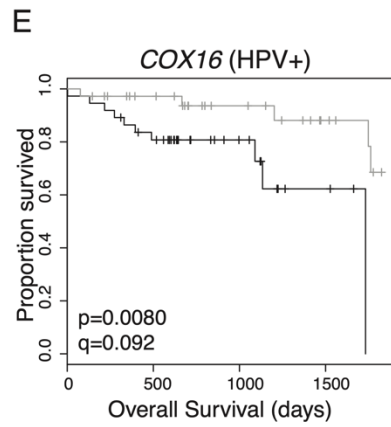
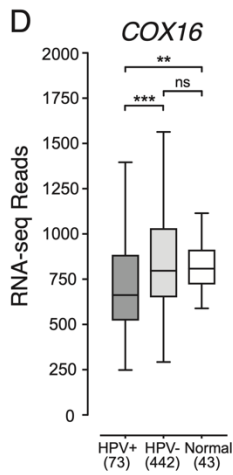
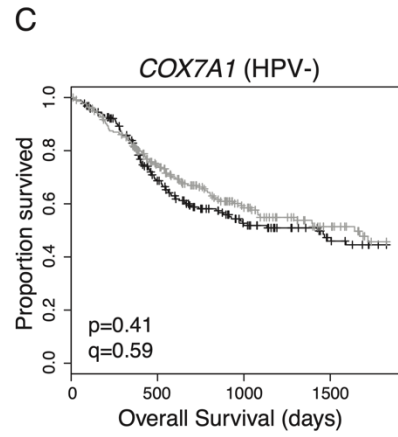
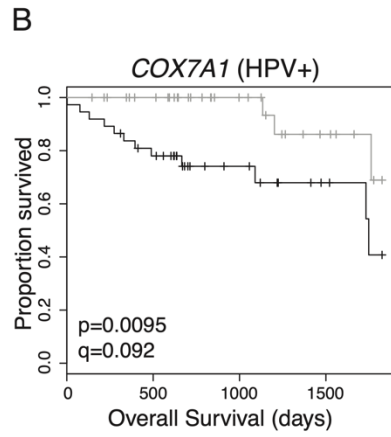
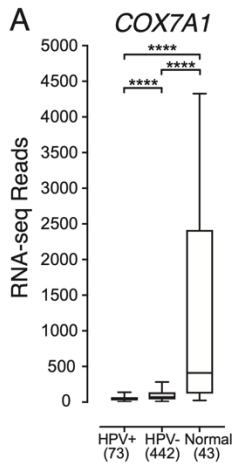
tissue (Figure 3.2A). HPV+ HNSCC patients with tumours exhibiting low *SDHC* expression had better overall five-year survival outcomes than HPV+ HNSCC patients with tumours exhibiting high *SDHC* expression ($p = 0.011$, FDR = 0.043) (Figure 3.2B). However, *SDHC* expression was not correlated with improved patient survival in HPV- HNSCC ($p = 0.34$, FDR = 0.45) (Figure 3.2C).

Consistent with the possibility that HPV+ HNSCCs are more reliant on cellular respiration than HPV- HNSCCs, three genes encoding components of the mitochondrial cellular respiration complex IV were also correlated with HPV+ HNSCC patient survival (Figure 3.3). These genes were *COX7A1* and *COX17*, which encode structural components of complex IV, and *COX16*, whose product is involved in complex IV assembly.

COX7A1 expression was significantly lower in both HPV+ and HPV- HNSCC samples compared to normal control tissues (Figure 3.3A). In addition, HPV+ HNSCC had significantly lower expression of *COX7A1* than HPV- HNSCC (Figure 3.3A). Overall survival of patients with HPV+ (Figure 3.3B) or HPV- HNSCC (Figure 3.3C) were dichotomized based on median *COX7A1* expression. We found that low expression of *COX7A1* was correlated with favourable survival outcomes in patients with HPV+ ($p = 0.0095$, FDR = 0.092) (Figure 3.3B), but not HPV- HNSCC ($p = 0.41$, FDR = 0.59) (Figure 3.3C).

Compared to normal control tissue, *COX16* expression was lower in HPV+, but not in HPV- HNSCC (Figure 3.3D). *COX16* expression was also significantly lower in HPV+ compared to HPV- HNSCC (Figure 3.3D). HPV+ and HPV- HNSCC samples were dichotomized based on median *COX16* expression. Low levels of *COX16* expression were correlated with improved survival in patients with HPV+ ($p = 0.0080$, FDR = 0.092) (Figure 3.3E), but not in patients with HPV- HNSCC ($p = 0.33$, FDR = 0.59) (Figure 3.3F).

In contrast to *COX7A1* and *COX16*, *COX17* expression was higher in HPV+ than HPV- HNSCC (Figure 3.3G). Expression of *COX17* across HPV+ and HPV- HNSCC samples was significantly higher than in normal control tissues (Figure 3.3G). However, the same



— High
— Low

Figure 3.3. Low expression of three mitochondrial respiration complex IV genes in HPV+ HNSCC is associated with improved survival. Expression of (A) *COX7A1*, (D) *COX16*, and (G) *COX17* in HNSCC tissues samples and normal control tissues. Overall 5-year survival outcomes in HPV+HNSCC patients and HPV- HNSCC dichotomized by median (B,C) *COX7A1* expression, (E,F) *COX16* expression, and (H,I) *COX17* expression. p = Two-sided log-rank test, q = Benjamini-Hochberg FDR method. Gray = low transcript expression, Black = high transcript expression. * $p \leq 0.05$, ** $p \leq 0.01$, *** $p \leq 0.001$, **** $p \leq 0.0001$, ns (not significant)

association between low expression of *COX17* and better overall 5-year patient survival was observed for patients with HPV+ HNSCC ($p = 0.00040$, FDR = 0.012) (Figure 3.3H), but not patients with HPV- HNSCC ($p = 0.35$, FDR = 0.59) (Figure 3.3I).

3.3.3 Low Expression of *ELOVL6*, Involved in Fatty Acid Synthesis, is Associated with Better Overall Survival in Patients with HPV+ HNSCC

ELOVL6 expression in HPV+ HNSCC was not significantly different from HPV- HNSCC. However, both HPV+ and HPV- HNSCC had significantly lower overall levels of *ELOVL6* expression than normal control tissues (Figure 3.4A). HPV+ HNSCC samples were dichotomized based on median *ELOVL6* expression. HPV+ patients with tumours expressing low levels of *ELOVL6* had significantly better five-year overall survival than patients with tumours expressing high levels of *ELOVL6* ($p = 0.0040$, $q = 0.084$) (Figure 3.4B). Reduced *ELOVL6* expression was not correlated with altered survival in HPV- HNSCC patients ($p = 0.34$, $q = 0.83$) (Figure 3.4C).

3.3.4 Low Expression of *GOT2*, Involved in Amino Acid Metabolism, is Associated with Better HPV+ HNSCC Patient Survival

GOT2 expression was significantly lower in HPV+ than HPV- HNSCC or normal control tissues and significantly lower in HPV- HNSCC than normal control tissues (Figure 3.4D). The high normalized RNA-seq read levels for *GOT2* suggest that it is abundantly expressed in normal head and neck tissues. HPV+ HNSCC samples were dichotomized based on median *GOT2* expression. Low expression of *GOT2* was associated with better five-year overall survival outcomes in patients with HPV+ HNSCC ($p = 0.012$, $q = 0.086$; Figure 3.4E). Although low *GOT2* expression appeared to be significantly correlated with favourable patient survival in HPV- HNSCC ($p = 0.029$; Figure 3.4F), it lost its significance after correcting for FDR ($q = 0.20$).

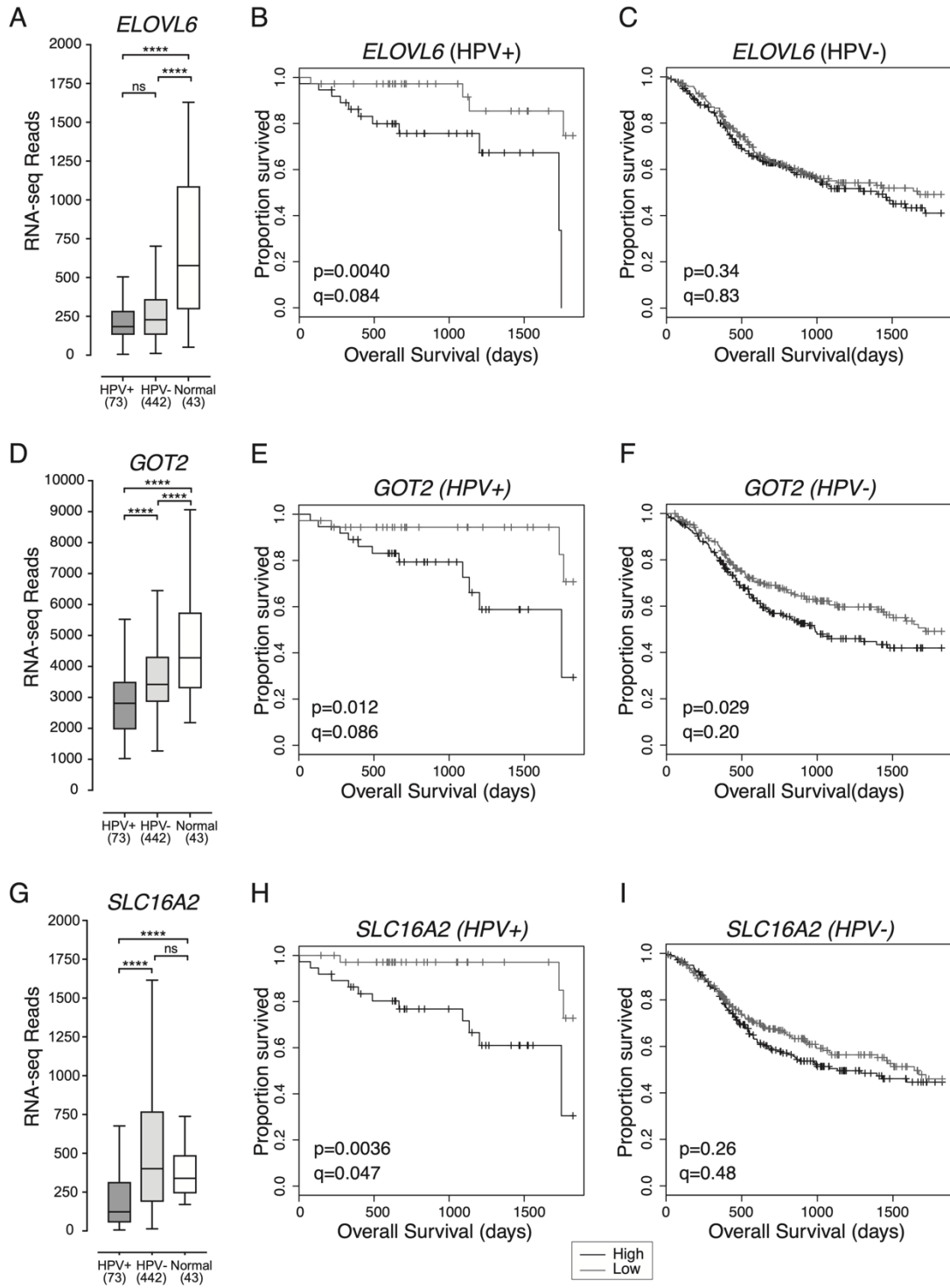


Figure 3.4. Low expression of ELOVL6, GOT2 and SLC16A2 is associated with improved patient survival in HPV+ HNSCC. Expression of (A) *ELOVL6*, (D) *GOT2*, and (G) *SLC16A2* in HPV+, HPV- HNSCC tissue samples and normal control tissues. Overall five-year survival outcomes in HPV+ HNSCC and HPV- HNSCC patients dichotomized by median (B,C) *ELOVL6* expression, (E,F) *GOT2* expression, and (H,I) *SLC16A2* expression. p = Two-sided log-rank test and q = Benjamini-Hochberg FDR method. Gray = low transcript expression, Black = high transcript expression. **** p ≤ 0.0001, ns (not significant)

3.3.5 Low Expression of SLC16A2, a Thyroid Hormone Transporter, in HPV+ HNSCC is Associated with Better Overall Survival.

Increased expression of the monocarboxylic acid transporter family member, *SLC16A1* (*MCT1*) was recently reported to be associated with poor survival outcomes in HNSCC (Fleming et al., 2019). Although, expression of *SLC16A1* was significantly higher than normal head and neck tissues for both HPV+ and HPV- HNSCC, and expression of *SLC16A1* was higher in HPV- HNSCC than HPV+ HNSCC, the impact of differential expression of *SLC16A1* on overall survival in either HPV+ or HPV- HNSCC was not significant ($p > 0.05$). Of the various family members, only expression of *SLC16A2* (*MCT8*), whose main function is thyroid hormone transport, appeared to be associated with altered overall survival (Figure 3.4G-I).

Expression of *SLC16A2* was significantly lower in HPV+ HNSCC when compared to either HPV- HNSCC or normal control tissues (Figure 3.4G). HPV+ HNSCC samples were dichotomized based on median *SLC16A2* expression. Again, low expression of *SLC16A2* was associated with improved patient survival in HPV+ HNSCC patients ($p = 0.0036$, FDR = 0.047) (Figure 3.4H), but not in patients with HPV- HNSCC ($p = 0.26$, FDR = 0.48) (Figure 3.4I).

3.3.6 COX16, COX17, and SLC16A2 are Independently Correlated with Favourable Survival Outcomes in HPV+ HNSCC

To determine the extent that each of the HPV+ HNSCC survival-associated genes could influence patient outcomes, we generated a hazard ratio (HR) for each gene and a variety of clinical variables by univariate analysis (Table 4.1). Each HR describes the relative increase in risk of death for the first variable x vs y (Spruance et al., 2004). As expected, the HR for each metabolic gene was significantly below 1, indicating a greatly reduced risk of death. In contrast, a comparison of the oral cavity vs the oropharynx subsites for HPV+ HNSCC generated a hazard ratio of 2.82, indicating that HPV+ HNSCC in the oral cavity is associated with a 2.82x increased risk of mortality compared to oropharynx.

As the contribution of these genes to overall survival might not be independent of one another, we also analyzed the relationship between survival and gene expression for all

Table 3.1. Univariate and multivariate analysis of the association of clinical variables and expression of metabolic genes with overall survival in HPV+ HNSCC.

	Variables	Univariate		Multivariate	
		HR (95% CI)	P value	HR (95% CI)	P value
Sex	Male vs Female	0.81 (0.18–3.62)	0.78		
Age	per every additional year	0.99 (0.94–1.04)	0.74		
Subsite	Oral cavity vs Oropharynx	2.82 (1.02–7.80)	0.045	13.59 (2.67–69.11)	0.002
	Larynx vs Oropharynx	1.52×10^{-8} (0–Inf)	1.00	3.67×10^{-10} (0–Inf)	1.00
	Hypopharynx vs Oropharynx	1.57×10^{-8} (0–Inf)	1.00	1.10×10^{-8} (0–Inf)	1.00
T Stage	T3–T4 vs T1–T2	1.03 (0.36–2.91)	0.96		
N Stage	N2b–N3 vs N0–N2a	0.41 (0.14–1.19)	0.10		
Overall Stage	IV vs I–III	0.76 (0.26–2.24)	0.62		
HPV Type	33, 35, 56 vs 16	3.33 (1.14–9.78)	0.028	16.88 (3.24–87.88)	0.0008
<i>COX16</i>	Low vs High Expression	0.19 (0.05–0.72)	0.015	0.059 (0.009–0.39)	0.003
<i>COX17</i>	Low vs High Expression	0.13 (0.03–0.47)	0.002	0.03 (0.003–0.35)	0.005
<i>COX7A1</i>	Low vs High Expression	0.22 (0.06–0.77)	0.018	0.25 (0.04–1.56)	0.14
<i>ELOVL6</i>	Low vs High Expression	0.17 (0.04–0.65)	0.009		
<i>GOT2</i>	Low vs High Expression	0.24 (0.07–0.79)	0.019		
<i>SDHC</i>	Low vs High Expression	0.23 (0.07–0.77)	0.018		
<i>SLC16A2</i>	Low vs High Expression	0.17 (0.04–0.63)	0.008	0.07 (0.01–0.37)	0.002

survival-associated metabolic genes and clinical variables concurrently by multivariate analysis (Table 4.1). The hazard ratios for *COX16*, *COX17*, and *SLC16A2* remained significant, indicating that low expression of each of these genes is a significant, and potentially independent, contributor to overall survival. *COX7A1* had a minor contribution to survival in this model. The multivariate model also included subsite (oral cavity vs. oropharynx) and HPV type as significant contributing factors to survival as previously reported in the literature (Bratman et al., 2016; Chatfield-Reed et al., 2020; Goodman et al., 2015; O'Rourke et al., 2012).

To test whether concurrent low expression of these genes had an additive effect on survival, we stratified the HPV+ HNSCCs into groups, based on high expression or low expression for a combination of any two of these seven survival-associated genes. When survival of HPV+ HNSCC patients with low expression of both *COX16* and *COX17* in their tumours was compared to survival of patients with high expression of both genes, survival was significantly greater in the *COX16* and *COX17* double low expression group ($p = 0.0015$) (Figure 3.5A). In patients with low expression of both *COX16* and *SLC16A2*, survival was almost 100% until approximately 4.75 years and significantly better ($p = 0.0021$) than samples expressing high levels of both genes (Figure 3.5B). In patients with low expression of both *COX17* and *SLC16A2* (Figure 3.5C), survival was 100%, which was significantly higher than patients expressing high levels of both *COX17* and *SLC16A2* ($p = 0.00027$; Figure 3.5C).

Figure 3.6 shows that there was no significant correlation between the expression of *SLC16A2* and *COX16* or *SLC16A2* and *COX17*. This provides further evidence that the improved survival associated with low expression for each of these genes may occur independently of one another. Additionally, the multivariate analysis indicates that *COX16* and *COX17* independently contribute to survival despite the correlation between these two genes (Figure 3.6).

3.4 Discussion

Our analysis identified many changes in expression of metabolism-associated genes between HPV+ and HPV- HNSCC when compared to normal control tissues. The

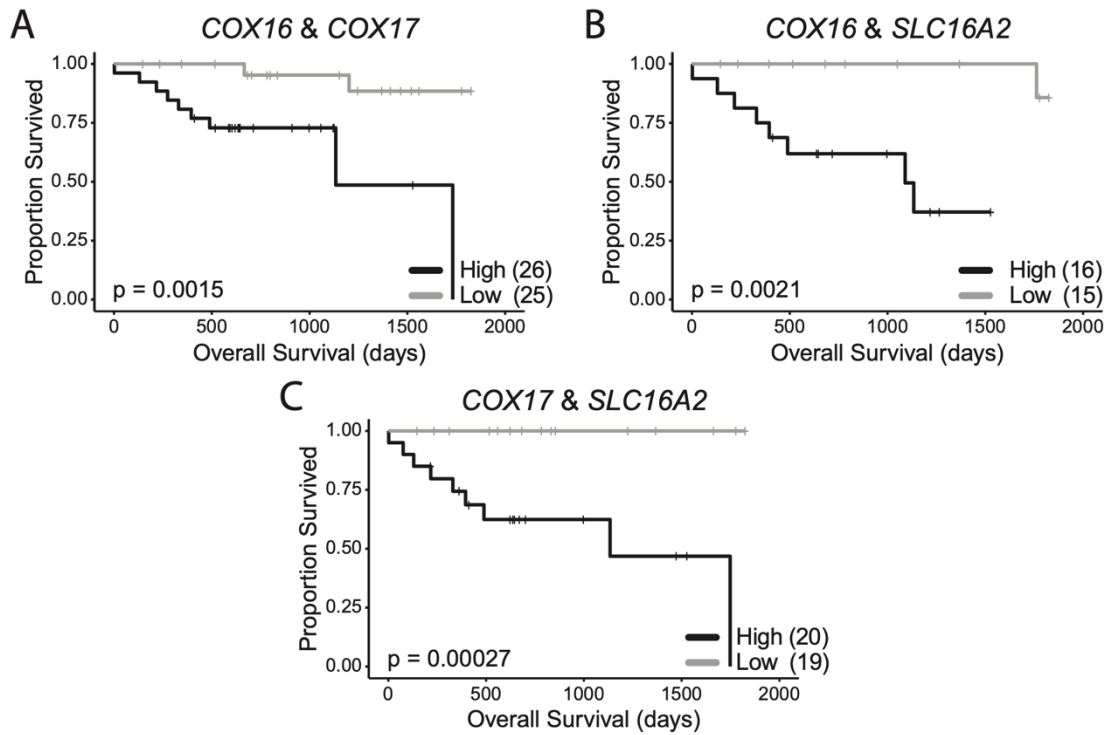


Figure 3.5. HPV+ HNSCC patient survival stratified by double low or double high expression of survival-associated metabolic genes. (A) *COX16* and *COX17*, (B) *COX16* and *SLC16A2*, (C) *COX17* and *SLC16A2*. Comparisons made with a two-sided log-rank test. Gray = low transcript expression, Black = high transcript expression. Bracketed value indicates number of HPV+ HNSCCs with double high or double low expression for genes of interest.

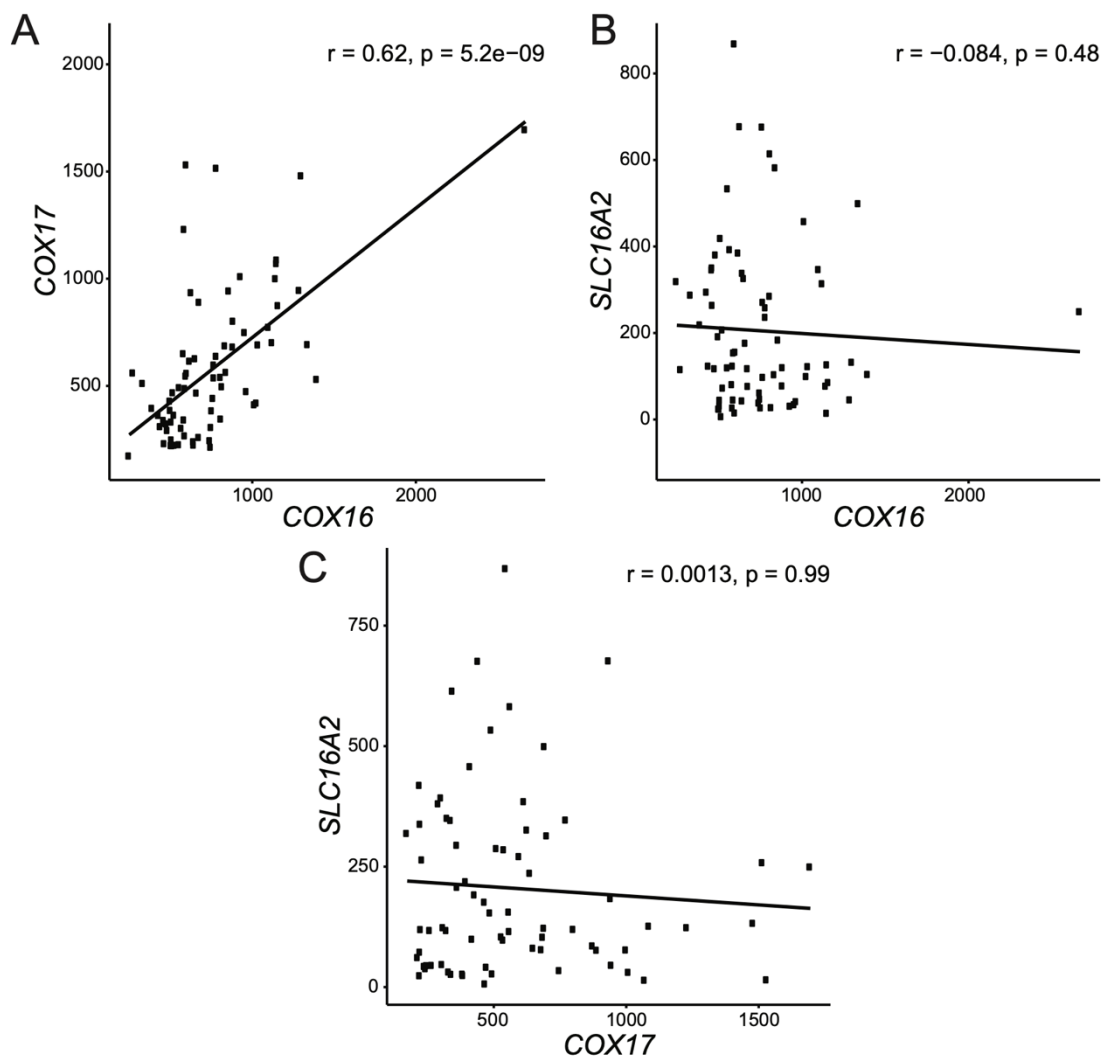


Figure 3.6. Correlation plots of independently significant genes identified by multivariate analysis. (A) Expression *COX16* and *COX17* were significantly correlated ($r=0.62$, $p=5.2 \times 10^{-9}$) in HPV+ HNSCCs. **(B)** Expression *SLC16A2* and *COX16* were not correlated ($r=-0.084$, $p=0.48$). **(C)** Expression of *SLC16A2* and *COX17* were not correlated ($r=0.0013$, $p=0.99$).

expression of seven genes was predictive of survival for HPV+ HNSCC patients. In each case, reduced expression correlated with improved survival, suggesting that reduced tumour cell metabolism is prognostically favorable. None of these genes were associated with altered survival in HPV- HNSCC, reinforcing the concept that HPV+ and HPV- HNSCC are distinct tumour entities (Gameiro et al., 2017, 2018; Seiwert et al., 2015; Worsham et al., 2013). This is not unexpected, as E6 from HPV16 and HPV18 can increase the expression of mitochondrial cellular respiration genes in a head and neck cancer cell line (Cruz-Gregorio et al., 2019), which matches our observation of increased expression of these genes in HPV+ HNSCCs when compared to HPV- HNSCCs. In addition, E6 and E7 may also be responsible for perturbing glycolysis in HPV+ cervical cancer cells (Guo et al., 2014; Ma et al., 2019), which could explain our observation of increased expression of glycolytic genes in HPV+ HNSCC as compared to normal control tissues. Interestingly, most of the survival-associated genes we identified in our study can be inhibited by small molecule inhibitors as outlined below.

As shown in our results, limiting *SDHC* may serve as a unique target in virally transformed HPV+ HNSCCs. *SDHC* encodes part of mitochondrial respiratory complex II, for which a few selective inhibitors exist. α -tocopheryl succinate (α -TOS) is a vitamin E analogue, which has selective growth inhibitory properties for some human cancer cells (Neuzil et al., 2007). α -TOS can induce apoptosis by increasing the levels of reactive oxidative species (ROS), triggering stress response pathways (Neuzil et al., 2007). α -TOS is also effective at inhibiting tumour growth (Kanai et al., 2010) in *in vivo* xenograft mouse models. Interestingly, α -TOS inhibited growth of several HNSCC cell lines *in vitro* and *in vivo* (Gu et al., 2008). Given that all of these experiments were done using HPV- HNSCC, α -TOS may be even more toxic to HPV+ HNSCCs based on the correlation between *SDHC* expression and HPV+ HNSCC survival outcomes we observed.

Specific small molecule inhibitors for both the *COX7A1* and *COX16* gene products have not yet been identified. However, as both are part of mitochondrial respiratory complex IV, it is possible that the complex IV inhibitors ADDA 5 (Oliva et al., 2016) and tetrathiomolybdate (Kim et al., 2015) could prove useful to phenocopy any metabolic effects associated with low gene expression, promoting enhanced survival in HPV+

HNSCC. It is also important to note that COX16 is an inhibitor of p53 activity, which means that non-mitochondrial functions of COX16 should not be discounted (Siebring-van Olst et al., 2017). E6 has been shown to inhibit expression of COX16 (Butz et al., 1999), which may contribute to the lower levels observed in HPV+ versus HPV- HNSCC (Figure 3.3D). MitoBloCK-6 is an inhibitor of mitochondrial respiratory complex IV that specifically targets the COX17 protein (Dabir et al., 2013). Whether inhibition of cellular respiration is less effective in HPV- HNSCCs because they are already more oxidatively stressed than HPV+ HNSCCs (The Cancer Genome Atlas Network, 2015), perhaps as a result of being less adapted to utilize cellular respiration, is an open question.

Two inhibitors of ELOVL6 were able to reduce the fatty acid composition of hepatocytes and the liver in a murine model of obesity (Shimamura et al., 2009, 2010), but the effects of these compounds on cancer cells have not been explored. Another potential druggable target to influence ELOVL6 expression is ATP citrate lyase (ACLY), which has a wide variety of inhibitors (Granchi, 2018). Expression of ELOVL6 has been shown to decrease concurrently with ACLY inhibition (Migita et al., 2014). Whether ELOVL6 inhibition would reduce the growth of HPV+ HNSCC cell lines remains to be examined.

In our study, we found that low expression of *GOT2* was associated with statistically significant survival in both groups ($p < 0.05$). However, only expression of *GOT2* in our HPV+ HNSCC group met the FDR cut-off of $q = 0.1$. This means that while *GOT2* may be important for survival outcomes in both HPV+ and HPV- HNSCC, it is likely that it has a more substantial contribution to patient survival in HPV+ HNSCC. In breast cancer, sensitivity to a nucleotide synthesis inhibitor, methotrexate, has been linked to high *GOT2* expression (Hong et al., 2019). This is likely due to the function of *GOT2* in providing aspartate for nucleotide biosynthesis (Hong et al., 2019). It is possible that HPV+ HNSCCs, or potentially any HNSCCs expressing high levels of *GOT2*, may be sensitive to methotrexate, but this remains to be explored.

SLC16A2 encodes a plasma membrane T3/T4 transporter. Once inside the cell, T3/T4 can bind nuclear and mitochondrial-localized thyroid hormone receptors, which are key regulators of mitochondrial biogenesis (Weitzel and Alexander Iwen, 2011). As HPV+

HNSCC may be more reliant on cellular respiration than HPV- HNSCC, it is possible that inhibiting SLC16A2-mediated thyroid hormone transport across the plasma membrane could preferentially inhibit ATP generation in HPV+ HNSCCs. Some TKIs, such as sunitinib, imatinib, dasatinib, and bosutinib, may inhibit SLC16A2 (Braun et al., 2012). These TKIs are already employed to treat a wide variety of cancers and are being evaluated for the treatment of HNSCC (Schmitz et al., 2014). As such, they may be especially suitable for the treatment of HPV+ HNSCCs expressing *SLC16A2* at high levels. We extracted data from our previous study of 27 HNSCC cell lines (6 HPV+ and 21 HPV- HNSCC cell lines) examining the effects of a variety of agents on cell growth and proliferation, including the TKI inhibitors mentioned above (Ghasemi et al., 2018). Of the TKIs tested, dasatinib was selectively cytotoxic to HPV+, but not HPV- HNSCC cell lines (Figure 3.7), suggesting that it could be used as a treatment for HPV+ HNSCC that expresses high levels of *SLC16A2*. A flavonoid, silychristin, also inhibits SLC16A2 (Johannes et al., 2016), but has not been studied in cancer models. Other antithyroid hormones used to treat hyperthyroidism, such as carbimazole, methimazole, and potassium perchlorate, could preferentially inhibit HPV+ HNSCC by mimicking inhibition of the SLC16A2 transporter. In one study, methimazole was used to experimentally treat patients with end-stage solid tumours and resulted in improved survival (Hercbergs et al., 2015). High levels of thyroid hormone can promote proliferation of some cancers (Hercbergs et al., 2018), and thyroid hormone mimetics which function as antagonists, such as tetraiodothyroacetic acid (tetrac) and triiodothyroacetic acid (triac) appear to exhibit an antiproliferative effect on breast cancer (Hercbergs et al., 2018) and T cell lymphomas (Cayrol et al., 2019).

While our univariate analysis of all seven genes confirmed that their expression was significantly correlated with survival, our multivariate analysis indicated that *COX16*, *COX17*, and *SLC16A2* were independently associated with overall survival. This suggested that the collective changes in the expression of these three genes could be a powerful predictor of clinical outcome. This was supported by our observation that the overall survival for the group of patients exhibiting simultaneously low expression of any two of these genes was far better than those simultaneously expressing high levels. Thus, expression of these genes may have prognostic utility. Furthermore, *COX16*, *COX17*, and

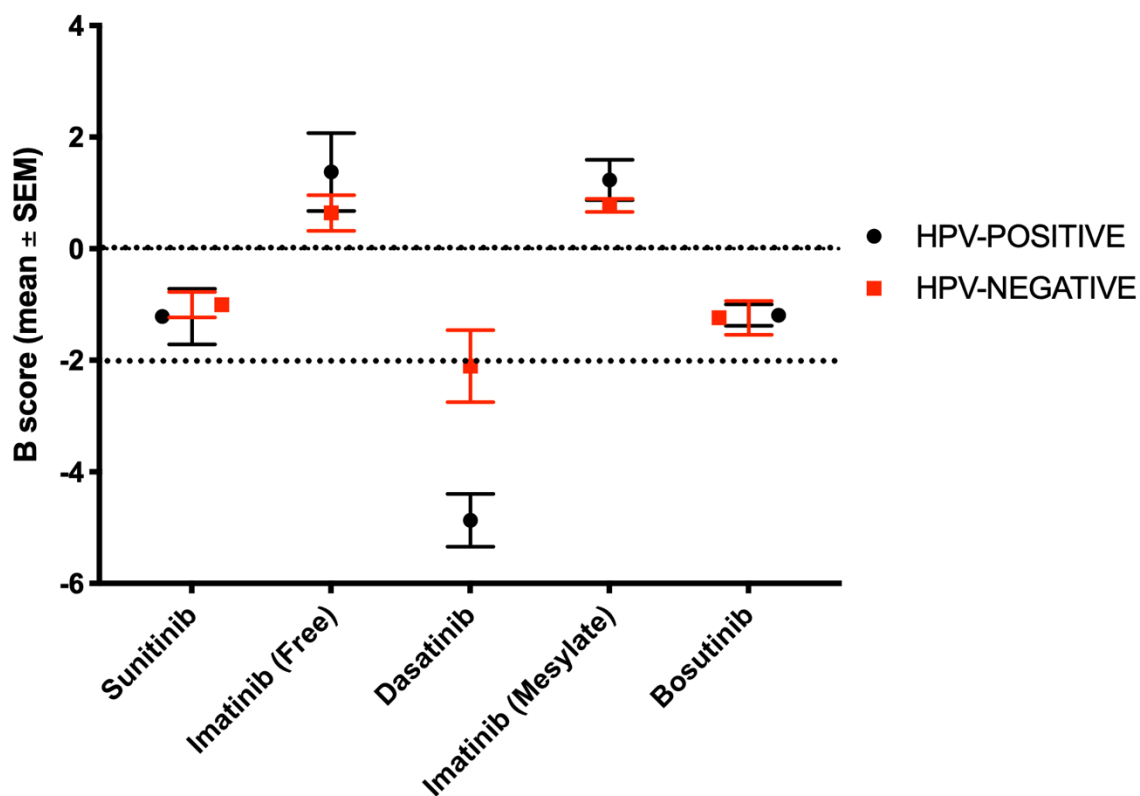


Figure 3.7. Tyrosine kinase inhibitor activity in 27 HNSCC cell lines based on HPV status. B-scores +/- SEM were calculated for HPV+ and HPV- HNSCC cell lines from a high throughput drug screen. Active drugs exhibit a B-score below -2. Red line = HPV-, Black line = HPV+. Figure adapted from data from a previously published study by the Mymryk and Nichols labs (Ghasemi et al., 2018).

SLC16A2 may represent attractive therapeutic targets for HPV+ HNSCC that warrant further exploration, especially considering that treatment with specific inhibitors may phenocopy the effects of low expression of these metabolic genes.

It is important to be cognizant of the limitations to this kind of study. One limitation to this study was the lack of protein data in the TCGA to corroborate the HPV+ HNSCC mRNA expression data. This is an important consideration, as levels of protein expression do not necessarily mirror mRNA expression (Fortelny et al., 2017). As with any high throughput dataset, batch effects that result from processing could be reflected in the data (Leek et al., 2010). In addition, the RNA-seq data contained within the TCGA reflects average mRNA expression within the whole tumour and does not identify expression differences between the various tumour cells as could be obtained from single-cell RNA sequencing platforms (Aran et al., 2015; Hwang et al., 2018). However, the bulk of the tissue that was sequenced is of tumour origin (Aran et al., 2015). Also, it is important to be aware that the TCGA contains HNSCC data from a single, albeit high quality, cohort and it would be useful to validate these genes of interest in other cohorts in the future. Finally, the concept of biomarker identification itself has its own caveats. Specifically, all of the survival-associated genes we identified in this study are only correlated with survival, which does not equal causation (Kaelin, 2017). In addition, as with all studies of this type, there exists the possibility that these correlations are due to chance or occur as the result of another confounder (Kaelin, 2017). However, despite these limitations, the seven metabolic genes identified in this study provide an interesting starting point for considering the metabolic differences between HPV+ and HPV- HNSCC as new prognostic markers or potential targets for therapy.

3.5 Conclusions

In summary, our analysis of HNSCC TCGA data stratified by HPV status indicated that the metabolic profile of HPV+ and HPV- HNSCC are strikingly different. HPV- HNSCCs may utilize glycolysis to a greater extent than HPV+ HNSCCs, while HPV+ HNSCCs may be more reliant on the TCA cycle, cellular respiration, and β -oxidation than HPV- HNSCCs. Despite this difference, both types of HNSCCs likely exhibit far less cellular

respiration than normal head and neck tissues, consistent with a cancer-associated Warburg phenotype (Pavlova and Thompson, 2016). Importantly, expression of genes involved in mitochondrial complex II and mitochondrial complex IV were associated with survival for HPV+ HNSCC patients. Namely, low expression of *SDHC*, *COX7A1*, *COX16*, or *COX17* was associated with better survival outcomes. Low expression of *ELOVL6*, involved in fatty acid elongation; *GOT2*, involved in amino acid metabolism; and *SLC16A2*, involved in thyroid hormone transport, were also all associated with better survival outcomes in HPV+ HNSCC patients. However, of these genes, only *COX16*, *COX17* and *SLC16A2* were independently correlated with survival outcomes according to our multivariate analysis. Importantly, *COX16*, *COX17*, and *SLC16A2* were associated with near 100% survival in all patients with low expression of any two of these genes. The products of these genes may represent useful new therapeutic targets for HPV+ HNSCC, as inhibition of their functions could phenocopy the metabolism of those tumours with low levels of metabolic gene expression, leading to improved survival in HPV+ HNSCC patients.

Chapter 4

4 Expression and patient survival associations for metabolic enzyme genes in Epstein-Barr virus associated gastric cancer

4.1. Introduction

Altered metabolism is a hallmark of a variety of cancers (Pavlova and Thompson, 2016). The first metabolic changes in cancer cells were observed in the 1920s with the discovery of the Warburg effect (Warburg, 1925), otherwise known as aerobic glycolysis. Aerobic glycolysis is an upregulation of glycolysis that occurs despite the presence of ample oxygen that would otherwise favour cellular respiration in most non-cancerous dividing cells. Since this time, it has becoming increasingly appreciated that the metabolic alterations that accompany cancer can vary drastically between cancer types. For example, many tumours also upregulate glutaminolysis (Jin et al., 2016), which is the breakdown of glutamine into constitutive components that can be utilized in the tricarboxylic acid (TCA) cycle for energy production or as precursors to other macromolecules required by the rapidly growing cancer cells. There are even unusual examples of tumours that preferentially upregulate and utilize cellular respiration (Vasan et al., 2020). In addition, fatty acid metabolism (Currie et al., 2013) and nucleotide metabolism (Patra and Hay, 2014) are two other pathways that are frequently reprogrammed during oncogenesis. In light of the complexity and interconnected nature of cellular metabolism and the potential for these pathways to vary from cancer to cancer, it is important to understand how metabolism is altered in specific cancer types in comparison to the corresponding non-cancerous tissue.

Gastric cancers, of which approximately 95% are stomach adenocarcinomas, can be divided into four different subtypes based on their molecular signature. These types are i) Epstein-Barr virus (EBV)-associated gastric cancer (EBVaGC), ii) microsatellite instable gastric cancer (MSI GC), which are highly mutated, iii) genomically stable gastric cancer (GS GC), which carry driver mutations primarily in genes encoding Rho-family proteins, and iv) those with chromosomal instability (CIN GC), with significant aneuploidy (Bass et al., 2014). As is the case with a variety of other cancers that can be subdivided based on

molecular characteristics, such as with human papillomavirus (HPV)-positive and negative head and neck squamous cell carcinoma (HNSCC) (Prusinkiewicz et al., 2020), it is quite likely that metabolic characteristics vary between these four subtypes. Interestingly, the majority of viruses, including EBV, reprogram cellular metabolism in a manner that can resemble the metabolic program of cancer cells (Goodwin et al., 2015). In terms of virally-induced cancers, including EBVaGC, tumours consistently retain expression of viral oncoproteins that drive growth, proliferation and altered metabolic function, which contributes to cancer progression (Mesri et al., 2014). However, as we have shown in our previous analysis of HPV+ and HPV- HNSCCs, these changes can differ between virally and non-virally induced cancer subtypes (Prusinkiewicz et al., 2020). In this study, we analyzed data for EBVaGC from The Cancer Genome Atlas (TCGA), a publicly available database comprised of multiple datatypes from radiologically or chemotherapeutically naive fresh frozen tissues (The Cancer Genome Atlas Research Network et al., 2013). These data types include RNAseq and corresponding anonymized patient survival data for the individuals from which the tumours were resected. We wanted to compare the transcriptomic metabolic profile of EBVaGC tissues to non-cancerous gastric tissues. To do this, we compared the expression of transcripts encoding metabolic enzymes from a variety of metabolic pathways, including glycolysis, the TCA cycle, cellular respiration, the pentose phosphate pathway (PPP) and fatty acid metabolism. We also determined whether differences in the expression of these transcripts within EBVaGCs were correlated with any differences in patient survival.

Our analysis identified that EBVaGCs display preferentially upregulated expression of mRNA for genes involved in glycolysis and the PPP, while transcripts encoding enzymes involved in the TCA cycle, cellular respiration, fatty acid beta-oxidation were downregulated. Additionally, it appeared that the expression of seven different metabolism-related transcripts were significantly associated with EBVaGC patient survival outcomes. Patients with EBVaGC tumours that had high expression of either *PFKM*, *ACLY*, *SCD*, *RPE*, or *SLC16A13* had better survival outcomes than EBVaGC patients whose tumours had low amounts of these transcripts. In addition, patients with EBVaGC tumours that had low expression of either *ALDOB* or *NDUFA4L2* appeared to have better survival outcomes than patients with tumours that had high expression of these genes.

Based on a comparison of data from our analysis to data in the literature for EBVaGC, we propose that EBVaGC is metabolically distinct from non-EBV associated gastric cancer. This could have implications on the metabolic function of the tumours and potentially serve as biomarkers for patient outcomes.

4.2. Materials and Methods

4.2.1. RNA Expression Analysis

As in our previous analysis (Ghasemi et al., 2020), we utilized the TCGA/PanCancer Atlas gastric carcinoma (STAD) cohort Level 3 RNA-Sequencing by Expectation Maximization (RSEM) normalized Illumina HiSeq RNA expression dataset, with merged clinical data, downloaded from the Broad Genome Data Analysis Centers Firehose Server (Cambridge, MA, USA; <https://gdac.broadinstitute.org>) (Broad Institute TCGA Genome Data Analysis Center, 2016). The gene level Firehose dataset was used. The data was curated as EBVaGC based on reported clinical data according to the 2018 TCGA PanCancer Atlas dataset from cBioPortal (<http://www.cbioportal.org/>). There were 30 EBVaGCs, 223 CIN GCs, 50 GS GCs, 73 MSI GCs and 35 non-cancerous tissue samples used for this analysis. Transcript expression levels from a manually curated list of metabolism associated genes, as described in (Prusinkiewicz et al., 2020), were compared between the GC subtypes and non-cancerous tissue using a Mann-Whitney U test, generating a p-value. This value was corrected using the Benjamini-Hochberg method with a threshold of significance at 0.1, generating a q-value.

4.2.2. Venn Diagram Visualization

To visualize the differences in metabolism-related gene regulation in each GC subtype, a Venn diagram illustrating the overlap between GC expression patterns was constructed with the web-based program InteractiVenn (Heberle et al., 2015) using the data generated from our RNA expression analysis (see Supplementary Table 4.1). Each gene that was significantly up or downregulated was included in the dataset for that GC subtype. Adobe Illustrator (San Jose, CA, USA) was used to further process the image to include the full gene abbreviations and typography designated to correspond to an upregulation (bold), downregulation (italics), or varied regulation dependent on GC subtype (regular font).

4.2.3. Survival analysis

Survival outcomes for GC patients were analyzed for a five-year period with a comparison between survival for patients with tumours that expressed high or low levels of each metabolic gene dichotomized by median expression as described in (Prusinkiewicz et al., 2020). For each Cox survival model, Log-rank statistical p-values were calculated. Additionally, the Benjamini-Hochberg analysis at a threshold of significance at 0.1, was used to generate a q-value.

4.3. Results

We analyzed mRNA expression data to compare the metabolic profile of EBVaGC tissues to non-cancerous gastric tissues. This analysis included transcripts encoding metabolic enzymes from several metabolic pathways, including glycolysis, the TCA cycle, cellular respiration, the PPP and fatty acid metabolism.

In certain metabolic pathways, such as glycolysis, there is a degree of functional redundancy that results from the presence of multiple different genes encoding metabolic enzymes that can perform the same function. For example, four different genes encode hexokinases, the enzymes responsible for the first step of glycolysis. However, expression of each of these genes may not be up or downregulated to the same extent or in the same direction for each step of a metabolic pathway. Understanding how the different enzymes involved in a certain step of glycolysis are up or downregulated can give insight as to which family-member EBVaGC may be reliant upon. Differentially regulated enzymes can then represent a targetable weak point or biomarker for the cancer. This is especially true when the expression data is combined with patient survival data, which can give a further level of insight as to how EBVaGC may be reliant on a certain metabolic enzyme.

4.3.1. Glycolysis

As mentioned above, hexokinase is the enzyme responsible for the conversion of glucose to glucose 6-phosphate in the first step of glycolysis. However, in EBVaGC, these four hexokinases were not necessarily regulated in the same direction. Specifically, transcripts for both hexokinase 2 (*HK2*) and hexokinase 3 (*HK3*) were upregulated while transcripts

for hexokinase 1 (*HK1*) and glucokinase (*GCK*) were downregulated when compared to non-cancerous tissue (Figure 4.1; Table 4.1). This suggested that EBVaGC may be more reliant on HK2 and HK3 for initiating glycolysis, which could have implications for the therapeutic inhibition of this step in the pathway. The upregulation of transcripts for the second enzyme involved in glycolysis, glucose 6-phosphate isomerase (*GPI*) in EBVaGC provided further evidence that glycolysis was upregulated in EBVaGC when compared to non-cancerous tissue.

However, in the third step of glycolysis the regulation of glycolytic transcripts was more complex. Phosphofructokinase (PFK) is responsible for the conversion of fructose-6-phosphate into fructose-1,6-biphosphate and is encoded by a variety of different genes. Transcripts for only one PFK family-member differed in EBVaGC when compared to non-cancerous tissue. Transcripts for phosphofructokinase, liver type (*PFKL*) were downregulated in EBVaGC. The potential dependence of EBVaGC on low levels of phosphofructokinases for cancer proliferation was supported by patient survival data corresponding to expression levels of another phosphofructokinase transcript, phosphofructokinase, muscle type (*PFKM*). EBVaGC patients with high levels of *PFKM* had better survival outcomes when compared to EBVaGC patients with low levels of *PFKM* (Figure 4.2A). However, the survival curve for *PFKM* did not meet the Benjamini-Hochberg FDR q-value cut-off (Supplementary Table 4.1).

For genes encoding the various aldolase (*ALDO*) enzymes in the steps of glycolysis that convert fructose 1,6-biphosphate into either glyceraldehyde 3-phosphate or dihydroxyacetone phosphate, transcripts for both *ALDOA* and *ALDOC* were decreased in EBVaGC when compared to non-cancerous tissue (Figure 4.1; Table 4.1). Interestingly, the amount of *ALDOB* transcript present in the tumours of EBVaGC patients was also correlated with survival outcomes. EBVaGC patients with high transcript levels of *ALDOB* had worse survival outcomes than patients with low levels of *ALDOB* (Figure 4.2B). This suggests that EBVaGC tumours are reliant on *ALDOB* to encode a functioning aldolase as levels of *ALDOA* and *ALDOC* transcript are lower than non-cancerous tissue (Figure 4.1; Table 4.1). Unlike phosphofructokinase, this step of glycolysis also does not represent a

Table 4.1 Glycolysis genes that were differentially regulated in EBVaGC.

Upregulated	<i>p</i>-value¹	<i>q</i>-value¹	Downregulated	<i>p</i>-value¹	<i>q</i>-value¹
<i>HK2</i>	6.50×10^{-4}	2.60×10^{-3}	<i>HK1</i>	1.48×10^{-6}	1.07×10^{-5}
<i>HK3</i>	2.45×10^{-8}	2.94×10^{-7}	<i>GCK</i>	1.59×10^{-7}	1.43×10^{-6}
<i>GPI</i>	4.31×10^{-4}	1.94×10^{-3}	<i>PFKL</i>	1.12×10^{-2}	2.69×10^{-2}
<i>PGK1</i>	4.43×10^{-3}	1.23×10^{-2}	<i>ALDOA</i>	8.36×10^{-4}	3.01×10^{-3}
<i>ENO1</i>	2.76×10^{-3}	9.03×10^{-3}	<i>ALDOC</i>	2.33×10^{-9}	8.30×10^{-8}
<i>PKM2</i>	1.25×10^{-4}	7.50×10^{-4}	<i>PGAM1</i>	7.27×10^{-3}	1.87×10^{-2}
<i>LDHA</i>	3.28×10^{-2}	6.95×10^{-2}	<i>PGAM2</i>	1.79×10^{-4}	9.21×10^{-4}
			<i>PGAM4</i>	3.11×10^{-3}	9.33×10^{-3}
			<i>LDHB</i>	2.97×10^{-2}	6.68×10^{-2}
			<i>SLC2A4</i>	4.61×10^{-9}	8.30×10^{-8}

¹ In comparison to matched non-cancerous tissue

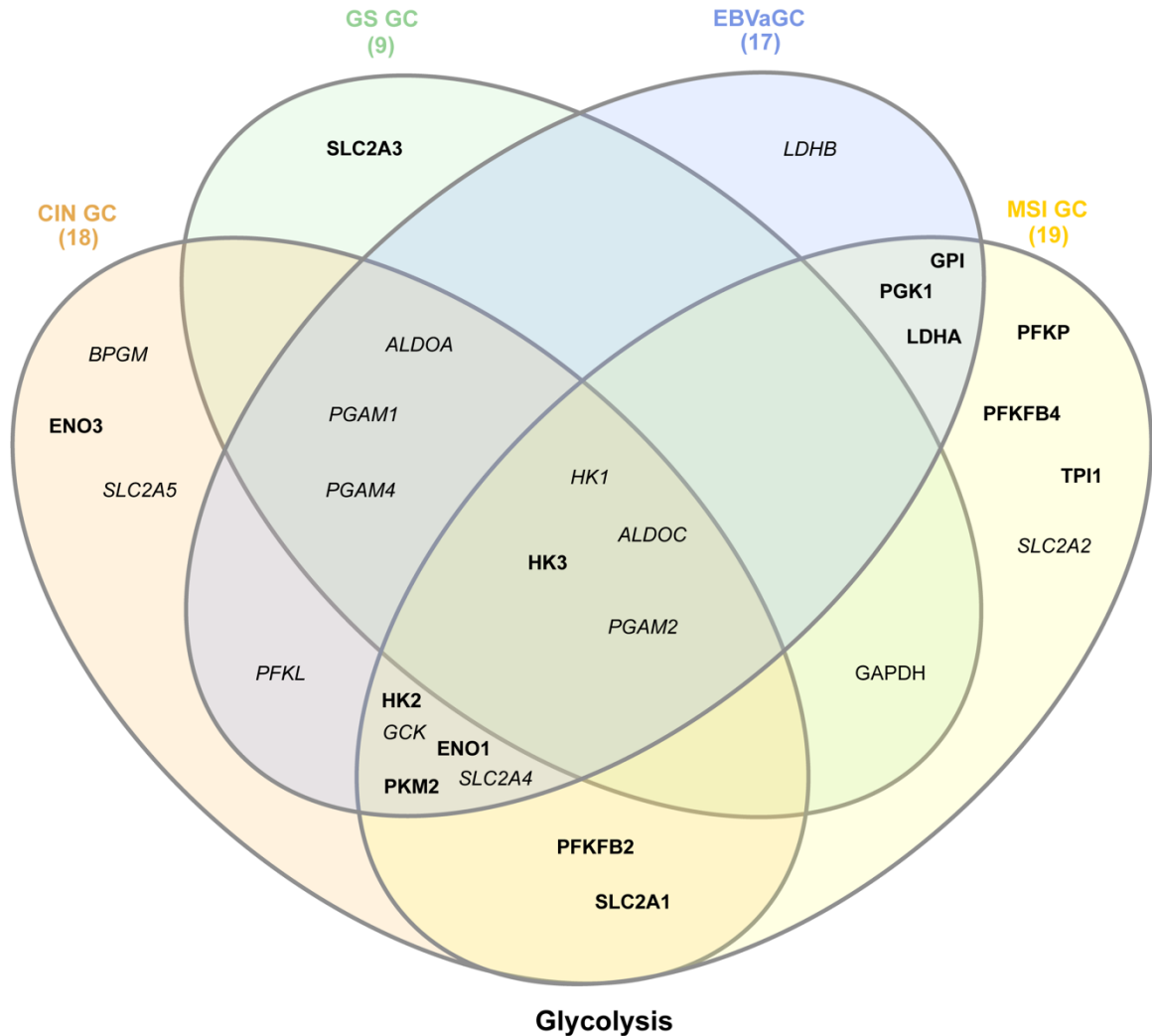


Figure 4.1. Venn diagram of differentially regulated glycolysis-related genes in GC. For each GC subtype, gene expression was compared to non-cancerous tissue. Gene names in italics were downregulated compared to non-cancerous tissue. Gene names in bold were upregulated compared to non-cancerous tissue. Gene names in regular font indicate that the gene was upregulated in one GC subtype, but downregulated in another. Each gene listed on this diagram met the significance threshold of $p = 0.05$ and an FDR cut-off of 0.1.

significant bottleneck or branching point. Note that the FDR value for the *ALDOB* survival curve did not meet the q-value cut-off of 0.1 (Supplementary Table 4.1).

The next glycolytic gene that displayed differential mRNA expression between EBVaGC and non-cancerous tissue was *PGK1*, which encodes phosphoglycerate kinase 1 (Figure 4.1; Table 4.1). Transcripts for *PGK1* were upregulated, as would be expected for a cancer cell more highly reliant on glycolysis than non-cancerous tissue. Transcripts encoding all functional phosphoglycerate mutases (*PGAM1*, *PGAM2*, *PGAM4*) were downregulated in EBVaGC when compared to non-cancerous tissue (Figure 4.1; Table 4.1). Expression of mRNAs encoding the final enzymes involved in glycolysis were also upregulated in EBVaGC. Transcripts for each of enolase 1 (*ENO1*), pyruvate kinase M1/2 (*PKM*), and lactate dehydrogenase A (*LDHA*) were all upregulated (Figure 4.1; Table 4.1). Corresponding to this, *LDHB* transcripts were downregulated in EBVaGC (Figure 4.1; Table 4.1), which was not unexpected since it appears that LDHA preferentially converts pyruvate to lactate while LDHB preferentially converts lactate to pyruvate (Urbańska and Orzechowski, 2019). Consequently, cancer cells employing anaerobic glycolysis typically express higher levels of LDHA (Urbańska and Orzechowski, 2019).

In regards to the other GC subtypes, each of the seven upregulated glycolysis genes in EBVaGC were also upregulated in MSI GC, while CIN GC only showed upregulation of *HK2*, *HK3*, *ENO1*, and *PKM2* in common with EBVaGC (Figure 4.1; Supplementary Table 4.1). *HK3* was the only glycolytic gene that was upregulated in both EBVaGC and MSI GC (Figure 4.1; Supplementary Table 4.1). As for the genes downregulated in EBVaGC, none of the other GC subtypes had a similar pattern of downregulation for all ten genes. CIN GC downregulated nine of the genes, with the exception of *LDHB* (Figure 4.1; Supplementary Table 4.1). GS GC shared downregulation of *HK1*, *ALDOA*, *ALDOC*, *PGAM1*, *PGAM2*, and *PGAM4* (Figure 4.1; Supplementary Table 4.1). Only 5 of the genes downregulated in MSI GC were in common with those downregulated in EBVaGC, these being *HK1*, *GCK*, *ALDOC*, *PGAM2*, and *SLC2A4* (Figure 4.1; Supplementary Table 4.1). Collectively, these differences provide evidence that each GC subtype may be metabolically distinct.

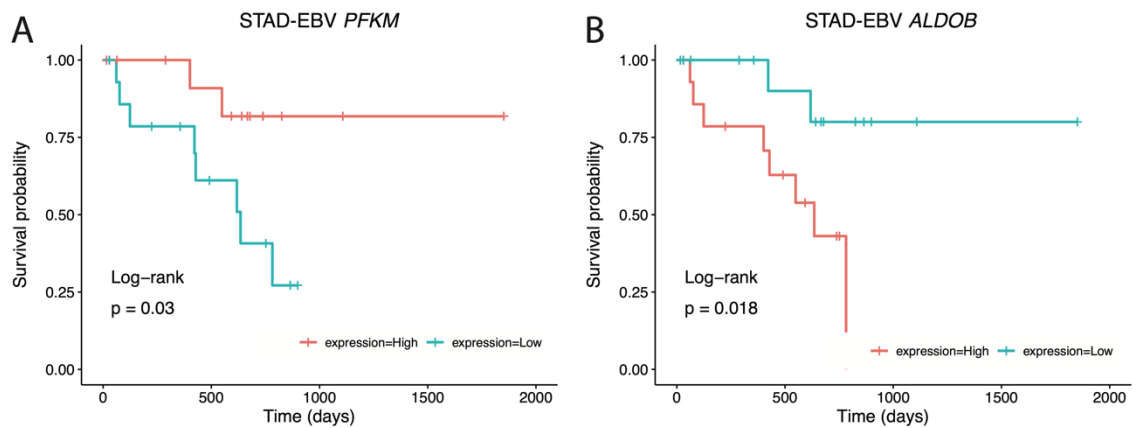


Figure 4.2. Expression of two transcripts that encode glycolytic enzymes were associated with EBVaGC patient survival outcomes. **(A)** Five-year survival outcomes dichotomized by median expression of PFKM. **(B)** Survival outcomes dichotomized by median expression of ALDOB. p = Two-sided log-rank test. Blue = low transcript expression, Red = high transcript expression.

4.3.2. Tricarboxylic Acid Cycle

Transcripts encoding enzymes within the TCA cycle tended to be downregulated in EBVaGC. For example, *PDHB*, which encodes the pyruvate dehydrogenase E1 beta subunit, was downregulated in EBVaGC when compared to non-cancerous tissue (Figure 4.3; Table 4.2). Paradoxically, the *PDPI* transcript, which encodes pyruvate dehydrogenase phosphatase catalytic subunit 1 and contributes to the activation of the pyruvate dehydrogenase complex, was upregulated in EBVaGC, as was the *PDHX* transcript, which encodes the pyruvate dehydrogenase complex component X (Figure 4.3; Table 4.2). Despite the upregulation of these two transcripts related to the pyruvate dehydrogenase complex in EBVaGC, the majority of TCA cycle enzyme-encoding transcripts were downregulated in EBVaGC (Table 4.2).

Interestingly, EBVaGCs exhibited differential regulation of *ACO1* and *ACO2* expression, which both encode an aconitase. These showed opposite trends. Transcripts for *ACO2* were upregulated, while transcripts for *ACO1* were downregulated in EBVaGC when compared to non-cancerous tissue (Figure 4.3; Table 4.2). However, the rest of the differentially regulated TCA cycle transcripts were downregulated in EBVaGC (Figure 4.3; Table 4.2). These transcripts include *IDH2* and *IDH3G*, which encode different isocitrate dehydrogenases; *OGDH*, which encodes oxoglutarate dehydrogenase; *SUCLA1*, *SUCLA2*, and *SUCLG2*, which encode components of succinate-COA ligase. Continuing through the TCA cycle, transcripts encoding the final enzymes in the cycle were also downregulated. These were *FH*, which encodes fumarate hydratase, and *MDHI*, which encodes a malate dehydrogenase. Although many of TCA cycle genes were downregulated when compared to non-cancerous tissue, high or low levels of any TCA cycle transcript between different cases of EBVaGC was not a prognostic indicator for patient survival.

As for the expression of these differentially regulated TCA cycle genes in other GC subtypes, both CIN GC and MSI GC shared upregulation of all three TCA cycle genes that were upregulated in EBVaGC (Figure 4.3; Supplementary Table 4.1). GS GC only shared upregulation of *PDPI* and *ACO2* (Figure 4.3; Supplementary Table 4.1). As for the TCA cycle genes that were downregulated in EBVaGC, GS GC downregulated the same ten genes as EBVaGC (Figure 4.3; Supplementary Table 4.1). Both CIN GC and MSI GC

Table 4.2. TCA cycle genes that were differentially regulated in EBVaGC.

Upregulated	<i>p</i>-value¹	<i>q</i>-value¹	Downregulated	<i>p</i>-value¹	<i>q</i>-value¹
<i>PDHX</i>	1.00×10^{-2}	1.60×10^{-2}	<i>PDHB</i>	6.23×10^{-8}	4.15×10^{-7}
<i>PDP1</i>	1.15×10^{-7}	5.75×10^{-7}	<i>ACO1</i>	2.47×10^{-5}	6.18×10^{-5}
<i>ACO2</i>	8.98×10^{-7}	3.00×10^{-6}	<i>IDH2</i>	4.79×10^{-7}	1.90×10^{-6}
			<i>IDH3G</i>	1.04×10^{-2}	1.60×10^{-2}
			<i>OGDH</i>	6.30×10^{-9}	6.30×10^{-8}
			<i>SUCLA2</i>	4.77×10^{-4}	9.54×10^{-4}
			<i>SUCLG1</i>	5.17×10^{-9}	6.30×10^{-8}
			<i>SUCLG2</i>	2.30×10^{-6}	6.60×10^{-6}
			<i>FH</i>	1.73×10^{-3}	3.15×10^{-3}
			<i>MDH1</i>	7.48×10^{-5}	1.66×10^{-4}

¹ In comparison to matched non-cancerous tissue

downregulated 7 genes in common with EBVaGC, the exceptions being *IDH3G*, *SUCLA2*, and *FH* in CIN GC, and *IDH2*, *SUCLA2*, and *FH* in MSI GC.

4.3.3. Cellular Respiration

We observed a consistent downregulation of transcripts encoding components of cellular respiration complexes, indicating that EBVaGCs were utilizing less oxidative phosphorylation than non-cancerous tissue. For all of the mitochondrial respiratory complexes, there were a large number of downregulated complex-subunit encoding transcripts (Tables 4.3-4.6; Figure 4.4).

Even in complex IV (Table 4.6; Figure 4.4D), the majority of differentially regulated EBVaGC transcripts were downregulated when compared to non-cancerous tissue, although there were a few which were upregulated. However, in light of the trend for transcripts in all four complexes, it is unlikely that the products of these upregulated transcripts would be sufficient to maintain cellular respiration in EBVaGC at levels present in normal control tissues (Table 4.6; Figure 4.4D).

GS GC downregulated the same set of cellular respiration complex I genes observed for EBVaGC, while CIN GC downregulated the same set of genes except for *NDUFV2*, *NDUFS2*, and *NDUFB9*, which remained at the same level as non-cancerous tissue (Figure 4.4A; Supplementary Table 4.1). MSI GC had the fewest number of downregulated respiration complex I genes that overlapped with those downregulated in EBVaGC. 10 respiration complex I genes that were downregulated in EBVaGC were not downregulated in MSI GC (Figure 4.4A; Supplementary Table 4.1). Both CIN GC and GS GC downregulated the same set of three respiratory complex II genes as EBVaGC, while MSI GC only shared downregulation of *SDHC* with EBVaGC (Figure 4.4B; Supplementary Table 4.1).

In cellular respiration complex III, both CIN GC and GS GC shared downregulation of 7 of the 8 genes downregulated by EBVaGC (Figure 4.4C; Supplementary Table 4.1). CIN GC did not downregulate *UQCRH*, while GS GC did not downregulate *UQCRB*. MSI GC only shared downregulation of 4 of the 8 genes downregulated by EBVaGC (Figure 4.4C;

Table 4.3. Respiratory complex I genes that were differentially regulated in EBVaGC.

Note that all genes were downregulated in EBVaGC.

Downregulated	<i>p</i>-value¹	<i>q</i>-value¹	Downregulated	<i>p</i>-value¹	<i>q</i>-value¹
<i>NDUFS4</i>	1.06 × 10 ⁻⁶	1.68 × 10 ⁻⁵	<i>NDUFA1</i>	2.79 × 10 ⁻⁵	2.00 × 10 ⁻⁴
<i>NDUFV1</i>	1.93 × 10 ⁻²	4.15 × 10 ⁻²	<i>NDUFA13</i>	7.65 × 10 ⁻⁴	2.35 × 10 ⁻³
<i>NDUFV2</i>	5.49 × 10 ⁻³	1.31 × 10 ⁻²	<i>NDUFB9</i>	1.24 × 10 ⁻³	3.33 × 10 ⁻³
<i>NDUFS1</i>	1.24 × 10 ⁻⁶	1.68 × 10 ⁻⁵	<i>NDUFB11</i>	4.99 × 10 ⁻²	8.25 × 10 ⁻²
<i>NDUFS2</i>	2.23 × 10 ⁻²	4.36 × 10 ⁻²	<i>NDUFA11</i>	1.19 × 10 ⁻⁴	4.26 × 10 ⁻⁴
<i>NDUFS7</i>	1.56 × 10 ⁻⁶	1.68 × 10 ⁻⁵	<i>NDUFAF1</i>	1.73 × 10 ⁻³	4.38 × 10 ⁻³
<i>NDUFS8</i>	1.03 × 10 ⁻³	2.95 × 10 ⁻³	<i>NDUFA8</i>	4.69 × 10 ⁻²	8.07 × 10 ⁻²
<i>NDUFS3</i>	4.60 × 10 ⁻⁵	2.16 × 10 ⁻⁴	<i>NDUFA2</i>	2.41 × 10 ⁻²	4.51 × 10 ⁻²
<i>NDUFA10</i>	2.68 × 10 ⁻²	4.80 × 10 ⁻²	<i>NDUFB7</i>	4.60 × 10 ⁻⁵	2.16 × 10 ⁻⁴
<i>NDUFV3</i>	1.56 × 10 ⁻⁶	1.68 × 10 ⁻⁵	<i>NDUFA6</i>	4.09 × 10 ⁻⁵	2.16 × 10 ⁻⁴
<i>NDUFB10</i>	5.20 × 10 ⁻⁵	2.16 × 10 ⁻⁴	<i>NDUFB8</i>	5.53 × 10 ⁻⁵	2.16 × 10 ⁻⁴
<i>NDUFC1</i>	3.67 × 10 ⁻⁴	1.21 × 10 ⁻³	<i>NDUFB1</i>	2.79 × 10 ⁻⁵	2.00 × 10 ⁻⁴
<i>NDUFAF3</i>	1.44 × 10 ⁻²	3.26 × 10 ⁻²	<i>NDUFA4</i>	2.14 × 10 ⁻²	4.36 × 10 ⁻²

¹ In comparison to matched non-cancerous tissue

Table 4.4. Respiratory complex II genes that were differentially regulated in EBVaGC. Note that all genes were downregulated in EBVaGC.

Downregulated	<i>p</i>-value¹	<i>q</i>-value¹
<i>SDHB</i>	3.28 × 10 ⁻²	4.37 × 10 ⁻²
<i>SDHC</i>	1.19 × 10 ⁻⁴	3.38 × 10 ⁻⁴
<i>SDHD</i>	1.69 × 10 ⁻⁴	3.38 × 10 ⁻⁴

¹ In comparison to matched non-cancerous tissue

Table 4.5. Respiratory complex III genes that were differentially regulated in EBVaGC. Note that all genes were downregulated in EBVaGC.

Downregulated	<i>p</i>-value¹	<i>q</i>-value¹
<i>UQCRFS1</i>	1.19 × 10 ⁻³	4.73 × 10 ⁻³
<i>UQCRC1</i>	1.58 × 10 ⁻³	4.73 × 10 ⁻³
<i>UQCRC2</i>	1.50 × 10 ⁻⁴	1.35 × 10 ⁻³
<i>UQCRB</i>	2.10 × 10 ⁻³	4.73 × 10 ⁻³
<i>UQCRQ</i>	7.91 × 10 ⁻³	1.19 × 10 ⁻²
<i>UQCRH</i>	4.39 × 10 ⁻²	4.94 × 10 ⁻²
<i>UQCR10</i>	1.17 × 10 ⁻²	1.50 × 10 ⁻²
<i>UQCR11</i>	2.76 × 10 ⁻³	4.97 × 10 ⁻³

¹ In comparison to matched non-cancerous tissue

Table 4.6. Respiratory complex IV genes that were differentially regulated in EBVaGC.

Upregulated	<i>p</i>-value¹	<i>q</i>-value¹	Downregulated	<i>p</i>-value¹	<i>q</i>-value¹
<i>COA1</i>	4.05 × 10 ⁻⁷	3.14 × 10 ⁻⁶	<i>COX6B1</i>	4.99 × 10 ⁻²	9.10 × 10 ⁻²
<i>COA7</i>	1.15 × 10 ⁻⁷	1.19 × 10 ⁻⁶	<i>COX8A</i>	1.19 × 10 ⁻³	3.69 × 10 ⁻³
<i>COX15</i>	1.26 × 10 ⁻²	3.00 × 10 ⁻²	<i>COX4I1</i>	2.00 × 10 ⁻⁴	8.86 × 10 ⁻⁴
<i>COX18</i>	4.54 × 10 ⁻²	8.80 × 10 ⁻²	<i>COX6A1</i>	1.26 × 10 ⁻²	3.00 × 10 ⁻²
<i>COX19</i>	3.79 × 10 ⁻⁹	1.17 × 10 ⁻⁷	<i>COX5B</i>	4.24 × 10 ⁻⁶	2.19 × 10 ⁻⁵
			<i>COX7A1</i>	8.98 × 10 ⁻⁷	5.57 × 10 ⁻⁶
			<i>COX7C</i>	4.77 × 10 ⁻⁴	1.64 × 10 ⁻³
			<i>COX6A2</i>	1.72 × 10 ⁻²	3.81 × 10 ⁻²
			<i>COX7B</i>	4.77 × 10 ⁻⁴	1.64 × 10 ⁻³
			<i>COA3</i>	3.11 × 10 ⁻³	8.76 × 10 ⁻³
			<i>COX14</i>	3.41 × 10 ⁻²	7.05 × 10 ⁻²
			<i>COX20</i>	6.78 × 10 ⁻⁸	1.05 × 10 ⁻⁶

¹ In comparison to matched non-cancerous tissue

Figure 4.4. Venn diagrams of differentially regulated cellular respiration complex genes in GC. (A) Cellular respiration complex I-related genes. (B) Cellular respiration complex II-related genes. (C) Cellular respiration complex III-related genes. (D) Cellular respiration complex IV-related genes in GC. For each GC subtype, gene expression was compared to non-cancerous tissue. Gene names in italics were downregulated compared to non-cancerous tissue. Gene names in bold were upregulated compared to non-cancerous tissue. Gene names in regular font indicate that the gene was upregulated in one GC subtype, but downregulated in another. Each gene listed on this diagram met the significance threshold of $p = 0.05$ and an FDR cut-off of 0.1.

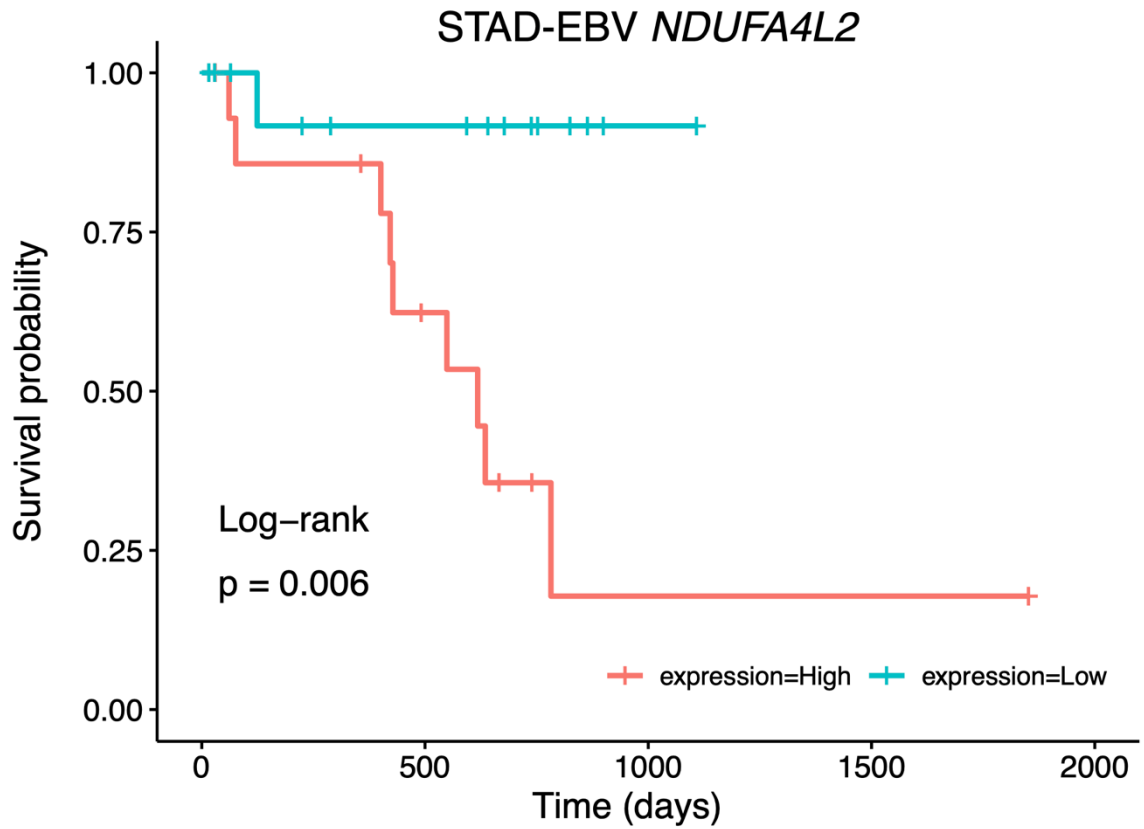


Figure 4.5. Five-year survival outcomes dichotomized by median expression of the cellular respiration complex I component encoding transcript *NDUFA4L2*. $p =$ Two-sided log-rank test. Blue = low transcript expression, Red = high transcript expression.

Supplementary Table 4.1). These were *UQCRC2*, *UQCRQ*, *UQCR10*, *UQCR11*. Of the 17 cellular respiration complex IV genes that were differentially regulated in EBVaGC, five of these did not share differential regulation in CIN GC. These genes were *COX6A2*, *COA3*, *COX15*, *COX18*, and *COX20*. GS CS shared differential expression of only 11 of the 17 cellular respiration complex IV genes differentially regulated by EBVaGC. The 6 genes that did not show differential regulation in GS CS were *COX7A1*, *COX6A2*, *COA1*, *COX15*, *COX18*, and *COX20*. MSI GC shared a pattern of differential regulation similar to EBVaGC for 15 of the 17 genes, with the exception of *COX6A1* and *COX20* (Figure 4.4D; Supplementary Table 4.1). Low expression of one cellular respiration complex I gene, *NDUFA4L2*, appeared to be associated with better survival in EBVaGC (Figure 4.5). However, this did not meet the q -value FDR cut-off of 0.1 after the Benjamini-Hochberg procedure.

4.3.4. Fatty Acid Metabolism

The regulation of fatty acid synthesis transcripts in EBVaGC were not consistently skewed towards upregulation or downregulation when compared to non-cancerous tissue. For example, transcripts encoding members of the *ELO* family of fatty acid elongases showed a split between upregulation and downregulation (Table 4.7; Figure 4.6A). Specifically, *ELOVL4*, *ELOVL5*, and *ELOVL6* were all downregulated in EBV+STAD while *ELOVL2*, *ELOVL3* and *ELOVL7* were all upregulated. *ACLY*, *FASN*, and *SCD* were three other fatty acid metabolism related transcripts that were upregulated in EBV+ STAD. In contrast, *ME1*, *ACACB*, *ACSSI* and *ACSS2* were all downregulated.

Interestingly, two of these fatty acid synthesis genes, *ACLY* and *SCD*, were also found to be associated with survival in EBVaGC (Figure 4.7). Specifically, better survival outcomes for EBVaGC patients were associated with high transcript expression of either *ACLY* (Figure 4.7A) or *SCD* (Figure 4.7B) when compared to EBVaGC patients with low transcript expression of either of these two genes. However, once again, the FDR values for *ACLY* and *SCD* did not meet the q -value cut-off of 0.1 (Supplementary Table 4.1).

When compared to other GC subtypes, no other type had an identical pattern of differentially regulated fatty acid synthesis genes (Figure 4.6A). Of the 13 differentially

Table 4.7. Fatty acid synthesis genes that were differentially regulated in EBVaGC.

Upregulated	<i>p</i> -value ¹	<i>q</i> -value ¹	Downregulated	<i>p</i> -value ¹	<i>q</i> -value ¹
<i>ACLY</i>	3.11×10^{-3}	1.09×10^{-2}	<i>ME1</i>	2.12×10^{-15}	4.45×10^{-14}
<i>FASN</i>	7.57×10^{-3}	1.77×10^{-2}	<i>ACSS1</i>	4.43×10^{-3}	1.33×10^{-2}
<i>ELOVL2</i>	1.00×10^{-2}	2.10×10^{-2}	<i>ACSS2</i>	1.34×10^{-2}	2.56×10^{-2}
<i>ELOVL3</i>	2.12×10^{-2}	3.42×10^{-2}	<i>ACACB</i>	3.94×10^{-8}	4.14×10^{-7}
<i>ELOVL7</i>	4.55×10^{-4}	2.39×10^{-3}	<i>ELOVL4</i>	2.96×10^{-5}	2.07×10^{-4}
<i>SCD</i>	8.79×10^{-4}	3.69×10^{-3}	<i>ELOVL5</i>	1.55×10^{-2}	2.71×10^{-2}
			<i>ELOVL6</i>	6.17×10^{-3}	1.62×10^{-2}

¹ In comparison to matched non-cancerous tissue

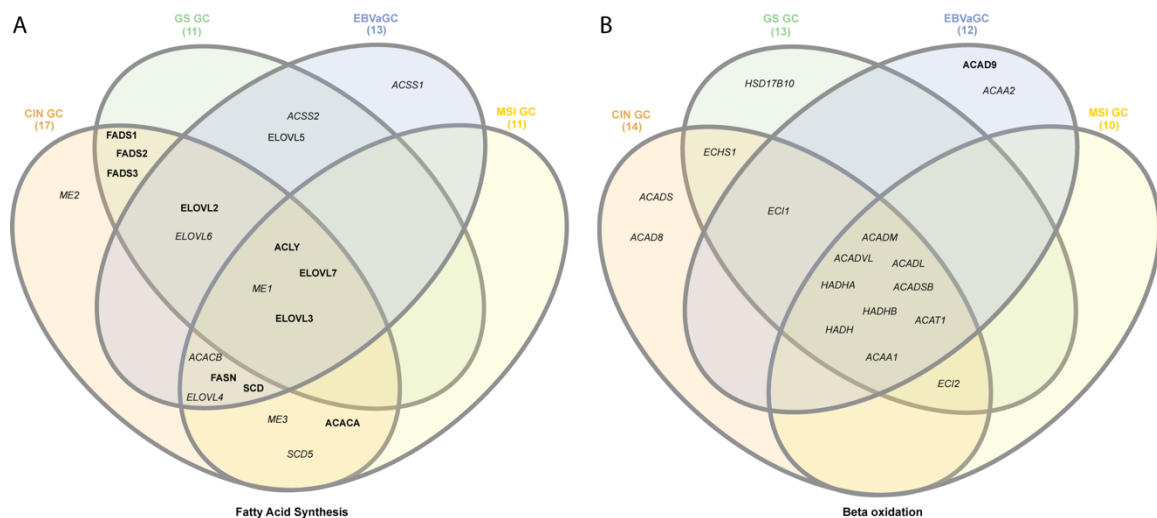


Figure 4.6. Venn diagrams of differentially regulated fatty acid synthesis-related genes, and beta-oxidation-related genes in GC. For each GC subtype, gene expression was compared to non-cancerous tissue. Gene names in *italics* were downregulated compared to non-cancerous tissue. Gene names in **bold** were upregulated compared to non-cancerous tissue. Gene names in regular font indicate that the gene was upregulated in one GC subtype, but downregulated in another. Each gene listed on this diagram met the significance threshold of $p = 0.05$ and an FDR cut-off of 0.1.

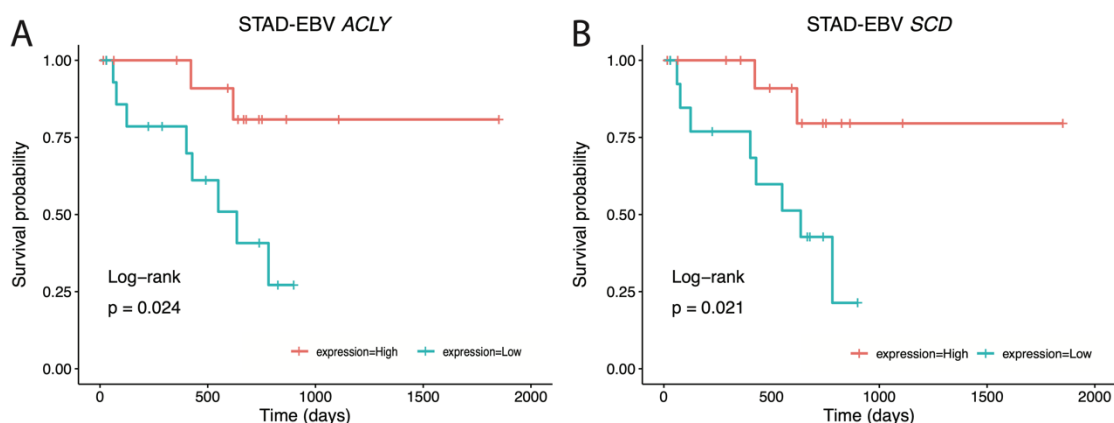


Figure 4.7. Two transcripts that encode fatty acid synthesis enzymes were associated with EBVaGC patient survival outcomes. (A) Five-year survival outcomes dichotomized by median expression of *ACLY*. **(B)** Survival outcomes dichotomized by median expression of *SCD*. p = Two-sided log-rank test. Blue = low transcript expression, Red = high transcript expression.

Table 4.8. Beta-oxidation genes that were differentially regulated in EBVaGC.

Upregulated	<i>p</i> -value ¹	<i>q</i> -value ¹	Downregulated	<i>p</i> -value ¹	<i>q</i> -value ¹
<i>ACAD9</i>	3.28×10^{-2}	4.92×10^{-2}	<i>ACADM</i>	7.43×10^{-15}	1.34×10^{-13}
			<i>ACADVL</i>	2.96×10^{-5}	7.61×10^{-5}
			<i>ACADL</i>	2.53×10^{-9}	1.14×10^{-8}
			<i>ACADSB</i>	1.56×10^{-6}	4.68×10^{-6}
			<i>HADHA</i>	6.89×10^{-12}	6.20×10^{-11}
			<i>HADHB</i>	1.05×10^{-9}	6.30×10^{-9}
			<i>HADH</i>	7.71×10^{-7}	2.78×10^{-6}
			<i>ECI1</i>	1.80×10^{-2}	2.95×10^{-2}
			<i>ACAA1</i>	1.60×10^{-4}	3.20×10^{-4}
			<i>ACAA2</i>	6.16×10^{-4}	1.11×10^{-3}
			<i>ACAT1</i>	6.60×10^{-5}	1.49×10^{-4}

¹ In comparison to matched non-cancerous tissue

regulated fatty acid synthesis genes in EBVaGC, CIN GC shared differential regulation of 10 of them, except for *ACSSI*, *ACSS2*, and *ELOVL5*. GS GC shared a similar pattern of differential regulation for 7 of the 13, with the exceptions being *ACSSI*, *ACACB*, *FASN*, *ELOVL4*, *SCD*, and *ELOVL5*. The expression of *ELOVL5* was upregulated in GS GC when compared to non-cancerous tissue, which was opposite to the downregulation of this gene in EBVaGC when compared to non-cancerous tissue. MSI GC shared a similar differential regulation pattern of 8 of the fatty acid synthesis genes with EBVaGC. *ACSSI*, *ACSS2*, *ELOVL2*, *ELOVL5*, and *ELOVL6* were the genes that were not differentially regulated in MSI GC that were differentially regulated in EBVaGC.

In contrast, transcripts involved in beta-oxidation, which is the breakdown of fatty acids, were highly downregulated in EBVaGC. There were a total of eleven beta-oxidation transcripts that were downregulated (Figure 4.6B; Table 4.8). Three of these genes *HADH*, *HADHA* and *HADHB* encode subunits of different hydroxyacyl-CoA dehydrogenase enzymes or complexes. Four transcripts encoding members of the ACAD Acyl-CoA dehydrogenase family, *ACADSB*, *ACADM*, *ACADVL*, *ACADL* were downregulated. Transcripts for two acetyl-CoA acyltransferases *ACAA1* and *ACAA2* were downregulated. Finally, *EC11* and *ACAT1* encoding other steps of beta-oxidation were also downregulated. There was only one beta-oxidation gene that was upregulated in EBVaGC, this being *ACAD9*. There was no correlation between level of transcript expression and EBVaGC patient survival for any of the beta-oxidation genes. Each of the other GC subtypes did not share differential regulation of *ACAD9* or *ACAA2* with EBVaGC, while MSI GC also did not have differential regulation of *EC11* (Figure 4.6B; Supplementary Table 4.1).

4.3.5. Glutaminolysis

In addition to the characteristic increase in aerobic glycolysis that occurs in many cancer cells, glutaminolysis, which is the conversion of glutamine into glutamate to provide energy and intermediates for rapid cell growth, occurs in many types of cancer. The first enzyme involved in this pathway is GLS and it is frequently upregulated in cancer (Akins et al., 2018). Indeed, *GLS2* transcripts were upregulated in EBVaGC when compared to non-cancerous tissue (Table 4.9; Figure 4.8). However, *GLS2* transcripts were the only upregulated glutaminolysis-related transcript in EBVaGC. There were two glutaminolysis

Table 4.9. Glutaminolysis genes that were differentially regulated in EBV+ STAD.

Upregulated	<i>p</i> -value ¹	<i>q</i> -value ¹	Downregulated	<i>p</i> -value ¹	<i>q</i> -value ¹
<i>GLS2</i>	8.40×10^{-5}	4.38×10^{-4}	<i>GPT</i>	1.25×10^{-4}	4.38×10^{-4}
			<i>GOT1</i>	3.07×10^{-2}	7.16×10^{-2}

¹ In comparison to matched non-cancerous tissue

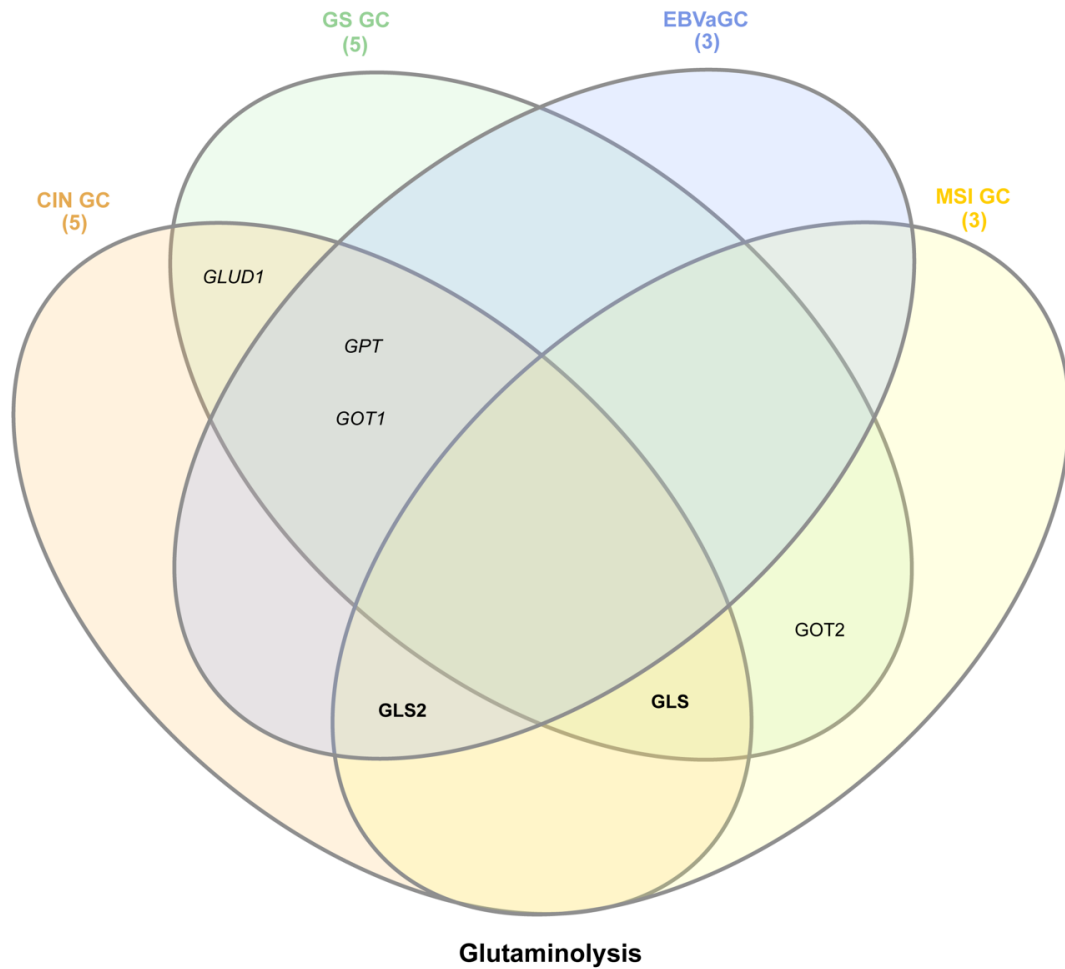


Figure 4.8. Venn diagram of differentially regulated glutaminolysis-related genes in GC. For each GC subtype, gene expression was compared to non-cancerous tissue. Gene names in italics were downregulated compared to non-cancerous tissue. Gene names in bold were upregulated compared to non-cancerous tissue. Gene names in regular font indicate that the gene was upregulated in one GC subtype, but downregulated in another. Each gene listed on this diagram met the significance threshold of $p = 0.05$ and an FDR cut-off of 0.1.

related transcripts that were downregulated in EBVaGC. These were transcripts for *GPT* and *GOT1* (Table 4.9; Figure 4.8), both of which are involved in the conversion of glutamate into alpha-ketoglutarate (Jin et al., 2016). Despite the differential regulation of these transcripts, there were no significant differences in EBVaGC patient survival outcomes with varied expression of any genes involved glutaminolysis. As for the other GC subtypes, CIN GC shared the differential expression pattern of all three genes with EBVaGC, while MSI GC only shared upregulation of *GLS* with EBVaGC. In contrast, GS GC did not share differential regulation of *GLS2* with EBVaGC (Figure 4.8; Supplementary Table 4.1).

Expression of *SLC16A2* was significantly lower in HPV+ HNSCC when compared to either HPV- HNSCC or normal control tissues (Figure 4.4G). HPV+ HNSCC samples were dichotomized based on median *SLC16A2* expression. Again, low expression of *SLC16A2* was associated with improved patient survival in HPV+ HNSCC patients ($p = 0.0036$, FDR = 0.047) (Figure 4.4H), but not in patients with HPV- HNSCC ($p = 0.26$, FDR = 0.48) (Figure 4.4I). However, *SLC16A2* did not meet the FDR q-value cut-off of 0.1 (Supplementary Table 4.1).

4.3.6. Pentose Phosphate Pathway

The PPP is responsible for the conversion of glucose into ribose, which is the sugar backbone of nucleotides. As cancer cells have an increased proliferation rate, which is accompanied by an increased demand for nucleotides, it is not usual for nucleotide production-related metabolic pathways, such as the PPP, to be upregulated (Jiang et al., 2014; Patra and Hay, 2014). Interestingly, transcripts encoding two PPP enzymes were upregulated in EBVaGC (Table 4.10; Figure 4.9). These were transcripts for ribulose-5-phosphate-3-epimerase (*RPE*) and ribulose-5-phosphate-3-epimerase like 1 (*RPEL1*). Both of these enzymes serve the same function in the PPP, which is the reversible conversion of D-xylulose 5-phosphate to D-ribulose 5-phosphate.

The expression level of *RPE* was correlated with survival in EBVaGC, as patients with high levels of this transcript had better survival than patients with low levels of this transcript (Figure 4.10). However, it should be noted that the significance of this survival

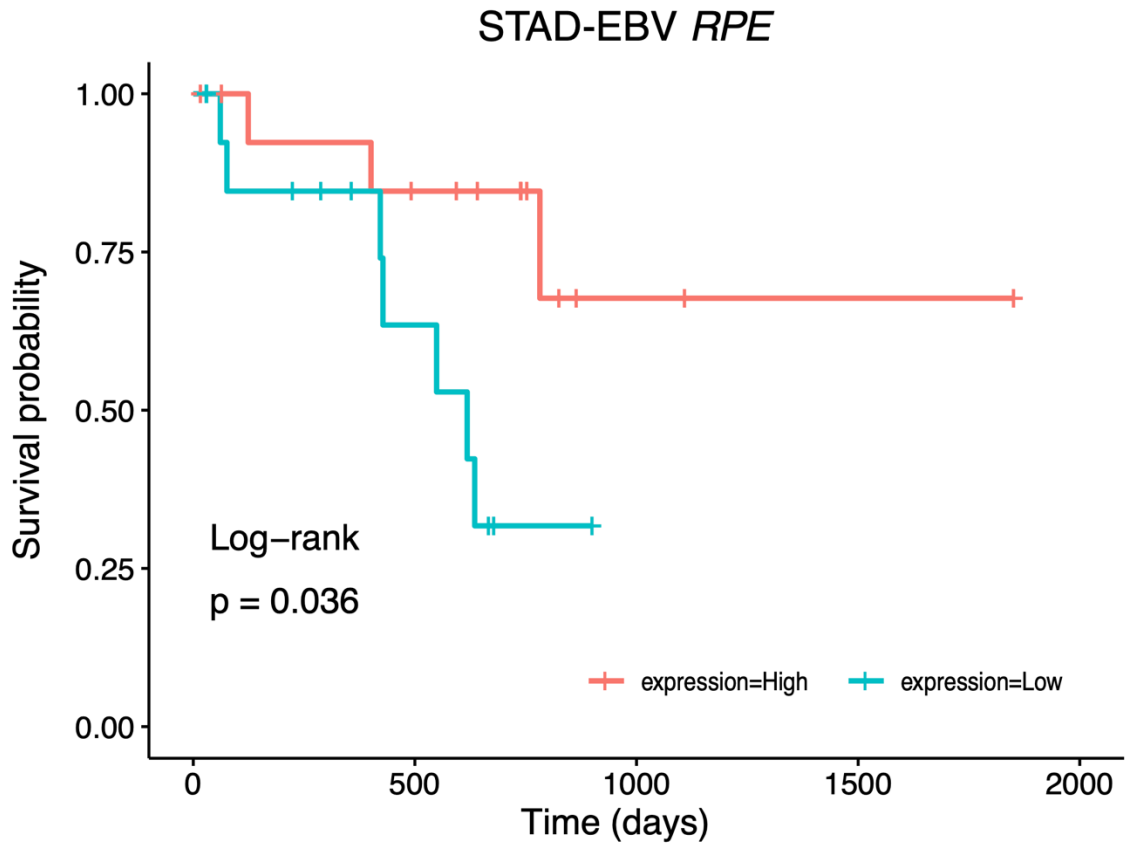


Figure 4.10. Five-year survival outcomes dichotomized by median expression of the pentose phosphate pathway enzyme-encoding transcript *RPE*. $p =$ Two-sided log-rank test. Blue = low transcript expression, Red = high transcript expression.

curve did not meet the FDR q-value cut-off of 0.1 (Supplementary Table 4.1). Expression of *RPE* was also upregulated in both CIN GC and MSI GC, while expression of *RPE* was upregulated in CIN GC (Figure 4.9; Supplementary Table 4.1).

4.3.7. Monocarboxylate Transporters

Monocarboxylate transporters (MCTs) are responsible for transporting the products of glycolysis and other metabolic pathways, such as pyruvate and lactate across the plasma membrane. Some transporters are capable of transporting multiple different products, while some are specific to only certain molecules. In EBVaGC, transcript for only one MCT family member, *SLC16A8*, which encodes the transporter MCT3, was upregulated when compared to non-cancerous tissue (Table 4.11). In contrast, transcripts for five MCT family members were downregulated (Table 4.11). These were *SLC16A2*, which encodes MCT8; *SLC16A7*, which encodes MCT2; *SLC16A9*, which encodes MCT9; *SLC16A11* which encodes MCT11; and *SLC16A14*, which encodes MCT14.

The intratumoral expression level of only one *SLC16A* family member transcript, *SLC16A13*, which encodes that transporter MCT13, appeared to be correlated with EBVaGC patient survival, albeit it did not meet the FDR q-value cut-off of 0.1 (Supplementary Table 4.1). Interestingly, this was not one of the transcripts that showed differential regulation between EBVaGC and non-cancerous tissue. Patients with EBVaGC tumours with high levels of this transcript had better survival outcomes than patients with low levels of this transcript (Figure 4.11).

When comparing expression of these genes across GC subtype, CIN GC shared the same expression pattern for four of the six differentially regulated genes in EBVaGC, however *SLC16A14* and *SLC16A2* were not expressed at levels significantly different from non-cancerous tissue in CIN GC (Figure 4.12; Supplementary Table 4.1). GS GC downregulated both *SLC16A11* and *SLC16A8* just as in EBVaGC, but *SLC16A2* was upregulated in GS GC, which was opposite to the downregulation of this gene in EBVaGC (Figure 4.12; Supplementary Table 4.1). Finally, MSI GC showed a similar expression trend as EBVaGC for four of the above six genes, with the exceptions of *SLC16A14* and *SLC16A8*.

Table 4.11. Monocarboxylic acid transport genes that were differentially regulated in EBVaGC.

Upregulated	<i>p</i> -value ¹	<i>q</i> -value ¹	Downregulated	<i>p</i> -value ¹	<i>q</i> -value ¹
<i>SLC16A8</i>	1.98×10^{-6}	5.15×10^{-6}	<i>SLC16A11</i>	2.77×10^{-9}	1.20×10^{-8}
			<i>SLC16A9</i>	2.46×10^{-9}	1.20×10^{-8}
			<i>SLC16A14</i>	1.15×10^{-5}	2.49×10^{-5}
			<i>SLC16A2</i>	2.06×10^{-7}	6.70×10^{-7}
			<i>SLC16A7</i>	1.14×10^{-9}	1.20×10^{-8}

¹ In comparison to matched non-cancerous tissue

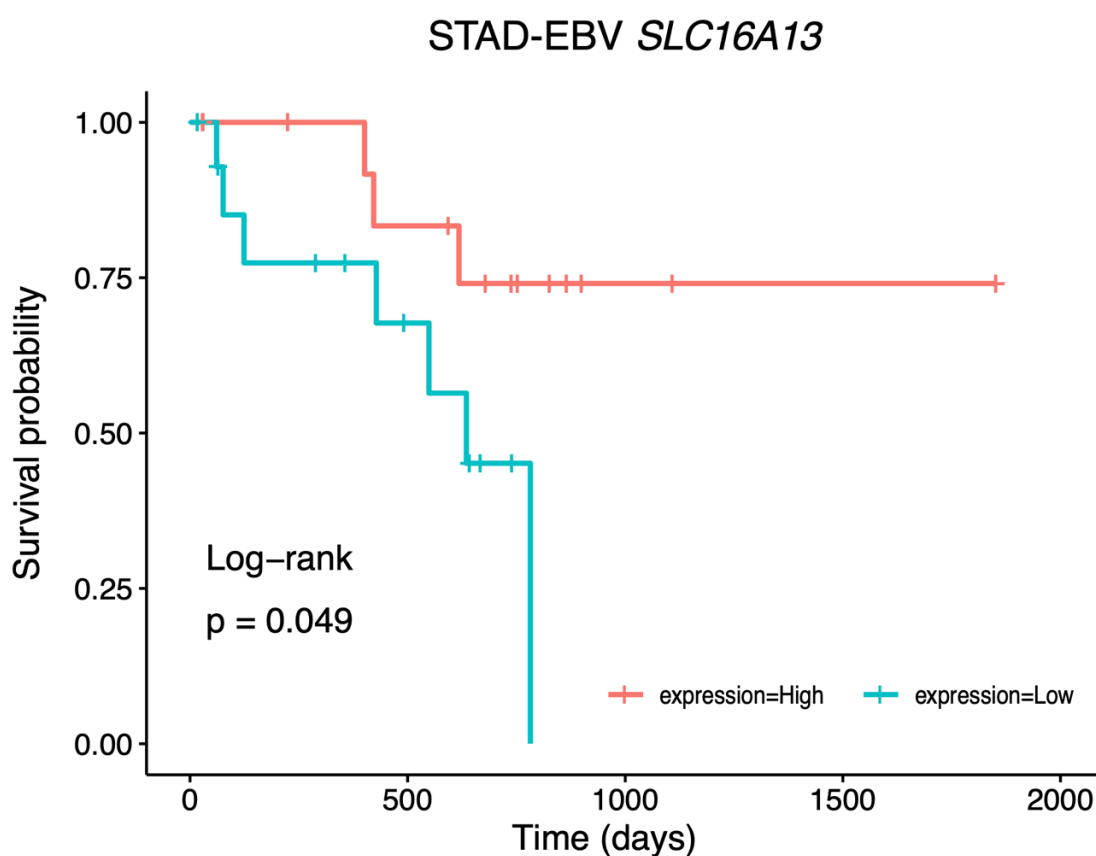


Figure 4.11. Five-year survival outcomes dichotomized by median expression of the monocarboxylate transporter encoding transcript *SLC16A13*. $p =$ Two-sided log-rank test. Blue = low transcript expression, Red = high transcript expression.

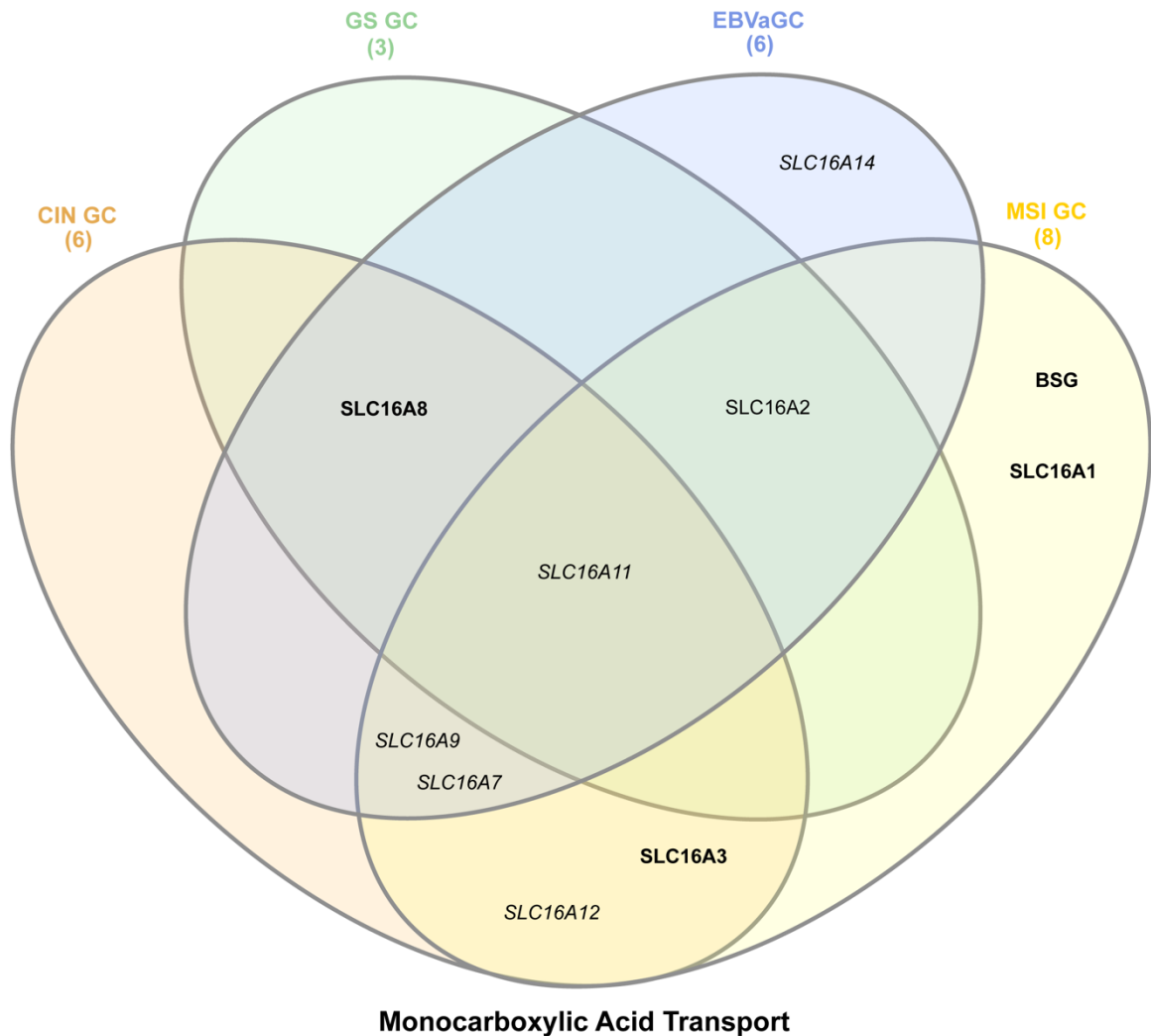


Figure 4.12. Venn diagram of differentially regulated monocarboxylic acid transport-related genes in GC. For each GC subtype, gene expression was compared to non-cancerous tissue. Gene names in italics were downregulated compared to non-cancerous tissue. Gene names in bold were upregulated compared to non-cancerous tissue. Gene names in regular font indicate that the gene was upregulated in one GC subtype, but downregulated in another. Each gene listed on this diagram met the significance threshold of $p = 0.05$ and an FDR cut-off of 0.1.

4.4. Discussion

Our analysis of differentially regulated metabolic gene expression in EBVaGC identified a number of genes with altered expression. While it generally appeared that EBVaGC was upregulating glycolysis, there were a few steps in the pathway where there appeared to be a downregulation of glycolysis enzyme-encoding transcripts. This might suggest that glycolysis is proceeding suboptimally, which is counterintuitive to the Warburg effect. However, some cancers have been observed to downregulate PFKs (Kim et al., 2017), the metabolic step of glycolysis which is also the branch point into the PPP. This ensures that sufficient glycolytic intermediates are funneled into the PPP for the generation of ribose, the sugar backbone of nucleotides. In addition, the only glycolytic enzyme encoding transcript that affected patient survival was *PFKM*. This suggested that low levels of this PFK isoform were beneficial to the tumour, because low levels of *PFKM* were associated with worse survival outcomes. Similarly, in renal cell carcinoma, low expression of *PFKM* has been associated with poor survival outcomes (Chen et al., 2020b), which illustrates how this phenomenon is not unique to EBVaGC.

Interestingly, for another glycolytic enzyme-encoding transcript, *ALDOB*, the trend in EBV-negative gastric cancers was opposite to the trend found in our analysis for EBVaGC. EBV-negative gastric cancer patients had worse outcomes when the tumours had low levels of *ALDOB* (He et al., 2016), while we observed that EBVaGC patients had better outcomes with low levels of *ALDOB*. It is possible that the metabolic pathways activated by the presence of EBV oncoproteins differs from those activated in EBV-negative gastric cancer. The only other potential contradiction to the idea that EBVaGC upregulated glycolysis when compared to non-cancerous tissue was the downregulation of transcripts encoding PGAM isoforms. While this is an unusual situation as upregulated *PGAM* transcripts are typically associated with upregulated glycolysis, there are some circumstances whereby *PGAM* transcripts are downregulated despite an upregulation in glycolysis (Mikawa et al., 2015). This typically occurs when p21-activated protein kinase (PAK) is involved in regulating glycolysis (Mikawa et al., 2015). All the other glycolytic-enzyme encoding transcripts were regulated as would be expected for cancer tissue performing increased glycolysis.

As for the TCA cycle, our analysis indicated that EBVaGC exhibit TCA cycle downregulation that was potentially similar to the downregulation of the TCA cycle observed in other cancers, such as breast cancer and melanomas (Luo et al., 2017; Tang et al., 2019). It remains unclear whether the metabolic regulation in EBVaGC is similar to or differs from EBV-negative gastric cancer. This is because in terms of metabolite concentrations, gastric carcinomas as a whole appeared to have higher levels of TCA cycle metabolites within the tumour tissue when compared to non-cancerous tissue (Aa et al., 2012). Whether this is indeed the case for EBVaGC remains to be explored. However, based on the overall reduced level of mRNA encoding TCA cycle genes in EBVaGC, it is quite possible that the concentrations of TCA cycle metabolites within EBVaGC will also be decreased.

Only one transcript encoding a component of a cellular respiration complex was associated with survival. This was *NDUFA4L2*, part of respiration complex I. Despite being a transcript associated with cellular respiration, this transcript can be found upregulated in a variety of other cancers, including hepatocellular carcinoma (Lai et al., 2016). This is because *NDUFA4L2* is tightly regulated by hypoxia-inducible genes and functions to reduce mitochondrial activity in order to prevent excessive ROS production (Lai et al., 2016). Therefore, downregulation of this gene may have a detrimental effect on tumour survival by allowing increased oxygen consumption and ROS levels. While this gene is not upregulated in EBVaGC when compared to non-cancerous tissue, EBVaGC may still be reliant on the activities of the *NDUFA4L2* protein. This could account for the improved survival outcomes in EBVaGC patients with low expression of this gene.

A number of differences were observed in the fatty acid metabolism pathways. It is possible that expression of certain key fatty acid metabolism-related genes might have specific pro-cancer or anticancer effects in EBVaGC. For example, *ELOVL7* overexpression has been noted in prostate cancer cells and appears to be a key element for its survival (Tamura et al., 2009). Perhaps, the upregulated *ELOVL7* transcripts in EBVaGC suggests a similar reliance on *ELOVL7*. In another parallel, *ELOVL5* has been reported to be downregulated in colorectal cancer (Boot et al., 2017), as it is in EBVaGC. Perhaps the most prominent upregulated transcript in the fatty acid metabolism pathway that EBVaGC shares with a

wide variety of cancers is *ACLY* (Zaidi et al., 2012). *ACLY* has been the focus of intense anticancer therapeutic scrutiny (Granchi, 2018). This is because *ACLY* encodes an enzyme that is responsible for linking glycolysis to the first step of *de novo* fatty acid synthesis, a process that is upregulated in many cancers due to their increased macromolecular demands from rapid proliferation (Granchi, 2018). Likewise, *FASN* is another fatty acid metabolism gene that is upregulated in a wide range of cancers (Menendez and Lupu, 2007), and this trend continues with EBVaGC. *FASN* is important to a wide variety of tumours because it encodes the terminal enzyme of fatty acid biosynthesis and is capable of linking energy production with anabolic and other oncogenic pathways (Menendez and Lupu, 2007). *SCD* has a crucial role in the production of phospholipids for cell membranes in cancer cells (Igal, 2010), and several cancers, including EBVaGC, as shown in this study, upregulate expression of this gene (Igal, 2010; Roongta et al., 2011).

Interestingly, the downregulation of *ME1* mRNA expression in EBVaGC, which encodes an enzyme that generates NADPH used in fatty acid and cholesterol biosynthesis, illustrates how this is a distinct gastric cancer subtype from other gastric cancer subtypes. A previous study using a pooled sample of gastric cancers found that *ME1* expression was upregulated and contributed to cancer proliferation (Lu et al., 2018). *ME1* was also correlated with poor patient survival outcomes (Lu et al., 2018). The contribution of *ME1* to cancer cell proliferation was further shown in an EBV-negative gastric cancer cell line (Shi et al., 2019). Similarly, expression of *ACSS2* is consistently high in a wide variety of cancers, while the expression of *ACSS1* can vary, but is typically lower (Yoshii et al., 2015). In this way, expression of these two genes in EBVaGC contrasts with what is known about the expression of these genes in other cancers since transcript levels for both *ACSS1* and *ACSS2* were low.

Within EBVaGCs, high expression of two genes, *ACLY* and *SCD*, were correlated with EBVaGC patient survival. Interestingly, as a whole, EBVaGCs had higher expression of these two genes compared to non-cancerous tissue. That a further increase in the expression of these genes within EBVaGC would be associated with patient survival is somewhat paradoxical. In a study correlating patient survival with the level of *ACLY* in EBV-negative GC, low levels were associated with survival (Qian et al., 2015). This once again illustrates

how EBVaGC is a metabolically distinct gastric cancer from EBV-negative gastric cancer. It is possible that the upregulation of *ACLY* and *SCD* could be a result of EBV infection (Wang et al., 2019b) rather than an unrelated pro-oncogenic pathway. Perhaps the upregulation of these transcripts serves a different function in EBVaGC when compared to EBV-negative GC and does not contribute to oncogenesis. In the future, it would be interesting to try to correlate the amount of viral EBV transcripts with the amount of *ACLY* and *SCD* transcripts, as perhaps they could act as a surrogate for a higher viral load and therefore a less severe course of STAD (Constanza Camargo et al., 2014). It is also interesting to note that a recent study measuring metabolite concentrations in EBVaGC cell lines identified many fluctuations in fatty acid metabolism (Yoon et al., 2019).

The trend in expression for transcripts encoding beta-oxidation enzymes was similar to that observed in a variety of other cancers. For example, expression of both *ACADM* and *ACADL* was lowered in hepatocellular carcinoma (HCC) cell lines and tumour models (Huang et al., 2014). This reduced cancer proliferation (Huang et al., 2014). The downregulation of *ACADM* and *ACADL* was mediated by hypoxia-related genes (Huang et al., 2014). It would be interesting to determine whether a similar mechanism is responsible for the downregulation of these transcripts in EBVaGC. *HADH* was another gene noted to be downregulated in multiple studies involving gastric cancers that were not stratified by EBV status (Enjoji et al., 2016; Shen et al., 2017). This implies that downregulation of this transcript in our analysis was unrelated to the EBV status of the cancer, but may rather be a general feature of gastric cancers. Both *HADHA* and *HADHB* were downregulated in breast cancers and HCCs (Mamtani and Kulkarni, 2012; Tanaka et al., 2013), which suggests that perhaps downregulation of these genes is a common feature of cancer-related metabolic reprogramming. Other beta-oxidation enzyme encoding transcripts that were downregulated in different cancer types in addition to EBVaGC were *ACAA1*, *ACAA2* and *ACAT1*. *ACAA1* has been found to be downregulated in colorectal cancer (Zhang et al., 2017b), while *ACAA2* was downregulated in a HeLa cervical cancer cells (Fang et al., 2020). *ACAT1* was found to be downregulated in both clear cell renal cell carcinoma (Chen et al., 2019; Zhao et al., 2015b) and colon cancer (Li et al., 2012). Presumably, downregulation serves to prevent beta-oxidation from occurring in cancer cells, which perhaps represents a significant, but underappreciated cancer metabolic

hallmark (Swinnen et al., 2006). That *ACAD9* was significantly upregulated in EBVaGC compared to non-cancerous tissue in our analysis may not necessarily have any functional ramifications, since there were a plethora of other downregulated beta-oxidation genes. It is also unusual for *ACAD9* to be upregulated in isolation. When *ACAD9* was upregulated in a study of breast cancer cell lines, the expression of other beta-oxidation genes were concurrently upregulated (Lamb et al., 2014).

In the PPP, EBVaGC displayed upregulation of two paralogous transcripts, *RPE* and *RPEL1*, the products of which perform a similar function, the conversion of D-xylulose 5-phosphate to D-ribulose 5-phosphate. This suggests that EBVaGC tumours would be especially vulnerable to downregulation of this transcript. However, and paradoxically, patients with tumours expressing high amounts of *RPE* transcript had better survival than patients with low levels of *RPE*. Other tumours that express high levels of *RPE* are pancreatic, breast, central nervous system, liver, lung, hematopoietic, pancreatic and prostate tumours (Rmaileh et al., 2020). In prostate tumours, inhibition of *RPE* suppressed tumour growth (Ying et al., 2012). Additionally, high transcript levels of *RPE* correlated with poor patient outcomes in liver and breast cancers (Rmaileh et al., 2020). Why EBVaGC showed the opposite survival trend, in which high numbers of *RPE* transcript were correlated with better outcomes, is unclear.

In terms of the MCT family of transporters in EBVaGC, there were some similarities with other cancers. The product of *SLC16A8*, MCT3, was frequently upregulated in hypoxic MCF7 breast cancer cells (Bando et al., 2003). It is possible that EBVaGCs are similarly hypoxic, thus causing the upregulation of this transcript. *SLC16A14*, which encodes MCT14, was downregulated in epithelial ovarian cancer when compared to non-cancerous tissue (Elsnerova et al., 2016, 2017), similar to EBVaGC. Expression of *SLC16A2* was downregulated in HPV+ HNSCC according to one of our previous analyses (Prusinkiewicz et al., 2020). This is notable because like EBVaGC, HPV+ HNSCCs are virally induced. Perhaps thyroid hormone transport is co-opted by DNA tumour viruses during oncogenesis. In another similarity between EBVaGC and other cancers, *SLC16A7* was downregulated in hepatocellular carcinoma (Alves et al., 2014). Little is known about the clinical relevance of MCT9 or MCT11 (Jones and Morris, 2016), encoded by the *SLC16A9*

and *SLC16A11*, respectively. The downregulation of *SLC16A9* and *SLC16A11* in EBVaGC may suggest unique roles for these transporters. Finally, high expression of *SLC16A13* could represent a novel prognostic indicator for patient survival in EBVaGC.

Understanding how the regulation of metabolism-related genes differs in EBVaGC from other GC subtypes is useful when considering these genes as prognostic indicators or druggable targets. Genes that are uniquely regulated in EBVaGC, but not other GCs, are especially attractive as specific targets for EBVaGC. Our analysis examining the differences in the expression of genes that are differentially regulated in EBVaGC when compared to other GCs indicated that no metabolic pathway is regulated in a completely identical manner to EBVaGC. Indeed, there were a number of metabolic genes that were uniquely regulated in EBVaGC and these could serve as a starting point for identification of effective and specific therapeutic compounds. These genes were *LDHB*, *COX20*, *ACSSI*, *ELOVL5*, *ACAD9*, *ACAA2* and *SLC16A14*. In addition, determining how differences in metabolic gene expression leads to different functional metabolic phenotypes across GCs is an interesting and open question. However, due to the relative paucity of EBVaGC cell lines, answering this question may first require the development of additional EBVaGC cell lines. That none of the significant survival curves comparing the effect of high or low expression of certain genes in EBVaGC met the FDR q-value cut-off suggests that the survival data should be validated in another independent cohort to confirm survival-associated differences.

4.5. Conclusions

EBVaGC represents a unique subtype of gastric cancer, which was illustrated in this analysis by the distinct expression of metabolism-related transcripts in EBVaGC. Expression of *LDHB*, *COX20*, *ACSSI*, *ACAD9*, *ACAA2*, and *SLC16A14* were uniquely regulated in EBVaGC. Additionally, the expression of certain transcripts could serve as potential prognostic indicators for survival outcomes, albeit after validation in another independent cohort. Low expression of the glycolytic enzyme-encoding transcript *ALDOB* was associated with improved survival outcomes in EBVaGC, while the literature indicated that low *ALDOB* expression was associated with worse survival outcomes in EBV-negative

gastric cancer (He et al., 2016). In yet another contrast, high expression of the fatty acid synthesis related transcript *ACLY* was associated with better survival outcomes in EBVaGC, while in the literature high *ACLY* expression was associated with worse survival outcomes for EBV-negative GC (Qian et al., 2015). It is possible these opposing patterns in EBVaGC could represent metabolic pathways that are altered as a result of EBV-related mechanisms. There were select commonalities in the regulation of genes in EBVaGC and other GC subtypes in most metabolic pathways including glycolysis (Figure 4.1), the TCA cycle (Figure 4.3), cellular respiration (Figure 4.4), fatty acid metabolism (Figure 4.6) and the MCT transporter encoding *SLC16A11*. These similarities could represent more general features of gastric cancer. Overall, EBVaGC appeared to exhibit a gene expression pattern that was indicative of an upregulation of glycolysis accompanied by a downregulation in the TCA cycle and oxidative phosphorylation. The pattern of the *SLC16A* transcripts were also consistent with increased glycolytic activity in EBVaGC. Finally, EBVaGC may exhibit a downregulation of beta-oxidation related metabolic pathways, a potentially unique metabolic feature of some cancers that remains underexplored and underappreciated.

Chapter 5

5 Discussion

5.1 Thesis Summary

This thesis investigated different aspects of the biology of metabolic reprogramming by DNA tumour viruses. The first sections of this thesis revolved around HAdV, which is a DNA tumour virus. HAdV serves a model for other DNA tumour viruses, such as HPV and EBV, even though HAdV has not been shown to cause cancer in humans. The reason HAdV is such an excellent model is because many important and conserved cancer-related pathways in both virally-induced and non-viral cancers were first discovered in HAdV due to its experimental tractability. In the introduction of my thesis, I discussed what was known about E4orf1, the first HAdV protein recognized to modulate cellular metabolism (Thai et al., 2014, 2015) and how, based on the literature, it was possible that E1A, another HAdV protein, could also be responsible for inducing changes in metabolism during HAdV infection.

This led to the chapter of this thesis in which I experimentally identified possible roles of E1A in changing functional metabolism and metabolism-related gene expression. Specifically, it appears that the 13S encoded isoform of E1A is responsible for the upregulation of transcripts related to glycolysis in addition to increasing the functional glycolytic rate. The 13S encoded isoform of E1A is also responsible for downregulating both cellular respiration related gene expression and the maximal cellular respiration rate. Interestingly, the 12S encoded isoform did not appear to alter functional metabolism in a manner that differed greatly from cells containing an empty vector. In the context of HAdV infection, IMR-90 cells infected with HAdV that contained the 13S encoded isoform of E1A, but not the 12S encoded isoform were capable of upregulating genes involved in glycolysis and the tricarboxylic acid cycle, while IMR-90 cells infected with HAdV that contained the 12S encoded isoform of E1A, but not the 13S encoded isoform, upregulated glycolytic genes to a lesser extent. This infection data supports the data obtained using E1A expression from a non-viral vector, in that the 13S encoded isoform of E1A appears to be

the predominant E1A isoform responsible for contributing to altered metabolism during infection.

However, as HAdV does not cause any human cancers, it was important to determine whether the presence of viral oncoproteins from other DNA tumour viruses lead to any appreciable metabolism-related gene expression differences in cancers of a viral etiology when compared to the corresponding non-virally induced cancer. To explore this question, RNAseq and patient survival data from the TCGA was analyzed for head and neck cancers and gastric cancers, a percentage of which can be induced by HPV or EBV, respectively. In the chapter comparing HPV+ HNSCCs to HPV- HNSCCs, HPV+ HNSCCs appeared to have lower expression of glycolysis related genes and higher expression of genes involved in the tricarboxylic acid cycle, cellular respiration, and beta-oxidation, a pathway that can potentially feed into the TCA cycle. This study also identified seven metabolism related genes that were associated with HPV+ HNSCC patient survival outcomes depending on the level of expression of each of these genes within the tumour. These genes were *SDHC*, *COX7A1*, *COX16*, *COX17*, *ELOVL6*, *GOT2*, and *SLC16A2*. The significance of identifying these genes is that they may potentially serve as prognostic indicators or, with further research, druggable therapeutic targets.

As for EBV-associated gastric carcinomas (EBVaGCs), there was more complexity in how these virally induced tumours compared to EBV-negative gastric carcinomas. This is because EBV-negative gastric carcinomas can be further subdivided based on their genomic features. For this reason, our analysis explored the overlap between the genes differentially regulated by EBVaGC and the other gastric cancer subtypes. While the expression of metabolism-related genes was never completely identical across the gastric cancer subtypes, the expression of many genes within these metabolic pathways was similar. To explicitly differentiate EBVaGC based on metabolic phenotype, it was important to identify the genes that were uniquely expressed when compared to other gastric cancer subtypes. The uniquely regulated genes in EBVaGC were *LDHB*, *COX20*, *ACSS1*, *ELOVL5*, *ACAD9*, *ACAA2*, and *SLC16A14*. These genes could represent novel weak points in EBVaGC that could be targeted therapeutically. In addition to these genes, there were a number of metabolic genes associated with EBVaGC patient survival

outcomes. Interestingly, these genes differed from those that were uniquely expressed in EBVaGC. The metabolism-related genes associated with survival in EBVaGC were *PFKM*, *ALDOB*, *NDUFA4L2*, *ACLY*, *SCD*, and *SLC16A13*. As with the survival-associated genes in HPV+ HNSCC, this set of survival-associated genes could serve as novel prognostic indicators or biomarkers, and potentially represent novel therapeutic targets.

In short, the purpose of this thesis was to illustrate that not only do viral oncoproteins contribute to metabolic reprogramming in the host-cell, but that this metabolic reprogramming is an aspect of the viral etiologies of these cancers. These etiologies are driven by the functions of these oncoproteins to generate a metabolic phenotype that is unique to that cancer subtype and can therefore be used to differentiate the cancer subtype from other subtypes. The remaining section of this chapter will: 1) discuss how viral oncogenes could specifically reprogram metabolism in light of the results presented in this thesis, 2) highlight how metabolic biomarkers are an important consideration in cancer, 3) discuss limitations of this work based on the approaches used, and 4) consider future work that could be performed based on the results of this thesis.

5.2 Viral Oncogenes and Metabolism

Virally encoded oncogenes are an essential component of modulating how DNA tumour viruses reprogram cellular metabolism. Despite the variety of sizes and functionalities between the different oncoproteins encoded by different viruses, there are a few common targets that could be attractive candidates for future work that attempts to explore methods of targeting virally induced metabolic reprogramming for therapy.

These common targets include *MYC*, which is a transcriptional regulator known to activate the transcription of genes involved in glycolysis, glutaminolysis, nucleotide synthesis and fatty acid synthesis (Wolf et al., 2015) (Figure 5.1). As *MYC* is a transcription factor, this typically occurs through *MYC*-induced transcriptional upregulation of metabolic genes. This includes *LDHA*, which converts pyruvate to lactate (Shim et al., 1997). Another *MYC*-upregulated metabolic gene is *GLUT1*, a major glucose transporter (Osthus et al., 2000). The glutamine transporter *SLC1A5* is also upregulated by *MYC* (Zhao et al., 2019). As a

result of increased MYC-induced glycolysis, the PPP is also upregulated (Morrish et al., 2009), and MYC is directly responsible for inducing the transcription of the PPP enzyme *PRPS2* (Mannava et al., 2008). Many other nucleotide synthesis genes are also upregulated by MYC (Liu et al., 2008). In addition, a multitude of genes involved in fatty acid synthesis are upregulated by MYC including *ACLY*, *ACACA*, *FASN* and *SCD* (Edmunds et al., 2014; Morrish et al., 2010). Finally, the mitochondrial processes of fusion and fission are also reported to be under some level of control by MYC (Graves et al., 2012). Given that MYC impinges on so many metabolic pathways, understanding which DNA tumour viruses are capable of altering MYC activity could be important for understanding the mechanisms behind DNA tumour virus metabolic reprogramming.

Another protein commonly affected by viral oncoproteins is the tumour suppressor p53 (Figure 5.2). Many viral oncoproteins inhibit the activity of p53, which in turn can increase the glycolytic activity of the infected cell (Ou et al., 2011). This is because activated wild type p53 can increase the activity of SCO2, which is involved in the assembly and regulation of the COX proteins that make up the mitochondrial cellular respiration complex IV (Matoba et al., 2006). Therefore, by inhibiting p53, the viral oncoproteins serve to inhibit mitochondrial function, which can subsequently trigger the upregulation of glycolytic pathways. p53 expression can also decrease levels of the glucose transporters Glut1, and Glut4 (Schwartzberg-Bar-Yoseph et al., 2004), as well as the glucose metabolism enzyme PGM (Kondoh et al., 2005). p53 expression also increases TP53 Induced Glycolysis Regulatory Phosphatase (TIGAR) expression, which can function to inhibit glycolysis (Bensaad et al., 2006).

DNA tumour viruses also commonly target the activity of pRb, which is responsible for inhibiting the E2F family of transcription factors (Figure 5.3). In addition to regulating cell growth and proliferation through the cell cycle, E2F regulates the expression of a multitude of metabolic enzymes that are involved in glycolysis, the TCA cycle, cellular respiration and nucleotide synthesis (Nicolay and Dyson, 2013). For example, E2F is responsible for regulating the expression of the glycolytic enzyme PFKFB (Darville et al., 1995; De Mattos et al., 2002). E2F can also increase the expression of PDK4, which inhibits the entry of pyruvate into the TCA cycle, further promoting glycolysis (Hsieh et al., 2008). Another

way in which E2F expression leads to a metabolic phenotype that is more akin to cancer cells is by activating glutaminolysis (Nicolay et al., 2013; Reynolds et al., 2014). E2F1 also plays a prominent role in inducing the expression of nucleotide synthesis genes (DeGregori et al., 1995). As certain oncoproteins are capable of binding pRb, thus activating E2F, the ability of E2F to influence cellular metabolism is a relevant area of future research to aid in understanding how the metabolic pathways that were outlined in the research chapters of this thesis are potentially altered by DNA tumour viruses during infection or in virus-dependent cancers.

5.2.1 Viral Oncoprotein Regulation of MYC

The most widely recognized oncoproteins in HAdV that can regulate MYC are E1A (Berk, 1986) and E1B (Barker and Berk, 1987) (Figure 5.1). E4orf1 (Javier, 1994) and E4orf6 (Nevels et al., 2000) are two other HAdV proteins that have a role in MYC regulation (Figure 5.1). Recent advances in proteomics have identified that HAdV consistently upregulates MYC throughout infection (Valdés et al., 2018). In a series of elegant experiments, E4orf1 was identified to be a significant HAdV protein responsible for upregulating MYC expression during infection and contributing to the associated increases in glycolysis and glutaminolysis (Thai et al., 2014, 2015). The HAdV oncoprotein E1A is reported to influence MYC activity through the TRRAP protein (Zhao et al., 2017), which could account for the findings in chapter three of this thesis, which illustrate that glycolysis can be regulated by E1A. E1A can also stabilize MYC itself (Löhr et al., 2003). The HAdV protein E4orf6 can influence an upregulation of MYC activity in two ways. One way is via stabilization of the amount of *MYC* transcript, presumably leading to greater production of MYC (Higashino et al., 2005). A second mechanism by which E4orf6 can influence MYC activity is through further stabilization of the interaction of E1A with MYC (Thai et al., 2014). In addition, E4orf4, which is not defined as an oncoprotein, inhibits MYC during infection (Ben-Israel et al., 2008), but this study was flawed as it was conducted in HEK293 cells, which already express E1A and E1B (Graham et al., 1977). In contradiction to this idea, E4orf4 has also been found to cause an increase in MYC protein levels (Arnold and Sears, 2006). Both E4orf6 and E1B-55K have also been reported downregulate MYC expression (Löhr et al., 2003), also a contradictory function for E4orf6.

Numerous reports outline the interactions and regulation of MYC by the HPV E6 and E7 oncoproteins (Figure 5.1). Both E6 and E7, albeit less efficiently, have been reported to upregulate MYC (Peta et al., 2018). However, more evidence exists for the association of E6 with MYC than E7 (Zhang et al., 2017c). Although some of that evidence is contradictory. For example, one study found that MYC merely associated with E6, but was not upregulated by the HPV oncoprotein (Veldman et al., 2003). Another study found that E6 may rely on another transcription factor, Sp1, to mediate the changes in transcription that occur as a result of the E6/MYC interaction (Oh et al., 2001). Somewhat confusingly, it was reported that E6 can also stimulate the degradation of MYC (Gross-Mesilaty et al., 1998). Despite all these reports, perhaps the most convincing evidence that E6 stimulates MYC activity was the ability of MYC overexpression to immortalize cells in conjunction with E7 in a manner similar, but not identical to E6 and E7 induced immortalization (Liu et al., 2007). As for the E7 oncoprotein, it is possible that HPV18 E7 can interact with MYC to promote MYC-regulated transcription (Wang et al., 2007). It is also possible that E7 can promote MYC activity indirectly, as a study utilizing HPV16 E7 found that E7 could inhibit a negative regulator of MYC activity, the protein MIZ1 (Morandell et al., 2012). The result of this was increased MYC function. Perhaps somewhat contradictorily, two studies of HPV+ HNSCC tissue samples did not identify an association between HPV+ HNSCC and increased MYC expression (Bhattacharya et al., 2005, 2009). However, another study of patient tissues found that HPV integration within the tonsillar crypt was associated with MYC amplification and overexpression (Kim et al., 2007b).

In B cell lymphomas, EBV appears to drive MYC expression in a variety of ways. Perhaps the most common EBV-induced change to MYC expression is in the form of a common *MYC*-translocation event in EBV-positive Burkitt's lymphoma (Dalla-Favera et al., 1982). In this translocation event, *MYC* is translocated to the immunoglobulin heavy locus gene, *IGH*, where it comes under control of the highly active *IGH* regulatory region (Allday, 2009). This leads to constitutive expression of MYC in Burkitt's lymphoma (Allday, 2009; Fitzsimmons and Kelly, 2017). However, the expression of multiple EBV viral proteins have been associated with MYC expression in the B cell cancers. EBNA2 was noted activate MYC transcription in primary B lymphocytes (Kaiser et al., 1999). EBNA2 can also upregulate protein expression of MYC (Zhao et al., 2011). There is evidence that

EBNA2 can increase interactions between enhancers and promoters upstream of *MYC* through the chromatin regulator SMARCA4 (Wood et al., 2016). EBNA2 can bind at regions termed EBV-super enhancers in which a complex of EBV latent proteins can increase the expression of host-cell genes, such as *MYC* (Zhou et al., 2015). EBNA2 may also increase expression of non-coding enhancer RNAs (eRNAs) that regulate *MYC* transcription (Liang et al., 2016). EBNA2-driven *MYC* expression can also upregulate mitochondrial one-carbon metabolism, specifically the *de novo* synthesis of serine, which contributes to nucleotide synthesis, mitochondrial NADPH production, and production of the antioxidant glutathione (Wang et al., 2019a). Other metabolic pathways upregulated by EBNA2-driven expression of *MYC* in B cells include cholesterol and lipid biosynthesis (Magon and Parish, 2021; Wang et al., 2019b). Two other EBNA proteins, EBNA3A and EBNA3C, also contribute to *MYC* expression. Both EBNA3A and EBNA3C contribute to the EBV-super enhancer structure that ensures the presence of transcription factors at the *MYC* transcription start site by enhancer-promoter looping (Jiang et al., 2017). Additionally, EBNA3C stabilizes the interaction between *MYC* and *MYC*-target promoters, essentially increasing *MYC* activity (Bajaj et al., 2008). To further augment *MYC* expression, EBNA3A and EBNA3C cooperate to epigenetically repress *BCL2L1* expression, which encodes a negative regulator of *MYC*. *BCL2L1* expression can be induced by *MYC* in the absence of EBNA3A and EBNA3C in a negative feedback mechanism (Anderton et al., 2008; Paschos et al., 2009; Styles et al., 2018)

The EBV latent membrane proteins (LMPs) also play a role in increasing *MYC* expression in EBV-driven cancers. In B cells, LMP1 can increase *MYC* transcription and resulting *MYC* protein expression via the JAK/STAT pathway (Dirmeier et al., 2005). STAT3 in particular is upregulated in EBV-positive nasopharyngeal carcinoma cell lines (Chen et al., 2003; Kwok Fung Lo et al., 2006). Also in EBV-induced nasopharyngeal carcinoma, LMP1 facilitates increased interactions between *MYC* and the *MYC*-target genes *HK2* and *IDH2*, which encodes an enzymes in glycolysis and the tricarboxylic acid cycle, respectively (Cao et al., 2021; Shi et al., 2020; Xiao et al., 2014). This *MYC* stabilization occurs through a LMP1 signalling pathway that involves PI3K/AKT/GSK3 β and FBXW7 signalling (Cao et al., 2021; Xiao et al., 2014). The importance of this LMP1-mediated *MYC* activation pathway is emphasized by a study in which the histone deacetylase

inhibitor romidepsin was found to be cytotoxic to an EBV-positive diffuse large B-cell lymphoma in both cell culture and a mouse xenograft model by reducing expression of both LMP1 and MYC (Shin et al., 2015). In addition to causing increased MYC expression and activity, LMP1 also downregulates the α -isoform of the MYC repressor PRDM1, which further accentuates LMP1-driven MYC activation (Vrzalikova et al., 2011). In a similar manner, LMP2A can facilitate MYC activity by enhancing degradation of the MYC inhibitor and tumour suppressor, CDKN1B (Fish et al., 2017). LMP2A can also increase translation of MYC, but not transcription of *MYC*, through the PI3K/AKT/mTOR signalling pathway (Moody et al., 2005). Finally, the EBV pro-survival BCL-2 homologue, BHRF1, has a synergistic effect with MYC to enhance MYC-activity in a mouse model of Burkitt's lymphoma (Fitzsimmons et al., 2020). EBV appears to tightly regulate MYC in infected B cells to modulate lytic reactivation that would otherwise occur with the absence of MYC (Guo et al., 2020).

Interestingly, the regulation of MYC by EBV oncoproteins appears to be relatively minimal (Figure 5.1). At most, MYC may be upregulated in EBVaGC during its early stages (Ishii et al., 2001). However at later times during the progression of EBVaGC, MYC was either downregulated (Ishii et al., 2001; Lima et al., 2008b) or MYC expression did not correlate with EBV expression at all (Lima et al., 2008a; Luo et al., 2006; Zhu et al., 2013). These findings suggest that MYC may not have a role in EBV induced metabolic alterations associated with EBVaGC.

5.2.2 Viral Oncoprotein Regulation of p53

p53 impinges on a variety of metabolic pathways, and its inhibition appears to be involved in the upregulation of glycolysis. It is possible that the action of certain viral oncoproteins on p53 may be responsible for the metabolic changes in virally induced cancers or DNA tumour virus infected cells discussed in this thesis. While there are some similarities between the mechanisms by which p53 is inhibited in HAdV, HPV or EBV (Figure 5.2), due to the differences in number and structure of viral oncoproteins between these viruses, there are also many distinct features.

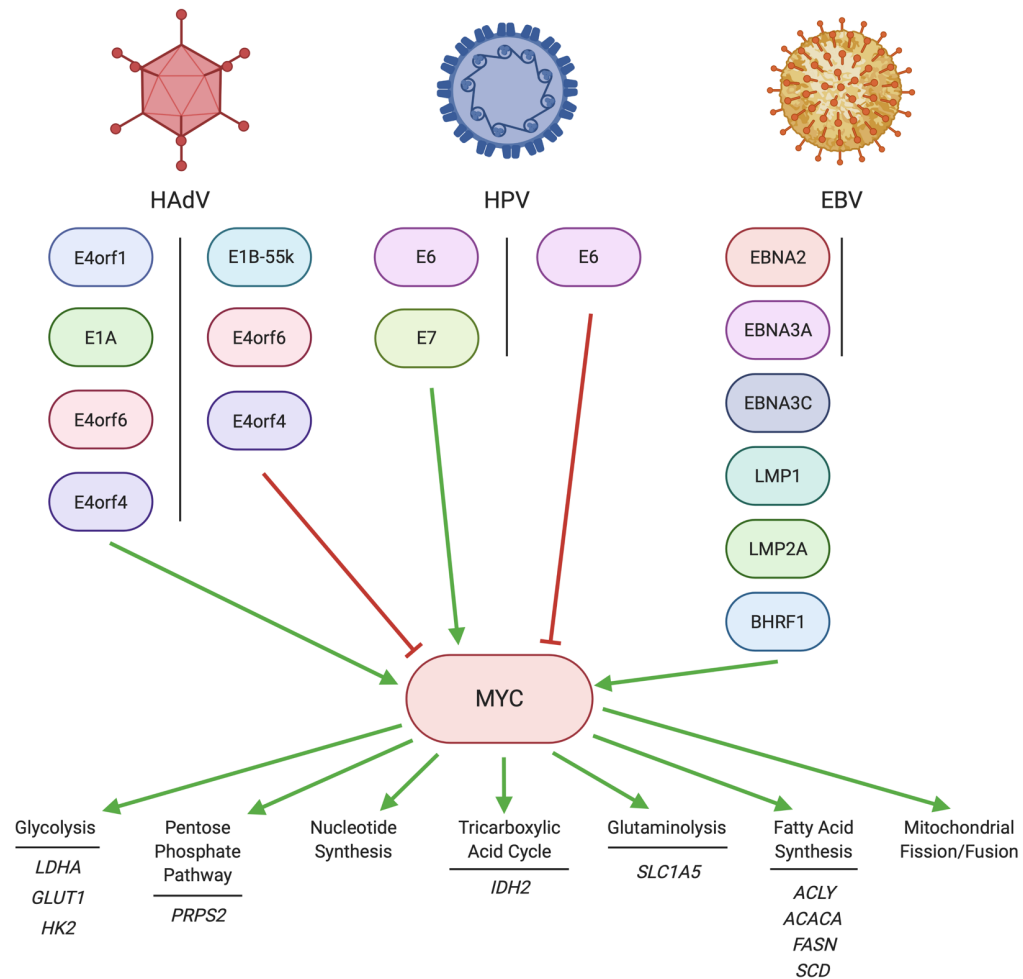


Figure 5.1. Regulation of MYC by DNA tumour virus oncoproteins. Both HAdV and HPV are capable of regulating MYC activity or expression. The HAdV oncoprotein E1A is reported to be a positive regulator of MYC activity while E1B-55k is a negative regulator of MYC. The HAdV protein E4orf1 is a well-established MYC regulator. Both E4orf4 and E4orf6 are reported to have both activating and inhibitory effects on MYC. The E6 and E7 HPV oncoproteins have been reported to positively regulate MYC, while E6 has also been reported to inhibit MYC. EBV oncoproteins do not appear to directly influence MYC in gastric cancers, but there are a number of EBV latent proteins that can positively regulate MYC in B cell infections. MYC is a key regulator, primarily as a transcription factor, for many metabolic genes and pathways.

The HAdV oncoprotein E1B is most directly responsible for binding to and inhibiting the transcriptional activation activity of p53 (Sarnow et al., 1982; Yew and Berk, 1992). The ability of E1A to interact with and affect p53 is more nuanced. It appears that E1A induces apoptosis through p53 and even triggers p53 accumulation (Lowe and Earl Ruley, 1993; Querido et al., 1997; Teodoro et al., 1995). However, E1A has also been reported to inhibit the transcriptional activation of target genes by p53 and repress its activity (Steege et al., 1996, 1999). Additionally, E1A and either mutant p53 or an absence of p53 entirely have been reported to transform cells (Horikoshi et al., 1995; Lowe et al., 1994), which would presumably lead to the induction of cancer-related metabolic pathways. Two of the E4 HAdV proteins have also been reported to contribute to p53 inhibition. E4orf6 directly inhibits the transcriptional activity of p53 (Nevels et al., 1999b), while E4orf3 can induce inhibitory H3K9 methylation of the promoters to which p53 would bind (Soria et al., 2010).

The HPV E6 oncoproteins, especially those of the most oncogenic types, HPV16 and HPV18, are responsible for modulating p53 activity by binding to and inducing degradation of p53 (Lechner et al., 1992; Scheffner et al., 1990; Werness et al., 1990). In contrast, the HPV E7 oncoprotein was reported to stabilize p53, which promoted apoptosis of infected cells (Jones et al., 1997). E6 can contribute to the bypassing of this apoptotic induction by E7, which bears some resemblance to the opposing activities of HAdV E1A and E1B. However, it has been reported that E7 may inhibit p53 transcriptional activity (Massimi and Banks, 1997). This implies that E7 could influence the changes in cellular metabolism that occur as a result of p53 inhibition.

EBV can influence the function of p53 through a variety of viral oncoproteins. These include the EBV latency protein EBNA3C, which has been noted to inhibit p53 DNA binding activity (Shukla et al., 2016; Yi et al., 2009). LMP1 is another EBV latency protein and oncoprotein that can inhibit the activity of p53 (Fries et al., 1996; Liu et al., 2005; Shao et al., 2004; Zeng et al., 2020). Interestingly, p53 also induces LMP1 expression, which is an example of a feedback loop in which the virus is directly responding to the activity of tumour suppressor pathways (Wang et al., 2017). Finally, the immediate early lytic protein BZLF1 can inhibit p53 transactivation of its targets (Zhang et al., 1994). It would be

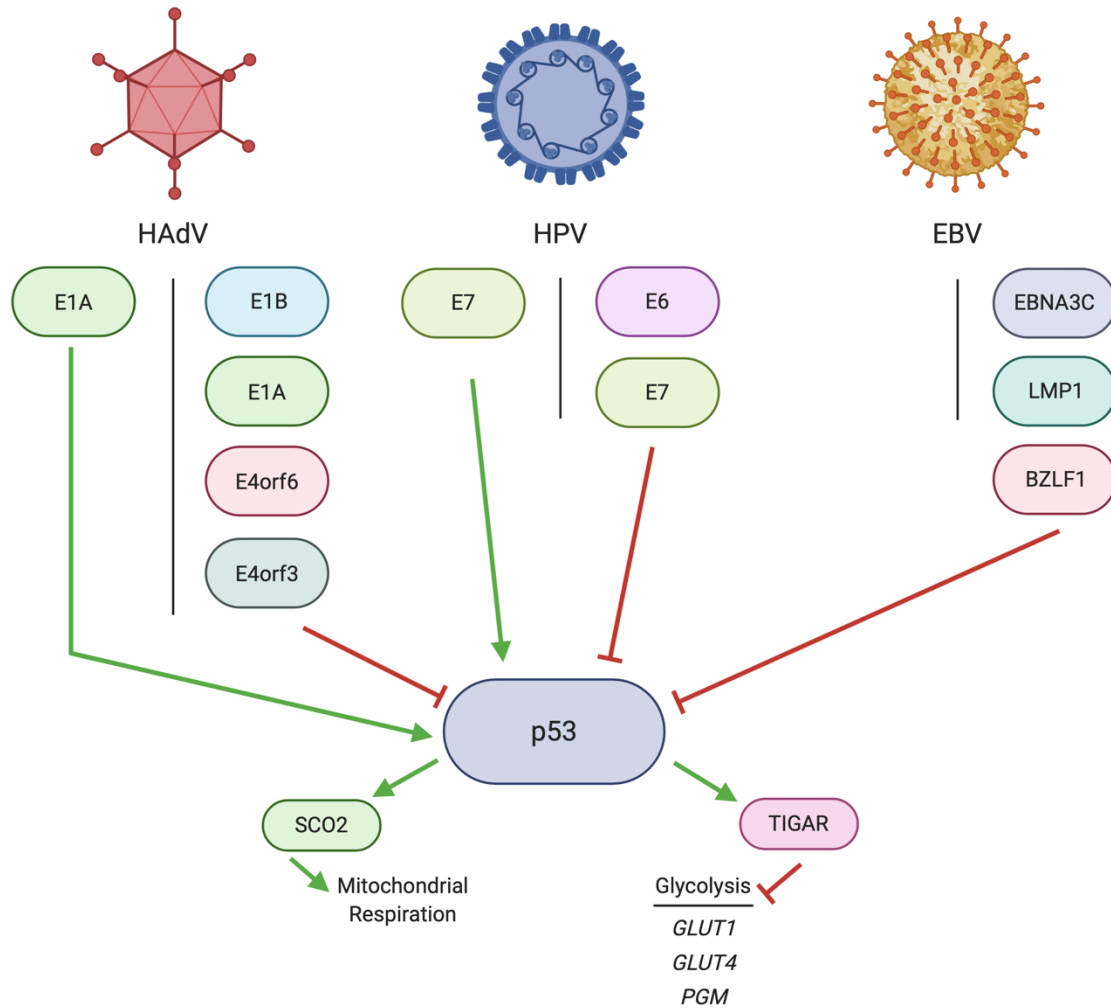


Figure 5.2. Regulation of p53 by DNA tumour virus oncoproteins. Each of HAAdV, HPV and EBV have been reported to influence the activity of p53. E1A is the only HAAdV oncoprotein reported to both activate or inhibit p53 depending on the infection context. Typically, the HAAdV oncoprotein E1B counteracts E1A-mediated activation of p53. The HAAdV viral proteins E4orf3 and E4orf6 have also been reported to inhibit p53 activity. The HPV oncoprotein E7 has also been reported to have both activating or inhibitory functions on p53, while the E6 oncoprotein has only been reported to inhibit p53. The EBV proteins EBNA3C, LMP1, and BZLF1 have also been reported to inhibit p53 activity. p53 can modulate metabolism by activating mitochondrial respiration through SCO2, while inhibiting glycolysis through the TIGAR protein or by negatively influencing the transcription of a subset of glycolytic genes.

interesting to explore whether there is a direct link between the expression of each of these oncoproteins within gastric cancer cell lines, the resulting expression of p53, and glycolytic upregulation or other associated metabolic changes.

5.2.3 Viral Oncoprotein Regulation of pRb/E2F

The only HAdV oncoprotein that appears to interact with pRb is E1A (Moran, 1993) (Figure 5.3). E1A can bind pRb directly to release E2F inhibition (Valdés et al., 2018), which allows for transcription of a variety of genes including metabolism-related genes. However, if E1A is bound to pRb and p300, this can have an inhibitory effect on the transcription of other metabolism related genes that are not transcribed by E2F due to the ability of this complex to lead to hypoacetylated and condensed chromatin (Ferrari et al., 2014). The p300 linked to E1A may acetylate pRb in the complex which prevents inhibitory pRb phosphorylation (Ferrari et al., 2014).

The E7 oncoprotein of HPV is primarily responsible for influencing pRb (Figure 5.3), especially at early stages of infection (Balsitis et al., 2005, 2003; Chellappan et al., 1992). Primarily, E7 induces the degradation of pRb (Gonzalez et al., 2001), but it is also capable of simply displacing pRb from E2F family members to induce DNA synthesis (Collins et al., 2005). Influencing pRb activity does not appear to be a major role for any of the other HPV encoded proteins, including the E6 HPV oncoprotein.

A variety of EBV-encoded viral proteins are capable of inducing E2F expression. One example is the immediate-early EBV protein BRLF1 (Swenson et al., 1999; Zacny et al., 1998). Some of the EBV-encoded EBNA proteins are also capable of binding pRb which results in E2F activity. Both EBNA3C (Parker et al., 2000) and EBNA5 (Szekely et al., 1993) can bind pRb to induce E2F dependent gene expression (Figure 5.3).

5.3 The Importance of Biomarkers in Metabolism

A large portion of this thesis was dedicated to identifying metabolism-related gene expression patterns in DNA tumour virus induced cancers. Genes with altered expression could potentially serve as metabolic biomarkers associated with patient outcomes, or help to differentiate virally induced cancers from their non-virally induced counterparts.

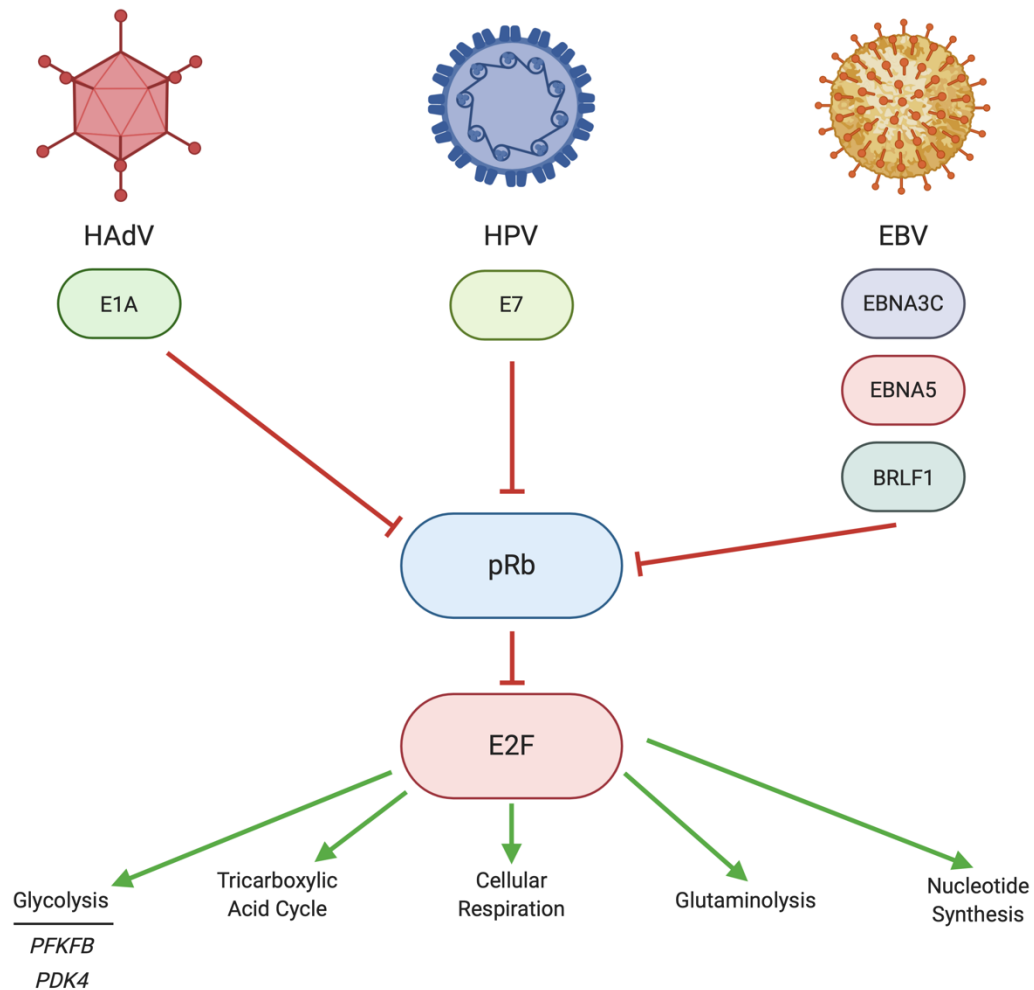


Figure 5.3. Regulation of pRb/E2F by DNA tumour virus oncoproteins. pRb is the inhibitory regulator associated with E2F to modulate its transcription factor activity. Each of HAdV, HPV and EBV are capable of inhibiting pRb, typically through a physical interaction, which releases E2F. The HAdV protein E1A can bind to pRb, which releases pRb inhibition of E2F. HPV E7 performs a similar role to remove pRb from E2F, thus permitting the transcriptional activity of E2F. EBV has three proteins which can inhibit pRb. These are EBNA3C, EBNA5, and BRLF1. E2F can transcribe genes that encode enzymes in a number of metabolic pathways.

However, as metabolism is a function and product-based process, with clearly discernable features, such as the metabolites themselves, a valid question is whether inferring metabolic function from gene expression is a valid approach. Existing literature appears to suggest that there is a high degree of concordance between gene expression and the resulting cellular metabolic function (Jerby and Ruppin, 2012). This is an important observation, as in a clinical setting it may be more logistically feasible to rapidly measure metabolite outputs, for example from urine or blood samples, than to sequence a tumour biopsy. Exploring whether the metabolites produced by virally induced tumours correspond to the altered expression of metabolic genes would be an interesting topic of future research. Another reason why the identification of metabolism-related biomarkers is important is that these differentially regulated genes may potentially serve as weak points in synthetic lethality (reviewed in (Mast et al., 2020)). The idea is that inhibiting one aspect of a metabolic process therapeutically may synergize with the altered metabolic profile of a tumour resulting from differential expression of a certain gene, which then makes that tumour especially susceptible to killing by the therapeutic compound. This would be especially useful if the therapeutic compound was administered at a dose that was non-lethal to the surrounding non-cancerous tissue.

The knowledge of which metabolic genes are affected by certain DNA tumour viruses could be combined with knowledge about which cellular transcription factors are utilized by the virus to enact these metabolic changes. For example, targeting certain glycolytic enzymes upregulated by MYC represented vulnerabilities that were not present in cells with non-dysregulated levels of MYC. (Cermelli et al., 2014; Toyoshima et al., 2012). Understanding which cellular regulatory protein is employed by a virus to induce metabolic changes could lead to a potentially targetable combination. Alternatively, targeting the viral oncoprotein and the cellular regulatory protein, or targeting the viral oncoprotein and an upregulated metabolic protein could also be potential avenues to explore for synthetic lethality (Mast et al., 2020).

5.4 Limitations of this Work

The material presented in the research chapters of this thesis provided novel insight into metabolic regulation by DNA tumour viruses, both in the context of infection and cancer. However, like all research, there are limitations associated with the work presented in this thesis.

The first limitation is a result of the especially dynamic nature of metabolism and the relatively static nature of data measurement. For example, both the qPCR data generated in chapter 2 of this thesis and the RNAseq data analyzed in chapters 2, 3 and 4 of this thesis are only representative of the metabolic state of the cell or tissue at the timepoint at which the samples were collected.

For data generated using cell lines, using different infection times or collecting cells after a shorter or longer period of growth could lead to different levels of metabolism-related transcripts. However, this does not necessarily mean that the metabolic states of the cells reflected in chapter 2 are not indicative of a metabolic program that the HAdV infected or E1A-isoform transduced cells are performing at least at some point during their lifespan or infection progression. However, time is another factor to be considered when translating the findings of this research into potential therapies. It could be that cells or diseased tissue may need to be treated at specific timepoints in order to target the desired metabolic pathway.

In terms of the TCGA data, which was generated from patient samples. The data represent an amalgamation of the differing timepoints and conditions from which the patient tissue was resected. This means that the median expression level of transcripts in certain tissues may be far from what could be observed in any one tissue individually. Hypothetically, it is possible that more advanced cancerous tissue may exhibit a completely different metabolic program than tissue from an earlier state of tumor progression. This adds complexity to translating the findings of these analyses, as timing and other physiological conditions may also be a factor. The TCGA does contain data about the stage and grade of resected tumours, but a larger dataset would be required to stratify tumours based on these parameters. However, considering the intricacies of obtaining patient tumour tissues in

high numbers, and matching them with non-cancerous tissue, the TCGA is an invaluable resource for determining which metabolism-genes of interest should be investigated further.

Another limitation to the studies presented in this thesis is that they primarily focus on RNA expression rather than protein expression. RNA expression levels do not necessarily correlate with protein levels (Fortelny et al., 2017). It is possible that the metabolic effects predicted to occur based on the RNA expression data may not occur if the levels of the correspondingly encoded protein do not change in a similar fashion. However, as shown in chapter 2, the functional metabolic data does appear to proceed as expected in cells transduced with E1A-isoforms, as was predicted based on the qPCR data from the same cell lines. In a corollary to this, miRNAs may be a factor in contributing to changes in both viral and host-cell gene expression, and miRNAs were not considered in this thesis. EBV is reliant on its own virally-encoded miRNAs to modulate gene expression and the cell cycle in infected cells, and these miRNAs may play a role in the genetic program of EBVaGC (Choy et al., 2008; Kim et al., 2007a). Additionally, both HPV (Lajer et al., 2012) and HAAdV (Huang et al., 2019; Manríquez et al., 2020; Zhao et al., 2015a) can induce altered expression of miRNAs encoded by the host cell, which may also have implications for metabolic reprogramming of the infected cell.

5.5 Future Work

The role of the mitochondria in promoting tumour growth, including tumours caused by DNA tumour viruses, may be one of the most important future avenues of cancer metabolism research. The conventional wisdom that increased glycolysis and limited mitochondrial activity leads to, or is associated with, increased tumour growth may not be entirely true. Functional mitochondria appear to be necessary for an increasing number of cancers, and other studies have shown that glycolysis is dispensable in many cases (Guo et al., 2011; Ju et al., 2014; Weinberg et al., 2010; Ždravlević et al., 2018). Indeed, the results from chapter 3 of this thesis suggest that HPV+ HNSCCs are more reliant on mitochondrial activity than HPV- HNSCCs, and even EBVaGCs utilized the TCA cycle as shown in chapter 4 of this thesis.

Linking metabolic pathways to other pathways that are reliant on components of cellular metabolism may also yield novel insight into how metabolism contributes to other cancer-related mechanisms in DNA tumour virus induced cancers. For example, EBV is thought to downregulate apoptosis, a process that is closely tied to the mitochondria, by downregulating mitochondria biogenesis (Gilardini Montani et al., 2019). This is especially interesting considering the analysis in chapter 4 of this thesis, in which EBVaGC showed broad downregulation of genes encoding mitochondrial components. Affecting mitochondrial biogenesis could be another way that DNA tumour viruses influence apoptosis aside from inhibiting p53 function. Necrosis is another mitochondria-related process of cell death that can occur in cancer and it remains relatively unexplored (Proskuryakov and Gabai, 2009), especially in the context of DNA tumour viruses.

Interestingly, compounds that attempt to treat cancers by targeting metabolism have been generally unsuccessful either due to a lack of efficacy or specificity (Faubert et al., 2020). However, the anti-diabetic compound metformin is increasingly becoming an attractive candidate to target tumour metabolism. In addition to its effects on insulin, it also is capable of inhibiting components of the mitochondria, which may be the key to targeting the altered metabolic profile of cancer cells (El-Mir et al., 2000; Wheaton et al., 2014). There are a multitude of studies showing the efficacy of this compound on a variety of cancer types, including a subset of HNSCCs (Davies et al., 2017; Madera et al., 2015) and a few clinical trials are underway (Arrieta et al., 2019; Brown et al., 2020). Additionally, recent studies show that inhibiting cancer cell metabolism with both metformin and a glycolytic inhibitor could be especially effective (Oshima et al., 2020). However, as demonstrated in the data chapters of this thesis, cancers do not have a homogenous metabolic profile. In the case of DNA tumour virus induced cancers, the particular viral oncoproteins expressed within the tumour could influence its metabolic profile, as demonstrated in chapter 2 of this thesis. For this reason, identifying and testing metabolic inhibitors on DNA tumour virus induced cancers could be an extremely valuable avenue for future research.

Another idea that will likely become central to the study of cancer-related metabolism, including DNA tumour virus induced cancers, is the concept of oncometabolites. Oncometabolites are metabolites that can induce oncogenic epigenetic changes within a

cell or promote other oncogenic changes (Nowicki and Gottlieb, 2015; Yong et al., 2020). For this reason, associating the levels of metabolism-related gene expression with metabolite concentrations and oncogenic epigenetic changes, and determining which parameter effects change, is another important area of future research.

5.6 Concluding Remarks

Understanding the intersection between the metabolism of virally infected cells and cancer cells is especially pertinent in the case of DNA tumour viruses, which both cause distinct diseases and in rare circumstances can lead to the development of cancer. Due to the close parallels between the metabolic program of a virally infected cell and a cancerous cell, understanding the metabolism of one disease can lead to new insights into the metabolism of the other disease. In cancers caused by DNA tumour viruses, at least some of the metabolic reprogramming that occurs is due to the presence of viral oncoproteins. It is interesting that these changes may resemble cancer counterparts with a non-viral origin, but have a distinct etiology.

An appreciation for viral metabolism is especially important considering that at the time of writing, the world is in the midst of a pandemic caused by a novel coronavirus, SARS-CoV-2. Part of the reason the emergence of SARS-CoV-2 is particularly concerning is because, unlike known endemic viruses and bacteria, such as Rabies virus or *Mycobacterium tuberculosis*, its biology is poorly characterized and therapeutic options to treat the virus are very limited. A landmark proteomic study of SARS-CoV-2 infection of Caco-2 cells indicated that glycolysis, cholesterol metabolism and nucleotide metabolism were upregulated by the virus in infected cells (Bojkova et al., 2020). Inhibition of either glycolysis with the hexokinase inhibitor 2-DG or guanosine synthesis with ribavirin inhibited replication of SARS-CoV-2 (Bojkova et al., 2020). It appears that metabolic pathways identified to affect well characterized viruses also play a role in the replication of emerging viruses such as SARS-CoV-2, highlighting the importance of studying the metabolic reprogramming of virally infected cells.

Finally, studying the metabolic profile of virally induced cancers, such as HPV+ HNSCC or EBVaGC are also of utmost importance even with the existence of an extremely

effective HPV vaccine that can prevent the occurrence of HNSCC (Petrosky et al., 2015). In the case of EBV, no effective vaccine for EBV induced cancer exists, which necessitates a full understanding of the phenotype of EBV-positive cancers. For HPV+ cancers, despite the safety and effectiveness of the vaccine, vaccine unawareness and anti-vaccine sentiment limit vaccine uptake amongst people in many different countries that have access to the vaccine (Chen et al., 2020a; Chido-Amajuoyi et al., 2020; Rančić et al., 2020; Simms et al., 2020). This is also compounded by potential disruption to HPV vaccination schedules due to the coronavirus pandemic (Pfeffer, 2020). For these reasons, understanding the effect of viral oncoproteins on host-cell metabolic reprogramming and how these may result in unique metabolic profiles in cancers caused by DNA tumour viruses remains a topic of utmost research significance.

References

- Aa, J., Yu, L., Sun, M., Liu, L., Li, M., Cao, B., Shi, J., Xu, J., Cheng, L., Zhou, J., et al. (2012). Metabolic features of the tumor microenvironment of gastric cancer and the link to the systemic macroenvironment. *Metabolomics* 8, 164–173.
- Ablack, J.N.G., Pelka, P., Yousef, A.F., Turnell, A.S., Grand, R.J.A., and Mymryk, J.S. (2010). Comparison of E1A CR3-Dependent Transcriptional Activation across Six Different Human Adenovirus Subgroups. *J. Virol.* 84, 12771–12781.
- Akins, N.S., Nielson, T.C., and Le, H. V. (2018). Inhibition of Glycolysis and Glutaminolysis: An Emerging Drug Discovery Approach to Combat Cancer. *Curr. Top. Med. Chem.* 18, 494–504.
- Allday, M.J. (2009). How does Epstein-Barr virus (EBV) complement the activation of Myc in the pathogenesis of Burkitt's lymphoma? *Semin. Cancer Biol.* 19, 366–376.
- Allday, M.J., Bazot, Q., and White, R.E. (2015). The EBNA3 Family: Two Oncoproteins and a Tumour Suppressor that Are Central to the Biology of EBV in B Cells. In *Epstein Barr Virus Volume 2: One Herpes Virus: Many Diseases*, C. Münz, ed. (Cham: Springer International Publishing), pp. 61–117.
- Allen, E.L., Ulanet, D.B., Pirman, D., Mahoney, C.E., Coco, J., Si, Y., Chen, Y., Huang, L., Ren, J., Choe, S., et al. (2016). Differential Aspartate Usage Identifies a Subset of Cancer Cells Particularly Dependent on OGDH. *Cell Rep.* 17, 876–890.
- Alves, V.A., Pinheiro, C., Morais-Santos, F., Felipe-Silva, A., Longatto-Filho, A., and Baltazar, F. (2014). Characterization of monocarboxylate transporter activity in hepatocellular carcinoma. *World J. Gastroenterol.* 20, 11780–11787.
- Anderton, E., Yee, J., Smith, P., Crook, T., White, R.E., and Allday, M.J. (2008). Two Epstein-Barr virus (EBV) oncoproteins cooperate to repress expression of the proapoptotic tumour-suppressor Bim: Clues to the pathogenesis of Burkitt's lymphoma. *Oncogene* 27, 421–433.
- Aran, D., Sirota, M., and Butte, A.J. (2015). Systematic pan-cancer analysis of tumour purity. *Nat. Commun.* 6, 1–12.
- Arnold, H.K., and Sears, R.C. (2006). Protein Phosphatase 2A Regulatory Subunit B56 α Associates with c-Myc and Negatively Regulates c-Myc Accumulation. *Mol. Cell. Biol.* 26, 2832–2844.

Arrieta, O., Barrón, F., Padilla, M.Á.S., Avilés-Salas, A., Ramírez-Tirado, L.A., Arguelles Jiménez, M.J., Vergara, E., Zatarain-Barrón, Z.L., Hernández-Pedro, N., Cardona, A.F., et al. (2019). Effect of Metformin Plus Tyrosine Kinase Inhibitors Compared with Tyrosine Kinase Inhibitors Alone in Patients with Epidermal Growth Factor Receptor-Mutated Lung Adenocarcinoma: A Phase 2 Randomized Clinical Trial. *JAMA Oncol.* 5.

Ashburner, M., Ball, C.A., Blake, J.A., Botstein, D., Butler, H., Cherry, J.M., Davis, A.P., Dolinski, K., Dwight, S.S., Eppig, J.T., et al. (2000). Gene Ontology: tool for the unification of biology. *Nat. Genet.* 25, 25–29.

Bajaj, B.G., Murakami, M., Cai, Q., Verma, S.C., Lan, K., and Robertson, E.S. (2008). Epstein-Barr Virus Nuclear Antigen 3C Interacts with and Enhances the Stability of the c-Myc Oncoprotein. *J. Virol.* 82, 4082–4090.

Balsitis, S., Dick, F., Lee, D., Farrell, L., Hyde, R.K., Griep, A.E., Dyson, N., and Lambert, P.F. (2005). Examination of the pRb-Dependent and pRb-Independent Functions of E7 In Vivo. *J. Virol.* 79, 11392–11402.

Balsitis, S.J., Sage, J., Duensing, S., Münger, K., Jacks, T., and Lambert, P.F. (2003). Recapitulation of the Effects of the Human Papillomavirus Type 16 E7 Oncogene on Mouse Epithelium by Somatic Rb Deletion and Detection of pRb-Independent Effects of E7 In Vivo. *Mol. Cell. Biol.* 23, 9094–9103.

Baltimore, D. (1970). Viral RNA-dependent DNA Polymerase: RNA-dependent DNA Polymerase in Virions of RNA Tumour Viruses. *Nature* 226, 1209–1211.

Baltimore, D. (1971). Expression of animal virus genomes. *Bacteriol. Rev.* 35, 235–241.

Bando, H., Toi, M., Kitada, K., and Koike, M. (2003). Genes commonly upregulated by hypoxia in human breast cancer cells MCF-7 and MDA-MB-231. *Biomed. Pharmacother.* 57, 333–340.

Barker, D.D., and Berk, A.J. (1987). Adenovirus proteins from both E1B reading frames are required for transformation of rodent cells by viral infection and DNA transfection. *Virology* 156, 107–121.

Bass, A.J., Thorsson, V., Shmulevich, I., Reynolds, S.M., Miller, M., Bernard, B., Hinoue, T., Laird, P.W., Curtis, C., Shen, H., et al. (2014). Comprehensive molecular characterization of gastric adenocarcinoma. *Nature* 513, 202–209.

Ben-Israel, H., Sharf, R., Rechavi, G., and Kleinberger, T. (2008). Adenovirus E4orf4 Protein Downregulates MYC Expression through Interaction with the PP2A-B55 Subunit. *J. Virol.* 82, 9381–9388.

Bensaad, K., Tsuruta, A., Selak, M.A., Vidal, M.N.C., Nakano, K., Bartrons, R., Gottlieb, E., and Vousden, K.H. (2006). TIGAR, a p53-Inducible Regulator of Glycolysis and Apoptosis. *Cell* 126, 107–120.

Bergvall, M., Melendy, T., and Archambault, J. (2013). The E1 proteins. *Virology* 445, 35–56.

Berk, A.J. (1986). Functions of adenovirus E1A. *Cancer Surv.* 5, 367–387.

van den Beucken, T., Koritzinsky, M., and Wouters, B.G. (2006). Translational control of gene expression during hypoxia. *Cancer Biol. Ther.* 5, 749–755.

Bhattacharya, N., Sabbir, M.G., Roy, A., Dam, A., Roychoudhury, S., and Panda, C.K. (2005). Approximately 580 Kb surrounding the MYC gene is amplified in head and neck squamous cell carcinoma of Indian patients. *Pathol. Res. Pract.* 201, 691–697.

Bhattacharya, N., Roy, A., Roy, B., Roychoudhury, S., and Panda, C.K. (2009). MYC gene amplification reveals clinical association with head and neck squamous cell carcinoma in Indian patients. *J. Oral Pathol. Med.* 38, 759–763.

Bojkova, D., Klann, K., Koch, B., Widera, M., Krause, D., Ciesek, S., Cinatl, J., and Münch, C. (2020). Proteomics of SARS-CoV-2-infected host cells reveals therapy targets. *Nature* 583, 469–472.

Bolaños, J.P., Almeida, A., and Moncada, S. (2010). Glycolysis: a bioenergetic or a survival pathway? *Trends Biochem. Sci.* 35, 145–149.

Boot, A., Oosting, J., van Eendenburg, J.D.H., Kuppen, P.J.K., Morreau, H., and van Wezel, T. (2017). Methylation associated transcriptional repression of ELOVL5 in novel colorectal cancer cell lines. *PLoS One* 12.

Boulanger, P.A., and Blair, G.E. (1991). Expression and interactions of human adenovirus oncoproteins. *Biochem. J.* 275, 281–299.

Braithwaite, A.W., Cheetham, B.F., Li, P., Parish, C.R., Waldron-Stevens, L.K., and Bellett, A.J. (1983). Adenovirus-induced alterations of the cell growth cycle: a requirement for expression of E1A but not of E1B. *J. Virol.* 45, 192–199.

Bratman, S. V., Bruce, J.P., O’Sullivan, B., Pugh, T.J., Xu, W., Yip, K.W., and Liu, F.F. (2016). Human papillomavirus genotype association with survival in head and neck squamous cell carcinoma. *JAMA Oncol.* 2, 823–826.

Braun, D., Kim, T.D., Le Coutre, P., Köhrle, J., Hershman, J.M., and Schweizer, U. (2012).

Tyrosine kinase inhibitors noncompetitively inhibit MCT8-mediated iodothyronine transport. *J. Clin. Endocrinol. Metab.* *97*, 100–105.

Bray, F., Ferlay, J., Soerjomataram, I., Siegel, R.L., Torre, L.A., and Jemal, A. (2018). Global cancer statistics 2018: GLOBOCAN estimates of incidence and mortality worldwide for 36 cancers in 185 countries. *CA. Cancer J. Clin.* *68*, 394–424.

Brito, A.F., and Pinney, J.W. (2017). Protein-protein interactions in virus-host systems. *Front. Microbiol.* *8*, 1–11.

Broad Institute TCGA Genome Data Analysis Center (2016). Analysis Overview for Stomach Adenocarcinoma (Primary solid tumor cohort) - 28 January 2016. Broad Inst. MIT Harvard doi:10.7908/C11V5DG4.

Brown, J.R., Chan, D.K., Shank, J.J., Griffith, K.A., Fan, H., Szulawski, R., Yang, K., Reynolds, R.K., Johnston, C., McLean, K., et al. (2020). Phase II clinical trial of metformin as a cancer stem cell-targeting agent in ovarian cancer. *JCI Insight* *5*, 0–12.

Buck, C.B., Day, P.M., and Trus, B.L. (2013). The papillomavirus major capsid protein L1. *Virology* *445*, 169–174.

Butz, K., Whitaker, N., Denk, C., Ullmann, A., Geisen, C., and Hoppe-Seyler, F. (1999). Induction of the p53-target gene GADD45 in HPV-positive cancer cells. *Oncogene* *18*, 2381–2386.

Caldwell, R.G., Wilson, J.B., Anderson, S.J., and Longnecker, R. (1998). Epstein-Barr virus LMP2A drives B cell development and survival in the absence of normal B cell receptor signals. *Immunity* *9*, 405–411.

Cao, Y., Xie, L., Shi, F., Tang, M., Li, Y., Hu, J., Zhao, L., Zhao, L., Yu, X., Luo, X., et al. (2021). Targeting the signaling in Epstein-Barr virus-associated diseases: mechanism, regulation, and clinical study. *Signal Transduct. Target. Ther.* *6*.

Carinhas, N., Koshkin, A., Pais, D.A.M., Alves, P.M., and Teixeira, A.P. (2017). 13C-metabolic flux analysis of human adenovirus infection: Implications for viral vector production. *Biotechnol. Bioeng.* *114*, 195–207.

Cayrol, F., Sterle, H.A., Díaz Flaqué, M.C., Barreiro Arcos, M.L., and Cremaschi, G.A. (2019). Non-genomic Actions of Thyroid Hormones Regulate the Growth and Angiogenesis of T Cell Lymphomas. *Front. Endocrinol. (Lausanne)*. *10*, 63.

Cen, O., and Longnecker, R. (2015). Latent Membrane Protein 2 (LMP2). In *Epstein Barr Virus Volume 2: One Herpes Virus: Many Diseases*, C. Münz, ed. (Cham: Springer

International Publishing), pp. 151–180.

Cermelli, S., Jang, I.S., Bernard, B., and Grandori, C. (2014). Synthetic lethal screens as a means to understand and treat MYC-driven cancers. *Cold Spring Harb. Perspect. Med.* 4.

Chang, Y., Moore, P.S., and Weiss, R.A. (2017). Human oncogenic viruses: Nature and discovery. *Philos. Trans. R. Soc. B Biol. Sci.* 372.

Chatfield-Reed, K., Gui, S., O'Neill, W.Q., Teknos, T.N., and Pan, Q. (2020). HPV33+ HNSCC is associated with poor prognosis and has unique genomic and immunologic landscapes. *Oral Oncol.* 100, 104488.

Chaturvedi, A.K., Engels, E.A., Pfeiffer, R.M., Hernandez, B.Y., Xiao, W., Kim, E., Jiang, B., Goodman, M.T., Sibug-Saber, M., Cozen, W., et al. (2011). Human papillomavirus and rising oropharyngeal cancer incidence in the United States. *J. Clin. Oncol.* 29, 4294–4301.

Chellappan, S., Kraus, V.B., Kroger, B., Munger, K., Howley, P.M., Phelps, W.C., and Nevins, J.R. (1992). Adeno virus E1A, simian virus 40 tumor antigen, and human papillomavirus E7 protein share the capacity to disrupt the interaction between transcription factor E2F and the retinoblastoma gene product. *Proc. Natl. Acad. Sci. U. S. A.* 89, 4549–4553.

Chen, J.Q., and Russo, J. (2012). Dysregulation of glucose transport, glycolysis, TCA cycle and glutaminolysis by oncogenes and tumor suppressors in cancer cells. *Biochim. Biophys. Acta - Rev. Cancer* 1826, 370–384.

Chen, H., Hutt-Fletcher, L., Cao, L., and Hayward, S.D. (2003). A Positive Autoregulatory Loop of LMP1 Expression and STAT Activation in Epithelial Cells Latently Infected with Epstein-Barr Virus. *J. Virol.* 77, 4139 LP – 4148.

Chen, L., Peng, T., Luo, Y., Zhou, F., Wang, G., Qian, K., Xiao, Y., and Wang, X. (2019). ACAT1 and Metabolism-Related Pathways Are Essential for the Progression of Clear Cell Renal Cell Carcinoma (ccRCC), as Determined by Co-expression Network Analysis. *Front. Oncol.* 9, 1–15.

Chen, L., Zhang, Y., Young, R., Wu, X., and Zhu, G. (2020a). Effects of Vaccine-related Conspiracy Theories on Chinese Young Adults' Perceptions of the HPV Vaccine: An Experimental Study. *Health Commun.* 00, 1–11.

Chen, Y., Yu, Q., Duan, X., Wu, W., and Zeng, G. (2020b). Phosphofructokinase-M inhibits cell growth via modulating the FOXO3 pathway in renal cell carcinoma cells. *Biochem. Biophys. Res. Commun.* 530, 67–74.

- Chido-Amajuoyi, O.G., Jackson, I., Yu, R., and Shete, S. (2020). Declining awareness of HPV and HPV vaccine within the general US population. *Hum. Vaccines Immunother.* *00*, 1–8.
- Choi, S.J., Jung, S.W., Huh, S., Cho, H., and Kang, H. (2018). Phylogenetic comparison of Epstein-Barr virus genomes. *J. Microbiol.* *56*, 525–533.
- Choo, K.-B., Pan, C.-C., Liu, M.-S., Han, S.-H., Ng, H.-T., Chen, C.-P., Lee, Y.-N., Chao, C.-F., Meng, C.-L., and Yeh, M.-Y. (1987). Presence of episomal and integrated human papillomavirus DNA sequences in cervical carcinoma. *J. Med. Virol.* *21*, 101–107.
- Chou, W.C., Cheng, A.L., Brotto, M., and Chuang, C.Y. (2014). Visual gene-network analysis reveals the cancer gene co-expression in human endometrial cancer. *BMC Genomics* *15*, 1–12.
- Choy, E.Y.W., Siu, K.L., Kok, K.H., Lung, R.W.M., Tsang, C.M., To, K.F., Kwong, D.L.W., Tsao, S.W., and Jin, D.Y. (2008). An Epstein-Barr virus-encoded microRNA targets PUMA to promote host cell survival. *J. Exp. Med.* *205*, 2551–2560.
- Chukkapalli, V., Heaton, N.S., and Randall, G. (2012). Lipids at the interface of virus-host interactions. *Curr. Opin. Microbiol.* *15*, 512–518.
- Chung, S.-H., Frese, K.K., Weiss, R.S., Prasad, B.V.V., and Javier, R.T. (2007). A new crucial protein interaction element that targets the adenovirus E4-ORF1 oncoprotein to membrane vesicles. *J. Virol.* *81*, 4787–4797.
- Collins, A.S., Nakahara, T., Do, A., and Lambert, P.F. (2005). Interactions with Pocket Proteins Contribute to the Role of Human Papillomavirus Type 16 E7 in the Papillomavirus Life Cycle. *J. Virol.* *79*, 14769–14780.
- Consigli, R.A., and Ginsberg, H.S. (1964). Activity of aspartate transcarbamylase in uninfected and type 5 adenovirus-infected HeLa cells. *J. Bacteriol.* *87*, 1034 LP – 1043.
- Constanza Camargo, M., Kim, W.H., Chiaravalli, A.M., Kim, K.M., Corvalan, A.H., Matsuo, K., Yu, J., Sung, J.J.Y., Herrera-Goepfert, R., Meneses-Gonzalez, F., et al. (2014). Improved survival of gastric cancer with tumour Epstein-Barr virus positivity: An international pooled analysis. *Gut* *63*, 236–243.
- Crawford, L. V. (1965). A study of human papilloma virus DNA. *J. Mol. Biol.* *13*, 362–372.
- Crick, F. (1970). Central Dogma of Molecular Biology. *Nature* *227*, 561–563.

Crisostomo, L., Soriano, A.M., Mendez, M., Graves, D., and Pelka, P. (2019). Temporal dynamics of adenovirus 5 gene expression in normal human cells. *PLoS One* *14*, e0211192.

Crow, J.M. (2012). HPV: The global burden. *Nature* *488*, S2–S3.

Cruz-Gregorio, A., Aranda-Rivera, A.K., Aparicio-Trejo, O.E., Coronado-Martínez, I., Pedraza-Chaverri, J., and Lizano, M. (2019). E6 oncoproteins from high-risk human papillomavirus induce mitochondrial metabolism in a head and neck squamous cell carcinoma model. *Biomolecules* *9*.

Currie, E., Schulze, A., Zechner, R., Walther, T.C., and Farese, R. V. (2013). Cellular fatty acid metabolism and cancer. *Cell Metab.* *18*, 153–161.

Dabir, D. V., Hasson, S.A., Setoguchi, K., Johnson, M.E., Wongkongkathep, P., Douglas, C.J., Zimmerman, J., Damoiseaux, R., Teitell, M.A., and Koehler, C.M. (2013). A Small Molecule Inhibitor of Redox-Regulated Protein Translocation into Mitochondria. *Dev. Cell* *25*, 81–92.

Dalla-Favera, R., Bregni, M., Erikson, J., Patterson, D., Gallo, R.C., and Croce, C.M. (1982). Human c-myc onc gene is located on the region of chromosome 8 that is translocated in Burkitt lymphoma cells. *Proc. Natl. Acad. Sci.* *79*, 7824 LP – 7827.

Darville, M.I., Antoine, I. V, Mertens-Strijthagen, J.R., Dupriez, V.J., and Rousseau, G.G. (1995). An E2F-dependent late-serum-response promoter in a gene that controls glycolysis. *Oncogene* *11*, 1509–1517.

Dashty, M. (2013). A quick look at biochemistry: Carbohydrate metabolism. *Clin. Biochem.* *46*, 1339–1352.

Davies, G., Lobanova, L., Dawicki, W., Groot, G., Gordon, J.R., Bowen, M., Harkness, T., and Arnason, T. (2017). Metformin inhibits the development, and promotes the resensitization, of treatment-resistant breast cancer. *PLoS One* *12*, 1–22.

Dawson, C.W., Port, R.J., and Young, L.S. (2012). The role of the EBV-encoded latent membrane proteins LMP1 and LMP2 in the pathogenesis of nasopharyngeal carcinoma (NPC). *Semin. Cancer Biol.* *22*, 144–153.

Debbas, M., and White, E. (1993). Wild-type p53 mediates apoptosis by E1A, which is inhibited by E1B. *Genes Dev.* *7*, 546–554.

DeBerardinis, R.J., Mancuso, A., Daikhin, E., Nissim, I., Yudkoff, M., Wehrli, S., and Thompson, C.B. (2007). Beyond aerobic glycolysis: transformed cells can engage in glutamine metabolism that exceeds the requirement for protein and nucleotide synthesis.

Proc. Natl. Acad. Sci. *104*, 19345–19350.

DeGregori, J., Kowalik, T., and Nevins, J.R. (1995). Cellular targets for activation by the E2F1 transcription factor include DNA synthesis- and G1/S-regulatory genes. *Mol. Cell. Biol.* *15*, 4215–4224.

Delecluse, H.J., Bartnizke, S., Hammerschmidt, W., Bullerdiek, J., and Bornkamm, G.W. (1993). Episomal and integrated copies of Epstein-Barr virus coexist in Burkitt lymphoma cell lines. *J. Virol.* *67*, 1292–1299.

Derks, S., Liao, X., Chiaravalli, A.M., Xu, X., Camargo, M.C., Solcia, E., Sessa, F., Fleitas, T., Freeman, G.J., Rodig, S.J., et al. (2016). Abundant PD-L1 expression in Epstein-Barr Virus-infected gastric cancers. *Oncotarget* *7*, 32925–32932.

Desvergne, B., Michalik, L., and Wahli, W. (2006). Transcriptional Regulation of Metabolism. *Physiol. Rev.* *86*, 465–514.

DiMaio, D., and Mattoon, D. (2001). Mechanisms of cell transformation by papillomavirus E5 proteins. *Oncogene* *20*, 7866–7873.

DiMaio, D., and Petti, L.M. (2013). The E5 proteins. *Virology* *445*, 99–114.

Dirmeier, U., Hoffmann, R., Kilger, E., Schultheiss, U., Briseño, C., Gires, O., Kieser, A., Eick, D., Sugden, B., and Hammerschmidt, W. (2005). Latent membrane protein 1 of Epstein-Barr virus coordinately regulates proliferation with control of apoptosis. *Oncogene* *24*, 1711–1717.

Dix, I., and Leppard, K.N. (1993). Regulated splicing of adenovirus type 5 E4 transcripts and regulated cytoplasmic accumulation of E4 mRNA. *J. Virol.* *67*, 3226–3231.

Dobin, A., Davis, C.A., Schlesinger, F., Drenkow, J., Zaleski, C., Jha, S., Batut, P., Chaisson, M., and Gingeras, T.R. (2013). STAR: Ultrafast universal RNA-seq aligner. *Bioinformatics* *29*, 15–21.

Domblides, C., Lartigue, L., and Faustin, B. (2018). Metabolic Stress in the Immune Function of T Cells, Macrophages and Dendritic Cells. *Cells* *7*, 68.

Doorbar, J. (2013). The E4 protein; structure, function and patterns of expression. *Virology* *445*, 80–98.

Dreer, M., van de Poel, S., and Stubenrauch, F. (2017). Control of viral replication and transcription by the papillomavirus E8^{E2} protein. *Virus Res.* *231*, 96–102.

- Dunmire, S.K., Hogquist, K.A., and Balfour, H.H. (2015). Infectious Mononucleosis. In Epstein Barr Virus Volume 1: One Herpes Virus: Many Diseases, C. Münz, ed. (Cham: Springer International Publishing), pp. 211–240.
- Dunmire, S.K., Verghese, P.S., and Balfour, H.H. (2018). Primary Epstein-Barr virus infection. *J. Clin. Virol.* *102*, 84–92.
- Durst, M., Gissmann, L., Ikenberg, H., and Zur Hausen, H. (1983). A papillomavirus DNA from a cervical carcinoma and its prevalence in cancer biopsy samples from different geographic regions. *Proc. Natl. Acad. Sci. U. S. A.* *80*, 3812–3815.
- Dyer, A., Schoeps, B., Frost, S., Jakeman, P.G., Scott, E.M., Freedman, J., and Seymour, L.W. (2018). Antagonism of glycolysis and reductive carboxylation of glutamine potentiates activity of oncolytic adenoviruses in cancer cells. *Cancer Res.*
- Edmunds, L.R., Sharma, L., Kang, A., Lu, J., Vockley, J., Basu, S., Uppala, R., Goetzman, E.S., Beck, M.E., Scott, D., et al. (2014). c-Myc programs fatty acid metabolism and dictates acetyl-CoA abundance and fate. *J. Biol. Chem.* *289*, 25382–25392.
- Eelen, G., De Zeeuw, P., Simons, M., and Carmeliet, P. (2015). Endothelial cell metabolism in normal and diseased vasculature. *Circ. Res.* *116*, 1231–1244.
- El-Mir, M.Y., Nogueira, V., Fontaine, E., Avéret, N., Rigoulet, M., and Leverve, X. (2000). Dimethylbiguanide inhibits cell respiration via an indirect effect targeted on the respiratory chain complex I. *J. Biol. Chem.* *275*, 223–228.
- Elsen, P. Van Den, Houweling, A., and Eb, A. Van Der (1983). Expression of region E1b of human adenoviruses in the absence of region E1a is not sufficient for complete transformation. *Virology* *128*, 377–390.
- Elsnerova, K., Mohelnikova-Duchonova, B., Cerovska, E., Ehrlichova, M., Gut, I., Rob, L., Skapa, P., Hrudá, M., Bartakova, A., Bouda, J., et al. (2016). Gene expression of membrane transporters: Importance for prognosis and progression of ovarian carcinoma. *Oncol. Rep.* *35*, 2159–2170.
- Elsnerova, K., Bartakova, A., Tihlarik, J., Bouda, J., Rob, L., Skapa, P., Hrudá, M., Gut, I., Mohelnikova-Duchonova, B., Soucek, P., et al. (2017). Gene expression profiling reveals novel candidate markers of ovarian carcinoma intraperitoneal metastasis. *J. Cancer* *8*, 3598–3606.
- Enjoji, M., Kohjima, M., Ohtsu, K., Matsunaga, K., Murata, Y., Nakamuta, M., Imamura, K., Tanabe, H., Iwashita, A., Nagahama, T., et al. (2016). Intracellular mechanisms underlying lipid accumulation (white opaque substance) in gastric epithelial neoplasms: A

pilot study of expression profiles of lipid-metabolism-associated genes. *J. Gastroenterol. Hepatol.* *31*, 776–781.

Enríquez, J.A. (2016). Supramolecular Organization of Respiratory Complexes. *Annu. Rev. Physiol.* *78*, 533–561.

Epstein, M.A., Achong, B.G., and Barr, Y.M. (1964). Virus Particles In Cultured Lymphoblasts From Burkitt's Lymphoma. *Lancet* *283*, 702–703.

Fakhry, C., Westra, W.H., Li, S., Cmelak, A., Ridge, J.A., Pinto, H., Forastiere, A., and Gillison, M.L. (2008). Improved survival of patients with human papillomavirus-positive head and neck squamous cell carcinoma in a prospective clinical trial. *J. Natl. Cancer Inst.* *100*, 261–269.

Fang, C.Y., Lee, C.H., Wu, C.C., Chang, Y.T., Yu, S.L., Chou, S.P., Huang, P.T., Chen, C.L., Hou, J.W., Chang, Y., et al. (2009). Recurrent chemical reactivations of EBV promotes genome instability and enhances tumor progression of nasopharyngeal carcinoma cells. *Int. J. Cancer* *124*, 2016–2025.

Fang, T., Shang, W., Liu, C., Liu, Y., and Ye, A. (2020). Single-Cell Multimodal Analytical Approach by Integrating Raman Optical Tweezers and RNA Sequencing. *Anal. Chem.*

Farina, A., Feederle, R., Raffa, S., Gonnella, R., Santarelli, R., Frati, L., Angeloni, A., Torrisi, M.R., Faggioni, A., and Delecluse, H.-J. (2005). BFRF1 of Epstein-Barr Virus Is Essential for Efficient Primary Viral Envelopment and Egress. *J. Virol.* *79*, 3703–3712.

Faubert, B., Solmonson, A., and DeBerardinis, R.J. (2020). Metabolic reprogramming and cancer progression. *Science.* *368*.

Faulkner, G.C., Krajewski, A.S., and Crawford, D.H. (2000). The ins and outs of EBV infection. *Trends Microbiol.* *8*, 185–189.

Fehrmann, F., and Laimins, L.A. (2003). Human papillomaviruses: Targeting differentiating epithelial cells for malignant transformation. *Oncogene* *22*, 5201–5207.

Ferlay, J., Colombet, M., Soerjomataram, I., Mathers, C., Parkin, D.M., Piñeros, M., Znaor, A., and Bray, F. (2018). Estimating the global cancer incidence and mortality in 2018: GLOBOCAN sources and methods. *Int. J. Cancer.*

Ferrari, R., Pellegrini, M., Horwitz, G.A., Xie, W., Berk, A.J., and Kurdistani, S.K. (2008). Epigenetic reprogramming by adenovirus e1a. *Science.* *321*, 1086–1088.

Ferrari, R., Gou, D., Jawdekar, G., Johnson, S.A., Nava, M., Su, T., Yousef, A.F., Zemke, N.R., Pellegrini, M., Kurdistani, S.K., et al. (2014). Adenovirus small E1A employs the lysine acetylases p300/CBP and tumor suppressor RB to repress select host genes and promote productive virus infection. *Cell Host Microbe* 16, 663–676.

Fish, K., Sora, R.P., Schaller, S.J., Longnecker, R., and Ikeda, M. (2017). EBV latent membrane protein 2A orchestrates p27kip1 degradation via Cks1 to accelerate MYC-driven lymphoma in mice. *Blood* 130, 2516–2526.

Fisher, T.N., and Ginsberg, H.S. (1957). Accumulation of organic acids by HeLa cells infected with type 4 adenovirus. *Proc. Soc. Exp. Biol. Med.* 95, 47–51.

Fitzsimmons, L., and Kelly, G.L. (2017). EBV and Apoptosis: The Viral Master Regulator of Cell Fate? *Viruses* 9.

Fitzsimmons, L., Cartlidge, R., Chang, C., Sejjic, N., Galbraith, L.C.A., Suraweera, C.D., Grant, D.C., Tierney, R.J., Bell, A.I., Herold, C.S.M.J., et al. (2020). EBV BCL-2 homologue BHRF1 drives chemoresistance and lymphomagenesis by inhibiting multiple cellular pro-apoptotic proteins. *Cell Death Differ.* 1554–1568.

Fleming, J.C., Woo, J., Moutasim, K., Mellone, M., Frampton, S.J., Mead, A., Ahmed, W., Wood, O., Robinson, H., Ward, M., et al. (2019). HPV, tumour metabolism and novel target identification in head and neck squamous cell carcinoma. *Br. J. Cancer* 120, 356–367.

Flint, J., and Shenk, T. (1989). Adenovirus E1A protein paradigm viral transactivator. *Annu. Rev. Genet.* 23, 141–161.

Fogh, J., and Trempe, G. (1975). New Human Tumor Cell Lines. In *Human Tumor Cells in Vitro*, J. Fogh, ed. (New York: Springer US), pp. 115–160.

Fortelny, N., Overall, C.M., Pavlidis, P., and Cohen Freue, G. V. (2017). Can we predict protein from mRNA levels? *Nature* 547, E19–E23.

Frappier, L. (2015). EBNA1. In *Epstein Barr Virus Volume 2: One Herpes Virus: Many Diseases*, C. Münz, ed. (Cham: Springer International Publishing), pp. 3–34.

Frese, K.K., Lee, S.S., Thomas, D.L., Latorre, I.J., Weiss, R.S., Glaunsinger, B.A., and Javier, R.T. (2003). Selective PDZ protein-dependent stimulation of phosphatidylinositol 3-kinase by the adenovirus E4-ORF1 oncoprotein. *Oncogene* 22, 710–721.

Fries, K.L., Miller, W.E., and Raab-Traub, N. (1996). Epstein-Barr virus latent membrane protein 1 blocks p53-mediated apoptosis through the induction of the A20 gene. *J. Virol.*

70, 8653–8659.

Gaglia, M.M., and Munger, K. (2018). More than just oncogenes: mechanisms of tumorigenesis by human viruses. *Curr. Opin. Virol.* 32, 48–59.

Gallimore, P.H., and Turnell, A.S. (2001). Adenovirus E1A: Remodelling the host cell, a life or death experience. *Oncogene* 20, 7824–7835.

Gallimore, P.H., Grand, R.J., and Byrd, P.J. (1986). Transformation of human embryo retinoblasts with simian virus 40, adenovirus and ras oncogenes. *Anticancer Res.* 6, 499–508.

Gameiro, S.F., Kolendowski, B., Zhang, A., Barrett, J.W., Nichols, A.C., Torchia, J., and Mymryk, J.S. (2017). Human papillomavirus dysregulates the cellular apparatus controlling the methylation status of H3K27 in different human cancers to consistently alter gene expression regardless of tissue of origin. *Oncotarget* 8, 72564–72576.

Gameiro, S.F., Ghasemi, F., Barrett, J.W., Koropatnick, J., Nichols, A.C., Mymryk, J.S., and Maleki Vareki, S. (2018). Treatment-naïve HPV+ head and neck cancers display a T-cell-inflamed phenotype distinct from their HPV- counterparts that has implications for immunotherapy. *Oncoimmunology* 7, 1–14.

Gey, G.O., Coffman, W.D., and Kubicek, M.T. (1952). Tissue culture studies of the proliferative capacity of cervical carcinoma and normal epithelium. *Cancer Res.* 12, 264–265.

Ghasemi, F., Black, M., Sun, R.X., Vizeacoumar, F., Pinto, N., Ruicci, K.M., Yoo, J., Fung, K., MacNeil, D., Palma, D.A., et al. (2018). High-throughput testing in head and neck squamous cell carcinoma identifies agents with preferential activity in human papillomavirus-positive or negative cell lines. *Oncotarget* 9, 26064–26071.

Ghasemi, F., Gameiro, S.F., Tessier, T.M., Maciver, A.H., and Mymryk, J.S. (2020). High Levels of Class I Major Histocompatibility Complex mRNA Are Present in Epstein–Barr Virus-Associated Gastric Adenocarcinomas. *Cells* 9.

Giard, D.J., Aaronson, S.A., Todaro, G.J., Arnstein, P., Kersey, J.H., and Parks, W.P. (1973). In Vitro Cultivation of Human Tumors: Establishment of Cell Lines Derived From a Series of Solid Tumors. *J. Natl. Cancer Inst.* 51, 1417–1423.

Gilardini Montani, M.S., Santarelli, R., Granato, M., Gonnella, R., Torrisi, M.R., Faggioni, A., and Cirone, M. (2019). EBV reduces autophagy, intracellular ROS and mitochondria to impair monocyte survival and differentiation. *Autophagy* 15, 652–667.

Gonzalez, S.L., Stremlau, M., He, X., Basile, J.R., and Münger, K. (2001). Degradation of the Retinoblastoma Tumor Suppressor by the Human Papillomavirus Type 16 E7 Oncoprotein Is Important for Functional Inactivation and Is Separable from Proteasomal Degradation of E7. *J. Virol.* 75, 7583–7591.

Goodman, M.T., Saraiya, M., Thompson, T.D., Steinau, M., Hernandez, B.Y., Lynch, C.F., Lyu, C.W., Wilkinson, E.J., Tucker, T., Copeland, G., et al. (2015). Human papillomavirus genotype and oropharynx cancer survival in the United States of America. *Eur. J. Cancer* 51, 2759–2767.

Goodwin, C.M., Xu, S., and Munger, J. (2015). Stealing the Keys to the Kitchen: Viral Manipulation of the Host Cell Metabolic Network. *Trends Microbiol.* 23, 789–798.

Graham, F.L., Smiley, J., Russell, W.C., and Nairn, R. (1977). Characteristics of a Human Cell Line Transformed by DNA from Human Adenovirus Type 5. *J. Gen. Virol* 36, 59–66.

Granato, M., Feederle, R., Farina, A., Gonnella, R., Santarelli, R., Hub, B., Faggioni, A., and Delecluse, H.-J. (2008). Deletion of Epstein-Barr Virus BFLF2 Leads to Impaired Viral DNA Packaging and Primary Egress as Well as to the Production of Defective Viral Particles. *J. Virol.* 82, 4042–4051.

Granberg, F., Svensson, C., Pettersson, U., and Zhao, H. (2006). Adenovirus-induced alterations in host cell gene expression prior to the onset of viral gene expression. *Virology* 353, 1–5.

Granchi, C. (2018). ATP citrate lyase (ACLY) inhibitors: An anti-cancer strategy at the crossroads of glucose and lipid metabolism. *Eur. J. Med. Chem.* 157, 1276–1291.

Graves, J.A., Wang, Y., Sims-Lucas, S., Cherok, E., Rothermund, K., Branca, M.F., Elster, J., Beer-Stolz, D., van Houten, B., Vockley, J., et al. (2012). Mitochondrial structure, function and dynamics are temporally controlled by c-Myc. *PLoS One* 7.

Green, H., and Kehinde, O. (1974). Sublines of mouse 3T3 cells that accumulate lipid. *Cell* 1, 113–116.

Green, M., Piña, M., Kimes, R., Wensink, P.C., MacHattie, L.A., and Thomas, C.A. (1967). Adenovirus DNA. I. Molecular weight and conformation. *Proc. Natl. Acad. Sci. U. S. A.* 57, 1302–1309.

Gross-Mesilaty, S., Reinstein, E., Bercovich, B., Tobias, K.E., Schwartz, A.L., Kahana, C., and Ciechanover, A. (1998). Basal and human papillomavirus E6 oncoprotein-induced degradation of Myc proteins by the ubiquitin pathway. *Proc. Natl. Acad. Sci. U. S. A.* 95, 8058–8063.

Gu, X., Song, X., Dong, Y., Cai, H., Walters, E., Zhang, R., Pang, X., Xie, T., Guo, Y., Sridhar, R., et al. (2008). Vitamin E Succinate Induces Ceramide-Mediated Apoptosis in Head and Neck Squamous Cell Carcinoma In vitro and In vivo. *Clin. Cancer Res.* *14*, 1840 LP – 1848.

Guillou, H., Zdravec, D., Martin, P.G.P., and Jacobsson, A. (2010). The key roles of elongases and desaturases in mammalian fatty acid metabolism: Insights from transgenic mice. *Prog. Lipid Res.* *49*, 186–199.

Guissoni, A.C.P., Soares, C.M.A., Badr, K.R., Ficcadori, F.S., Parente, A.F.A., Parente, J.A., Baeza, L.C., Souza, M., and Cardoso, D.D.P. (2018). Proteomic analysis of A-549 cells infected with human adenovirus 40 by LC-MS. *Virus Genes* *54*, 351–360.

Guo, H., Shen, S., Wang, L., and Deng, H. (2010). Role of tegument proteins in herpesvirus assembly and egress. *Protein Cell* *1*, 987–998.

Guo, J.Y., Chen, H.Y., Mathew, R., Fan, J., Strohecker, A.M., Karsli-Uzunbas, G., Kamphorst, J.J., Chen, G., Lemons, J.M.S., Karantza, V., et al. (2011). Activated Ras requires autophagy to maintain oxidative metabolism and tumorigenesis. *Genes Dev.* *25*, 460–470.

Guo, R., Gu, J., Wu, M., and Yang, M. (2016). Amazing structure of respirasome: unveiling the secrets of cell respiration. *Protein Cell* *7*, 854–865.

Guo, R., Jiang, C., Zhang, Y., Govande, A., Trudeau, S.J., Chen, F., Fry, C.J., Puri, R., Wolinsky, E., Schineller, M., et al. (2020). MYC Controls the Epstein-Barr Virus Lytic Switch. *Mol. Cell* *78*, 653-669.e8.

Guo, Y., Meng, X., Ma, J., Zheng, Y., Wang, Q., Wang, Y., and Shang, H. (2014). Human papillomavirus 16 E6 contributes HIF-1 α induced warburg effect by attenuating the VHL-HIF-1 α interaction. *Int. J. Mol. Sci.* *15*, 7974–7986.

Haley, K.P., Overhauser, J., Babiss, L.E., Ginsberg, H.S., and Jones, N.C. (1984). Transformation properties of type 5 adenovirus mutants that differentially express the E1A gene products. *Proc. Natl. Acad. Sci. U. S. A.* *81*, 5734–5738.

Hamrahian, A.H., Zhang, J.Z., Elkhairi, F.S., Prasad, R., and Ismail-Beigi, F. (1999). Activation of Glut1 glucose transporter in response to inhibition of oxidative phosphorylation. Role of sites of mitochondrial inhibition and mechanism of Glut1 activation. *Arch. Biochem. Biophys.* *368*, 375–379.

Hanahan, D., and Weinberg, R.A. (2000). The Hallmarks of Cancer. *Cell* *100*, 57–70.

Hanover, J.A., Chen, W., and Bond, M.R. (2018). O-GlcNAc in cancer: An Oncometabolism-fueled vicious cycle. *J. Bioenerg. Biomembr.* *50*, 155–173.

Harlow, E., Franza, B.R., and Schley, C. (1985). Monoclonal antibodies specific for adenovirus early region 1A proteins: extensive heterogeneity in early region 1A products. *J. Virol.* *55*, 533–546.

Hatzivassiliou, G., Zhao, F., Bauer, D.E., Andreadis, C., Shaw, A.N., Dhanak, D., Hingorani, S.R., Tuveson, D.A., and Thompson, C.B. (2005). ATP citrate lyase inhibition can suppress tumor cell growth. *Cancer Cell* *8*, 311–321.

zur Hausen, H., Schulte-Holthausen, H., Klein, G., Henle, W., Henle, G., Clifford, P., and Santesson, L. (1970). Epstein–Barr Virus in Burkitt’s Lymphoma and Nasopharyngeal Carcinoma: EBV DNA in Biopsies of Burkitt Tumours and Anaplastic Carcinomas of the Nasopharynx. *Nature* *228*, 1056–1058.

Zur Hausen, H. (2002). Papillomaviruses and cancer: From basic studies to clinical application. *Nat. Rev. Cancer* *2*, 342–350.

Hayashi, M., Hayashi, M.N., and Spiegelman, S. (1963). Restriction of in Vivo Genetic Transcription To One of the Complementary Strands of Dna. *Proc. Natl. Acad. Sci.* *50*, 664–672.

Hayes, J.D., and Dinkova-Kostova, A.T. (2014). The Nrf2 regulatory network provides an interface between redox and intermediary metabolism. *Trends Biochem. Sci.* *39*, 199–218.

He, J., Jin, Y., Chen, Y., Yao, H.B., Xia, Y.J., Ma, Y.Y., Wang, W., and Shao, Q.S. (2016). Downregulation of ALDOB is associated with poor prognosis of patients with gastric cancer. *Onco. Targets. Ther.* *9*, 6099–6109.

Heaton, N.S., and Randall, G. (2011). Multifaceted roles for lipids in viral infection. *Trends Microbiol.* *19*, 368–375.

Heberle, H., Meirelles, V.G., da Silva, F.R., Telles, G.P., and Minghim, R. (2015). InteractiVenn: A web-based tool for the analysis of sets through Venn diagrams. *BMC Bioinformatics* *16*, 1–7.

Vander Heiden, M.G., and DeBerardinis, R.J. (2017). Understanding the Intersections between Metabolism and Cancer Biology. *Cell* *168*, 657–669.

Vander Heiden, M.G., Cantley, L.C., and Thompson, C.B. (2009). Understanding the Warburg effect: the metabolic requirements of cell proliferation. *Science*. *324*, 1029–1033.

Heinz, S., Benner, C., Spann, N., Bertolino, E., Lin, Y.C., Laslo, P., Cheng, J.X., Murre, C., Singh, H., and Glass, C.K. (2010). Simple Combinations of Lineage-Determining Transcription Factors Prime cis-Regulatory Elements Required for Macrophage and B Cell Identities. *Mol. Cell* 38, 576–589.

Hercbergs, A., Johnson, R.E., Ashur-Fabian, O., Garfield, D.H., and Davis, P.J. (2015). Medically Induced Euthyroid Hypothyroxinemia May Extend Survival in Compassionate Need Cancer Patients: An Observational Study. *Oncologist* 20, 72–76.

Hercbergs, A., Mousa, S.A., Leinung, M., Lin, H.Y., and Davis, P.J. (2018). Thyroid Hormone in the Clinic and Breast Cancer. *Horm. Cancer* 1–5.

Herrero, R., Castellsagué, X., Pawlita, M., Lissowska, J., Kee, F., Balaram, P., Rajkumar, T., Sridhar, H., Rose, B., Pintos, J., et al. (2003). Human papillomavirus and oral cancer: the International Agency for Research on Cancer multicenter study. *J. Natl. Cancer Inst.* 95, 1772–1783.

Hidalgo, P., Anzures, L., Hernández-Mendoza, A., Guerrero, A., Wood, C.D., Valdés, M., Dobner, T., and Gonzalez, R.A. (2016). Morphological, Biochemical, and Functional Study of Viral Replication Compartments Isolated from Adenovirus-Infected Cells. *J. Virol.* 90, 3411–3427.

Higashino, F., Aoyagi, M., Takahashi, A., Ishino, M., Taoka, M., Isobe, T., Kobayashi, M., Totsuka, Y., Kohgo, T., and Shindoh, M. (2005). Adenovirus E4orf6 targets pp32/LANP to control the fate of ARE-containing mRNAs by perturbing the CRM1-dependent mechanism. *J. Cell Biol.* 170, 15–20.

Hino, R., Uozaki, H., Inoue, Y., Shintani, Y., Ushiku, T., Sakatani, T., Takada, K., and Fukayama, M. (2008). Survival advantage of EBV-associated gastric carcinoma: Survivin up-regulation by viral latent membrane protein 2A. *Cancer Res.* 68, 1427–1435.

Hoebe, E.K., Le Large, T.Y.S., Greijer, A.E., and Middeldorp, J.M. (2013). BamHI-A rightward frame 1, an Epstein–Barr virus-encoded oncogene and immune modulator. *Rev. Med. Virol.* 23, 367–383.

Hong, R., Zhang, W., Xia, X., Zhang, K., Wang, Y., Wu, M., Fan, J., Li, J., Xia, W., Xu, F., et al. (2019). Preventing BRCA1/ZBRK1 repressor complex binding to the GOT2 promoter results in accelerated aspartate biosynthesis and promotion of cell proliferation. *Mol. Oncol.* 13, 959–977.

Horikoshi, N., Usheva, A., Chen, J., Levine, A.J., Weinmann, R., and Shenk, T. (1995). Two domains of p53 interact with the TATA-binding protein, and the adenovirus 13S E1A protein disrupts the association, relieving p53-mediated transcriptional repression. *Mol. Cell. Biol.* 15, 227–234.

Hošek, T., Calçada, E.O., Nogueira, M.O., Salvi, M., Pagani, T.D., Felli, I.C., and Pierattelli, R. (2016). Structural and Dynamic Characterization of the Molecular Hub Early Region 1A (E1A) from Human Adenovirus. *Chem. - A Eur. J.* 22, 13010–13013.

Houten, S.M., and Wanders, R.J.A. (2010). A general introduction to the biochemistry of mitochondrial fatty acid β -oxidation. *J. Inherit. Metab. Dis.* 33, 469–477.

Houweling, A., Van Den Elsen, P.J., and Van Der Eb, A.J. (1980). Partial transformation of primary rat cells by the leftmost 4.5% fragment of adenovirus 5 DNA. *Virology* 105, 537–550.

Hsieh, M.C.F., Das, D., Sambandam, N., Zhang, M.Q., and Nahlé, Z. (2008). Regulation of the PDK4 isozyme by the Rb-E2F1 complex. *J. Biol. Chem.* 283, 27410–27417.

Huang, M., and Graves, L.M. (2003). De novo synthesis of pyrimidine nucleotides; emerging interfaces with signal transduction pathways. *Cell. Mol. Life Sci. C.* 60, 321–336.

Huang, D., Li, T., Li, X., Zhang, L., Sun, L., He, X., Zhong, X., Jia, D., Song, L., Semenza, G.L., et al. (2014). HIF-1-mediated suppression of acyl-CoA dehydrogenases and fatty acid oxidation is critical for cancer progression. *Cell Rep.* 8, 1930–1942.

Huang, F., Bai, J., Zhang, J., Yang, D., Fan, H., Huang, L., Shi, T., and Lu, G. (2019). Identification of potential diagnostic biomarkers for pneumonia caused by adenovirus infection in children by screening serum exosomal microRNAs. *Mol. Med. Rep.* 49, 4306–4314.

Hwang, B., Lee, J.H., and Bang, D. (2018). Single-cell RNA sequencing technologies and bioinformatics pipelines. *Exp. Mol. Med.* 50.

Ichikawa, M., Scott, D.A., Losfeld, M.E., and Freeze, H.H. (2014). The metabolic origins of mannose in glycoproteins. *J. Biol. Chem.* 289, 6751–6761.

Igal, R.A. (2010). Stearoyl-coa desaturase-1: A novel key player in the mechanisms of cell proliferation, programmed cell death and transformation to cancer. *Carcinogenesis* 31, 1509–1515.

Iizasa, H., Nanbo, A., Nishikawa, J., Jinushi, M., and Yoshiyama, H. (2012). Epstein-barr virus (EBV)-associated gastric carcinoma. *Viruses* 4, 3420–3439.

Imai, S., Nishikawa, J., and Takada, K. (1998). Cell-to-Cell Contact as an Efficient Mode of Epstein-Barr Virus Infection of Diverse Human Epithelial Cells. *J. Virol.* 72, 4371–4378.

Ip, W.H., and Dobner, T. (2019). Cell transformation by the adenovirus oncogenes E1 and E4. *FEBS Lett.* 1–13.

Ishii, H., Gobé, G., Kawakubo, Y., Sato, Y., and Ebihara, Y. (2001). Interrelationship between Epstein-Barr virus infection in gastric carcinomas and the expression of apoptosis-associated proteins. *Histopathology* 38, 111–119.

Javier, R.T. (1994). Adenovirus type 9 E4 open reading frame 1 encodes a transforming protein required for the production of mammary tumors in rats. *J Virol* 68, 3917–3924.

Jerby, L., and Ruppin, E. (2012). Predicting drug targets and biomarkers of cancer via genome-scale metabolic modeling. *Clin. Cancer Res.* 18, 5572–5584.

Jiang, P., Du, W., and Wu, M. (2014). Regulation of the pentose phosphate pathway in cancer. *Protein Cell* 5, 1–11.

Jiang, S., Zhou, H., Liang, J., Gerdt, C., Wang, C., Ke, L., Schmidt, S.C.S., Narita, Y., Ma, Y., Wang, S., et al. (2017). The Epstein-Barr Virus Regulome in Lymphoblastoid Cells. *Cell Host Microbe* 22, 561-573.e4.

Jin, L., Alesi, G.N., and Kang, S. (2016). Glutaminolysis as a target for cancer therapy. *Oncogene* 35, 3619–3625.

Johannes, J., Jayarama-Naidu, R., Meyer, F., Wirth, E.K., Schweizer, U., Schomburg, L., Köhrle, J., and Renko, K. (2016). Silychristin, a flavonolignan derived from the milk thistle, is a potent inhibitor of the thyroid hormone transporter MCT8. *Endocrinology* 157, 1694–1701.

Johannsen, E., Luftig, M., Chase, M.R., Weicksel, S., Cahir-McFarland, E., Illanes, D., Sarracino, D., and Kieff, E. (2004). Proteins of purified Epstein-Barr virus. *Proc. Natl. Acad. Sci. U. S. A.* 101, 16286–16291.

Jonckheere, A.I., Smeitink, J.A.M., and Rodenburg, R.J.T. (2012). Mitochondrial ATP synthase: Architecture, function and pathology. *J. Inherit. Metab. Dis.* 35, 211–225.

Jones, R.S., and Morris, M.E. (2016). Monocarboxylate Transporters: Therapeutic Targets and Prognostic Factors in Disease. *Clin. Pharmacol. Ther.* 100, 454–463.

Jones, D.L., Thompson, D.A., and Münger, K. (1997). Destabilization of the RB tumor suppressor protein and stabilization of p53 contribute to HPV type 16 E7-induced apoptosis. *Virology* 239, 97–107.

Ju, Y.S. eo., Alexandrov, L.B., Gerstung, M., Martincorena, I., Nik-Zainal, S.,

- Ramakrishna, M., Davies, H.R., Papaemmanuil, E., Gundem, G., Shlien, A., et al. (2014). Origins and functional consequences of somatic mitochondrial DNA mutations in human cancer. *Elife* 3, 1–28.
- Kaddurah-Daouk, R., Lillie, J.W., Daouk, G.H., Green, M.R., Kingston, R., and Schimmel, P. (1990). Induction of a cellular enzyme for energy metabolism by transforming domains of adenovirus E1a. *Mol. Cell. Biol.* 10, 1476–1483.
- Kaelin, W.G. (2017). Common pitfalls in preclinical cancer target validation. *Nat. Rev. Cancer* 17, 441–450.
- Kaiser, C., Laux, G., Eick, D., Jochner, N., Bornkamm, G.W., and Kempkes, B. (1999). The Proto-Oncogene c-myc Is a Direct Target Gene of Epstein-Barr Virus Nuclear Antigen 2. *J. Virol.* 73, 4481–4484.
- Kanai, K., Kikuchi, E., Mikami, S., Suzuki, E., Uchida, Y., Kodaira, K., Miyajima, A., Ohigashi, T., Nakashima, J., and Oya, M. (2010). Vitamin E succinate induced apoptosis and enhanced chemosensitivity to paclitaxel in human bladder cancer cells in vitro and in vivo. *Cancer Sci.* 101, 216–223.
- Kang, M.S., and Kieff, E. (2015). Epstein-Barr virus latent genes. *Exp. Mol. Med.* 47, 1–16.
- Kanzler, H., Küppers, R., Hansmann, M.L., and Rajewsky, K. (1996). Hodgkin and Reed-Sternberg cells in Hodgkin's disease represent the outgrowth of a dominant tumor clone derived from (crippled) germinal center B cells. *J. Exp. Med.* 184, 1495–1505.
- Kempkes, B., and Ling, P.D. (2015). EBNA2 and Its Coactivator EBNA-LP. In *Epstein Barr Virus Volume 2: One Herpes Virus: Many Diseases*, C. Münz, ed. (Cham: Springer International Publishing), pp. 35–59.
- Kieser, A., and Sterz, K.R. (2015). The Latent Membrane Protein 1 (LMP1). In *Epstein Barr Virus Volume 2: One Herpes Virus: Many Diseases*, C. Münz, ed. (Cham: Springer International Publishing), pp. 119–149.
- Kim, D.N., Chae, H.-S., Oh, S.T., Kang, J.-H., Park, C.H., Park, W.S., Takada, K., Lee, J.M., Lee, W.-K., and Lee, S.K. (2007a). Expression of Viral MicroRNAs in Epstein-Barr Virus-Associated Gastric Carcinoma. *J. Virol.* 81, 1033–1036.
- Kim, K.K., Abelman, S., Yano, N., Ribeiro, J.R., Singh, R.K., Tipping, M., and Moore, R.G. (2015). Tetrathiomolybdate inhibits mitochondrial complex IV and mediates degradation of hypoxia-inducible factor-1 α in cancer cells. *Sci. Rep.* 5, 14296.

- Kim, N.H., Cha, Y.H., Lee, J., Lee, S.H., Yang, J.H., Yun, J.S., Cho, E.S., Zhang, X., Nam, M., Kim, N., et al. (2017). Snail reprograms glucose metabolism by repressing phosphofructokinase PFKP allowing cancer cell survival under metabolic stress. *Nat. Commun.* 8.
- Kim, S.H., Koo, B.S., Kang, S., Park, K., Kim, H., Lee, K.R., Lee, M.J., Kim, J.M., Choi, E.C., and Cho, N.H. (2007b). HPV integration begins in the tonsillar crypt and leads to the alteration of p16, EGFR and c-myc during tumor formation. *Int. J. Cancer* 120, 1418–1425.
- King, C.R., Zhang, A., Tessier, T.M., Gameiro, S.F., and Mymryk, J.S. (2018). Hacking the Cell: Network Intrusion and Exploitation by Adenovirus E1A. *MBio* 9, e00390-18.
- Kluckova, K., Bezawork-Geleta, A., Rohlena, J., Dong, L., and Neuzil, J. (2013). Mitochondrial complex II, a novel target for anti-cancer agents. *Biochim. Biophys. Acta - Bioenerg.* 1827, 552–564.
- Klug, A., and Finch, J.T. (1965). Structure of viruses of the papilloma-polyoma type: I. Human wart virus. *J. Mol. Biol.* 11, 403–423.
- Ko, Y.H. (2015). EBV and human cancer. *Exp. Mol. Med.* 47, 14–16.
- Kondoh, H., Leonart, M.E., Gil, J., Wang, J., Degan, P., Peters, G., Martinez, D., Carnero, A., and Beach, D. (2005). Glycolytic enzymes can modulate cellular life span. *Cancer Res.* 65, 177–185.
- Kosulin, K., Haberler, C., Hainfellner, J.A., Amann, G., Lang, S., and Lion, T. (2007). Investigation of Adenovirus Occurrence in Pediatric Tumor Entities. *J. Virol.* 81, 7629–7635.
- Kosulin, K., Hoffmann, F., Clauditz, T.S., Wilczak, W., and Dobner, T. (2013). Presence of Adenovirus Species C in Infiltrating Lymphocytes of Human Sarcoma. *PLoS One* 8, 1–8.
- Kosulin, K., Rauch, M., Ambros, P.F., Pötschger, U., Chott, A., Jäger, U., Drach, J., Nader, A., and Lion, T. (2014). Screening for adenoviruses in haematological neoplasia: High prevalence in mantle cell lymphoma. *Eur. J. Cancer* 50, 622–627.
- Koundouros, N., and Poulogiannis, G. (2019). Reprogramming of fatty acid metabolism in cancer. *Br. J. Cancer.*
- Koutsky, L.A., and Harper, D.M. (2006). Chapter 13: Current findings from prophylactic HPV vaccine trials. *Vaccine* 24, 114–121.

- Kreimer, A.R., Clifford, G.M., Boyle, P., and Franceschi, S. (2005). Human papillomavirus types in head and neck squamous cell carcinomas worldwide: A systemic review. *Cancer Epidemiol. Biomarkers Prev.* *14*, 467–475.
- Kuo, C.Y., and Ann, D.K. (2018). When fats commit crimes: Fatty acid metabolism, cancer stemness and therapeutic resistance. *Cancer Commun.* *38*, 1–12.
- Küppers, R. (2003). B cells under influence: Transformation of B cells by Epstein-Barr virus. *Nat. Rev. Immunol.* *3*, 801–812.
- Kurth, J., Hansmann, M.L., Rajewsky, K., and Küppers, R. (2003). Epstein-Barr virus-infected B cells expanding in germinal centers of infectious mononucleosis patients do not participate in the germinal center reaction. *Proc. Natl. Acad. Sci. U. S. A.* *100*, 4730–4735.
- Kuwano, K., Kawasaki, M., Kunitake, R., Hagimoto, N., Nomoto, Y., Matsuba, T., Nakanishi, Y., and Hara, N. (1997). Detection of group C adenovirus DNA in small-cell lung cancer with the nested polymerase chain reaction. *J. Cancer Res. Clin. Oncol.* *123*, 377–382.
- Kwok Fung Lo, A., Wai Lo, K., Tsao, S.W., Wong, H.L., Ying Hui, J.W., To, K.F., Hayward, S.D., Chui, Y.L., Lau, Y.L., Takada, K., et al. (2006). Epstein-Barr Virus Infection Alters Cellular Signal Cascades in Human Nasopharyngeal Epithelial Cells. *Neoplasia* *8*, 173–180.
- Lai, D., Tan, C.L., Gunaratne, J., Quek, L.S., Nei, W., Thierry, F., and Bellanger, S. (2013). Localization of HPV-18 E2 at Mitochondrial Membranes Induces ROS Release and Modulates Host Cell Metabolism. *PLoS One* *8*, 1–14.
- Lai, R.K.H., Xu, I.M.J., Chiu, D.K.C., Tse, A.P.W., Wei, L.L., Law, C.T., Lee, D., Wong, C.M., Wong, M.P., Ng, I.O.L., et al. (2016). NDUFA4L2 fine-tunes oxidative stress in hepatocellular carcinoma. *Clin. Cancer Res.* *22*, 3105–3117.
- Lajer, C.B., Garnæs, E., Friis-Hansen, L., Norrild, B., Therkildsen, M.H., Glud, M., Rossing, M., Lajer, H., Svane, D., Skotte, L., et al. (2012). The role of miRNAs in human papilloma virus (HPV)-associated cancers: Bridging between HPV-related head and neck cancer and cervical cancer. *Br. J. Cancer* *106*, 1526–1534.
- Lamb, R., Harrison, H., Hult, J., Smith, D.L., Lisanti, M.P., and Sotgia, F. (2014). Mitochondria as new therapeutic targets for eradicating cancer stem cells: Quantitative proteomics and functional validation via MCT1/2 inhibition. *Oncotarget* *5*, 11029–11037.
- Lechner, M.S., Mack, D.H., Finicle, A.B., Crook, T., Vousden, K.H., and Laimins, L.A. (1992). Human papillomavirus E6 proteins bind p53 in vivo and abrogate p53-mediated

repression of transcription. *EMBO J.* *11*, 3045–3052.

Lee, J.S., Zhang, X., and Shin, Y. (1996). Differential interactions of the CREB/ATF family of transcription factors with p300 and adenovirus E1A. *J. Biol. Chem.* *271*, 17666–17674.

Lee, S.S., Weiss, R.S., and Javier, R.T. (1997). Binding of human virus oncoproteins to hDlg/SAP97, a mammalian homolog of the *Drosophila* discs large tumor suppressor protein. *Proc. Natl. Acad. Sci. U. S. A.* *94*, 6670–6675.

Leek, J.T., Scharpf, R.B., Bravo, H.C., Simcha, D., Langmead, B., Johnson, W.E., Geman, D., Baggerly, K., and Irizarry, R.A. (2010). Tackling the widespread and critical impact of batch effects in high-throughput data. *Nat. Rev. Genet.* *11*, 733–739.

Leemans, C.R., Braakhuis, B.J.M., and Brakenhoff, R.H. (2011). The molecular biology of head and neck cancer. *Nat. Rev. Cancer* *11*, 9–22.

Leiprecht, N., Munoz, C., Alesutan, I., Siraskar, G., Sopjani, M., Föller, M., Stubenrauch, F., Iftner, T., and Lang, F. (2011). Regulation of Na⁺-coupled glucose carrier SGLT1 by human papillomavirus 18 E6 protein. *Biochem. Biophys. Res. Commun.* *404*, 695–700.

Lenaerts, L., De Clercq, E., and Naesens, L. (2008). Clinical features and treatment of adenovirus infections. *Pertanika J. Soc. Sci. Humanit.* *18*, 357–374.

Levy, H.B., Baron, S., and Rowe, W.P. (1957). Metabolic effects of animal viruses in tissue culture. In *Federation of American Societies for Experimental Biology*, p. 422.

Li, J.N., Zhao, L., Wu, J., Wu, B., Yang, H., Zhang, H.H., and Qian, J.M. (2012). Differences in gene expression profiles and carcinogenesis pathways between colon and rectal cancer. *J. Dig. Dis.* *13*, 24–32.

Li, Z., Xu, X., Leng, X., He, M., Wang, J., Cheng, S., and Wu, H. (2017). Roles of reactive oxygen species in cell signaling pathways and immune responses to viral infections. *Arch. Virol.* *162*, 603–610.

Liang, J., Zhou, H., Gerdt, C., Tan, M., Colson, T., Kaye, K.M., Kieff, E., and Zhao, B. (2016). Epstein-Barr virus super-enhancer eRNAs are essential for MYC oncogene expression and lymphoblast proliferation. *Proc. Natl. Acad. Sci. U. S. A.* *113*, 14121–14126.

Lillie, J.W., Loewenstein, P.M., Green, M.R., and Green, M. (1987). Functional domains of adenovirus type 5 E1a proteins. *Cell* *50*, 1091–1100.

Lima, M.A.P., Ferreira, M.V.P., Barros, M.A.P., Pardini, M.I.M.C., Ferrasi, A.C., Mota, R.M.S., and Rabenhorst, S.H.B. (2008a). Relationship Between EBV Infection and Expression of Cellular Proteins c-Myc, Bcl-2, and Bax in Gastric Carcinomas. *Diagnostic Mol. Pathol.* 17.

Lima, V.P., de Lima, M.A.P., André, A.R., Ferreira, M.V.P., Barros, M.A.P., and Rabenhorst, S.H.B. (2008b). H pylori (CagA) and Epstein-Barr virus infection in gastric carcinomas: Correlation With p53 mutation and c-Myc, Bcl-2 and Bax expression. *World J. Gastroenterol.* 14, 884–891.

Line, E.C., Soule, H.D., Maloney, T.M., Wolman, S.R., Peterson, W.D., Brenz, R., Mcgrath, C.M., Russo, J., Pauley, R.J., Jones, R.F., et al. (1990). Isolation and Characterization of a Spontaneously Immortalized Human Breast Epithelial Cell Line, MCF-10. *Cancer Res.* 50, 6075–6086.

Lion, T. (2014). Adenovirus infections in immunocompetent and immunocompromised patients. *Clin. Microbiol. Rev.* 27, 441–462.

Liu, F., and Green, M.R. (1990). A specific member of the ATF transcription factor family can mediate transcription activation by the adenovirus E1a protein. *Cell* 61, 1217–1224.

Liu, M.T., Chang, Y.T., Chen, S.C., Chuang, Y.C., Chen, Y.R., Lin, C.S., and Chen, J.Y. (2005). Epstein-Barr virus latent membrane protein 1 represses p53-mediated DNA repair and transcriptional activity. *Oncogene* 24, 2635–2646.

Liu, X., Disbrow, G.L., Yuan, H., Tomaić, V., and Schlegel, R. (2007). Myc and Human Papillomavirus Type 16 E7 Genes Cooperate To Immortalize Human Keratinocytes. *J. Virol.* 81, 12689–12695.

Liu, Y.C., Li, F., Handler, J., Huang, C.R.L., Xiang, Y., Neretti, N., Sedivy, J.M., Zeller, K.I., and Dang, C. V. (2008). Global regulation of nucleotide biosynthetic genes by c-myc. *PLoS One* 3.

Livak, K.J., and Schmittgen, T.D. (2001). Analysis of relative gene expression data using real-time quantitative PCR and the 2- $\Delta\Delta$ CT method. *Methods* 25, 402–408.

Löhr, K., Hartmann, O., Schäfer, H., and Dobbelstein, M. (2003). Mutual Interference of Adenovirus Infection and myc Expression. *J. Virol.* 77, 7936–7944.

Love, M.I., Huber, W., and Anders, S. (2014). Moderated estimation of fold change and dispersion for RNA-seq data with DESeq2. *Genome Biol.* 15, 1–21.

Lowe, S.W., and Earl Ruley, H. (1993). Stabilization of the p53 tumor suppressor is

induced by adenovirus 5 E1A and accompanies apoptosis. *Genes Dev.* 7, 535–545.

Lowe, S.W., Jacks, T., Housman, D.E., and Ruley, H.E. (1994). Abrogation of oncogene-associated apoptosis allows transformation of p53- deficient cells. *Proc. Natl. Acad. Sci. U. S. A.* 91, 2026–2030.

Lu, Y.X., Ju, H.Q., Liu, Z.X., Chen, D.L., Wang, Y., Zhao, Q., Wu, Q.N., Zeng, Z. lei, Qiu, H.B., Hu, P.S., et al. (2018). ME1 regulates NADPH homeostasis to promote gastric cancer growth and metastasis. *Cancer Res.* 78, 1972–1985.

Lunt, S.Y., and Vander Heiden, M.G. (2011). Aerobic Glycolysis: Meeting the Metabolic Requirements of Cell Proliferation. *Annu. Rev. Cell Dev. Biol.* 27, 441–464.

Luo, B., Wang, Y., Wang, X.F., Gao, Y., Huang, B.H., and Zhao, P. (2006). Correlation of Epstein-Barr virus and its encoded proteins with *Helicobacter pylori* and expression of c-met and c-myc in gastric carcinoma. *World J. Gastroenterol.* 12, 1842–1848.

Luo, S., Li, Y., Ma, R., Liu, J., Xu, P., Zhang, H., Tang, K., Ma, J., Liu, N., Zhang, Y., et al. (2017). Downregulation of PCK2 remodels tricarboxylic acid cycle in tumor-repopulating cells of melanoma. *Oncogene* 36, 3609–3617.

Ma, D., Huang, Y., and Song, S. (2019). Inhibiting the HPV16 oncogene-mediated glycolysis sensitizes human cervical carcinoma cells to 5-fluorouracil. *Onco. Targets. Ther.* 12, 6711–6720.

Madera, D., Vitale-Cross, L., Martin, D., Schneider, A., Molinolo, A.A., Gangane, N., Carey, T.E., McHugh, J.B., Komarck, C.M., Walline, H.M., et al. (2015). Prevention of tumor growth driven by PIK3CA and HPV oncogenes by targeting mTOR signaling with metformin in oral squamous carcinomas expressing OCT3. *Cancer Prev. Res.* 8, 197–207.

Madhu, B., Narita, M., Jauhiainen, A., Menon, S., Stubbs, M., Tavaré, S., Narita, M., and Griffiths, J.R. (2015). Metabolomic changes during cellular transformation monitored by metabolite–metabolite correlation analysis and correlated with gene expression. *Metabolomics* 11, 1848–1863.

Madison, D.L., Yaciuk, P., Kwok, R.P.S., and Lundblad, J.R. (2002). Acetylation of the adenovirus-transforming protein E1A determines nuclear localization by disrupting association with importin- α . *J. Biol. Chem.* 277, 38755–38763.

Magon, K.L., and Parish, J.L. (2021). From infection to cancer: how DNA tumour viruses alter host cell central carbon and lipid metabolism. *Open Biol.* 11, 210004.

Mahr, J.A., and Gooding, L.R. (1999). Immune evasion by adenoviruses. *Immunol. Rev.*

168, 121–130.

Mamtani, M., and Kulkarni, H. (2012). Association of HADHA expression with the risk of breast cancer: Targeted subset analysis and meta-analysis of microarray data. *BMC Res. Notes* 5.

Mannava, S., Grachtchouk, V., Wheeler, L.J., Im, M., Zhuang, D., Slavina, E.G., Mathews, C.K., Shewach, D.S., and Nikiforov, M.A. (2008). Direct role of nucleotide metabolism in C-MYC-dependent proliferation of melanoma cells. *Cell Cycle* 7, 2392–2400.

Manríquez, V., Gutierrez, A., Morales, A., Brito, R., Pavez, M., Sapunar, J., Fonseca, L., Molina, V., Ortiz, E., Barra, M.I., et al. (2020). Influence of adenovirus 36 seropositivity on the expression of adipogenic microRNAs in obese subjects. *Int. J. Obes.*

Mansilla, N., Racca, S., Gras, D.E., Gonzalez, D.H., and Welchen, E. (2018). The complexity of mitochondrial complex iv: An update of cytochrome c oxidase biogenesis in plants. *Int. J. Mol. Sci.* 19.

Markowitz, L.E., Hariri, S., Lin, C., Dunne, E.F., Steinau, M., McQuillan, G., and Unger, E.R. (2013). Reduction in human papillomavirus (HPV) prevalence among young women following HPV vaccine introduction in the United States, National Health and Nutrition Examination Surveys, 2003-2010. *J. Infect. Dis.* 208, 385–393.

de Martel, C., Plummer, M., Vignat, J., and Franceschi, S. (2017). Worldwide burden of cancer attributable to HPV by site, country and HPV type. *Int. J. Cancer* 141, 664–670.

Massimi, P., and Banks, L. (1997). Repression of p53 transcriptional activity by the HPV E7 proteins. *Virology* 227, 255–259.

Mast, F.D., Navare, A.T., van der Sloot, A.M., Coulombe-Huntington, J., Rout, M.P., Baliga, N.S., Kaushansky, A., Chait, B.T., Aderem, A., Rice, C.M., et al. (2020). Crippling life support for SARS-CoV-2 and other viruses through synthetic lethality. *J. Cell Biol.* 219, 1–15.

Matoba, S., Kang, J.-G., Patino, W.D., Wragg, A., Boehm, M., Gavrilova, O., Hurley, P.J., Bunz, F., and Hwang, P.M. (2006). p53 Regulates Mitochondrial Respiration. *Science*. 312, 1650 LP – 1653.

Matsukura, T., Koi, S., and Sugase, M. (1989). Both episomal and integrated forms of human papillomavirus type 16 are involved in invasive cervical cancers. *Virology* 172, 63–72.

De Mattos, S.F., Lam, E.W.F., and Tauler, A. (2002). An E2F-binding site mediates the

activation of the proliferative isoform of 6-phosphofructo-2-kinase/fructose-2,6-bisphosphatase by phosphatidylinositol 3-kinase. *Biochem. J.* *368*, 283–291.

Mauser, A., Saito, S., Appella, E., Anderson, C.W., Seaman, W.T., and Kenney, S. (2002). The Epstein-Barr Virus Immediate-Early Protein BZLF1 Regulates p53 Function through Multiple Mechanisms. *J. Virol.* *76*, 12503–12512.

Mayyasi, S.A., Traul, K.A., Garon, C., and Wright, B. (1970). Antigenic characteristics of Rauscher virus cultivated in human embryonic kidney cells. In *American Association for Cancer Research*, p. 54.

Mazurek, S., Zwerschke, W., Jansen-Dürr, P., and Eigenbrodt, E. (2001a). Metabolic cooperation between different oncogenes during cell transformation: Interaction between activated ras and HPV-16 E7. *Oncogene* *20*, 6891–6898.

Mazurek, S., Zwerschke, W., Jansen-Dürr, P., and Eigenbrodt, E. (2001b). Effects of the human papilloma virus HPV-16 E7 oncoprotein on glycolysis and glutaminolysis: Role of pyruvate kinase type M2 and the glycolytic-enzyme complex. *Biochem. J.* *356*, 247–256.

McBride, A.A. (2013). The Papillomavirus E2 proteins. *Virology* *445*, 57–79.

McBride, A.A., and Warburton, A. (2017). The role of integration in oncogenic progression of HPV-associated cancers. *PLoS Pathog.* *13*, 1–7.

McFadden, K., Hafez, A.Y., Kishton, R., Messinger, J.E., Nikitin, P.A., Rathmell, J.C., and Luftig, M.A. (2016). Metabolic stress is a barrier to Epstein-Barr virus-mediated B-cell immortalization. *Proc. Natl. Acad. Sci. U. S. A.* *113*, E782–E790.

McIntosh, K., Payne, S., and Russell, W.C. (1971). Studies on lipid metabolism in cells infected with adenovirus. *J. Gen. Virol.* *10*, 251–265.

Menendez, J.A., and Lupu, R. (2007). Fatty acid synthase and the lipogenic phenotype in cancer pathogenesis. *Nat. Rev. Cancer* *7*, 763–777.

Mesri, E.A., Feitelson, M.A., and Munger, K. (2014). Human viral oncogenesis: A cancer hallmarks analysis. *Cell Host Microbe* *15*, 266–282.

Mi, H., Muruganujan, A., Ebert, D., Huang, X., and Thomas, P.D. (2019). PANTHER version 14: More genomes, a new PANTHER GO-slim and improvements in enrichment analysis tools. *Nucleic Acids Res.* *47*, D419–D426.

Michaud, D.S., Langevin, S.M., Eliot, M., Nelson, H.H., Pawlita, M., McClean, M.D., and Kelsey, K.T. (2014). High-risk HPV types and head and neck cancer. *Int. J. Cancer* *135*,

1653–1661.

Michmerhuizen, N.L., Birkeland, A.C., Bradford, C.R., and Brenner, J.C. (2016). Genetic determinants in head and neck squamous cell carcinoma and their influence on global personalized medicine. *Genes Cancer* 7.

Migita, T., Okabe, S., Ikeda, K., Igarashi, S., Sugawara, S., Tomida, A., Soga, T., Taguchi, R., and Seimiya, H. (2014). Inhibition of ATP citrate lyase induces triglyceride accumulation with altered fatty acid composition in cancer cells. *Int. J. Cancer* 135, 37–47.

Mikawa, T., Lleonart, M.E., Takaori-Kondo, A., Inagaki, N., Yokode, M., and Kondoh, H. (2015). Dysregulated glycolysis as an oncogenic event. *Cell. Mol. Life Sci.* 72, 1881–1892.

Miller, A.D., and Rosman, G.J. (1989). Improved retroviral vectors for gene transfer and expression. *Biotechniques* 7, 980–990.

Miller, D.L., Myers, C.L., Rickards, B., Collier, H.A., and Flint, S.J. (2007). Adenovirus type 5 exerts genome-wide control over cellular programs governing proliferation, quiescence, and survival. *Genome Biol.* 8.

Möhl, B.S., Chen, J., Sathiyamoorthy, K., Jardetzky, T.S., and Longnecker, R. (2016). Structural and Mechanistic Insights into the Tropism of Epstein-Barr Virus. *Mol. Cells* 39, 286–291.

Montell, C., Fisher, E.F., Caruthers, M.H., and Berk, A.J. (1982). Resolving the functions of overlapping viral genes by site-specific mutagenesis at a mRNA splice site. *Nature* 295, 380–384.

Montrose, D.C., and Galluzzi, L. (2019). Drugging cancer metabolism: Expectations vs. reality. *Int. Rev. Cell Mol. Biol.* 347, 1–26.

Moody, C.A., Scott, R.S., Amirghahari, N., Nathan, C.-A., Young, L.S., Dawson, C.W., and Sixbey, J.W. (2005). Modulation of the Cell Growth Regulator mTOR by Epstein-Barr Virus-Encoded LMP2A. *J. Virol.* 79, 5499–5506.

Moran, E. (1993). Interaction of adenoviral proteins with pRB and p53. *FASEB J.* 7, 880–885.

Moran, E., and Mathews, M.B. (1987). Multiple functional domains in the adenovirus E1A gene. *Cell* 48, 177–178.

Moran, E., Grodzicker, T., Roberts, R.J., Mathews, M.B., and Zerler, B. (1986). Lytic and transforming functions of individual products of the adenovirus E1A gene. *J. Virol.* 57,

765–775.

Morandell, D., Kaiser, A., Herold, S., Rostek, U., Lechner, S., Mitterberger, M.C., Jansen-Dürr, P., Eilers, M., and Zwerschke, W. (2012). The human papillomavirus type 16 E7 oncoprotein targets Myc-interacting zinc-finger protein-1. *Virology* 422, 242–253.

Morrish, F., Isern, N., Sadilek, M., Jeffrey, M., and Hockenbery, D.M. (2009). C-Myc activates multiple metabolic networks to generate substrates for cell-cycle entry. *Oncogene* 28, 2485–2491.

Morrish, F., Noonan, J., Perez-Olsen, C., Gafken, P.R., Fitzgibbon, M., Kelleher, J., VanGilst, M., and Hockenbery, D. (2010). Myc-dependent mitochondrial generation of acetyl-CoA contributes to fatty acid biosynthesis and histone acetylation during cell cycle entry. *J. Biol. Chem.* 285, 36267–36274.

Mosialos, G. (2001). Cytokine signaling and Epstein-Barr virus-mediated cell transformation. *Cytokine Growth Factor Rev.* 12, 259–270.

Moss, B. (2013). Poxvirus DNA replication. *Cold Spring Harb. Perspect. Biol.* 5.

Mullen, A.R., Wheaton, W.W., Jin, E.S., Chen, P.H., Sullivan, L.B., Cheng, T., Yang, Y., Linehan, W.M., Chandel, N.S., and Deberardinis, R.J. (2012). Reductive carboxylation supports growth in tumour cells with defective mitochondria. *Nature* 481, 385–388.

Munger, J., Bajad, S.U., Collier, H.A., Shenk, T., and Rabinowitz, J.D. (2006). Dynamics of the cellular metabolome during human cytomegalovirus infection. *PLoS Pathog.* 2, 1165–1175.

Murata, T., and Tsurumi, T. (2014). Switching of EBV cycles between latent and lytic states. *Rev. Med. Virol.* 24, 142–153.

Murata, T., Sato, Y., and Kimura, H. (2014). Modes of infection and oncogenesis by the Epstein-Barr virus. *Rev. Med. Virol.* 24, 242–253.

Murphy, G., Pfeiffer, R., Camargo, M.C., and Rabkin, C.S. (2009). Meta-analysis Shows That Prevalence of Epstein-Barr Virus-Positive Gastric Cancer Differs Based on Sex and Anatomic Location. *Gastroenterology* 137, 824–833.

Nanbo, A., Terada, H., Kachi, K., Takada, K., and Matsuda, T. (2012). Roles of Cell Signaling Pathways in Cell-to-Cell Contact-Mediated Epstein-Barr Virus Transmission. *J. Virol.* 86, 9285–9296.

Nanbo, A., Kachi, K., Yoshiyama, H., and Ohba, Y. (2016). Epstein-Barr virus exploits

host endocytic machinery for cell-to-cell viral transmission rather than a virological synapse. *J. Gen. Virol.* *97*, 2989–3006.

Nash, L.A., and Parks, R.J. (2017). Adenovirus Biology and Development as a Gene Delivery Vector. In *Therapeutic Applications of Adenoviruses*, P. Ng, and N. Brunetti-Pierri, eds. (Boca Raton: CRC Press), pp. 1–36.

Neuzil, J., Dyason, J.C., Freeman, R., Dong, L.F., Prochazka, L., Wang, X.F., Scheffler, I., and Ralph, S.J. (2007). Mitocans as anti-cancer agents targeting mitochondria: Lessons from studies with vitamin e analogues, inhibitors of complex II. *J. Bioenerg. Biomembr.* *39*, 65–72.

Nevels, M., Täuber, B., Kremmer, E., Spruss, T., Wolf, H., and Dobner, T. (1999a). Transforming Potential of the Adenovirus Type 5 E4orf3 Protein. *J. Virol.* *73*, 1591–1600.

Nevels, M., Spruss, T., Wolf, H., and Dobner, T. (1999b). The adenovirus E4orf6 protein contributes to malignant transformation by antagonizing E1A-induced accumulation of the tumor suppressor protein p53. *Oncogene* *18*, 9–17.

Nevels, M., Rubenwolf, S., Spruss, T., Wolf, H., and Dobner, T. (2000). Two Distinct Activities Contribute to the Oncogenic Potential of the Adenovirus Type 5 E4orf6 Protein. *J. Virol.* *74*, 5168–5181.

Nevins, J.R. (1981). Mechanism of activation of early viral transcription by the adenovirus E1A gene product. *Cell* *26*, 213–220.

Nevins, J.R. (1987). Regulation of early adenovirus gene expression. *Microbiol. Rev.* *51*, 419–430.

Nichols, W.W., Murphy, D.G., Cristofalo, V.J., Toji, L.H., Greene, A.E., and A, D.S. (1977). Characterization of a New Human Diploid Cell Strain, IMR-90. *Science*. *196*, 60–63.

Nicolay, B.N., and Dyson, N.J. (2013). The multiple connections between pRB and cell metabolism. *Curr. Opin. Cell Biol.* *25*, 735–740.

Nicolay, B.N., Gameiro, P.A., Tschöp, K., Korenjak, M., Heilmann, A.M., Asara, J.M., Stephanopoulos, G., Iliopoulos, O., and Dyson, N.J. (2013). Loss of RBF1 changes glutamine catabolism. *Genes Dev.* *27*, 182–196.

Niller, H.H., Salamon, D., Ilg, K., Koroknai, A., Banati, F., Bäuml, G., Rucker, O.L., Schwarzmann, F., Wolf, H., and Minarovits, J. (2003). The in vivo binding site for oncoprotein c-Myc in the promoter for Epstein-Barr virus (EBV) encoding RNA (EBER)

1 suggests a specific role for EBV in lymphomagenesis. *Med. Sci. Monit.* 9, 1–9.

Noch, E., and Khalili, K. (2012). Oncogenic viruses and tumor glucose metabolism: Like kids in a candy store. *Mol. Cancer Ther.* 11, 14–23.

Nowicki, S., and Gottlieb, E. (2015). Oncometabolites: Tailoring our genes. *FEBS J.* 282, 2796–2805.

O’Rorke, M.A., Ellison, M. V, Murray, L.J., Moran, M., James, J., and Anderson, L.A. (2012). Human papillomavirus related head and neck cancer survival: A systematic review and meta-analysis. *Oral Oncol.* 48, 1191–1201.

Oh, S.T., Kyo, S., and Laimins, L.A. (2001). Telomerase Activation by Human Papillomavirus Type 16 E6 Protein: Induction of Human Telomerase Reverse Transcriptase Expression through Myc and GC-Rich Sp1 Binding Sites. *J. Virol.* 75, 5559–5566.

Oliva, C.R., Markert, T., Ross, L.J., White, E.L., Rasmussen, L., Zhang, W., Everts, M., Moellering, D.R., Bailey, S.M., Suto, M.J., et al. (2016). Identification of small molecule inhibitors of human cytochrome c oxidase that target chemoresistant glioma cells. *J. Biol. Chem.* 291, 24188–24199.

Oshima, N., Ishida, R., Kishimoto, S., Beebe, K., Brender, J.R., Yamamoto, K., Urban, D., Rai, G., Johnson, M.S., Benavides, G., et al. (2020). Dynamic Imaging of LDH Inhibition in Tumors Reveals Rapid In Vivo Metabolic Rewiring and Vulnerability to Combination Therapy. *Cell Rep.* 30, 1798-1810.e4.

Osthus, R.C., Shim, H., Kim, S., Li, Q., Reddy, R., Mukherjee, M., Xu, Y., Wonsey, D., Lee, L.A., and Dang, C. V. (2000). Deregulation of glucose transporter 1 and glycolytic gene expression by c-Myc. *J. Biol. Chem.* 275, 21797–21800.

Ou, H.D., May, A.P., and O’Shea, C.C. (2011). The critical protein interactions and structures that elicit growth deregulation in cancer and viral replication. *Wiley Interdiscip. Rev. Syst. Biol. Med.* 3, 48–73.

Owens, K.M., Kulawiec, M., Desouki, M.M., Vanniarajan, A., and Singh, K.K. (2011). Impaired OXPHOS complex III in breast cancer. *PLoS One* 6.

Oyervides-Muñoz, M.A., Pérez-Maya, A.A., Rodríguez-Gutiérrez, H.F., Gómez-Macias, G.S., Fajardo-Ramírez, O.R., Treviño, V., Barrera-Saldaña, H.A., and Garza-Rodríguez, M.L. (2018). Understanding the HPV integration and its progression to cervical cancer. *Infect. Genet. Evol.* 61, 134–144.

- Pajic, A., Staeger, M.S., Dudziak, D., Schuhmacher, M., Spitkovsky, D., Eissner, G., Brielmeier, M., Polack, A., and Bornkamm, G.W. (2001). Antagonistic effects of c-myc and Epstein-Barr virus latent genes on the phenotype of human B cells. *Int. J. Cancer* *93*, 810–816.
- Parker, G.A., Touitou, R., and Allday, M.J. (2000). Epstein-Barr virus EBNA3C can disrupt multiple cell cycle checkpoints and induce nuclear division divorced from cytokinesis. *Oncogene* *19*, 700–709.
- Paschos, K., Smith, P., Anderton, E., Middeldorp, J.M., White, R.E., and Allday, M.J. (2009). Epstein-Barr virus latency in B cells leads to epigenetic repression and CpG methylation of the tumour suppressor gene Bim. *PLoS Pathog.* *5*.
- Patra, K.C., and Hay, N. (2014). The pentose phosphate pathway and cancer. *Trends Biochem. Sci.* *39*, 347–354.
- Pavlova, N.N., and Thompson, C.B. (2016). The Emerging Hallmarks of Cancer Metabolism. *Cell Metab.* *23*, 27–47.
- Pelka, P., Ablack, J.N.G., Fonseca, G.J., Yousef, A.F., and Mymryk, J.S. (2008). Intrinsic Structural Disorder in Adenovirus E1A: a Viral Molecular Hub Linking Multiple Diverse Processes. *J. Virol.* *82*, 7252–7263.
- Pelka, P., Ablack, J.N.G., Torchia, J., Turnell, A.S., Grand, R.J.A., and Mymryk, J.S. (2009). Transcriptional control by adenovirus E1A conserved region 3 via p300/CBP. *Nucleic Acids Res.* *37*, 1095–1106.
- Pelka, P., Miller, M.S., Cecchini, M., Yousef, A.F., Bowdish, D.M., Dick, F., Whyte, P., and Mymryk, J.S. (2011). Adenovirus E1A Directly Targets the E2F/DP-1 Complex. *J. Virol.* *85*, 8841–8851.
- Perlmutter, J.D., and Hagan, M.F. (2015). Mechanisms of virus assembly. *Annu. Rev. Phys. Chem.* *66*, 217–239.
- Peta, E., Sinigaglia, A., Masi, G., Di Camillo, B., Grassi, A., Trevisan, M., Messa, L., Loregian, A., Manfrin, E., Brunelli, M., et al. (2018). HPV16 E6 and E7 upregulate the histone lysine demethylase KDM2B through the c-MYC/miR-146a-5p axis. *Oncogene* *37*, 1654–1668.
- Petrosky, E., Bocchini, J.A., Hariri, S., Chesson, H., Curtis, C.R., Saraiya, M., Unger, E.R., and Markowitz, L.E. (2015). Use of 9-valent human papillomavirus (HPV) vaccine: updated HPV vaccination recommendations of the advisory committee on immunization practices. *MMWR. Morb. Mortal. Wkly. Rep.* *64*, 300–304.

Pfeffer, A. (2020). Fewer in-school HPV vaccinations could cause rise in preventable cancers, doctors warn. *Can. Broadcast. Corp.*

Vande Pol, S.B., and Klingelutz, A.J. (2013). Papillomavirus E6 oncoproteins. *Virology* 445, 115–137.

Proskuryakov, S., and Gabai, V. (2009). Mechanisms of Tumor Cell Necrosis. *Curr. Pharm. Des.* 16, 56–68.

Prusinkiewicz, M.A., and Mymryk, J.S. (2019). Metabolic Reprogramming of the Host Cell by Human Adenovirus Infection. *Viruses* 11, 141.

Prusinkiewicz, M.A., Gameiro, S.F., Ghasemi, F., Dodge, M.J., Zeng, P.Y.F., Maekebay, H., Barrett, J.W., Nichols, A.C., and Mymryk, J.S. (2020). Survival-Associated Metabolic Genes in Human Papillomavirus-Positive Head and Neck Cancers. *Cancers (Basel)*. 12, 1–17.

Puchhammer-Stöckl, E., and Görzer, I. (2006). Cytomegalovirus and Epstein-Barr virus subtypes-The search for clinical significance. *J. Clin. Virol.* 36, 239–248.

Qian, X., Hu, J., Zhao, J., and Chen, H. (2015). ATP citrate lyase expression is associated with advanced stage and prognosis in gastric adenocarcinoma. *Int. J. Clin. Exp. Med.* 8, 7855–7860.

Querido, E., Teodoro, J.G., and Branton, P.E. (1997). Accumulation of p53 induced by the adenovirus E1A protein requires regions involved in the stimulation of DNA synthesis. *J. Virol.* 71, 3526–3533.

Racker, E. (1972). Bioenergetics and the problem of tumor growth: an understanding of the mechanism of the generation and control of biological energy may shed light on the problem of tumor growth. *Am. Sci.* 60, 56–63.

Radko, S., Jung, R., Olanubi, O., and Pelka, P. (2015). Effects of adenovirus type 5 E1A isoforms on viral replication in arrested human cells. *PLoS One* 10, 1–18.

Rančić, N.K., Golubović, M.B., Ilić, M. V., Ignjatović, A.S., Živadinović, R.M., Đenić, S.N., Momčilović, S.D., Kocić, B.N., Milošević, Z.G., and Otašević, S.A. (2020). Knowledge about cervical cancer and awareness of human papillomavirus (HPV) and HPV vaccine among female students from Serbia. *Med.* 56, 1–15.

Ressing, M.E., van Gent, M., Gram, A.M., Hooykaas, M.J.G., Piersma, S.J., and Wiertz, E.J.H.J. (2015). Immune Evasion by Epstein-Barr Virus. In *Epstein Barr Virus Volume 2*, C. Münz, ed. (Cham: Springer International Publishing), pp. 355–381.

Reynolds, M.R., Lane, A.N., Robertson, B., Kemp, S., Liu, Y., Hill, B.G., Dean, D.C., and Clem, B.F. (2014). Control of glutamine metabolism by the tumor suppressor Rb. *Oncogene* 33, 556–566.

Ridgway, N.D. (2013). The role of phosphatidylcholine and choline metabolites to cell proliferation and survival. *Crit. Rev. Biochem. Mol. Biol.* 48, 20–38.

Rmaileh, A.A., Solaimuthu, B., Tanna, M., Khatib, A., Yosef, M. Ben, Hayashi, A., Lichtenstein, M., and Shaul, Y.D. (2020). Large-scale differential gene expression transcriptomic analysis identifies a metabolic signature shared by all cancer cells. *Biomolecules* 10.

Roman, A., and Munger, K. (2013). The papillomavirus E7 proteins. *Virology* 445, 138–168.

Roongta, U. V., Pabalan, J.G., Wang, X., Ryseck, R.P., Fagnoli, J., Henley, B.J., Yang, W.P., Zhu, J., Madireddi, M.T., Lawrence, R.M., et al. (2011). Cancer cell dependence on unsaturated fatty acids implicates stearyl-CoA desaturase as a target for cancer therapy. *Mol. Cancer Res.* 9, 1551–1561.

Roos, W.H., Ivanovska, I.L., Evilevitch, A., and Wuite, G.J.L. (2007). Viral capsids: Mechanical characteristics, genome packaging and delivery mechanisms. *Cell. Mol. Life Sci.* 64, 1484–1497.

Rowe, W.P., Huebner, R.J., Gilmore, L.K., Parrott, R.H., and Ward, T.G. (1953). Isolation of a cytopathogenic agent from human adenoids undergoing spontaneous degeneration in tissue culture. *Proc. Soc. Exp. Biol. Med.* 84, 570–573.

Rozee, K.R., Ottey, L.J., and Van Rooyen, C.E. (1957). Some metabolic effects of adenovirus infection in HeLa cells. *Can. J. Microbiol.* 3, 1015–1020.

Rozenblatt-Rosen, O., Deo, R.C., Padi, M., Adelmant, G., Calderwood, M.A., Rolland, T., Grace, M., Dricot, A., Askenazi, M., Tavares, M., et al. (2012). Interpreting cancer genomes using systematic host network perturbations by tumour virus proteins. *Nature* 487, 491–495.

Sanchez, E.L., and Lagunoff, M. (2015). Viral activation of cellular metabolism. *Virology* 479–480, 609–618.

Sarnow, P., Ho, Y.S., Williams, J., and Levine, A.J. (1982). Adenovirus E1b-58kd tumor antigen and SV40 large tumor antigen are physically associated with the same 54 kd cellular protein in transformed cells. *Cell* 28, 387–394.

- Scheffner, M., Werness, B.A., Huibregtse, J.M., Levine, A.J., and Howley, P.M. (1990). The E6 oncoprotein encoded by human papillomavirus types 16 and 18 promotes the degradation of p53. *Cell* 63, 1129–1136.
- Schlattner, U., Klaus, A., Ramirez Rios, S., Guzun, R., Kay, L., and Tokarska-Schlattner, M. (2016). Cellular compartmentation of energy metabolism: creatine kinase microcompartments and recruitment of B-type creatine kinase to specific subcellular sites. *Amino Acids* 48, 1751–1774.
- Schmitz, S., Ang, K.K., Vermorken, J., Haddad, R., Suarez, C., Wolf, G.T., Hamoir, M., and Machiels, J.-P. (2014). Targeted therapies for squamous cell carcinoma of the head and neck: Current knowledge and future directions. *Cancer Treat. Rev.* 40, 390–404.
- Scholle, F., Bendt, K.M., and Raab-Traub, N. (2000). Epstein-Barr Virus LMP2A Transforms Epithelial Cells, Inhibits Cell Differentiation, and Activates Akt. *J. Virol.* 74, 10681–10689.
- Schulte-Holthausen, H., and Hausen, H. zur (1970). Partial purification of the Epstein-Barr virus and some properties of its DNA. *Virology* 40, 776–779.
- Schwartzenberg-Bar-Yoseph, F., Armoni, M., and Karnieli, E. (2004). The Tumor Suppressor p53 Down-Regulates Glucose Transporters GLUT1 and GLUT4 Gene Expression. *Cancer Res.* 64, 2627–2633.
- Seiwert, T.Y., Zuo, Z., Keck, M.K., Khattri, A., Pedomallu, C.S., Stricker, T., Brown, C., Pugh, T.J., Stojanov, P., Cho, J., et al. (2015). Integrative and comparative genomic analysis of HPV-positive and HPV-negative head and neck squamous cell carcinomas. *Clin. Cancer Res.* 21, 632–641.
- Shair, K.H.Y., Bendt, K.M., Edwards, R.H., Nielsen, J.N., Moore, D.T., and Raab-Traub, N. (2012). Epstein-Barr Virus-Encoded Latent Membrane Protein 1 (LMP1) and LMP2A Function Cooperatively To Promote Carcinoma Development in a Mouse Carcinogenesis Model. *J. Virol.* 86, 5352–5365.
- Shao, J.Y., Ernberg, I., Biberfeld, P., Heiden, T., Zeng, Y.X., and Hu, L.F. (2004). Epstein-Barr virus LMP1 status in relation to apoptosis, p53 expression and leucocyte infiltration in nasopharyngeal carcinoma. *Anticancer Res.* 24, 2309–2318.
- Sharma, L.K., Lu, J., and Bai, Y. (2009). Mitochondrial respiratory complex I: structure, function and implication in human diseases. *Curr. Med. Chem.* 16, 1266–1277.
- Sharma, V., Ichikawa, M., and Freeze, H.H. (2014). Mannose metabolism: More than meets the eye. *Biochem. Biophys. Res. Commun.* 453, 220–228.

Shen, C., Song, Y.H., Xie, Y., Wang, X., Wang, Y., Wang, C., Liu, S., Xue, S.L., Li, Y., Liu, B., et al. (2017). Downregulation of HADH promotes gastric cancer progression via Akt signaling pathway. *Oncotarget* 8, 76279–76289.

Shi, F., He, Y., Li, J., Tang, M., Li, Y., Xie, L., Zhao, L., Hu, J., Luo, X., Zhou, M., et al. (2020). Wild-type IDH2 contributes to Epstein–Barr virus-dependent metabolic alterations and tumorigenesis. *Mol. Metab.* 36, 1–11.

Shi, Y., Zhou, S., Wang, P., Guo, Y., Xie, B., and Ding, S. (2019). Malic enzyme 1 (ME1) is a potential oncogene in gastric cancer cells and is associated with poor survival of gastric cancer patients. *Onco. Targets. Ther.* 12, 5589–5599.

Shim, H., Dolde, C., Lewis, B.C., Wu, C.S., Dang, G., Jungmann, R.A., Dalla-Favera, R., and Dang, C. V. (1997). c-Myc transactivation of LDH-A: Implications for tumor metabolism and growth. *Proc. Natl. Acad. Sci. U. S. A.* 94, 6658–6663.

Shimamura, K., Kitazawa, H., Miyamoto, Y., Kanesaka, M., Nagumo, A., Yoshimoto, R., Aragane, K., Morita, N., Ohe, T., Takahashi, T., et al. (2009). 5,5-Dimethyl-3-(5-methyl-3-oxo-2-phenyl-2,3-dihydro-1H-pyrazol-4-yl)-1-phenyl-3-(trifluoromethyl)-3,5,6,7-tetrahydro-1H-indole-2,4-dione, a Potent Inhibitor for Mammalian Elongase of Long-Chain Fatty Acids Family 6. *J. Pharmacol. Exp. Ther.* 330, 249 LP – 256.

Shimamura, K., Nagumo, A., Miyamoto, Y., Kitazawa, H., Kanesaka, M., Yoshimoto, R., Aragane, K., Morita, N., Ohe, T., Takahashi, T., et al. (2010). Discovery and characterization of a novel potent, selective and orally active inhibitor for mammalian ELOVL6. *Eur. J. Pharmacol.* 630, 34–41.

Shin, D.Y., Kim, A., Kang, H.J., Park, S., Kim, D.W., and Lee, S.S. (2015). Histone deacetylase inhibitor romidepsin induces efficient tumor cell lysis via selective down-regulation of LMP1 and c-myc expression in EBV-positive diffuse large B-cell lymphoma. *Cancer Lett.* 364, 89–97.

Shukla, S.K., Jha, H.C., El-Naccache, D.W., and Robertson, E.S. (2016). An EBV recombinant deleted for residues 130-159 in EBNA3C can deregulate p53/Mdm2 and Cyclin D1/CDK6 which results in apoptosis and reduced cell proliferation. *Oncotarget* 7, 18116–18134.

Siebring-van Olst, E., Blijlevens, M., de Menezes, R.X., van der Meulen-Muileman, I.H., Smit, E.F., and van Beusechem, V.W. (2017). A genome-wide siRNA screen for regulators of tumor suppressor p53 activity in human non-small cell lung cancer cells identifies components of the RNA splicing machinery as targets for anticancer treatment. *Mol. Oncol.* 11, 534–551.

Silva, A.C., Simão, D., Küppers, C., Lucas, T., Sousa, M.F.Q., Cruz, P., Carrondo, M.J.T.,

Kochanek, S., and Alves, P.M. (2015). Human amniocyte-derived cells are a promising cell host for adenoviral vector production under serum-free conditions. *Biotechnol. J.* *10*, 760–771.

Silva, A.C., P. Teixeira, A., and M. Alves, P. (2016). Impact of Adenovirus infection in host cell metabolism evaluated by ¹H-NMR spectroscopy. *J. Biotechnol.* *231*, 16–23.

Simms, K.T., Hanley, S.J.B., Smith, M.A., Keane, A., and Canfell, K. (2020). Impact of HPV vaccine hesitancy on cervical cancer in Japan: a modelling study. *Lancet Public Heal.* *5*, e223–e234.

Skalsky, R.L., and Cullen, B.R. (2015). EBV Noncoding RNAs. In *Epstein Barr Virus Volume 2: One Herpes Virus: Many Diseases*, C. Münz, ed. (Cham: Springer International Publishing), pp. 181–217.

Smallwood, H.S., Duan, S., Morfouace, M., Rezinciuc, S., Shulkin, B.L., Shelat, A., Zink, E.E., Milasta, S., Bajracharya, R., Oluwaseun, A.J., et al. (2017). Targeting Metabolic Reprogramming by Influenza Infection for Therapeutic Intervention. *Cell Rep.* *19*, 1640–1653.

Smatti, M.K., Al-Sadeq, D.W., Ali, N.H., Pintus, G., Abou-Saleh, H., and Nasrallah, G.K. (2018). Epstein-barr virus epidemiology, serology, and genetic variability of LMP-1 oncogene among healthy population: An update. *Front. Oncol.* *8*.

Song, H.J., Srivastava, A., Lee, J., Kim, Y.S., Kim, K.M., Ki Kang, W., Kim, M., Kim, S., Park, C.K., and Kim, S. (2010). Host Inflammatory Response Predicts Survival of Patients With Epstein-Barr Virus-Associated Gastric Carcinoma. *Gastroenterology* *139*, 84-92.e2.

Soria, C., Estermann, F.E., Espantman, K.C., and Oshea, C.C. (2010). Heterochromatin silencing of p53 target genes by a small viral protein. *Nature* *466*, 1076–1081.

Soriano, A.M., Crisostomo, L., Mendez, M., Graves, D., Frost, J.R., Olanubi, O., Whyte, P.F., Hearing, P., and Pelka, P. (2019). Adenovirus 5 E1A Interacts with E4orf3 To Regulate Viral Chromatin Organization. *J. Virol.* *93*, e00157-19.

Spruance, S.L., Reid, J.E., Grace, M., and Samore, M. (2004). Hazard ratio in clinical trials. *Antimicrob. Agents Chemother.* *48*, 2787–2792.

Stark, R., Pasquel, F., Turcu, A., Pongratz, R.L., Roden, M., Cline, G.W., Shulman, G.I., and Kibbey, R.G. (2009). Phosphoenolpyruvate cycling via mitochondrial phosphoenolpyruvate carboxykinase links anaplerosis and mitochondrial GTP with insulin secretion. *J. Biol. Chem.* *284*, 26578–26590.

Steegenga, W.T., van Laar, T., Riteco, N., Mandarino, A., Shvarts, A., van der Eb, A.J., and Jochemsen, A.G. (1996). Adenovirus E1A proteins inhibit activation of transcription by p53. *Mol. Cell. Biol.* *16*, 2101–2109.

Steegenga, W.T., Shvarts, A., Riteco, N., Bos, J.L., and Jochemsen, A.G. (1999). Distinct Regulation of p53 and p73 Activity by Adenovirus E1A, E1B, and E4orf6 Proteins. *Mol. Cell. Biol.* *19*, 3885–3894.

Stevens, J.L., Cantin, G.T., Wang, G., Shevchenko, A., Shevchenko, A., and Berk, A.J. (2002). Transcription control by E1A and MAP kinase pathway via Sur2 Mediator subunit. *Science*. *296*, 755–758.

Stine, Z.E., Walton, Z.E., Altman, B.J., Hsieh, A.L., and Dang, C. V. (2015). MYC, Metabolism, and Cancer. *Cancer Discov.* *5*, 1024–1039.

Styles, C.T., Paschos, K., White, R.E., and Farrell, P.J. (2018). The cooperative functions of the EBNA3 proteins are central to EBV persistence and latency. *Pathogens* *7*.

Swenson, J.J., Mauser, A.E., Kaufmann, W.K., and Kenney, S.C. (1999). The Epstein-Barr Virus Protein BRLF1 Activates S Phase Entry through E2F1 Induction. *J. Virol.* *73*, 6540–6550.

Swinnen, J. V., Brusselmans, K., and Verhoeven, G. (2006). Increased lipogenesis in cancer cells: New players, novel targets. *Curr. Opin. Clin. Nutr. Metab. Care* *9*, 358–365.

Szekely, L., Selivanova, G., Magnusson, K.P., Klein, G., and Wiman, K.G. (1993). EBNA-5, an Epstein-Barr virus-encoded nuclear antigen, binds to the retinoblastoma and p53 proteins. *Proc. Natl. Acad. Sci. U. S. A.* *90*, 5455–5459.

Tamura, K., Makino, A., Hullin-Matsuda, F., Kobayashi, T., Furihata, M., Chung, S., Ashida, S., Miki, T., Fujioka, T., Shuin, T., et al. (2009). Novel lipogenic enzyme ELOVL7 is involved in prostate cancer growth through saturated long-chain fatty acid metabolism. *Cancer Res.* *69*, 8133–8140.

Tanaka, M., Masaki, Y., Tanaka, K., Miyazaki, M., Kato, M., Sugimoto, R., Nakamura, K., Aishima, S., Shirabe, K., Nakamuta, M., et al. (2013). Reduction of fatty acid oxidation and responses to hypoxia correlate with the progression of de-differentiation in HCC. *Mol. Med. Rep.* *7*, 365–370.

Tang, K., Yu, Y., Zhu, L., Xu, P., Chen, J., Ma, J., Zhang, H., Fang, H., Sun, W., Zhou, L., et al. (2019). Hypoxia-reprogrammed tricarboxylic acid cycle promotes the growth of human breast tumorigenic cells. *Oncogene* *38*, 6970–6984.

Temin, H.M., and Mizutami, S. (1970). RNA-dependent DNA polymerase in virions of Rous sarcoma virus. *Nature* 226, 1211–1213.

Teodoro, J.G., Shore, G.C., and Branton, P.E. (1995). Adenovirus E1A proteins induce apoptosis by both p53-dependent and p53-independent mechanisms. *Oncogene* 11, 467–474.

Thai, M., Graham, N.A., Braas, D., Nehil, M., Komisopoulou, E., Kurdistani, S.K., McCormick, F., Graeber, T.G., and Christofk, H.R. (2014). Adenovirus E4ORF1-induced MYC activation promotes host cell anabolic glucose metabolism and virus replication. *Cell Metab.* 19, 694–701.

Thai, M., Thaker, S.K., Feng, J., Du, Y., Hu, H., Ting Wu, T., Graeber, T.G., Braas, D., and Christofk, H.R. (2015). MYC-induced reprogramming of glutamine catabolism supports optimal virus replication. *Nat. Commun.* 6, 8873.

Thaker, S.K., Ch'ng, J., and Christofk, H.R. (2019). Viral hijacking of cellular metabolism. *BMC Biol.* 17, 59.

The Cancer Genome Atlas Network (2015). Comprehensive genomic characterization of head and neck squamous cell carcinomas. *Nature* 517, 576–582.

The Cancer Genome Atlas Research Network, Chang, K., Creighton, C.J., Davis, C., Donehower, L., Drummond, J., Wheeler, D., Ally, A., Balasundaram, M., Birol, I., et al. (2013). The Cancer Genome Atlas Pan-Cancer analysis project. *Nat. Genet.* 45, 1113.

The Gene Ontology Consortium (2018). The Gene Ontology Resource: 20 years and still GOing strong. *Nucleic Acids Res.* 47, D330–D338.

Thomas, D.L., Shin, S., Jiang, B.H., Vogel, H., Ross, M.A., Kaplitt, M., Shenk, T.E., and Javier, R.T. (1999). Early Region 1 Transforming Functions Are Dispensable for Mammary Tumorigenesis by Human Adenovirus Type 9. *J. Virol.* 73, 3071–3079.

Thompson, M.P., and Kurzrock, R. (2004). Epstein-Barr Virus and Cancer. *Clin. Cancer Res.* 10, 803 LP – 821.

Tindle, R.W. (2002). Immune evasion in human papillomavirus-associated cervical cancer. *Nat. Rev. Cancer* 2, 59–64.

Toyoshima, M., Howie, H.L., Imakura, M., Walsh, R.M., Annis, J.E., Chang, A.N., Frazier, J., Chau, B.N., Loboda, A., Linsley, P.S., et al. (2012). Functional genomics identifies therapeutic targets for MYC-driven cancer. *Proc. Natl. Acad. Sci. U. S. A.* 109, 9545–9550.

Trentin, J.J., Yabe, Y., and Taylor, G. (1962). The quest for human cancer viruses. *Science*. *137*, 835–841.

Tsao, S.W., Tsang, C.M., To, K.F., and Lo, K.W. (2015). The role of Epstein-Barr virus in epithelial malignancies. *J. Pathol.* *235*, 323–333.

Tumban, E. (2019). A current update on human papillomavirus-associated head and neck cancers. *Viruses* *11*.

Urbanczyk-Wochniak, E., Willmitzer, L., and Fernie, A.R. (2007). Integrating profiling data: using linear correlation to reveal coregulation of transcript and metabolites. *Methods Mol Biol* *358*, 77–85.

Urbańska, K., and Orzechowski, A. (2019). Unappreciated role of LDHA and LDHB to control apoptosis and autophagy in tumor cells. *Int. J. Mol. Sci.* *20*, 1–15.

Valdés, A., Zhao, H., Pettersson, U., and Lind, S.B. (2018). Time-resolved proteomics of adenovirus infected cells. *PLoS One* *13*, 1–23.

Vasan, K., Werner, M., and Chandel, N. (2020). Mitochondrial Metabolism as a Target for Cancer Therapy. *Cell Metab.*

Vastag, L., Koyuncu, E., Grady, S.L., Shenk, T.E., and Rabinowitz, J.D. (2011). Divergent effects of human cytomegalovirus and herpes simplex virus-1 on cellular metabolism. *PLoS Pathog.* *7*.

Veldman, T., Liu, X., Yuan, H., and Schlegel, R. (2003). Human papillomavirus E6 and Myc proteins associate in vivo and bind to and cooperatively activate the telomerase reverse transcriptase promoter. *Proc. Natl. Acad. Sci. U. S. A.* *100*, 8211–8216.

De Villiers, E.M., Fauquet, C., Broker, T.R., Bernard, H.U., and Zur Hausen, H. (2004). Classification of papillomaviruses. *Virology* *324*, 17–27.

Vousden, K.H., and Ryan, K.M. (2009). P53 and Metabolism. *Nat. Rev. Cancer* *9*, 691–700.

Vrzalikova, K., Vockerodt, M., Leonard, S., Bell, A., Wei, W., Schrader, A., Wright, K.L., Kube, D., Rowe, M., Woodman, C.B., et al. (2011). Down-regulation of BLIMP1 α by the EBV oncogene, LMP-1, disrupts the plasma cell differentiation program and prevents viral replication in B cells: implications for the pathogenesis of EBV-associated B-cell lymphomas. *Blood* *117*, 5907–5917.

Walboomers, J., Jacobs, M., Manos, M., Bosch, F., Kummer, J., Shah, K., Snijders, Peter,

J.F., Peto, J., Meijer, C.J., L., and Munoz, N. (1999). Human Papillomavirus Is a Necessary Cause. *J. Pathol.* *189*, 12–19.

Wang, J.W., and Roden, R.B.S. (2013). L2, the minor capsid protein of papillomavirus. *Virology* *445*, 175–186.

Wang, L.W., Shen, H., Nobre, L., Ersing, I., Paulo, J.A., Trudeau, S., Wang, Z., Smith, N.A., Ma, Y., Reinstadler, B., et al. (2019a). Epstein-Barr-Virus-Induced One-Carbon Metabolism Drives B Cell Transformation. *Cell Metab.* *30*, 539-555.e11.

Wang, L.W., Wang, Z., Ersing, I., Nobre, L., Guo, R., Jiang, S., Trudeau, S., Zhao, B., Weekes, M.P., and Gewurz, B.E. (2019b). Epstein-Barr virus subverts mevalonate and fatty acid pathways to promote infected B-cell proliferation and survival.

Wang, M., Yu, F., Wu, W., Wang, Y., Ding, H., and Qian, L. (2018). Epstein-Barr virus-encoded microRNAs as regulators in host immune responses. *Int. J. Biol. Sci.* *14*, 565–576.

Wang, M., Gu, B., Chen, X., Wang, Y., Li, P., and Wang, K. (2019c). The Function and Therapeutic Potential of Epstein-Barr Virus-Encoded MicroRNAs in Cancer. *Mol. Ther. - Nucleic Acids* *17*, 657–668.

Wang, Q., Lingel, A., Geiser, V., Kwapnoski, Z., and Zhang, L. (2017). Tumor Suppressor p53 Stimulates the Expression of Epstein-Barr Virus Latent Membrane Protein 1. *J. Virol.* *91*, 1–14.

Wang, X., Kenyon, W.J., Li, Q., Müllberg, J., and Hutt-Fletcher, L.M. (1998). Epstein-Barr Virus Uses Different Complexes of Glycoproteins gH and gL To Infect B Lymphocytes and Epithelial Cells. *J. Virol.* *72*, 5552–5558.

Wang, Y.W., Chang, H.S., Lin, C.H., and Yu, W.C.Y. (2007). HPV-18 E7 conjugates to c-Myc and mediates its transcriptional activity. *Int. J. Biochem. Cell Biol.* *39*, 402–412.

Warburg, O. (1925). The metabolism of carcinoma cells. *J. Cancer Res.* *9*, 148–163.

Warburg, O., Wind, F., and Negelein, E. (1927). The metabolism of tumors in the body. *J. Gen. Physiol.* *8*, 519–530.

Watson, E., Yilmaz, L.S., and Walhout, A.J.M. (2015). Understanding Metabolic Regulation at a Systems Level: Metabolite Sensing, Mathematical Predictions, and Model Organisms. *Annu. Rev. Genet.* *49*, 553–575.

Wegner, A., Meiser, J., Weindl, D., and Hiller, K. (2015). How metabolites modulate

metabolic flux. *Curr. Opin. Biotechnol.* *34*, 16–22.

Weinberg, F., Hamanaka, R., Wheaton, W.W., Weinberg, S., Joseph, J., Lopez, M., Kalyanaraman, B., Mutlu, G.M., Budinger, G.R.S., and Chandel, N.S. (2010). Mitochondrial metabolism and ROS generation are essential for Kras-mediated tumorigenicity. *Proc. Natl. Acad. Sci. U. S. A.* *107*, 8788–8793.

Weitzel, J.M., and Alexander Iwen, K. (2011). Coordination of mitochondrial biogenesis by thyroid hormone. *Mol. Cell. Endocrinol.* *342*, 1–7.

Weitzman, M.D. (2005). Functions of the adenovirus E4 proteins and their impact on viral vectors. *Front. Biosci.* *10*, 1106–1117.

Wellen, K.E., and Thompson, C.B. (2012). A two-way street: Reciprocal regulation of metabolism and signalling. *Nat. Rev. Mol. Cell Biol.* *13*, 270–276.

Weller, M.A., Ward, M.C., Berriochoa, C., Reddy, C.A., Trosman, S., Greskovich, J.F., Nwizu, T.I., Burkey, B.B., Adelstein, D.J., and Koyfman, S.A. (2017). Predictors of distant metastasis in human papillomavirus-associated oropharyngeal cancer. *Head Neck* *39*, 940–946.

Werness, B.A., Levine, A.J., and Howley, P.M. (1990). Association of human papillomavirus types 16 and 18 E6 proteins with p53. *Science.* *248*, 76–79.

Wheaton, W.W., Weinberg, S.E., Hamanaka, R.B., Soberanes, S., Sullivan, L.B., Anso, E., Glasauer, A., Dufour, E., Mutlu, G.M., Scott Budigner, G.R., et al. (2014). Metformin inhibits mitochondrial complex I of cancer cells to reduce tumorigenesis. *Elife* *2014*, 1–18.

Whyte, P., Ruley, H.E., and Harlow, E. (1988a). Two regions of the adenovirus early region 1A proteins are required for transformation. *J Virol* *62*, 257–265.

Whyte, P., Buchkovich, K.J., Horowitz, J.M., Friend, S.H., Raybuck, M., Weinberg, R.A., and Harlow, E. (1988b). Association between an oncogene and an anti-oncogene: the adenovirus E1A proteins bind to the retinoblastoma gene product. *Nature* *334*, 124.

Wolf, E., Lin, C.Y., Eilers, M., and Levens, D.L. (2015). Taming of the beast: Shaping Myc-dependent amplification. *Trends Cell Biol.* *25*, 241–248.

Wood, C.D., Veenstra, H., Khasnis, S., Gunnell, A., Webb, H.M., Shannon-Lowe, C., Andrews, S., Osborne, C.S., and West, M.J. (2016). MYC activation and BCL2L1 silencing by a tumour virus through the large-scale reconfiguration of enhancer-promoter hubs. *Elife* *5*, 1–23.

- Worsham, M.J., Chen, K.M., Ghanem, T., Stephen, J.K., and Divine, G. (2013). Epigenetic modulation of signal transduction pathways in HPV-associated HNSCC. *Otolaryngol. - Head Neck Surg. (United States)* *149*, 409–416.
- Xiao, L., Hu, Z.Y., Dong, X., Tan, Z., Li, W., Tang, M., Chen, L., Yang, L., Tao, Y., Jiang, Y., et al. (2014). Targeting Epstein-Barr virus oncoprotein LMP1-mediated glycolysis sensitizes nasopharyngeal carcinoma to radiation therapy. *Oncogene* *33*, 4568–4578.
- Yanai, H., Takada, K., Shimizu, N., Mizugaki, Y., Tada, M., and Okita, K. (1997). Epstein-Barr virus infection in non-carcinomatous gastric epithelium. *J. Pathol.* *183*, 293–298.
- Yang, M., and Vousden, K.H. (2016). Serine and one-carbon metabolism in cancer. *Nat. Rev. Cancer* *16*, 650.
- Yateman, M.E. (1995). Regulation of human fibroblast insulin-like growth factor (IGF)-binding proteins by IGF-1 and cytokines, mechanisms of action and effects upon IGF bioactivity. University of London.
- Ye, J., Coulouris, G., Zaretskaya, I., Cutcutache, I., Rozen, S., and Madden, T.L. (2012). Primer-BLAST: a tool to design target-specific primers for polymerase chain reaction. *BMC Bioinformatics* *13*, 134.
- Yew, P.R., and Berk, A.J. (1992). Inhibition of p53 transactivation required for transformation by adenovirus early 1B protein. *Nature* *357*, 82–85.
- Yi, F., Saha, A., Murakami, M., Kumar, P., Knight, J.S., Cai, Q., Choudhuri, T., and Robertson, E.S. (2009). Epstein-Barr virus nuclear antigen 3C targets p53 and modulates its transcriptional and apoptotic activities. *Virology* *388*, 236–247.
- Ying, H., Kimmelman, A.C., Lyssiotis, C.A., Hua, S., Chu, G.C., Fletcher-Sananikone, E., Locasale, J.W., Son, J., Zhang, H., Coloff, J.L., et al. (2012). Oncogenic kras maintains pancreatic tumors through regulation of anabolic glucose metabolism. *Cell* *149*, 656–670.
- Yong, C., Stewart, G.D., and Frezza, C. (2020). Oncometabolites in renal cancer. *Nat. Rev. Nephrol.* *16*, 156–172.
- Yoon, S.J., Kim, J.Y., Long, N.P., Min, J.E., Kim, H.M., Yoon, J.H., Anh, N.H., Park, M.C., Kwon, S.W., and Lee, S.K. (2019). Comprehensive Multi-Omics Analysis Reveals Aberrant Metabolism of Epstein-Barr-Virus-Associated Gastric Carcinoma. *Cells* *8*.
- Yoshii, Y., Furukawa, T., Saga, T., and Fujibayashi, Y. (2015). Acetate/acetyl-CoA metabolism associated with cancer fatty acid synthesis: Overview and application. *Cancer Lett.* *356*, 211–216.

Yuan, J.S., Reed, A., Chen, F., and Stewart, C.N. (2006). Statistical analysis of real-time PCR data. *BMC Bioinformatics* 7, 1–12.

Zacny, V.L., Wilson, J., and Pagano, J.S. (1998). The Epstein-Barr Virus Immediate-Early Gene Product, BRLF1, Interacts with the Retinoblastoma Protein during the Viral Lytic Cycle. *J. Virol.* 72, 8043–8051.

Zaidi, N., Swinnen, J. V., and Smans, K. (2012). ATP-citrate lyase: A key player in cancer metabolism. *Cancer Res.* 72, 3709–3714.

Ždravlević, M., Brand, A., Ianni, L. Di, Dettmer, K., Reinders, J., Singer, K., Peter, K., Schnell, A., Bruss, C., Decking, S.M., et al. (2018). Double genetic disruption of lactate dehydrogenases A and B is required to ablate the “Warburg effect” restricting tumor growth to oxidative metabolism. *J. Biol. Chem.* 293, 15947–15961.

Zeng, M., Chen, Y., Jia, X., and Liu, Y. (2020). The anti-apoptotic role of EBV-LMP1 in lymphoma cells. *Cancer Manag. Res.* 12, 8801–8811.

Zerler, B., Roberts, R., Mathews, M., and Moran, E. (1987). Different functional domains of the adenovirus E1A gene are involved in regulation of host cell cycle products. *Mol. Cell. Biol.* 7, 821–829.

Zhang, W., and Huang, L. (2019). Genome Analysis of A Novel Recombinant Human Adenovirus Type 1 in China. *Sci. Rep.* 9, 1–10.

Zhang, A., Tessier, T.M., Galpin, K.J.C., King, C.R., Gameiro, S.F., Anderson, W.W., Yousef, A.F., Qin, W.T., Li, S.S.C., and Mymryk, J.S. (2018). The transcriptional repressor bs69 is a conserved target of the e1a proteins from several human adenovirus species. *Viruses* 10.

Zhang, J., Jia, L., Tsang, C.M., and Tsao, S.W. (2017a). EBV Infection and Glucose Metabolism in Nasopharyngeal Carcinoma. In *Infectious Agents Associated Cancers: Epidemiology and Molecular Biology*, Q. Cai, Z. Yuan, and K. Lan, eds. (Singapore: Springer Singapore), pp. 75–90.

Zhang, M., Zhang, M., Hu, S., Hu, S., Min, M., Ni, Y., Lu, Z., Sun, X., Sun, X., Wu, J., et al. (2020). Dissecting transcriptional heterogeneity in primary gastric adenocarcinoma by single cell RNA sequencing. *Gut* 1–12.

Zhang, Q., Gutsch, D., and Kenney, S. (1994). Functional and physical interaction between p53 and BZLF1: implications for Epstein-Barr virus latency. *Mol. Cell. Biol.* 14, 1929–1938.

Zhang, S., Jin, J., Tian, X., and Wu, L. (2017b). hsa-miR-29c-3p regulates biological function of colorectal cancer by targeting SPARC. *Oncotarget* 8, 104508–104524.

Zhang, Y., Dakic, A., Chen, R., Dai, Y., Schlegel, R., and Liu, X. (2017c). Direct HPV E6/Myc interactions induce histone modifications, Pol II phosphorylation, and hTERT promoter activation. *Oncotarget* 8, 96323–96339.

Zhao, B., Zou, J., Wang, H., Johannsen, E., Peng, C.W., Quackenbush, J., Mar, J.C., Morton, C.C., Freedman, M.L., Blacklow, S.C., et al. (2011). Epstein-Barr virus exploits intrinsic B-lymphocyte transcription programs to achieve immortal cell growth. *Proc. Natl. Acad. Sci. U. S. A.* 108, 14902–14907.

Zhao, H., Granberg, F., and Pettersson, U. (2007). How adenovirus strives to control cellular gene expression. *Virology* 363, 357–375.

Zhao, H., Chen, M., Tellgren-Roth, C., and Pettersson, U. (2015a). Fluctuating expression of microRNAs in adenovirus infected cells. *Virology* 478, 99–111.

Zhao, L., Loewenstein, P.M., and Green, M. (2017). Enhanced MYC association with the NuA4 histone acetyltransferase complex mediated by the adenovirus E1A N-terminal domain activates a subset of MYC target genes highly expressed in cancer cells. *Genes Cancer* 8.

Zhao, X., Petrashen, A.P., Sanders, J.A., Peterson, A.L., and Sedivy, J.M. (2019). SLC1A5 glutamine transporter is a target of MYC and mediates reduced mTORC1 signaling and increased fatty acid oxidation in long-lived Myc hypomorphic mice. *Aging Cell* 18, 1–6.

Zhao, Z., Wu, F., Ding, S., Sun, L., Liu, Z., Ding, K., and Lu, J. (2015b). Label-free quantitative proteomic analysis reveals potential biomarkers and pathways in renal cell carcinoma. *Tumor Biol.* 36, 939–951.

Zheng, L.L., Li, C., Ping, J., Zhou, Y., Li, Y., and Hao, P. (2014). The domain landscape of virus-host interactomes. *Biomed Res. Int.* 2014.

Zhou, H., Schmidt, S.C.S., Jiang, S., Willox, B., Bernhardt, K., Liang, J., Johannsen, E.C., Kharchenko, P., Gewurz, B.E., Kieff, E., et al. (2015). Epstein-Barr Virus Oncoprotein Super-enhancers Control B Cell Growth. *Cell Host Microbe* 17, 205–216.

Zhu, S., Sun, P., Zhang, Y., Yan, L., and Luo, B. (2013). Expression of c-myc and PCNA in Epstein-Barr virus-associated gastric carcinoma. *Exp. Ther. Med.* 5, 1030–1034.

Appendix

Appendix A: Calculation for RT-qPCR data using the $2^{-\Delta\Delta Ct}$ method

Step 1: Average technical replicate values for each biological replicate. The standard deviation between technical replicates should be less than 0.5.

Step 2: Calculate the geometric mean of the reference genes for each biological replicates. In Excel this function is “=GEOMEAN(Ref1,Ref2)” Note: this is only applicable if more than one reference gene was used. In this example B-actin and H2AFY were the reference genes.

D2 fx | =GEOMEAN(C2,C11)

	A	B	C	D
1	Gene	Sample	Ct	Ref Geomean
2	B-actin	EV 1	21.544	24.861997
3		EV 2	21.501	24.94558
4		EV 3	21.221	24.721748
5		12S 1	22.38	25.273899
6		12S 2	21.07	24.33589
7		12S 3	22.108	25.396868
8		13S 1	21.298	24.730844
9		13S 2	21.752	25.160454
10		13S 3	21.833	25.261333
11	H2AFY	EV 1	28.691	
12		EV 2	28.942	
13		EV 3	28.8	
14		12S 1	28.542	
15		12S 2	28.108	
16		12S 3	29.175	
17		13S 1	28.717	
18		13S 2	29.103	
19		13S 3	29.228	

Biological replicate Ct

Calculated geometric mean

Step 3: Calculate a ΔCt for each biological replicate by subtracting the Ct for a gene of interest, such as *ACO2*, by the corresponding geometric mean.

E20 fx =C20-D2

	A	B	C	D	E
	Gene	Sample	Ct	Ref Geomean	ΔCt (Gene of Interest - Geomean Ref Genes)
1	B-actin	EV 1	21.544	24.8619972	
2		EV 2	21.501	24.9455796	
3		EV 3	21.221	24.7217475	
4		12S 1	22.38	25.2738988	
5		12S 2	21.07	24.3358904	
6		12S 3	22.108	25.3968679	
7		13S 1	21.298	24.7308444	
8		13S 2	21.752	25.1604542	
9		13S 3	21.833	25.2613326	
10	H2AFY	EV 1	28.691		
11		EV 2	28.942		
12		EV 3	28.8		
13		12S 1	28.542		
14		12S 2	28.108		
15		12S 3	29.175		
16		13S 1	28.717		
17		13S 2	29.103		
18		13S 3	29.228		
19	ACO2	EV 1	26.324		1.46200282
20		EV 2	26.569		1.62342039
21		EV 3	26.487		1.76525249
22		12S 1	26.626		1.35210121
23		12S 2	25.871		1.53510963
24		12S 3	26.869		1.47213208
25		13S 1	24.987		0.25615557
26		13S 2	25.464		0.30354579
27		13S 3	25.885		0.62366741

Annotations:
 - Red arrow: Geometric mean for Ct of reference genes (points to D20)
 - Green arrow: ΔCt for a biological replicate (points to E20)
 - Blue arrow: Ct for gene of interest (points to C20)

Step 4: Calculate an average ΔCt value (ΔCt_{avg}) for each biological replicate using the Excel formula “=AVERAGE” and the corresponding standard deviation using the formula “=STDEV.S”.

	A	B	C	D	E	F	G
	Gene	Sample	Ct	Ref Geomean	ΔCt (Gene of Interest - Geomean Ref Genes)	Average ΔCt	SD
1	ACO2	EV 1	26.324		1.46200282	1.6168919	0.15173021
2		EV 2	26.569		1.62342039		
3		EV 3	26.487		1.76525249		
4		12S 1	26.626		1.35210121	1.45311431	0.09297461
5		12S 2	25.871		1.53510963		
6		12S 3	26.869		1.47213208		
7		13S 1	24.987		0.25615557	0.39445626	0.19991191
8		13S 2	25.464		0.30354579		
9		13S 3	25.885		0.62366741		

Annotations:
 - Green arrow: Biological replicate values used to calculate ΔCt Avg and SD for A549-EV (points to E20)
 - Blue arrow: Biological replicate values used to calculate ΔCt Avg and SD for A549-12S (points to F4)
 - Red arrow: Biological replicate values used to calculate ΔCt Avg and SD for A549-13S (points to F7)

Step 5: Calculate the $\Delta\Delta Ct$ value was calculated by subtracting the ΔCt of the condition (A549-13S or A549-12S), from the ΔCt of the control sample (A549-EV).

	A	B	C	D	E
			Average		$\Delta\Delta CT$ (Condition - Control Sample)
1	Gene	Sample	ΔCt	SD	
2	ACO2	EV 1	1.6168919	0.15173021	0
3		EV 2			
4		EV 3			
5		12S 1	1.45311431	0.09297461	-0.1637776
6		12S 2			
7		12S 3			
8		13S 1	0.39445626	0.19991191	-1.2224356
9		13S 2			
10		13S 3			

Step 6: Standard deviation ΔCt_{SD} values are added or subtracted from the $\Delta\Delta Ct$ values.

	A	B	C	D	E	F	G	H
			Average		$\Delta\Delta CT$ (Condition - Control Sample)	RQ 2 ⁻ ($\Delta\Delta CT$)	$\Delta\Delta CT+SD$	$\Delta\Delta CT-SD$
1	Gene	Sample	ΔCt	SD				
2	ACO2	EV 1	1.6168919	0.1517302	0	1	0.1517302	-0.1517302
3		EV 2						
4		EV 3						
5		12S 1	1.4531143	0.0929746	-0.1637776	1.1202165	-0.070803	-0.2567522
6		12S 2						
7		12S 3						
8		13S 1	0.3944563	0.1999119	-1.2224356	2.3334032	-1.0225237	-1.4223476
9		13S 2						
10		13S 3						

Step 7: $RQ = 2^{-\Delta\Delta Ct}$, $RQ_{Max} = 2^{-(\Delta\Delta Ct - \Delta Ct_{SD})}$, and $RQ_{Min} = 2^{-(\Delta\Delta Ct + \Delta Ct_{SD})}$ are calculated.

	A	B	C	D	E	F	G	H
			$\Delta\Delta CT$ (Condition - Control Sample)	RQ 2 ⁻ ($\Delta\Delta CT$)	$\Delta\Delta CT+SD$	$\Delta\Delta CT-SD$	RQ Min 2 ⁻ ($\Delta\Delta CT+SD$)	RQ Max 2 ⁻ ($\Delta\Delta CT-SD$)
1	Gene	Sample						
2	ACO2	EV 1	0	1	0.15173021	-0.1517302	0.90017025	1.11090097
3		EV 2						
4		EV 3						
5		12S 1	-0.1637776	1.12021651	-0.070803	-0.2567522	1.0503011	1.19478597
6		12S 2						
7		12S 3						
8		13S 1	-1.2224356	2.33340323	-1.0225237	-1.4223476	2.03146953	2.6802128
9		13S 2						
10		13S 3						

Step 8: The biological replicate ΔCt values are used to calculate statistical significance with a student's two-tailed t-test.

M8 fx =T.TEST(D2:D4,D8:D10,2,2)

Gene	Sample	Ct	ΔCt (Gene of Interest - Geomean Ref Genes)	Average	SD	$\Delta\Delta Ct$ (Condition - Control Sample)	RQ 2 ⁻ ($\Delta\Delta Ct$)	$\Delta\Delta Ct+SD$	$\Delta\Delta Ct-SD$	RQ Min 2 ⁻ ($\Delta\Delta Ct+SD$)	RQ Max 2 ⁻ ($\Delta\Delta Ct-SD$)	P-value vs Control
ACO2	EV 1	26.324	1.4620028	1.6168919	0.1517302	0	1	0.1517302	-0.1517302	0.9001702	1.110901	
	EV 2	26.569	1.6234204									
	EV 3	26.487	1.7652525									
12S	12S 1	26.626	1.3521012	1.4531143	0.0929746	-0.1637776	1.1202165	-0.070803	-0.2567522	1.0503011	1.194786	0.186138
	12S 2	25.871	1.5954096									
	12S 3	26.869	1.4721321									
13S	13S 1	24.987	0.2561556	0.3944563	0.1999119	-1.2224356	2.3334032	-1.0225237	-1.4223476	2.0314695	2.6802128	0.0010811
	13S 2	25.464	0.3035458									
	13S 3	25.885	0.6236674									

ΔCt of A549-EV (control) → C2
 ΔCt of A549-13S → C3
 T-test formula and p-value → M8

Curriculum Vitae

Martin A. Prusinkiewicz, M.Sc. B.Sc. (Hon.)

EDUCATION

- Doctor of Philosophy (Ph.D.)** **2015 – 2021**
 Supervisor: Dr. Joseph Mymryk
 Department of Microbiology and Immunology
 Schulich School of Medicine and Dentistry
 Western University
- Master of Science (M.Sc.)** **2012 – 2015**
 Supervisor: Dr. Troy Harkness
 Department of Anatomy and Cell Biology
 University of Saskatchewan
- Bachelor of Science (B.Sc. Hon.)** **2008 – 2012**
 Major in Anatomy and Cell Biology
 University of Saskatchewan

SCHOLARSHIPS AND AWARDS

- Natural Science and Engineering Research Council of Canada Post-graduate Alexander Graham Bell Doctoral Program Scholarship **September 2016 – August 2019**
 • \$35,000/year
- Western University Dr. FW Luney Graduate Travel Award in Microbiology & Immunology **July 2016**
 • \$2,000
- Western University Dr. FW Luney Graduate Entrance Scholarship in Microbiology & Immunology **September 2015**
 • \$3,000
- Western University Dean's PhD Stipend for Graduate Research **September 2015 – August 2019**
(Superseded by the NSERC Alexander Graham Bell Scholarship in 2016)
 • \$25,000/year
- University of Saskatchewan College of Medicine Graduate Scholarship **September 2014 – August 2015**
 • \$17,000

- University of Saskatchewan 21st Annual Life and Health Science Research Day **March 2014**
(Second place, cell biology category)
- \$50
- University of Saskatchewan Student Travel Award **October 2013**
- \$350
- University of Saskatchewan College of Medicine Graduate Student/Post-Doctoral Fellows Conference Travel Fund **October 2013**
- \$1,000
- University of Saskatchewan College of Medicine Graduate Scholarship **September 2013 – August 2014**
- \$17,000
- Natural Science and Engineering Research Council of Canada Post-graduate Alexander Graham Bell Master's Program Scholarship **September 2012 – August 2013**
- \$17,500
- Saskatchewan Innovation and Opportunity Post-graduate Scholarship **September 2012**
- \$10,000
- Natural Science and Engineering Research Council of Canada Undergraduate Student Research Award **May 2012 – August 2012**
(Under the supervision of Dr. Troy Harkness, University of Saskatchewan)
- \$6,000
- Natural Science and Engineering Research Council of Canada Undergraduate Student Research Award **May 2011 – August 2011**
(Under the supervision of Dr. Susan Kaminskyj, University of Saskatchewan)
- \$6,000
- Natural Science and Engineering Research Council of Canada Undergraduate Student Research Award **May 2010 – August 2010**
(Under the supervision of Dr. Susan Kaminskyj, University of Saskatchewan)
- \$6,000
- American Gastroenterological Association Student Research Fellowship Award **May 2009 – August 2009**
(Under the supervision of Dr. Gilaad Kaplan, University of Calgary)
- \$3,000

University of Saskatchewan Entrance Award
 • \$3,000

September 2008

ACADEMIC POSITIONS

Teaching Assistantship (3) **September – December 2016, 2017, 2018**
MICROIMM 3610F: Microbiology Laboratory
 Course Coordinator: Dr. Bryan Heit
 Western University

Teaching Assistantship (3) **January – April 2013, 2014, 2015**
BMSC 240: Lab Techniques
 Course Coordinator: Ms. Dawn Giesbrecht
 University of Saskatchewan

Teaching Assistantship **September – December 2014**
BMSC 220: Cell Biology
 Course Coordinator: Dr. Pat Krone
 University of Saskatchewan

Teaching Assistantship (2) **September – December 2013, 2014**
ACB 331: Methods in Cell and Developmental Biology
 Course Coordinator: Ms. Dawn Giesbrecht
 University of Saskatchewan

SUPERVISORY EXPERIENCE

4th year Thesis Research Project **September 2019 – April 2020**
Student Supervisor
 Trainee: Sarah Denford

Undergraduate Research Volunteer Student Supervisor **May 2019 – March 2020**
 Trainee: Jessie Tu

Partners in Experiential Learning Student Supervisor **February 2018 – June 2018**
 Trainee: Hanna Maekebay

PEER-REVIEWED PUBLICATIONS (*co-first authorship)

- Prusinkiewicz MA, Tu J, Dodge MJ, MacNeil KM, Pelka P, Mymryk JS.**
 Differential Effects of E1A Isoforms on Aerobic Glycolysis. *Viruses*. 2020 June;
 12(6):610.

2. **Prusinkiewicz MA***, Gameiro SF*, Ghasemi F, Dodge MJ, Zeng PY, Maekebay H, Barrett JW, Nichols AC, Mymryk JS. Survival-Associated Metabolic Genes in Human Papillomavirus-Positive Head and Neck Cancers. *Cancers*. 2020 Jan;12(1):253.
3. Tessier TM, Dodge MJ, **Prusinkiewicz MA**, Mymryk JS. Viral Appropriation: Laying Claim to Host Nuclear Transport Machinery. *Cells*. 2019 Jun;8(6):559.
4. **Prusinkiewicz MA**, Mymryk JS. Metabolic reprogramming of the host cell by human adenovirus infection. *Viruses*. 2019 Feb;11(2):141.
5. Ghavidel A, Baxi K, **Prusinkiewicz M**, Swan C, Belak ZR, Eskiw CH, Carvalho CE, Harkness TA. Rapid nuclear exclusion of Hcm1 in aging *Saccharomyces cerevisiae* leads to vacuolar alkalization and replicative senescence. *G3: Genes, Genomes, Genetics*. 2018 May 1;8(5):1579-92.
6. Ghavidel A, Baxi K, Ignatchenko V, **Prusinkiewicz M**, Arnason TG, Kislinger T, Carvalho CE, Harkness TA. A genome scale screen for mutants with delayed exit from mitosis: Ire1-independent induction of autophagy integrates ER homeostasis into mitotic lifespan. *PLoS genetics*. 2015 Aug;11(8).
7. Menzel J, Malo ME, Chan C, **Prusinkiewicz M**, Arnason TG, Harkness TA. The anaphase promoting complex regulates yeast lifespan and rDNA stability by targeting Fob1 for degradation. *Genetics*. 2014 Mar 1;196(3):693-709.
8. Raj MT, **Prusinkiewicz M**, Cooper DM, George B, Webb MA, Boughner JC. Technique: imaging earliest tooth development in 3D using a silver-based tissue contrast agent. *Anatomical Record*. 2014 Feb;297(2):222-33.
9. **Prusinkiewicz MA***, Farazkhorasani F*, Dynes JJ, Wang J, Gough KM, Kaminskyj SG. Proof-of-principle for SERS imaging of *Aspergillus nidulans* hyphae using in vivo synthesis of gold nanoparticles. *Analyst*. 2012;137(21):4934-42.
10. Ma C, Crespin M, Proulx MC, DeSilva S, Hubbard J, **Prusinkiewicz M**, Nguyen GC, Panaccione R, Ghosh S, Myers RP, Quan H, Kaplan GG. Postoperative complications following colectomy for ulcerative colitis: a validation study. *BMC gastroenterology*. 2012 Dec;12(1):39.
11. DeSilva S, Ma C, Proulx MC, Crespin M, Kaplan BS, Hubbard J, **Prusinkiewicz M**, Fong A, Panaccione R, Ghosh S, Beck PL, MacLean A, Buie D, Kaplan GG. Postoperative complications and mortality following colectomy for ulcerative colitis. *Clinical Gastroenterology and Hepatology*. 2011 Nov 1;9(11):972-80.

POSTERS/CONFERENCES (* denotes presenting author)

1. **Prusinkiewicz M***, Gameiro S, Ghasemi F, Denford S, Dodge M, Maekebay H, Barrett J, Nichols A, Mymryk J. Seven Metabolism Genes are Associated With Survival in Human Papillomavirus-positive Head and Neck Squamous Cell Carcinoma. 14th Infection and Immunity Research Forum. London, ON. 2019 (Poster)
2. **Prusinkiewicz M***, Gameiro S, Ghasemi F, Dodge M, Maekebay H, Barrett J, Nichols A, Mymryk J. Metabolic Genes Associated With Survival in HPV+ HNSCC. The DNA Tumour Virus Meeting. Trieste, Italy. 2019. (Poster)
3. Tu J*, **Prusinkiewicz M**, Mymryk J. Metabolic Gene Expression of E1A-Expressing Cells. Lawson's 1st Summer Student Research Symposium. London, ON. 2019. (Oral Presentation)
4. **Prusinkiewicz M***, Gameiro S, Ghasemi F, Dodge M, Maekebay H, Barrett J, Nichols A, Mymryk J. Survival Associated Metabolic Genes in HPV+ HNSCC. 16th Annual Oncology Research and Education Day. London, ON. 2019. (Oral Presentation)
5. **Prusinkiewicz M***, Cohen M, Mymryk J. A Snapshot of Metabolic Changes in HAdV5 Infected Cells. London Health Research Day. London, ON. 2019. (Poster)
6. **Prusinkiewicz M***, Dodge M, Gameiro S, Maekebay H, Ghasemi F, Barrett J, Nichols A, Mymryk J. Metabolic Gene Expression of Head and Neck Squamous Cell Carcinomas Indicate A Sensitivity to Cellular Respiration Inhibitors. 13th annual Infection and Immunity Research Forum. Stratford, ON. 2018. (Poster)
7. **Prusinkiewicz M***, Cohen M, Buensuceso A, Shepherd T, Mymryk J. Cellular metabolic changes associated with Δ E1A human adenovirus infection. The DNA Tumour Virus Meeting. Madison, WI. 2018. (Oral Presentation)
8. **Prusinkiewicz M***, Cohen M, Buensuceso A, Shepherd T, Mymryk J. Cancer metabolism insight from metabolic changes induced by human adenovirus 5. 15th Annual Oncology Research and Education Day. London, ON. 2018. (Poster)
9. **Maekebay H***, Prusinkiewicz M, Gameiro S, Ghasemi F, Barrett J, Nichols A, Mymryk J. The expression of metabolic genes in HPV+ vs HPV- Head and Neck Squamous Cell Carcinoma. 15th Annual Oncology Research and Education Day. London, ON. 2018. (Poster)
10. **Prusinkiewicz M***, Buensuceso A, Cohen M, Shepherd T, Mymryk J. E1A affects adenovirus induced metabolic changes. London Health Research Day. London, ON. 2018. (Poster)
11. **Prusinkiewicz M***, Buensuceso A, Cohen M, Shepherd T, Mymryk J. Metabolic

- reprogramming by human adenovirus E1A protein. 12th annual Infection and Immunity Research Forum. London, ON. 2017. (Poster)
12. **Prusinkiewicz M***, Buensuceso A, Lucien F, Cohen M, Leong H, Shepherd T, Mymryk J. Adenovirus E1A influences host-cell glycolysis and oxidative phosphorylation during infection. The DNA Tumour Virus Meeting, Birmingham, UK. 2017. (Oral Presentation)
 13. **Prusinkiewicz M***, Buensuceso A, Lucien F, Cohen M, Leong H, Shepherd T, Mymryk J. Effects of the adenovirus oncogene E1A on host-cell metabolism. Oncology Research and Education Day. London, ON. 2017. (Poster)
 14. **Prusinkiewicz M***, Buensuceso A, Cohen M, Shepherd T, Mymryk J. Adenovirus E1A influences host cell metabolism during infection. London Health Research Day. London, ON. 2017. (Poster)
 15. **Prusinkiewicz M***, Cohen M, Mymryk J. Metabolic parallels between virally infected cells and cancer. Abcam Symposium: Metabolic and transcriptional reprogramming leads to cancer vulnerabilities. Toronto, ON. 2016. (Poster)
 16. **Prusinkiewicz M***, Cohen M, Mymryk J. Adenovirus regulation of nucleotide biosynthesis gene transcription. 11th annual Infection and Immunity Research Forum. London, ON. 2016. (Poster)
 17. **Prusinkiewicz M***, Mymryk J. Appropriate Reference Gene Selection for RT-PCR Studies of Human Adenovirus 5 Infected Cells. The DNA Tumour Virus Meeting. Montréal, QC. 2016. (Poster)
 18. **Prusinkiewicz M***, Ghavidel A, Harkness T. Iron importers are required for *Saccharomyces cerevisiae* caloric restriction response. Molecular Genetics of Aging. Cold Spring Harbor Laboratory, NY. 2014. (Poster)
 19. Uganbayar S, Jones H, **Prusinkiewicz M**, Malo M, Harkness T*. Small peptides homologous to the histone variant Htz1 extend yeast lifespan in an anaphase promoting complex-dependent manner. 2nd Canadian Conference on Epigenetics. London, ON. 2014. (Poster)
 20. **Prusinkiewicz M***, Ghavidel A, Harkness T. The yeast iron transporter, Fet3, has a significant role in lifespan maintenance. 2nd Annual Protein Structure, Function and Malfunction Meeting. University of Saskatchewan, Saskatoon, SK. 2014. (Oral Presentation)
 21. **Prusinkiewicz M***, He S, Kaminskyj S, Ghavidel A, Harkness T. Synergistic interactions between iron transporters affect replicative lifespan in *Saccharomyces cerevisiae*. 21st Annual Life and Health Sciences Research Day. University of Saskatchewan, Saskatoon, SK. 2014. (Poster)

22. **Prusinkiewicz M***, Ghavidel A, Harkness T. Hsp70 gene deletions and mitotic longevity. 42nd Annual Scientific and Educational Meeting of the Canadian Association on Gerontology. Halifax NS, Canada. 2013. (Poster)
23. Raj MT, **Prusinkiewicz M**, Cooper DML, Belev G, Webb A, Boughner JC*. Synchrotron 3D Imaging of Earliest Tooth Formation in Mouse. 10th International Congress of Vertebrate Morphology. Barcelona, Spain. 2013. (Oral Presentation)
24. Farazkhorasani F, **Prusinkiewicz M**, Gough K, Kaminskyj S*. Beyond green mining: analysis of fungal cytochemistry using gold nanoparticles. 27th Fungal Genetics Conference. Pacific Grove, CA. 2013. (Poster)
25. **Prusinkiewicz M***, Ghavidel A. Harkness T. Replicative lifespan for *Saccharomyces cerevisiae* with individual metal metabolism and heat shock protein genes deleted. College of Graduate Studies and Research celebrating student success poster competition. University of Saskatchewan, Saskatoon, SK. 2012. (Poster)
26. Farazkhorasani F*, **Prusinkiewicz M**, Kaminskyj, S, Gough, K. SERS imaging of fungi via in vivo synthesis of gold nanoparticles. SciX National meeting of the Society for Applied Spectroscopy, Kansas City, MO. 2012. (Poster)
27. Raj MT*, **Prusinkiewicz M**, Cooper DML, Belev G, Boughner JC. Silver K-edge micro-CT of mandible and tooth germ in embryonic mouse. BMIT research symposium, University of Saskatchewan, Saskatoon SK. 2012. (Poster)
28. Farazkhorasani F*, Gough K, **Prusinkiewicz M**, Kaminskyj S. SERS for intracellular imaging of fungi. 95th Canadian Chemistry Conference, Calgary AB. 2012. (Poster)
29. Kaminskyj S*, **Prusinkiewicz M**, Farazkhorasani F, Isenor M, Gough K. Gold nanoparticles in *Aspergillus nidulans* hyphae: can we study real-time physiology? 8th international *Aspergillus* meeting (ASPERFEST 8), Pacific Grove, CA. 2011 (Oral Presentation)
30. Farazkhorasani F*, **Prusinkiewicz M**, Dynes J, Wang J, Kaminskyj S, Gough K. SERS imaging of fungi with gold nanoparticles synthesized in vivo. Sixth international conference on advanced vibrational spectroscopy, Sonoma Country, CA. 2011 (Poster)
31. **Prusinkiewicz M***, Farazkhorasani F, Dynes J, Wang J, Gough K, Kaminskyj S. Nanoparticles, high-resolution imaging and *Aspergillus nidulans*. Prairie University Biology Symposium, University of Saskatchewan, Saskatoon SK. 2011. (Poster)
32. **Prusinkiewicz M***, Farazkhorasani F, Dynes J, Wang J, Gough K, Kaminskyj S. Gold nanoparticles grown in living cells of the fungus *Aspergillus nidulans* have potential for studying real-time physiology. 1 st Annual Undergraduate Life Sciences

- Conference, St. Boniface General Hospital Research Centre, Winnipeg MB. 2010. (Poster)
33. Farazkhorasani F, Isenor M, Liao CR, **Prusinkiewicz M**, Kaminskyj SGW, Nasse MJ, Hirschmugl C, Gough KM*. FTIR, Raman, and SERS imaging of fungi. Synchrotron- based FTIR imaging workshop and SRC Users meeting. Synchrotron Radiation Center, Madison WI. 2010.
 34. **Prusinkiewicz M***, Farazkhorasani F, Dynes J, Wang J, Gough K, Kaminskyj S. Growing gold nanoparticles in *Aspergillus nidulans*. Natural Sciences and Engineering Council of Canada Undergraduate Student Research Awards Poster Event. Saskatoon, SK. 2010. (Poster)
 35. Ma C*, Crespin M, Proulx M, DeSilva S, Hubbard J, **Prusinkiewicz M**, Panaccione R, Ghosh S, Myers R, Kaplan G. Accuracy of Administrative Data in Identifying Ulcerative Colitis Patients Presenting with Acute Flare and Undergoing Colectomy. American College of Gastroenterology Annual Scientific Meeting. 2010. (Oral Presentation)
 36. Crespin M*, Ma C, Proulx M, DeSilva S, **Prusinkiewicz M**, Seow C, Panaccione R, Ghosh S, Hubbard J, Myers R, Kaplan G. Validity of Administrative Data in Identifying In-hospital Complications in Ulcerative Colitis Patients Undergoing Colectomy. Canadian Digestive Diseases Week. 2010. (Poster)
 37. DeSilva S*, Crespin M, Ma C, **Prusinkiewicz M**, Panaccione R, Ghosh S, MacLean A, Buie D, Devlin S, Seow C, Leung Y, and Kaplan GG. Predictors of Complications Following a Colectomy for Ulcerative Colitis Patients: A Population-Based Study. United European Gastroenterology Week. 2009. (Oral Presentation)

SCHOLARLY ACTIVITIES

Chair

October 2017

Infection and Immunity Research Forum (IIRF)

Western University

- IIRF is organized by the graduate students from microbiology and immunology to showcase work the work of graduate and students and post-doctoral fellows from southwestern Ontario. As the chair I was responsible for coordinating multiple aspects of the forum from contacting the keynote speaker, organizing the venue, and overseeing other logistical concerns.

Co-chair

September 2016

Infection and Immunity Research Forum (IIRF)

Western University

- I was responsible for helping host the keynote speaker and aspects of forum organization and planning

Master of Ceremonies **November 2015**
Infection and Immunity Research Forum (IIRF)
Western University

- I was a joint MC for this event, which involved introducing speakers and moderating questions and their presentations.

Anatomy & Cell Biology Grad Life Committee **September – April 2015**
University of Saskatchewan

- This committee introduced new graduate students to the department of Anatomy and Cell Biology at the University of Saskatchewan

Graduate Student Association Course Councillor **September – April 2013**
University of Saskatchewan

- I represented the College of Medicine Graduate Students' Society at the general Graduate Student Association (GSA) meetings.

VOLUNTEER WORK

Judge **March 2017, 2018, 2019**
Western Student Research Conference
Western University

- An undergraduate student research day that featured both oral and poster presentations.

Scholarship Reviewer **February 2017, 2018**
Western University National Scholarships

- Ranked a selection of scholarship applications from high-achieving secondary students across Canada applying to Western University

Judge **March 2016, 2017**
SciNapse Undergraduate Case Competition
Western University

- An undergraduate student case competition that featured poster presentations from hypothetical subjects revolving around a select theme.

Experience US Demonstrator for Anatomy & Cell Biology **October 2013**
University of Saskatchewan

- I spoke to high school students who were considering attending the University of Saskatchewan about the Department of Anatomy & Cell Biology.